IDENTIFYING FUNCTIONAL SINGLE NUCLEOTIDE POLYMORPHISMS IN TWO CANDIDATE GENES (*PROC* and *PCSK9*) IN SEPSIS

by

KATHERINE ROBERTA THAIN

B.Sc.Hons., Simon Fraser University, 2008

A THESIS SUBMITTED IN PARTIAL FULFILLMENT OF
THE REQUIREMENTS FOR THE DEGREE OF

DOCTOR OF PHILOSOPHY

in

THE FACULTY OF GRADUATE STUDIES

(Experimental Medicine)

THE UNIVERSITY OF BRITISH COLUMBIA

(Vancouver)

July 2013

Abstract

Genetic variation contributes to outcome from sepsis. A large number of associations have been observed between genetic variants and sepsis outcome, however, identification of causal single nucleotide polymorphisms (SNPs), or their mechanisms of action, have not been successfully elucidated. The aims of this project are to identify causal variants in two candidate genes and determine whether these variants are involved in the mechanisms leading to altered outcomes in sepsis.

The known pathophysiology of sepsis is complex and involves dysregulation of several systemic processes, including the coagulation and inflammatory systems. Based on this knowledge, and known literature on genetic variation in coagulation genes, *PROC* was chosen as a candidate gene in which to search for causal SNPs. In addition, based on the known role of lipids in sepsis, as well as the already identified causal SNPs in the *PCSK9* gene, *PCSK9* was selected as a second candidate gene to test the hypothesis that genetic variation in lipid mediators alters outcome in sepsis.

Two intronic SNPs were found in the *PROC* gene (rs2069915 and rs2069916) that are in high linkage disequilibrium and appear to modify untranslated mRNA, leading to lower concentrations of circulating protein C in individuals homozygous for the major alleles of these SNPs. Furthermore, in the *PCSK9* gene, an intronic SNP (rs644000) was found that appears to mark known Loss-of-Function and Gain-of-Function coding SNPs, and was associated with outcome in two cohorts of patients with septic shock, and with a reduction of cytokine levels in a subset of these patients. Additionally, using murine genetic *Pcsk9* knock-out and pharmacologic inhibition strategies in a murine model of systemic bacteremia, a markedly attenuated global, cardiovascular and inflammatory cytokine response to

lipopolysaccharide administration was observed. Furthermore, increased endotoxin clearance was measured after PCSK9 knock-out. Together these results indicate that reduction of *PCSK9* activity in both mice and humans reduces the inflammatory response and improves outcome in septic shock.

The work presented here furthers the understanding of the role played by non-coding SNPs in protein expression and has implications for a new, potentially personal, drug strategy for sepsis patients in intensive care units.

Preface

Parts of this thesis have been published in peer-reviewed journals, listed below in chronological order.

1. **Katherine R. Thain**, Taka-aki Nakada, John H. Boyd, James A. Russell, Keith R. Walley. A common polymorphism in the 5' region of the human protein C gene binds USF1. *Thromb Res*. 2012. 130(3):451-7. Epub 2012 Mar 17 doi:10.1016.

   I designed and performed all the experiments, analyzed the data and wrote the manuscript. TN and JHB assisted with experimental design, data analysis and editing of the manuscript. JAR contributed to design and analysis of experiments. KRW designed the research study, analyzed the data and edited the manuscript.

This published work appears in Chapters 1, 2, 3 and 5.

2. Keith R. Walley*, **Katherine R. Thain***, James A. Russell, Taka-aki Nakada, Simone A. Thair, Yingjin Wang, John H. Boyd. Reduced PCSK9 function protects against adverse outcomes in murine systemic inflammation and human septic shock. Manuscript in preparation.

   ∗KRW and I contributed equally to this work: we designed the experiments, performed the analyses and wrote the manuscript. In addition, I prepared the mouse plasma samples and performed the mouse cytokine assays. JHB designed the mouse experiments, contributed to data analysis and critically

edited the manuscript. TN helped with the human data analysis. SAT prepared the human plasma samples for the human cytokine assay. YW performed all the mouse physiological measurements and harvested the mouse blood and JAR contributed to experimental design and offered critical insight to analyses and manuscript preparation. All animal work was approved by the UBC Animal Care Committee, certificate number A10-0238.

Parts of this prepared manuscript appear in Chapters 1, 2, 4 and 5.

The work in this thesis is conducted with approval from University of British Columbia Office of Research and in accordance with the University of British Columbia Policies and procedures, Biosafety Practices and Public Health Agency of Canada Guidelines. Work with radioactive materials was approved by the University of British Columbia Committee on Radioisotopes and Radiation Hazards.

Radioisotope Licenses: MEDI-3104-11 and MEDI-3258-16

Table of Contents

List of Tables

List of Figures

List of Abbreviations

Abbreviation	Definition
°C	Degrees Celsius
aa	Amino acid
ANOVA	Analysis of Variance
AP1	Adapter protein 1
APACHE II	Acute Physiological and Chronic Health Evaluation II
aPC	Activated protein C
APOB	Apolipoprotein B
APOE	Apolipoprotein E
ARE	AU-rich element
Arg6	Argenine 6
ARIC	Atherosclerosis Risk in Communities
ATCC	American Type Culture Collection
ATP	Adenosine triphosphate
BCA	Bicinchoninic acid assay
bp	Base pair
BSA	Bovine serum albumin
CC	Cysteine-cysteine
CD40	Cluster of Differentiation 40 (TNF receptor family)
cDNA	Complementary DNA
CEPB	CCAAT/enhancer binding protein
CEU	Utah Residents (CEPH) with Northern and Western European ancestry
CFTR	Cystic fibrosis transmembrane conductance regulator
CLP	Cecal ligation and puncture
CO_2	Carbon dioxide
COP1	Caspase recruitment domain-containing protein 16
CXC	Cysteine-X-cysteine

Abbreviation	Definition
DAMP	Damage (or danger) Associated Molecular Patterns
DIC	Diseminated intravascular coagulation
DMEM	Dulbecco's modified minimum essential medium
DTT	Dichlorodiphenyltrichloroethane
ECHO	Echocardiogram
EDTA	Ethylenediaminetetraacetic acid
EMEM	Eagle's minimum essential medium
EMSA	Electrophoretic mobility shift assay
ENCODE	Encyclopedia of DNA Elements
EPCR	Endothelial Protein C receptor
F2R	Coagulation factor II (thrombin) receptor (also PAR-1)
FBS	Fetal bovine serum
FDA	Federal Drug Administration
gDNA	Genomic DNA
GOF	Gain of function
GR/PR	Glucocorticoid receptor
GWAS	Genome-wide assocoation study
HCV	Hepatitis C virus
HDL	High density lipoprotein
HGF	Hepatocyte growth factor
HMGB1	High mobility group box 1
HNF1	Hepatocyte nuclear factor 1
HNRPM	N-acetylglucosamine receptor
i.p.	Intraperitoneal injection
ICAM1	Intercellular adhesion molecule 1
ICU	Intensive care unit
IFNG	Interferon gamma
IL10	Interleukin 10
IL6	Interleukin 6
IL8	Interleukin 8
IRE	Iron response element

Abbreviation	Definition
IRF1	Interferon regulatory factor 1
JE	Platelet-derived growth factor-inducible protein JE
KCl	Potassium chloride
LAL	Limulus amebocyte lysate
LB	Lysogeny broth
LD	Linkage disequilibrium
LDL	Low density lipoprotein
LDLR	Low density lipoprotein receptor (Human and murine)
LDLR/Ldlr	Low density lipoprotein receptor gene (Human/Murine)
LOF	Loss of function
LPS	Lipopolysaccharide
LRP8	Low density lipoprotein receptor-related protein 8
LTA	Lipoteichoic acid
LXR	Liver X receptor
Lys4	Lysine 4
MAF	Minor allele frequency
MIP-2	Macrophage inflammatory protein 2
miRNA	Micro RNA
NaCl	Sodium chloride
NARC-1	Neural apoptosis-regulated convertase 1
NCBI	National Center for Biotechnology Information
NFKB	Nuclear factor kappa B
NHP2	Non-histone protein 2
NIH	National Institute of Health
(e)NOS	(endothelial) Nitric oxide synthase
NRF1	Nuclear respiratory factor 1
PAF	Population attributable fraction
PAMP	Pathogen-associated molecular patterns
PAR-1	Protease-activated receptor 1
PBS	Phosphate buffered saline
PCSK9/Pcsk9	Proprotein convertase subtilisin/kexin type 9 gene (Human/murine)

Abbreviation	Definition
PCSK9	Proprotein convertase subtilisin/kexin type 9 protein (Human and murine)
PPAR	Peroxisome proliferator-activated receptor
PROC	Protein C gene (Human)
RAGE	Receptor for advanced glycation end products
rhAPC	Recombinant human activated Protein C
rpm	Revolutions per minute
RT-qPCR	Real time-quantitative PCR
RUNX1	Runt-related transcription factor 1(formerly AML1)
S1P	Sphingosine-1-phosphate
SILAC	Stable isotope labeling by amino acids in cell culture
siRNA	Small interfering RNA
SNP	Single nucleotide polymorphism
SOC	Super optimal broth with catabolite repression
SPH	St Paul's Hospital
STAT3	Signa transducer and activator of transcription
Streptavidin-PE	Streptavidin-phycoerythrin
TEAD1	TEA domain family member 1
TGFB1	Transforming growth factor - beta 1
TLR(2)(4)	Toll like receptor 2 or 4
TNF-alpha	Tumour necrosis factor alpha
Tris-HCl	Tris(hydroxymethyl)aminomethane-hydrochloride
USF1	Upstream stimulatory factor 1
UTR	Untranslated region
UV	Ultraviolet
VASST	Vasopressin and septic shock trial
VLDL	Very low density lipoprotein

Acknowledgements

I owe a huge debt of thanks to my supervisor Dr Keith Walley for his support and encouragement from the very beginning of my year-long undergraduate co-op studentship through to the end of my PhD study. During this time Dr Walley inspired me to think critically, to recognize the medical implications and always understand those statistics! My sincere gratitude must also go to my graduate committee members, Dr Mike Allard, Dr John Boyd and Dr David Huntsman whose enthusiasm and constructive suggestions kept my project on track. In particular I would like to thank Dr John Boyd for his guidance, patience in answering my many questions and his innate ability to determine the quickest, least expensive route to the answer – a skill I am still trying to emulate. In addition, I thank my graduate committee for their advice and interest in my future career.

I acknowledge financial support from the Heart and Stroke Foundation, the Canadian Institutes of Health Research and the University of British Columbia.

I extend special thanks to Ms Loubna Akhibir, Dr Samuel Wadsworth, Dr Michael Silverman (SFU), Dr Mike Allard, Dr Vince Duronio and Dr Andy Sandford for their advice and support that made completing my studies possible.

I thank Dr Taka-aki Nakada for the knowledge and good work practices he imparted to me over the 3 years he spent in our lab as a research fellow from Japan. I also thank other members of our team: Yingjin Wang for his surgical skills with anything mouse-related and Sumeet Mathur for his unfailing good-nature, enthusiasm and interest in music which made long days in the lab more enjoyable. Thanks also to David Ngan and Adrian Png for extensive practical help with computer software, for advice freely offered and for introducing me to new sports that continue to enhance my life. I am grateful to many others at the James

Hogg Research Centre for many hours of useful discussion, assistance and advice that helped my work proceed more smoothly and to Dr Leonard Foster for his kind gift of the solutions containing “heavy and “light” isotopes of argenine and lysine.

Last but not least, I am eternally grateful to my family and friends for always being prepared to listen, despite not understanding what I was talking about, for being so concerned for my physical well-being and for being there when I needed them.

Completion of this thesis would not have been possible without the contributions of all these people – it truly has been a team effort, thank you all!

I dedicate this dissertation to all those who, over the years, have believed in me and have encouraged me to think and to question everything.

"If you want to be happy, set a goal that commands your thoughts, liberates your energy and inspires your hopes."

Andrew Carnegie

Chapter 1: Introduction

Many genetic variations have been associated with a diverse array of complex diseases, from diabetes [1], cardiovascular disease [2] and chronic obstructive pulmonary disease [3], to asthma [4], atherosclerosis [5] and sepsis [6], to name but a few. Elucidating the actual causal or functional variations has proven to be far more challenging.

Compounding this difficulty is the likely contribution of many variations from several genes to the outcome or phenotype of a single disease.

A variety of treatments have been trialed for treatment of sepsis but to date none have proven to be the "silver bullet" that physicians are looking for. The likelihood exists that the most effective treatment for sepsis will vary between individuals as each individual possesses a unique background of genetic variation upon which any disease will act.

Performing functional studies on every variation in the human genome is not feasible therefore potentially functional variations need to be selected for in-depth testing using the collection of knowledge amassed in the literature, including previously published association data and knowledge of biologic pathways active during the course of the disease.

1.1 Sepsis – Clinical Definition

Sepsis is a complex condition resulting from an overwhelming systemic host response to a systemic infection initiated mainly by Gram-positive and Gram-negative bacterial pathogens [7], but also by viral, fungal and protozoan pathogens [8]. Occasionally, hyperinfections by metazoans such as *Strongyloides stercoralis* have been known to initiate sepsis in immunocompromised individuals [9]. Sepsis is defined as a systemic inflammatory

response syndrome (SIRS) in response to an infection, and is considered severe when combined with acute organ dysfunction [10]. Severe sepsis combined with hypotension despite adequate fluid resuscitation is termed septic shock [10].

1.2 Incidence of Sepsis

In 2004 sepsis was the 10th leading cause of mortality in adults and the leading cause of death in intensive care units (ICUs) in developed countries [11] and accounted for as many deaths as heart attacks [12]. Incidence of severe sepsis in the United States increases by 1.5% annually due, in part, to the aging population [12] which, by 2020, will increase incidence by an additional million cases per year [13]. Prognosis of patients with severe sepsis is poor, with in-hospital mortality rates ranging between 30% and 40% [14]. There are ~750 000 cases of severe sepsis in the United States every year, of which ~215 000 (approx. 30%) will die [14]. The long-term outcome for survivors of severe sepsis is also affected as their quality of life is lower than before the critical illness [15] and 2-year mortality rate is high (~45%) [15] moreover, long-term survival is reduced with an increased 5-year mortality rate, even after controlling for co-morbidities [16]. Altogether this represents an enormous burden on the health care system; it is estimated that in 2008 the United States spent approximately $14.6 billion on hospital costs for sepsis [17]. With average costs of more than $38 000 for survivors (not including costs incurred after discharge) and $49 000 for non-survivors [12], coupled with an increasing incidence, it is easy to see these costs escalating in the future. These high costs are not restricted to the United States - a small 1999 study in the United Kingdom found median daily ICU costs of treating a patient with sepsis varied between $930 and $1079, depending on severity [18].

1.3 Heritability of Genetic Predisposition to Sepsis

Is the susceptibility to inflammatory or infective conditions inherited or a product of environmental conditions? There have been several studies that have attempted to answer this question. A key 1988 study by Sørensen *et al.* found that death due to infections and vascular causes is strongly linked to the genetic background of the individual [19]. They found that adoptees have a 5.81 relative risk of dying from an infection if their biologic parent died of infection before the age of 50, which is greater than their relative risk for a cardiovascular or cerebrovascular event (4.52) or for cancer (1.19) [19].

Further evidence of a genetic contribution to outcome of infectious diseases comes from twin studies: A study in India found a 60% concordance among monozygotic twins for the risk of contracting leprosy compared to a 20% concordance for dizygotic twins [20]. Further, a 2010 study by Obel *et al.* found a consistent concordance rate for monozygotic twin pairs compared to dizygotic twin pairs over the three definitions of death due to infection used in the analyses (narrow, broad, broadest) [21]. Although the concordance rates were low, this nonetheless demonstrates a genetic influence on the risk of death from infectious diseases.

These infections are not genetic diseases, therefore the similarities in outcome of genetically linked, but not environmentally linked, adopted individuals points to a genetic influence. Determination of a genetic link to susceptibility is also seen in twin studies where the siblings usually share the same environment and the genetic contribution to susceptibility is determined by the different concordance rates between the more-genetically-similar monozygotic twin pair compared to the dizygotic twin pair. Genotype could contribute to susceptibility to any infection or to specific pathogens but also could contribute to the

response to an infectious agent. Determining which genotypes are likely to develop sepsis, or survive a severe sepsis or septic shock episode, may help in developing or targeting new treatment therapies.

1.4 Pathophysiology of Sepsis

Initially, within the first 24 – 48 hours after infection, sepsis manifests as an intense inflammatory response of the host to an invading pathogen (see Figure 1.1), which includes production of many pro-inflammatory mediators such as tumor necrosis factor-alpha (TNF-alpha), interferon-gamma (IFNG), interleukin 1 beta (IL1B), interleukin 6 (IL6), nitric oxide and activated complement factors C3a and C5a [7, 22, 23]. At the same time, large numbers of immune cells are recruited to the damaged tissue and release anti-inflammatory mediators such as interleukin 10 (IL10) and transforming growth factor beta 1 (TGFB1) [24-26]. The cellular damage caused by the invading pathogen and these mediators leads to further release of pro-inflammatory mediators and amplification of the pro-inflammatory response, leading to a vicious cycle resulting in hypoperfusion, disseminated intravascular coagulation, acute organ dysfunction and shock [23-26].

There is increasing evidence of a biphasic aspect to the immune response in patients with sepsis: those who survive the initial "cytokine storm" may succumb to a secondary infection, often one which would not normally be pathogenic in a healthy individual [27, 28]. It has been suggested that as sepsis progresses, some patients may suffer "immuno-paralysis" caused, in part, by a sustained release of the anti-inflammatory mediators and characterized by decreased cytokine and chemokine production as well as defective antigen presentation and phagocytosis [29-32].

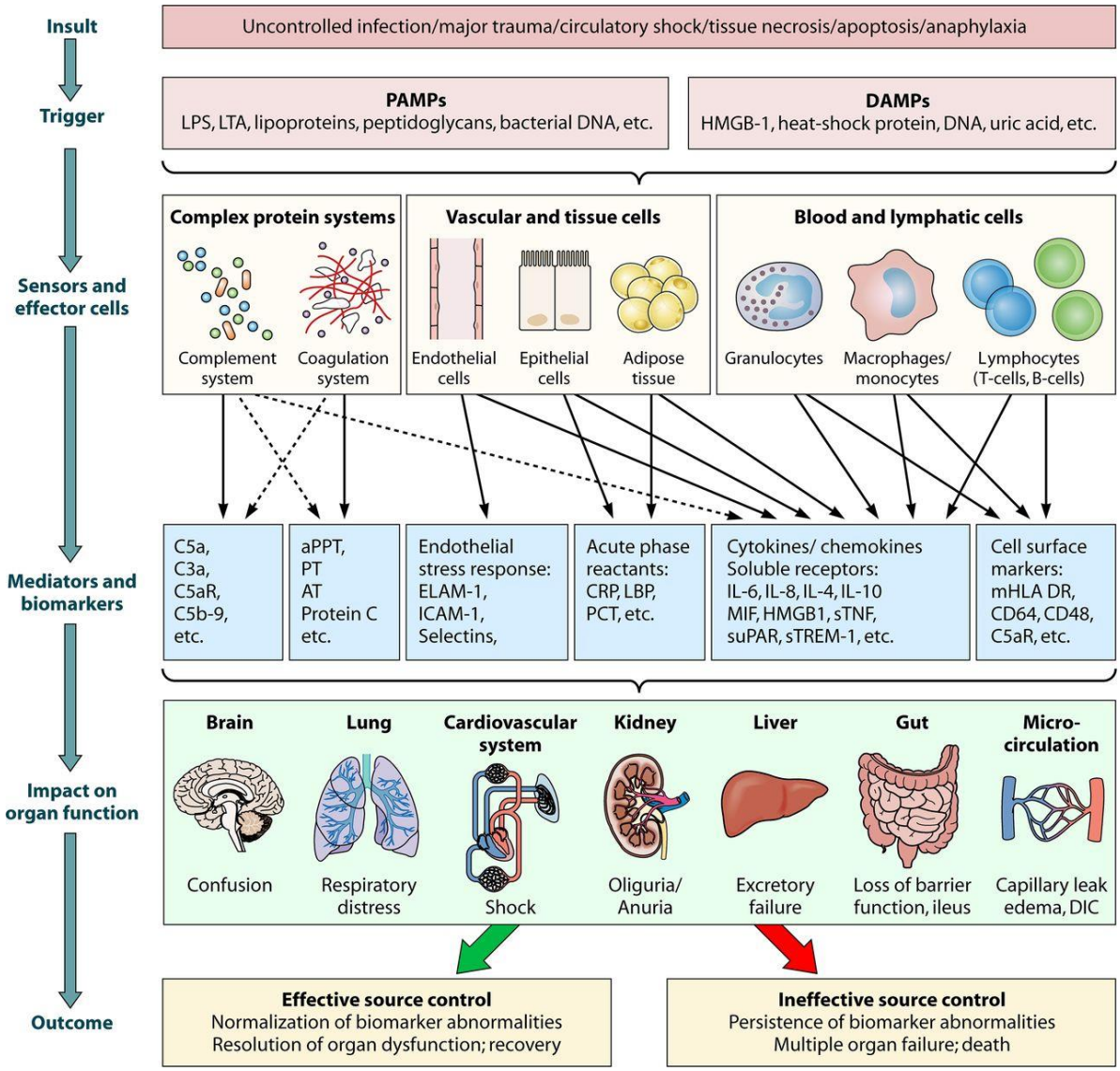

Figure 1.1 Overview of the inflammatory response.

Even a simplified overview of the inflammatory response highlights the complex interplay between molecules and tissues: the initial immune response, triggered by a variety of insults, invokes pathogen-associated and/or danger-associated molecular patterns (PAMPs and DAMPs, respectively), which results in the release of an exuberant inflammatory response. A vast array of inflammatory mediators acts on all the physiological systems and various cell types, ultimately causing organ dysfunction. Some individuals able to resolve the insult will survive, while many will be unable to combat either the insult or the overwhelming response and will succumb. *Reprinted with permission from The American Society for Microbiology: Reinhart K et al. Clin. Microbiol. Rev. 2012;25:609-634.*

Otto *et al.* (2011) found re-infection rates by opportunistic pathogens, specifically *Candida spp*., increased in later stages of sepsis. Concomitantly, they found mortality rates peaked in the early phase (0-5 days) after sepsis diagnosis and then again later, with the majority of deaths (63.3%) occurring after the first 5 days [28].

1.4.1 Lipids in sepsis

Serum total cholesterol, high density lipoprotein (HDL) and low density lipoprotein (LDL) levels are important in the hosts' response to Gram-negative and Gram-positive infections (eg., sepsis) [33]. Triglyceride-rich lipoproteins clear pathogens by binding to lipopolysaccharide (LPS) and lipoteichoic acid (LTA) fragments of Gram-negative and Gram-positive pathogens, respectively (see Figure 1.2), and forming complexes which are then internalized via the LDL receptor (LDLR) and cleared by the liver through bile excretions [34, 35]. Patients with sepsis due to Gram–negative bacteria commonly display brief increases in plasma free fatty acids and triglycerides and a sustained drop in cholesterol, LDL, HDL and apolipoprotein B (APOB) levels [33]. Most adults and children admitted to the ICU with severe sepsis have low or undetectable serum lipoprotein levels and an increased risk of death [36]. Both LDL and HDL are able to bind pathogen fragments and neutralize their harmful effects prior to expulsion by the liver [37], in fact, reconstituted HDL has been used in several species, including humans [38-40] to treat septic shock and prevent the harmful release of pro-inflammatory cytokines, while having minimal effect on anti-inflammatory cytokines [41].

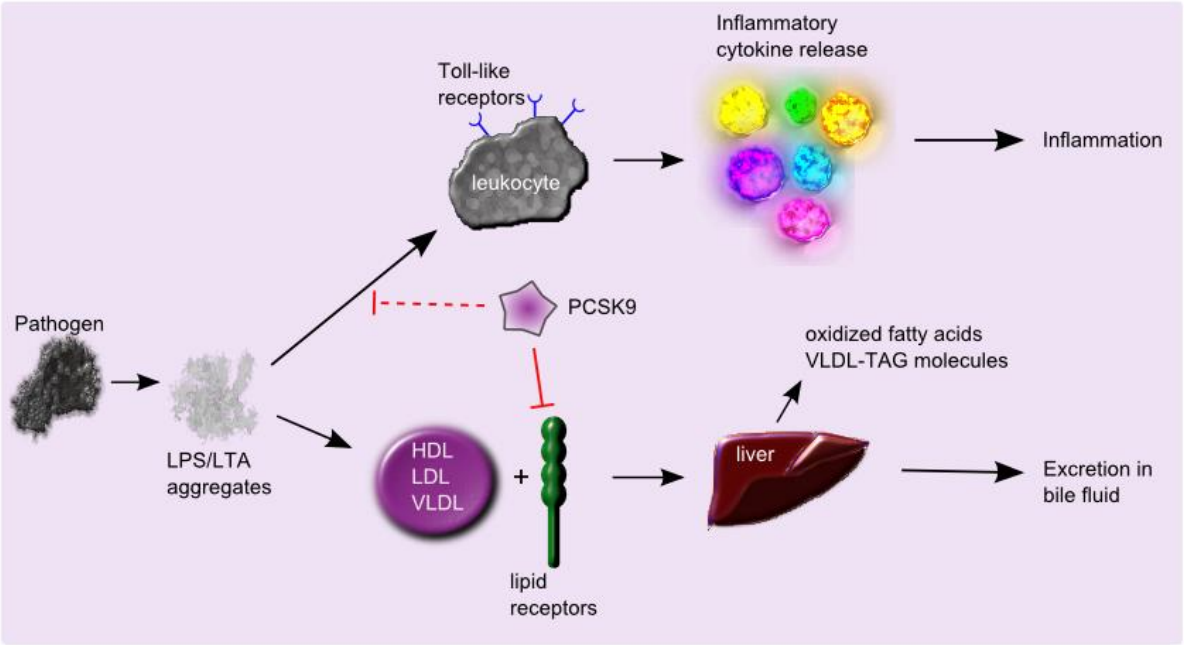

Figure 1.2 Clearance of pathogens by lipids.

Pathogenic aggregates increase expression of pro-inflammatory mediators via innate-immune receptors on leukocytes, which is indirectly inhibited by PCSK9: PCSK9 mediates uptake of LDL, very low density lipoprotein (VLDL) and HDL molecules via the LDL receptor by directly binding to the LDL receptor, and reducing receptor numbers on the cell surface by preventing receptor recycling. PCSK9 may also have this effect on other lipid receptors, such as the very low density receptor (VLDLR). Reduction of PCSK9 increases uptake of these pathogen/ lipid complexes, allowing removal of pathogen-bound lipid molecules via the liver for excretion in bile fluids. Non-esterified fatty acids are either re-esterified to form triacylglycerol (TAG) or oxidized. *Figure created using Inkscape software version 0.48.4*

1.4.1.1 Oxidized lipoproteins

In septic patients, levels of oxidized lipoproteins are high and are associated with both the pro- and anti-inflammatory aspects of sepsis. Oxygen free radicals cause tissue damage to a variety of cells, in particular to endothelial cells, which leads to vascular dysfunction and, ultimately, organ failure [42]. In contrast, oxidized lipoproteins are also able to neutralize pathogen fragments, to suppress signaling via some nuclear factor of kappa light

polypeptide gene enhancer in B-cells 1 (NFKB1, commonly known as NFKB) pathways [42] as well as to augment the anticoagulant activity of activated protein C (aPC), a natural anticoagulant always in short supply during severe sepsis and septic shock [43]. Oxidized LDL concentrations increase steadily during the first 7 days in patients with severe sepsis and, given its opposing roles, may change the course of the response from an acute event to a more chronic condition [42].

1.4.1.2 The role of apolipoprotein E in the inflammatory response

Apolipoprotein E (APOE) has also been shown to bind strongly to LPS fragments and intensify the uptake and degradation of LPS by the liver and also to decrease the levels of pro-inflammatory cytokines by precluding any association between LPS and pro-inflammatory cells such as macrophages [44] as well as possibly directly down-regulating macrophage pro-inflammatory activity [45, 46]. Apolipoprotein E has been shown to have several different immunomodulatory effects, from protection against LPS infection to modulating T-cell activation and clearance of apoptotic bodies [47], suppression of Type I inflammatory response [48] and antigen presentation to natural killer cells [49]. Apolipoprotein E has also shown protective effects against diverse diseases such as malaria [50], *Listeria monocytogenes* [51] and *Klebsiella pneumoniae* [52].

Other lipoproteins have displayed protective affects against LPS-induced infection, possibly also, like APOE, by reducing pro-inflammatory cytokine production. One such lipoprotein is apolipoprotein A-1 (APOA1), a major component of HDL [37], which has been shown to decrease the development of atherosclerosis in response to LPS in mice that are APOE-deficient and have high plasma concentrations of other lipids [53].

1.5 Treatment of Sepsis

Currently the standard treatment for patients with sepsis is early administration of broad spectrum antibiotics, early goal-directed fluid resuscitation, control of infection source and appropriate organ support [10]. There is no FDA–approved drug treatment specifically used to reduce mortality from sepsis. Many different treatment regimens have been tested, including treatments aimed at supporting the immune system, reducing coagulation, blocking the host inflammatory response and aggressive support of cardiac function and global oxygen delivery but none has been wholly successful. An early study by Rivers *et al.* (2001) found early goal-directed therapy, compared to standard therapy, reduced 28-day mortality in patients with severe sepsis and septic shock, and suggested that adequate, rather than supranormal, levels of oxygen delivery be achieved rapidly [54], which correlates with findings from two other groups that found increased in-hospital mortality [55], or no decrease in mortality [56], in the groups assigned to receive a high level of oxygen delivery.

To date, in addition to system support, there have been many potential pharmacological therapies for sepsis but all have either failed completely or not proved as efficacious as expected [13].

1.5.1 Pharmacological agents against inflammatory mediators

1.5.1.1 Anti-tumour necrosis factor therapy

Tumour necrosis factor alpha is a well described cytokine with a central role in the stimulation of the acute phase response. Produced primarily by activated macrophages it induces fever, apoptotic cell death, inflammation and sepsis via induction of IL1 and IL6 [57] and contributes to the organ dysfunction, shock and mortality seen in severe infections [58].

Several studies have linked polymorphisms in the TNF-alpha [59, 60] and TNF-beta [61, 62] genes with outcome in septic patients. Several anti-TNF therapies have been trialed but none have so far been as effective as expected, for example the MONARCS trial saw a small benefit after adjusting for covariates but no benefit overall [58, 63] and the small treatment effect has not been replicated [13]. Furthermore, a meta-analysis of randomized control trials of anti-TNF therapies for rheumatoid arthritis found an increased risk of serious infection and development of malignancies [64], while other studies found necrosis of extremities occurred after anti-TNF therapy [65, 66].

1.5.1.2 Nuclear factor kappa B (NFKB) therapy

A central player in the inflammatory cascade is NFKB, a transcription factor activated by stimuli such as cellular stress, cytokines and pathogens whereby it then modulates expression of several genes involved in the immune response to infection [67, 68]. When lung epithelial cells are stimulated with LPS derived from *Escherichia coli*, the LPS binds pattern recognition receptors on the cell surface such as toll-like receptors (TLRs) which initiates a signaling cascade through myeloid differentiation primary response 88 (MYD88), and other intermediates, to phosphorylate nuclear factor of kappa light polypeptide gene enhancer in B-cells inhibitor alpha (NFKBIA). Phosphorylated NFKBIA then releases NFKB allowing it to translocate to the nucleus where it regulates transcription of various genes [69-71]. Clinical studies of patients with infection-induced sepsis have shown high nuclear concentrations of NFKB in neutrophils which have been associated with a worse outcome. In experimental models, inhibition of NFKB translocation results in less inflammation and less injury to the lungs [69].

In addition, NFKB is involved in other cellular processes such as embryonic development, cell growth and proliferation, blocking apoptosis [72], promotion of angiogenesis and neuronal development such that it is known to regulate approximately 400 genes in a temporal and tissue-specific manner [73-77]. Mutations in the *NFKB* gene leads to several known human defects [78]: NFKB has been associated with varied disease states such as atherosclerosis, asthma, arthritis, stroke, diabetes and septic shock [79]. Dysregulation of NFKB pathways has been implicated in many types of cancer and inflammatory conditions and over 750 different NFKB pathway-inhibiting compounds have been identified and many are being tested for use as NFKB-blocking therapies [76, 80, 81].

As a drug target for sepsis NFKB appears to be a good candidate; inhibiting a main player involved in the amplification of the inflammatory response should reduce the cytokine storm that often overwhelms the patient, but NFKB is also involved in normal cellular processes and blocking NFKB systemically could have dire consequences for the host.

1.5.2 Anticoagulant therapies

There is extensive cross-talk between inflammation and coagulation; not least because the three important anticoagulant systems (Protein C/thrombomodulin, antithrombin and tissue factor pathway inhibitor (TFPI) systems) are located on endothelial cell surfaces where they can participate in both functions [82]. Molecules that act in the coagulation cascade (see Figure 1.3) are obvious candidates to investigate as potential treatments to combat the excessive dysregulation of this system regularly seen during severe sepsis and septic shock and many have been trialed with limited success.

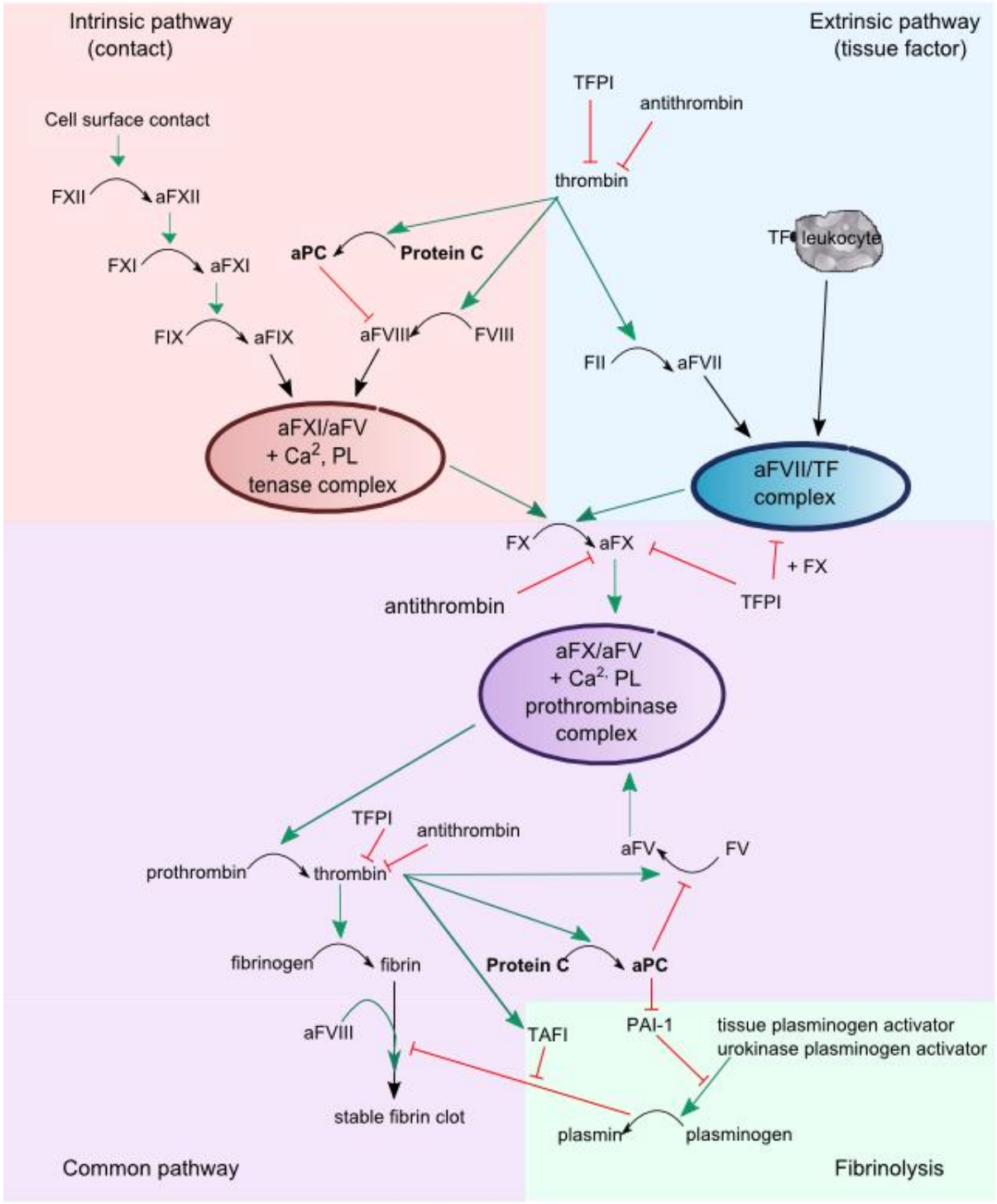

Figure 1.3 The complexity of the coagulation cascade

Many players interact in a carefully choreographed interplay to maintain balance between excessive coagulation and runaway hemorrhage. Thrombin and activated protein C (aPC) are major players in both the coagulation and fibrinolytic pathways. *Figure created using Inkscape software version 0.48.4*

1.5.2.1 Tissue factor pathway inhibitor (TFPI) therapy

The main inhibitor of the tissue factor/Factor VIIa complex is tissue factor pathway inhibitor (TFPI) [82]. This molecule has been tested extensively in experimental and clinical settings and although high concentrations of TFPI seem to reduce tissue-factor-mediated coagulation, a large study in patients with severe sepsis (OPTIMIST trial) displayed no survival benefit [83-85]. Although one study using recombinant TFPI in baboons with septic shock did show a survival benefit for the group treated with TFPI 30 minutes after LPS challenge, this benefit was vastly reduced in animals treated 4 hours after LPS challenge [86].

1.5.2.2 Antithrombin therapy

Endothelial damage caused, in part, by excessive cytokine production leads to generation and activation of thrombin. Excess thrombin contributes to the excess blood clotting seen in deep vein thrombosis and severe sepsis [87]. In addition, recently it has been found that histones in the plasma, likely a result of apoptosis of damaged cells, induce thrombin generation [88].

Antithrombin is a serine protease inhibitor and is the main inhibitor of thrombin and Factor Xa [89]. Heparin and heparin-sulphates enhance activity of antithrombin by at least 1000-fold [89]. During a severe inflammatory incidence, expression of antithrombin is inhibited by acute-phase response proteins. Antithrombin levels are further reduced due to continued consumption and degradation, while thrombin continues to be generated by activated neutrophils [89]. Plasma levels of antithrombin are known to be low in patients with sepsis, and treatment by antithrombin replacement therapy has been used since the 1980s [90]. A large randomized-controlled clinical trial (KyberSept trial) in patients with

severe sepsis did not show an overall benefit of antithrombin treatment except in a sub-group of patients who were not also receiving heparin [91]. Earlier studies used plasma-derived antithrombin concentrate whereas more recently recombinant antithrombin has been made available and has shown efficacy in reversing heparin resistance in patients undergoing cardiac bypass surgery [92].

1.5.2.3 Activated protein C and protein C therapy

In addition to anti-coagulant functions, activated protein C (aPC) has been shown to have several cytoprotective functions: it is essential for immune-mediated elimination of cancer cells [93], promotes coagulation factor II (thrombin) receptor (F2R) - commonly known as proteinase-activated receptor 1 (PAR-1) - cytoprotective signaling through arrestin beta-1 and dishevelled-2 scaffolds in endothelial cells [94], and through protease activated receptor 3 (PAR-3; approved name coagulation factor II (thrombin) receptor-like 2 (F2RL2)) in podocytes [95]. Signaling by aPC via the PAR-1/arrestin beta -1/disheveled-2 complex leads to endothelial barrier protection, in contrast to thrombin signaling through PAR-1 which does not require the same co-factors and leads to barrier permeability [94]. The initial large prospective, randomized, double-blind, placebo-controlled, multicenter PROWESS trial showed a 6.1% reduction of risk for all-cause mortality in their cohort of 1690 patients with sepsis and septic shock after treatment with recombinant human aPC (drotrecogin alfa, Xigris®, abbreviation rhAPC) [96], but this result did not replicate in a follow-up study (PROWESS-SHOCK Trial) [97]. In both studies there was a slightly increased risk of serious bleeding events in the drotrecogin alfa group. Studies are underway to test synthesized aPC molecules that have little or no anticoagulant function but retain anti-inflammatory and anti-apoptotic function [98], but this may not be as effective as hoped in

light of a recent discovery by Schuepbach *et al*. (2011) who found aPC upregulates procoagulant factors on endothelial cells, in a manner dependent on aPC binding to the endothelial protein C receptor (PROCR; commonly designated EPCR) but independent of PAR-1 signalling [99].

Instead of using aPC, Baratto *et al.* (2008) tested the use of endogenous protein C as a therapy, reasoning that protein C is normally reduced in patients with sepsis, and serious bleeding events would be minimized if only the required amount of aPC was generated [100]. They conducted a small pilot study with 20 patients who had protein C levels <50% of normal in the setting of severe sepsis or septic shock [100]. Patients received an infusion of protein C (Ceprotin®, Baxter, Deerfield, IL) over 72 hours to maintain protein C activity between 70% and 120% of normal. They found a significant reduction in coagulopathy, disseminated intravascular coagulation (DIC) score and lactate levels and a significant increase in platelets and anticoagulant molecules, however, the results are difficult to interpret as there was no control group. Further studies into protein C as an adjunct therapy are warranted.

1.5.3 Lipids as inflammatory mediators

1.5.3.1 High density lipoprotein therapy

High density lipoproteins (HDLs) have been shown to be important mediators in sepsis and septic shock by mediating the inflammatory response via both endotoxin and non-endotoxin binding mechanisms [101]. Patients with sepsis are known to have reduced plasma HDL cholesterol, with the lowest levels seen in the most severely ill, and correlated to patient outcome [102]. The known anti-inflammatory effects of HDL (Figure 1.2) include

clearing of LPS molecules from plasma [103], modulation of cytokine expression [104], repression of adhesion molecule expression [105, 106], increasing expression and capacity for activation of endothelial nitric oxide synthase (eNOS) [107, 108] and preventing oxidative damage to LDL molecules [109, 110]. Levine *et al.* (1993) showed a survival benefit in endotoxin-challenged mice given reconstituted HDL therapy but also showed a mild toxicity to plasma HDL and no benefit from HDL apoprotein alone [38]. Recombinant HDL (rHDL) therapy in rabbits with sepsis displayed a reduction in TNF signaling [111], however, a drawback to rHDL therapy is that infusion of this molecule has been shown to increase incidence of *Candida albicans* [112]. Another group found growth of *Staphylococcus aureus* substantially increased in the presence of cholesterol [113]. Taken together, these results suggest that in septic patients, HDL therapy should be used with caution because of the risk of life-threatening secondary infections. More recent work by Gautier and Lagrost (2011) suggests that neutralization of LPS by lipoproteins is mediated by phospholipid-transfer protein (PLTP) and, indeed, this protein has demonstrated effects in diverse biological processes including the inflammatory response and innate immunity and may be a better molecule to pursue as a drug target in the treatment of sepsis [114].

1.5.3.2 Statin drugs as anti-inflammatory agents

The metabolism of cholesterol is a highly regulated process, balancing uptake of cholesterol from diet with synthesis and degradation of cholesterol in the liver [115]. The rate limiting step in cholesterol synthesis is an enzymatic step mediated by 3-hydroxy-3-methylglutaryl-coenzyme A (HMG-CoA) reductase [115]. Drugs commonly prescribed to inhibit HMG-CoA reductase in patients with high serum cholesterol levels at risk of cardiovascular disease or atherosclerosis are universally called “statins” [115]. In addition to

their lipid-lowering affects, statins are now also thought to play a separate, independent role in reducing inflammation in infectious conditions such as sepsis and septic shock [115, 116].

Studies looking at the anti-inflammatory effects of statins in reducing mortality in patients with sepsis have been inconclusive. Most studies involving statins and sepsis show a significant decline in mortality for patients already taking statins and for at-risk patients pre-treated with statins, although the mechanism has not been elucidated as yet [117, 118]. Studies using animal models of sepsis where statins were given after the onset of infection did not show a significant benefit [119]. Much of the anti-inflammatory effects of statins are mediated in endothelial cells which exhibit a reduction in inflammatory cytokine production caused by a statin-induced inhibition of CD40 molecule, TNF receptor superfamily member 5 [120]. In addition, statins inhibit small GTPase prenylation which results in inhibition of several transcription factors (for example, NFKB and activator protein-1 (AP-1)) involved in the transcription of pro-inflammatory mediators [121]. Statins inhibit adhesion molecules, particularly P-selectin and intercellular adhesion factor 1 (ICAM1), but also affect many others by altering either gene expression or protein distribution in tissue [121].

1.5.4 Other therapies tested in treatment of sepsis

Clinical trials for many other potential therapies for sepsis targeting the coagulation, inflammatory or innate immune systems or the endotoxins themselves have failed: p55 tumour necrosis factor fusion protein, anti-endotoxin monoclonal antibodies, recombinant human IL1 antagonist, NOS inhibitor, platelet activating factor acetylhydrolase, group IIA secretory phospholipase A, bactericidal/permeability-increasing protein, ibuprofen, pentoxifylline and others (reviewed in Wheeler, 2009 [13]). Other trials have targeted the

apoptotic pathway [122], corticosteroids [123, 124], nutrition [125], oxidative stress [126] and nitric oxide [127]. Efficacies of most drug therapies in the treatment of sepsis have been mixed. This may be due, in part, to diversity of the initiating pathogen type or enrollment of patients with no bacterial infection, the duration of infection prior to enrollment in the study, the definition of sepsis used in the study, underlying morbidities of the patients and non-uniformity of initial patient support [58]. It has been shown, by sub-analyses of study data, that tight stratification of the study group identifies a greater benefit of some treatments in the patients with the highest risk of death compared to those with less severe disease [58]. In addition, the efficacy of any potential drug therapy has been determined largely by the risk of death in the control group and this varied between studies [128].

Sepsis is a complex condition involving all physiological systems therefore it is unlikely that a pharmaceutical agent targeting one single system is likely to lead to complete resolution of all symptoms. In addition, patient presentation and the responses of individuals to different pathogens and therapies vary markedly and suggest that elucidation of functional variations in key genes may be useful in predicting responses to pharmacological therapies as well as outcome. Use of biomarkers such as single nucleotide polymorphisms (SNPs) in identifying host responses to infection and inflammation may elucidate individuals likely to develop more severe disease or have a better or worse response to particular treatments, thereby enabling specific therapies to be personally targeted, leading to better patient outcomes.

1.6 Polymorphisms in the Genome

There is very little genetic difference between individuals: human genomes vary by only about 0.1% [129]. Mutation rates are lower in females than males [130]. Several common types of variations exist: small insertions and deletions of base pairs, micro-satellite regions (varying number of short, repeated base pair sequences) and SNPs [131]. The smallest genotypic change is the SNP, a change to a single base pair; it is relatively common and makes up about 90% of all human genetic variations [132, 133]. The most common variation is a nucleotide change from CpG to TpG and accounts for approximately 25% of all mutations in the human genome [134]. The allele that occurs most frequently in the population is known as the major allele, while the less common allele is known as the minor allele. A mutation is known as a SNP if the minor allele occurs with a frequency of ≥0.1%, these variations occur approximately every 100 – 300 bases along the length of the genome (http://genomics.energy.gov). Very common SNPs, where the minor allele occurs with a frequency of ≥10%, are found approximately every 500 - 1000 base pairs. Since the human genome was sequenced, >10 million SNPs had been identified by early 2005 (International HapMap Project, http://hapmap.ncbi.nlm.nih.gov, release #19). All SNPs have been deposited in a publicly accessible NCBI database (dbSNP, http://www.ncbi.nlm.nih.gov/projects/SNP/, build 123). Through genome-wide association studies, microarray expression studies and candidate gene studies, many SNPs have been associated with outcome in a variety of disease states [135-141] but few have been shown to be the causal or functional SNP. Church *et al.* (2009) estimated the functional proportion of protein coding sequences in the human genome to be 1.06% [142], whereas another group, using an evolutionary method and including constrained non-coding regions as well,

estimated the functional proportion of the human genome to be much higher at between 6.7% and 10.0% [143].

1.7 Identification of Functional Polymorphisms in Disease

Cis-acting gene regulatory regions may be situated up to 1Mb up- or down-stream of the gene they regulate [144] and may incorporate binding sites for enhancers, repressors or insulators [145, 146], see Figure 1.4. Moreover, these regulatory regions may be inside intronic regions of unrelated genes [146]. Although most regulatory regions are found in the proximal promoter region and in the first few introns [147], some have been discovered up to 150kb away from the gene being regulated [145].

Studies have shown that disruption of distal regulatory regions can lead to disease phenotypes [144-146, 148], therefore linkage disequilibrium (LD) between SNPs that are significantly associated with outcome or phenotype may be very important. Linkage disequilibrium is the frequency of occurrence of allele haplotypes more often than would be expected by chance, assuming random distribution [149].

In any region of the genome, LD reflects all past forces that have led to the frequency of each allele, such as natural selection, mutation and transpositions [149]. The effect of a SNP often varies between individuals and may be due to either environmental causes or genetic effects or both: one individual may carry more co-morbidities than another and/or SNPs in other genes may modulate the effect of the SNP of interest [150].

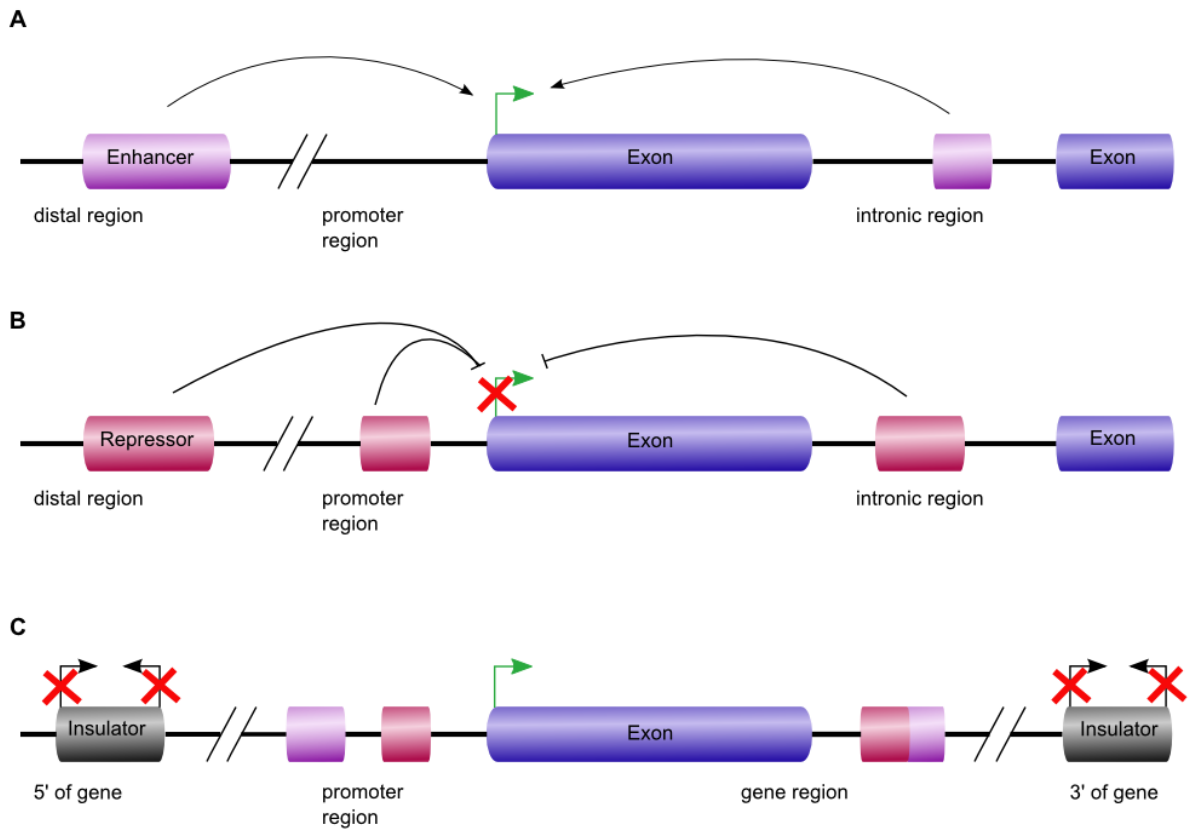

Figure 1.4 Regulation of transcription.

A. Enhancer elements promote transcription of genes from regions far from the gene, close to, or within the gene itself. **B.** Repressor elements decrease transcription of genes and are found in similar genomic regions as enhancers. **C.** Insulators at either end of a gene region prevent transcription from neighboring genes encroaching on the gene region, as well as preventing the gene's own transcription from beginning or continuing inappropriately. Interaction of all elements ensures transcription occurs correctly at the right time and only in the required tissues. *Figure created using Inkscape software version 0.48.4*

A 2006 study by Drake *et al.* show that SNPs in conserved non-coding regions of the genome are less densely distributed and more likely to be functional than SNPs in non-conserved regions, particularly if the SNP is common and intronic [151]. However, evidence

of conservation is not sufficient to identify functional SNPs – the evolutionary forces that selectively constrained the region may not be relevant to the human genome.

Several well studied SNPs have repeatedly been significantly associated with outcome or a phenotype such as increased/decreased plasma levels of a protein which correlates with outcome [137, 152-157] but to date the mechanisms whereby these SNPs exert their influences have remained elusive. Therefore functional studies of SNPs are necessary to determine whether they are indeed the functional SNPs or whether they are merely in LD with the causal SNP.

The least complicated SNP effects to interpret functionally are those that alter an amino acid in coding regions of a gene coding for a binary trait inherited in a Mendelian fashion, but most SNPs (~95%) [158] are in non-coding regions and effects of these SNPs are far more difficult to elucidate, particularly in genes that exert pleiotropic effects.

1.7.1 Coding SNPs

SNPs in coding regions may alter the amino acid (non-synonymous SNPs) or may code for an alternate codon of the same amino acid (synonymous SNPs) and any of these changes may alter the functionality of the protein [159]. Several research groups have long been trying to predict the effects of these amino acid changes using computational modeling techniques [160, 161]. For example, Xia *et al.* (2002) developed a model to predict the propensity of a particular amino acid change occurring due to the preference of the amino acid to be like its neighbors and forming part of a particular secondary structure such as α-helices or β-sheets [162], but ultimately, functional assays need to be performed to determine the validity of these predictions.

1.7.1.1 Non-synonymous amino acid changes

Non-synonymous amino acid changes are either missense or nonsense mutations occurring in coding regions of genes. Both are caused by point mutations that change the original codon to one that codes for a different amino acid. Nonsense mutations result from an amino acid change that forms an unexpected stop codon which usually results in a truncated protein. This truncated protein may not be functional at all, may have reduced function or may have a different function altogether [163]. Examples of diseases caused by prematurely shortened transcripts include β-thalassemia [164], Duchenne Muscular Dystrophy [165], Cystic Fibrosis [166] and Hurler Syndrome [167].

Although missense mutations also change the amino acid, the affects can range from neutral to severe depending where in the resulting protein the change occurs: an amino acid change in a region that does not affect protein secondary structure or function may pass unnoticed whereas an amino acid change in a protein's active site, DNA-binding site or subunit attachment domain could have dire consequences for the functionality of the protein [168]. Disruption of protein function may be caused by the new amino acid having a different charge, a different shape or different biochemical properties. For example, if a hydrophobic amino acid forming part of the transmembrane portion of a receptor protein changes to a hydrophilic amino acid, the protein may not get incorporated into the membrane or may compromise the integrity of the membrane [163]. Correct folding of a protein or proper interaction with binding partners or chaperones may not occur if the new amino acid is a different shape, carries a different charge, has disrupted post-secondary modification sites or causes aggregation of proteins [168-171]. Alterations in amino acids forming part of signal peptides may cause aberrant protein localization leading to proteins not being secreted,

proteins not inserted into membranes or proteins that get "stuck" in the endoplasmic reticulum or Golgi apparatus. All these will have an effect on cell homeostasis and some effects may be deleterious [168].

1.7.1.2 Synonymous amino acid changes

When a mutation in a codon does not result in a change in translation it is called a synonymous mutation and is a result of the degenerate coding of some amino acids which have several different codon options for the same amino acid. For example Leucine (Leu) has six possible codons, namely TTA, TTG, CTT, CTC, CTA or CTG. Synonymous amino acid changes are not always neutral and can affect the function of a protein. All organisms, from bacteria to vertebrates, display codon bias whereby some codons are translated less efficiently than others resulting in reduced protein production or reduced function [172]. In addition, synonymous mutations near exon/intron boundaries can disrupt splicing signals resulting in exon skipping. For example, in the cystic fibrosis transmembrane conductance regulator (*CFTR*) gene 25% of synonymous mutations in exon 12 cause that exon to be skipped, resulting in an inactive protein [173].

Although the 5' and 3' untranslated regions (UTRs) are not translated, they are transcribed, and variations in these regions can be as destructive as those in exons. Sequences in the 5'UTR region have been shown to regulate gene expression and export of mRNA, promote or inhibit the initiation of translation, contain riboswitches [174] or sequences such as iron-response elements (IREs) that regulate expression [175]. The 3'UTR contains regulatory sequences such as the poly-A tail [176] and AU-rich elements (AREs) which stabilize or destabilize the transcript when bound by particular proteins [177] as well as microRNA (miRNA) binding sites [178, 179].

1.7.2 Non-coding SNPs

Approximately 95% of SNPs in the human genome are non-coding SNPs [158] and although many will have no apparent influence on phenotype, many will have significant effects. Non-coding SNPs are those that lie outside the coding regions, which includes the 5' and 3' UTRs, hence those in the promoter region and introns, but also includes intergenic regions and regions far from the gene being regulated [158].

Functional effects of SNPs in non-coding regions are more difficult to determine and present their own set of unique challenges, not least of which is the genomic distance which is often involved. Many genes have extremely long introns or the SNP of interest is far from the gene it potentially regulates [180, 181], both features which present huge challenges for functional assays such as cloning-based assays.

A non-coding SNP can have one of many functions: it can modulate expression by altering binding of enhancer or suppression transcription factors [181], by modifying effects of insulator regions or by altering methylation sites. In addition, a SNP can generate alternate transcripts by affecting nucleotides at splicing sites [182]. These alternate transcripts may or may not code for functional proteins, moreover these alternate transcripts may themselves be regulators of genes or mRNA transcripts. In addition, non-coding SNPs may alter the binding of structural proteins, such as histones or histone-associated proteins, affecting chromatin remodeling which may lead to a change in open or closed DNA conformation with a concomitant alteration of transcription efficiency [181]. Alteration of binding sites for proteins such as chaperones may contribute to protein mis-folding and such proteins may get degraded quickly or form inactive aggregates [168], may be unable to leave the endoplasmic reticulum or Golgi apparatus [168] or may be unable to accept post-

translational modifications such as glycosylation which may be important for correct localization or function of the protein [168].

Non-coding SNPs that lead to an increase or decrease in mRNA decay may disrupt cellular homeostasis as delayed mRNA decay allows more protein to be translated [182], this may increase protein activity or cause it to reach a "critical threshold" which overwhelms the cell or over-activates other pathways, whereas an increase in mRNA decay would have the opposite effect. By introducing novel polyadenylation sites, non-coding SNPs may generate novel protein isoforms which may or may not be active [183].

In some instances, non-coding SNPs may not interfere with the normal transcription of a gene but may affect the stability of the pre-mRNA transcript by altering miRNA binding sites [184]. MicroRNAs have been implicated in a range of diseases from deafness, cardiac disease and diabetes to various types of cancer [185]. Disrupting miRNA target binding sites or creating novel miRNA binding sites also increases the risk of developing a broad range of diseases [178].

Methylation of DNA is another method of regulation of gene expression (for review, see Law 2010 [186]) and is essential for normal processes such as X-chromosome inactivation, genomic imprinting and suppressing repetitive elements and has also been implicated in cancer. In mammals most CpGs are methylated [187]. Methylation in promoter regions results in suppression of transcription. Erroneous methylation or disruption of methylated CpGs caused by SNPs leads to inappropriate suppression or activation of gene transcription with a concomitant increase in disease risk [188].

1.8 Candidate Gene Selection

The 'common disease – common variant' hypothesis suggests that there are a limited number of common variants in the human genome [189] and these can be tested for association with phenotypes of common disease states, eventually leading to a catalogue of all gene variants that influence outcome of complex, polygenic diseases. Several examples have already been reported: alleles of the APOE*E4 gene have been associated with Alzheimer's disease [190] and the Factor V Leiden mutation was found to be a risk for deep-vein thrombosis [191].

For this study, in order to elucidate functional genetic factors that may alter the outcome of patients with severe sepsis or septic shock, a candidate gene approach was employed. Initially, the *PROC* gene was selected as plasma levels of this protein and of aPC, the activated form of protein C, is well known to modulate outcome in patients with sepsis, severe sepsis and septic shock [14, 96, 192, 193]. In addition, at the time this study began, recombinant human activated protein C (rhAPC) was the only FDA-approved drug for treatment of severe sepsis and septic shock in the ICU.

Next, as both statin drugs and HDL have shown some efficacy in modulating outcome in sepsis, and there is a known connection between lipids and inflammation [33, 37, 42], we selected *PCSK9*, a known lipid modulator, as a second candidate gene.

1.8.1 Protein C (*PROC*)

Protein C was discovered twice: first in 1960 by Mammen EF *et al.* [194] and then again by Stenflo in 1976 [195], in both cases discovery was pertinent to the coagulation cascade. Today protein C has been well studied and has been shown to function not only in

the coagulation cascade but also as an anti-inflammatory, anti-apoptotic, pro-fibrinolytic molecule and has an innate immune function [96].

Human protein C is a proenzyme of a serine protease that is vitamin K-dependent [196]. In humans, protein C is synthesized, primarily in the liver, as an inactive zymogen in a single chain [197] containing 461 amino acids [198], see Figure 1.5.

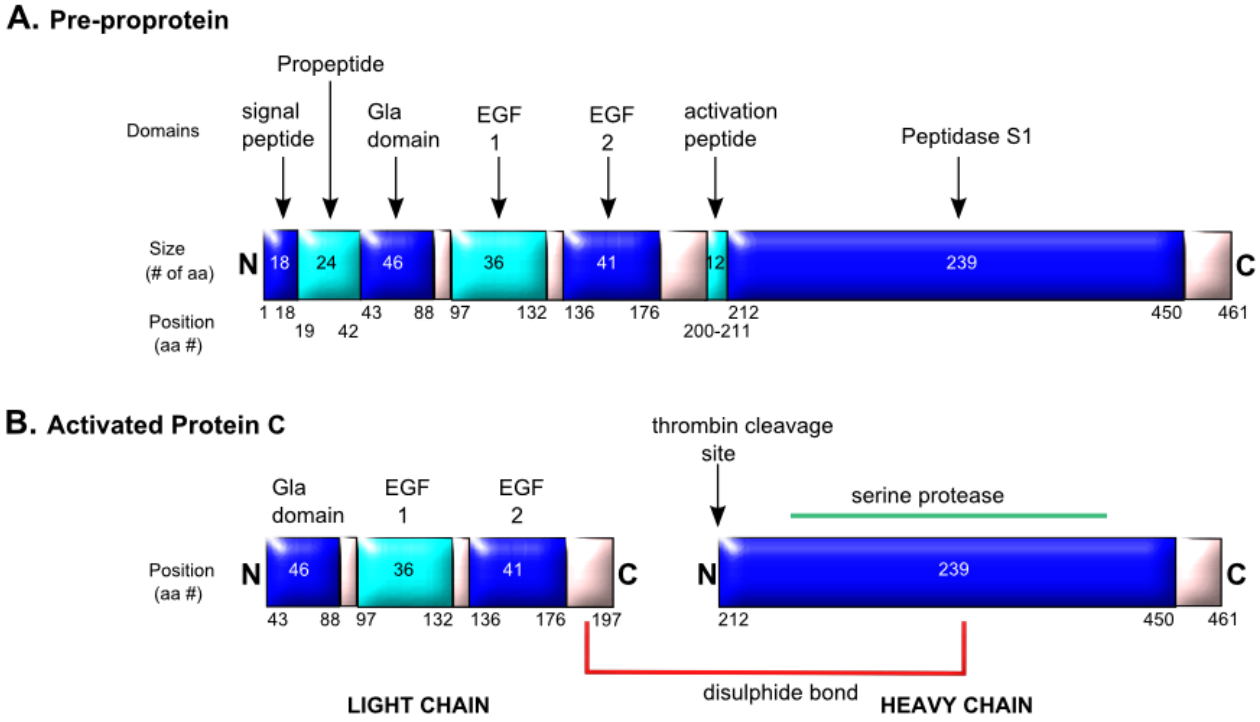

Figure 1.5 Domains in the *PROC* gene.

A. The signal sequence of the single-chain pre-proprotein is cleaved off to allow secretion of the protein out of the cell and into the plasma. The propeptide sequence, required for γ-carboxylation of nine particular glutamic residues in the Gla-domain, which is necessary for biologic activity, is also cleaved off in the mature protein. Residues 199 and 198 (Lys-Arg) are cleaved to allow generation of the light and heavy chains (21kDa and 41kDa, respectively). **B.** The 12 amino acids of the activation peptide are cleaved off the N-terminal of the heavy chain by thrombin to effect activation of the mature protein. *Figure created using Inkscape software version 0.48.4*

Cleavage of the signal peptide is required for transport of the proprotein out of the cell into plasma [199], and, required for anti-coagulant function, the proprotein undergoes co- and post-translational modifications that includes cleavage of the 24 amino acid propeptide, γ-carboxylation and glycosylation [198]. Unlike other human vitamin K-dependent proteases, autoproteolytic removal of two amino acids results in a light chain (21kDa) and a heavy chain (41kDa) linked by disulphide bonds [196, 200, 201]. The N-terminal has a region containing nine γ-carboxyglutamic acids (Gla domain) that interacts with negatively charged phospholipids on cell surfaces as well as the EPCR [200, 202, 203]. Limited proteolysis by thrombin of 12 amino acids (activation peptide) on the N-terminal of the heavy chain converts the zymogen protein C into activated protein C [200]. The rate of protein C activation is increased if protein C and thrombin are bound to their respective transmembrane receptors, EPCR and thrombomodulin, on the surface of endothelial cells [204]. In fact, when protein C is bound to EPCR, conversion to aPC occurs 20 times faster [204], and 1000 times faster when thrombin is bound to thrombomodulin [205]. Following the Gla domain are two epidermal growth factor-like domains (EGF domains) and a serine protease domain [203] (Figure 1.5).

Activated protein C, in the presence of co-factors protein S, calcium and phospholipids, plays an important role in the anticoagulation pathway by inhibiting blood clotting through degradation of factors Va and VIIIa [205], see Figure 1.3. The significance of this anticoagulation activity is seen in individuals who are homozygous for an abnormal protein C gene that results in low levels of aPC. These individuals usually have a life-threatening form of thrombosis called purpura fulminans, which causes extensive blood

clotting throughout the body [206], while heterozygotes are predisposed to venous or pulmonary thrombosis [152, 207].

In healthy individuals, the circulating levels of protein C (2800 - 5600ng/mL) are normally about 2000 times that of aPC (1-3ng/mL), while in >80% of patients with an excessive inflammatory response due to infection, as is found in severe sepsis or septic shock, the circulating level of protein C is below the lower limit of normal [193]. Previously, another group had described similar plasma concentrations of protein C as normal (mean 4000ng/mL in 699 healthy adults), and had described heterozygous protein C deficiency (or the lower end of normal) as 55-65% of normal [208].

A small increase in aPC (<20ng/mL) is seen in fewer than 20% of patients with sepsis [209] and protein C levels that remain low are correlated to a poor outcome [193]. The half-life of protein C is about 10 hours, while the half-life of circulating aPC is only about 20 minutes but despite this difference, it has been suggested that it is not only the conversion of protein C to aPC that causes the protein C levels to remain low in patients with sepsis [193]. One study in which exogenous protein C was given to children with severe meningococcal sepsis showed a dose-dependent increase in the amount of circulating aPC and a reduction in mortality, however the study was small with ≤10 patients in each group [210]. Another clinical study showed a 40% reduction in endogenous protein C levels in neutropenic patients who developed severe sepsis or septic shock while their aPC levels showed a small transient, statistically insignificant increase [209].

1.8.1.1 Protein C deficiency

Congenital protein C deficiency was first described in 1981 [211] and occurs in about 0.2% of the general population. It is inherited as an autosomal dominant condition with

variable penetrance [207, 211, 212]. There are two types of congenital protein C deficiency: Type I describes protein C that functions normally but is synthesized in insufficient quantities to control the coagulation cascade [213]. In Type II deficiency, the protein is produced in normal quantities but is defective in structure and is unable to interact with other proteins in the coagulation cascade [214]. Individuals who are heterozygous for defective *PROC* are at risk of developing pulmonary embolisms or deep vein thrombosis [215], while homozygotes or compound heterozygotes are at risk of early development of purpura fulminans, a systemic coagulopathy, resulting in death unless treated [216, 217]. The latter is a recessive form of *PROC* deficiency [206].

Protein C deficiency can also be acquired. Purported mechanisms for acquired protein C deficiency in sepsis may be the increased consumption of protein C as it is converted to aPC [209] and the increased expression of protein C inhibitors in sepsis [218]. In addition, the increased sepsis-induced expression of soluble EPCR [219] may lead to increased sequestration of protein C in the plasma and, in conjunction with the failure of the endothelial surface to support the necessary receptors (thrombomodulin and EPCR) for conversion of protein C to aPC, could contribute to the persistently low protein C levels seen in sepsis patients [209].

1.8.1.2 Mechanisms of protein C in sepsis

In sepsis, an exuberant host response to invading pathogens results in excess inflammation, apoptosis and coagulation leading to vascular injury, organ dysfunction and often death [96]. Protein C and/or aPC have now been shown to positively affect all these pathways:

1.8.1.2.1 Coagulation and fibrinolysis

Under normal physiologic conditions the balance between coagulation and fibrinolysis is tightly regulated [220] (Figure 1.3). In patients with severe sepsis this hemostasis is often dysregulated and is associated with increased mortality [87]. Disseminated intravascular coagulation is the result of constant, systemic stimulation of the coagulation cascade and down regulation of the fibrinolytic and anti-coagulant pathways by invading pathogens [87]. It is characterized by excess fibrin deposition in the microvasculature leading to proliferation of microthrombi in small blood vessels and increasing organ dysfunction [87, 221]. Over time, the pro-coagulant molecules are consumed and cannot be replaced quickly enough which may lead to the concomitant uncontrolled hemorrhage complication frequently observed in critically ill patients [220].

The initial host response to infection is a rapid release of pro-inflammatory cytokines such as TNF-alpha, IL1-beta and IL6 which are able to induce coagulation and inhibit fibrinolysis [222-224]. The major pro-coagulant molecule, thrombin, adds to the inflammatory response by inducing activation of several pro-inflammatory pathways [225]. Activated protein C has been shown to inhibit release of these cytokines [226-228] as well as indirectly inhibiting thrombin [204]. Effects of aPC on these pathways can be seen in mice with heterozygous *Proc* deficiency that evinced more DIC, a greater pro-inflammatory response and increased mortality compared to wild-type mice [224].

The formation of fibrin clots is an important first host defense against infection [229] as the clots are able to trap certain bacterial pathogens. Mutations resulting in impairment of fibrin clot formation leads to increased host susceptibility to some bacterial infections such as Group A streptococci [230, 231]. Conversely, trapping of *Staphylococcus aureus* in fibrin

clots leads to increased host susceptibility to infection, so clearly the benefits of increased coagulation after pathogen attack are pathogen dependent [232].

Bacterial endotoxins are able to initiate the pro-inflammatory and intrinsic coagulation cascades by activating endothelial cells [233, 234]. Activated factor XII (FXIIa) on activated endothelial cells triggers the contact-phase system [235], which results in the release of the nine amino acid peptide, bradykinin [236], leading to pain, vasodilation and increased vascular permeability [237]. A study by Herwald *et al.* (1998) showed that interaction of surface proteins on Gram-negative bacteria such as *Salmonella typhimurium* and *Escherichia coli* with the host contact-phase factors resulted in increased vascular permeability and pathogen penetration into the surrounding tissue [233]. This vascular permeability also allows plasma to leak out which contributes not only to the hypovolemic hypotension and shock seen in severe sepsis and septic shock, but possibly also serves as a rich source of nutrients for the invading pathogens [233].

The two receptors, low density lipoprotein receptor-related protein 8 (LRP8, commonly known as APOER2) and glycoprotein 1b alpha polypeptide (GP1BA), on platelets, monocytes and endothelial cells are known to mediate intracellular signaling leading to adverse outcomes in thrombotic disease, such as antiphospholipid syndrome [238, 239]. Both protein C and aPC have been shown to bind to the LDLR-family receptor, APOER2, and GP1BA on platelets, resulting in an intracellular calcium flux and platelet spreading, necessary for plug formation [240]. Conversely, aPC plays a role in the stimulation of fibrinolysis, resulting in the removal of small blood clots by breaking down the fibrin in the clots [192], while SERPINE1 (previously known as PAI-1), sharply induced by the introduction of endotoxin, has the opposite effect [83]. Clearly, dysregulation of the

coagulation system is important in the clinical progression of sepsis, severe sepsis and septic shock, and switching between pro and anticoagulant states provides costs and benefits for both host and pathogen.

1.8.1.2.2 Inflammation

Monocytes are another key player in the host immune response, secreting pro-inflammatory cytokines and ingesting pathogens [241]. Treatment with aPC reduced secretion of pro-inflammatory mediators from monocytes (Figure 1.6) but did not affect phagocytosis of pathogens in either primary blood monocytes or THP1 cells, a cultured human monocyte cell line [226, 241].

Similar results were obtained in human neutrophils, where aPC abolished neutrophil chemotaxis towards interleukin 8 (IL8) but did not affect phagocytic behavior [242]. Activated protein C also downregulates expression of adhesion molecules and NFKB subunits in activated endothelial cells and monocytes [243, 244] as well as inhibiting nuclear translocation of NFKB in monocytes [245].

Downregulation of pro-inflammatory cytokines in monocytes by aPC possibly occurs by interfering with Wnt signaling (Pereira, 2008). Activated protein C is also purported to upregulate anti-inflammatory cytokine IL10 while downregulating pro-thrombotic tissue factor in an LPS model of sepsis in monocytes, and in patients with severe sepsis [246].

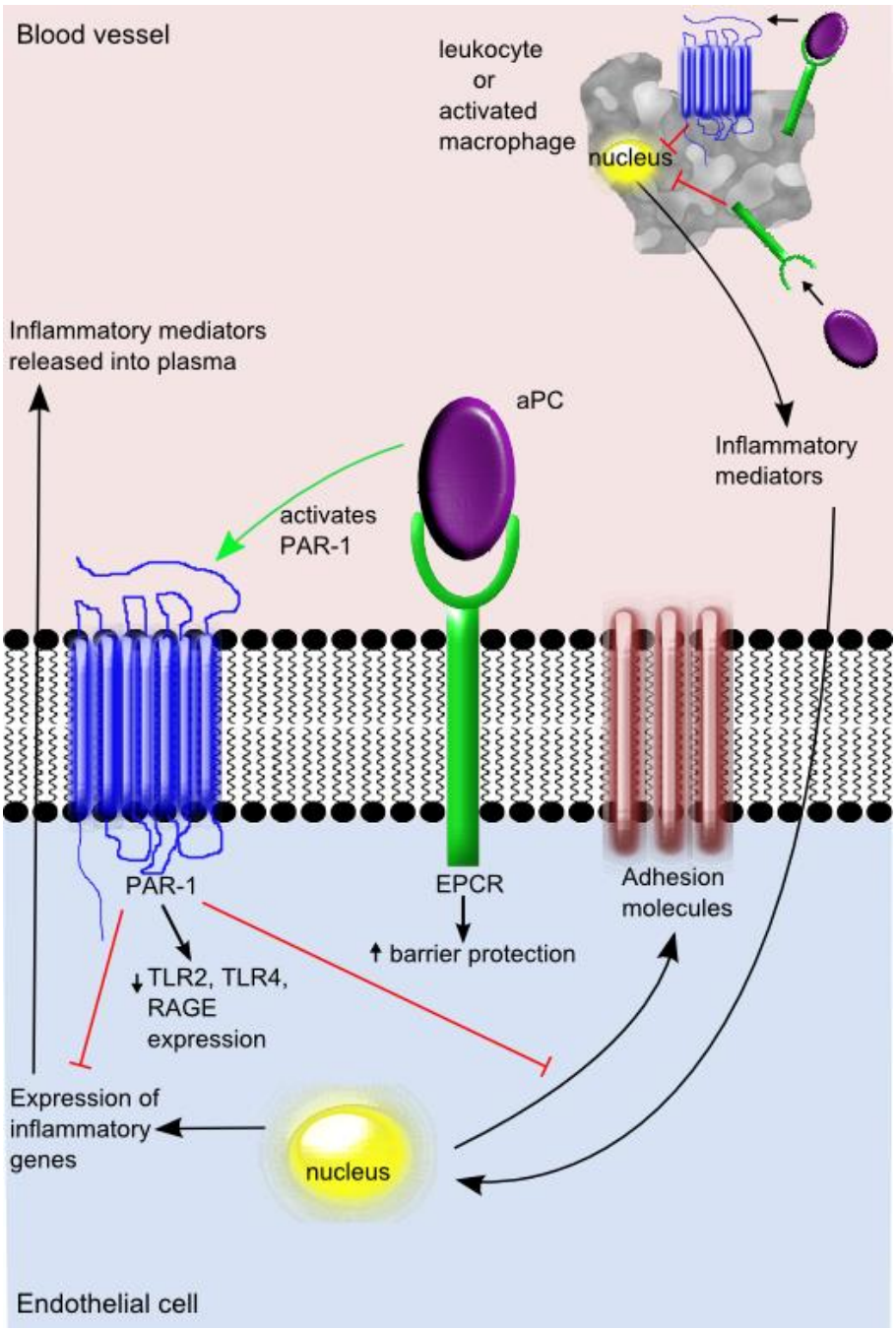

Figure 1.6 Activated protein C and inflammation

Activated protein C bound to EPCR on endothelial cells signals directly to increase expression of genes involved in maintaining barrier integrity and via PAR-1 to decrease expression of innate receptors, adhesion molecules and pro-inflammatory genes. In addition, on activated macrophages or leukocytes, aPC signals in an EPCR-independent and EPCR/PAR-1 dependent manner to reduce expression of pro-inflammatory mediators.

Figure created using Inkscape software version 0.48.4

Acute lung injury is a common complication of severe infection and results in a large number of neutrophils accumulating in the lungs, as well as increased levels of pro-inflammatory cytokines and chemokines [69], contributing to severe organ dysfunction and mortality [227, 247]. Recombinant human activated protein C has been shown to decrease the accumulation of leukocytes such as neutrophils in air spaces in the lungs, which may improve survival in patients with sepsis [247].

As part of host defense strategies against invading organisms, platelets express toll-like receptors and secrete pro-inflammatory mediators such as IL1-beta and high mobility group box 1 (HMGB1) to activate endothelial cells and various leukocytes [229, 248]. Platelet TLR4 activation leads to the release of neutrophil extracellular traps (NETS) which function to trap and kill microbial particles but, unfortunately, also increases coagulation and suppresses protein C activation [249]. The free histones derived from degraded NETS are cytotoxic and contribute to late mortality in sepsis [250]. Activated protein C protects cells against histone cytotoxicity by proteolytic cleavage of histones, independent of any EPCR and PAR-1 interaction [250].

The HMGB1 protein is a late mediator of mortality in sepsis [251], binding to several innate immunity receptors (TLR2, TLR4 and RAGE) on endothelial cells and leading to the release of pro-inflammatory cytokines and adhesion molecules, resulting in increased leukocyte adherence, coagulation and vascular permeability [252, 253]. Recently it has shown by Bae *et al*. (2011), that in an EPCR/PAR-1 dependent manner (Figure 1.6), aPC down-regulates expression of TLR2, TLR4 and RAGE receptors on endothelial cells, resulting in reduced pro-inflammatory signaling by HMGB1 [254].

Increased apoptosis has been shown to increase multiple organ dysfunction in patients with severe sepsis [243, 255], and aPC bound to EPCR is able to signal via PAR-1 to reduce apoptosis [241].

During inflammation the normal permeability barrier function of the endothelium is breached which results in edema, hypotension and the promotion of inflammation. These symptoms are an integral part of severe sepsis, acute lung injury and organ failure [256]. Activated protein C protects barrier function in an EPCR/PAR-1/S1P manner [257, 258].

1.8.1.3 The PROC gene

Protein C is coded for by the gene *PROC* (accession number NM_ 000312.3), which is located on human chromosome 2 (2q14.3). The gene is 10 827bp (base pairs) in size, spans a range from 128 175 996 – 128 186 822 (UCSC, Feb 2009 build) on the forward (+) strand and contains nine exons in adults. The coding region contains eight exons and covers 1389bp. The primary site of *PROC* synthesis is in the liver from where it is secreted into the plasma in its inactive form. Secondary sites of *PROC* expression include the kidney, testis, brain, lung, and some epithelial cells [259].

1.8.1.4 Genetic variants in the PROC gene

UniProt Knowledgebase (http://www.uniprot.org/uniprot/P04070) describes more than 70 natural variants in coding regions of *PROC* that result in protein C deficiency and thrombosis, however, the majority of these mutations are extremely rare (minor allele frequency (MAF) <1%) and have not been shown to affect mortality in sepsis and septic shock. In contrast, the Ensemble database (http://uswest.ensembl.org) lists >230 coding SNPs and almost 200 intronic SNPs with a further >150 situated 5' and 3' of the gene for a total of 719 SNPs affecting the *PROC* gene, again, the majority of these SNPs are rare.

Several groups have found rare disease-associated SNPs in non-coding regions of the *PROC* gene, including the promoter region [213, 260-264]. Two well-studied SNPs in the promoter region, commonly referred to as -1654 and -1641 (rs1799808[C/T] and rs1799809[A/G], respectively) have been associated with outcome in deep vein thrombosis, pulmonary embolism, and severe sepsis [260, 265, 266] and are also well represented in the general population with a MAF of more than 10%. These two SNPs are only 13bp apart therefore are usually studied as a haplotype and, most commonly, the C-G and C-A haplotypes are correlated with the lowest levels of protein C [265]. The T-G haplotype is rarely seen in most populations. Conversely, by studying the SNPs independently, Walley *et al*. (2007) found a greater association with mortality and more organ dysfunction in severe sepsis patients homozygous for the -1641 A-allele [137]. In addition, carriers of the -1641 AA genotype mounted a more robust IL6 response after cardiopulmonary surgery than patients without this genotype. Moreover, the SNP -1654 was not implicated in outcome in either of the two cohorts studied [137].

1.8.2 Proprotein convertase subtilisin/kexin type 9 (PCSK9)

Proprotein convertase subtilisin/kexin type 9 (PCSK9) was discovered in 2003 when it was initially known as neural apoptosis-regulated convertase-1 (NARC-1) [267], however it is now officially known as PCSK9.

Initially, PCSK9 was thought to play a role in the differentiation of cortical neurons [267], more recently it is acknowledged as a mediator of cholesterol homeostasis, which affects outcome in diseases such as cardiovascular disease, familial hypercholesterolemia and atherosclerosis [268-270].

1.8.2.1 Mechanisms of PCSK9 in sepsis

To date, very little is known about the function of PCSK9 in patients with sepsis. A search of Google, Pubmed and Medline (search terms: PCSK9 AND sepsis) uncovered no studies relating to the role of PCSK9 in human patients with sepsis.

1.8.2.1.1 PCSK9 in inflammation

However, PCSK9 is known to interact with the inflammatory response: PCSK9 results in up-regulation of genes involved in sterol biosynthesis and down-regulation of stress-response genes and specific inflammatory pathways [271]. In addition, PCSK9 has pro-apoptotic effects [272]. Labonte and colleagues (2009) found an antiviral effect of circulating liver-derived PCSK9 on Hepatitis C virus (HCV) in cells and showed that PCSK9 down-regulates the level of mouse liver CD81 expression *in vivo* [273]. Cells expressing PCSK9 are resistant to HCV infection [273]. The addition of purified soluble PCSK9 to cell culture supernatant impeded HCV infection in a dose-dependent manner [273]. It has been shown that infection and inflammation upregulates PCSK9 itself [274] and, for example, PCSK9 concentrations are increased in patients who have periodontal infections [275].

1.8.2.2 The PCSK9 protein

In mammals, PCSK9 is a member of the serine proprotein convertase family [276] and is related to proteinase K [277]. The PCSK9 protein is synthesized as a soluble zymogen which contains an N-terminal signal peptide that is followed in turn by a pro-domain, a subtilisin-like catalytic domain and a C-terminal domain [278] (Figure 1.7). The zymogen undergoes autocatalytic cleavage of the pro-domain to allow secretion from the endoplasmic reticulum, however the pro-domain remains attached, serving as a chaperone to mediate correct folding and as an inhibitor of the catalytic site [268, 278].

The inactive 74kDa pre-pro-protein undergoes autocatalytic cleavage in the endoplasmic reticulum resulting in secretion of a ~14kDa fragment and a ~60kDa fragment held together by non-covalent bonds [279, 280], see Figure 1.7.

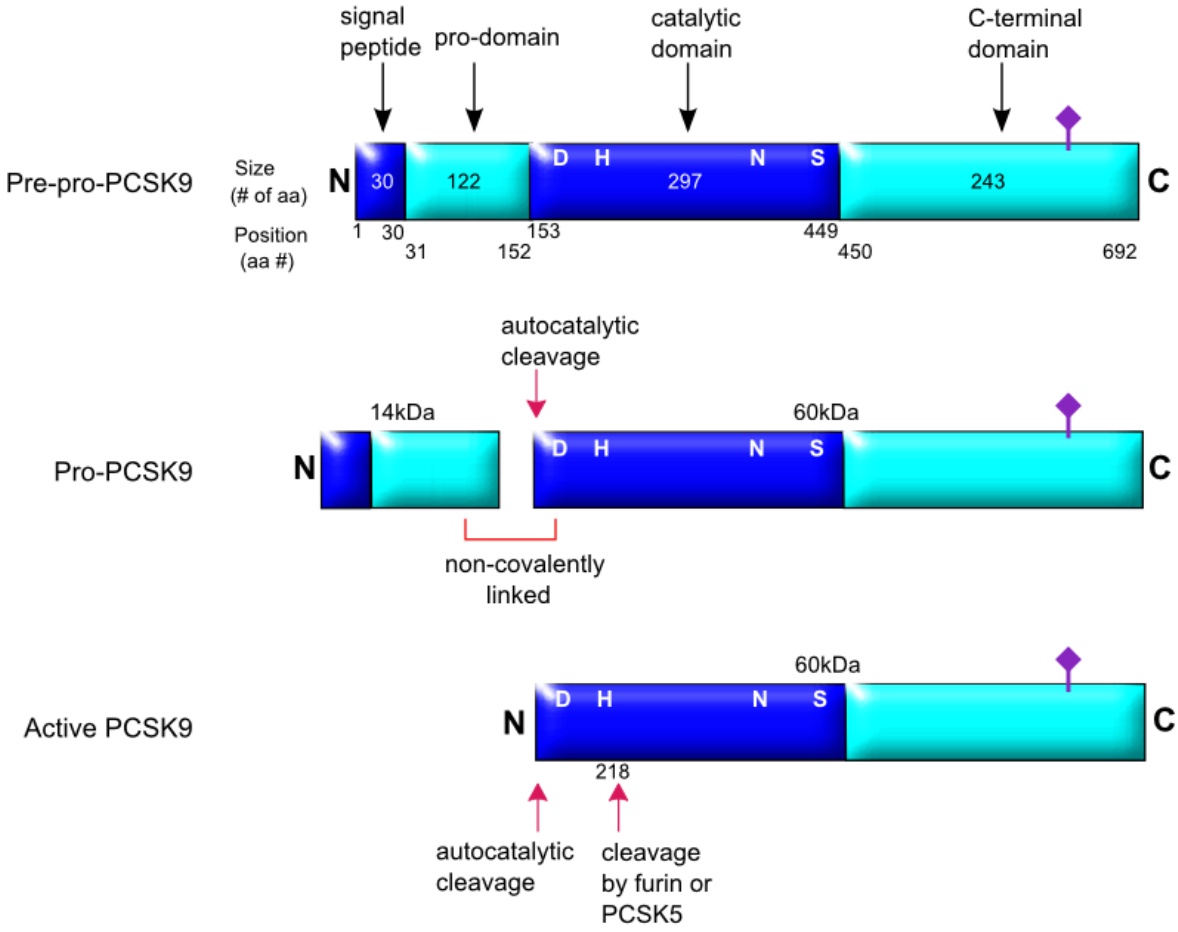

Figure 1.7 Domains of *PCSK9* protein before and after activation

Although usually found as a monomer, the catalytic domain may mediate self-association of the pre-pro-protein. Cleavage of the 74kDa pre-pro-protein is required for transport out of the endoplasmic reticulum, through the Golgi apparatus and out of the cell. The resulting 14kDa and 60kDa fragments of the pro-protein are held together by non-covalent bonds – the 14kDa fragment blocks the active sites, rendering the protein enzymatically inactive. Via the C-terminus, the secreted pro-protein is able to interact with the LDL receptor and mediate its degradation. Further autocatalytic cleavage of the 14kDa fragment renders PCSK9

enzymatically active. Cleavage at residue 218 by either furin or PCSK5 results in an inactive, truncated protein. The catalytic triad is shown as D (Asp), H (His), S (Ser) and the oxyanion hole as N (Asn). The purple diamond indicates the sole site of N-linked glycosylation, a post translational modification.

Figure created using Inkscape software version 0.48.4

This cleavage is necessary to allow transport out of the endoplasmic reticulum as well as for secretion, correct folding and regulation of catalytic activity [279, 281].

Unlike all other proprotein convertases, catalytic cleavage of PCSK9 does not require calcium [279]. Also unlike most other proprotein convertases, PCSK9 lacks a P-domain, required for correct folding and regulation of protease activity, rather, these functions are mediated via the cysteine- and histidine-rich C-terminal region [282]. Moreover, intramolecular cleavage does not occur after a basic residue [283] but rather after the sequence LVFAQ↓ [277]. Further autocatalytic cleavage of the ~14kDa fragment renders the pro-protein enzymatically active. The PCSK9 proprotein is phosphorylated at Ser47 and Ser688 which may protect it from proteolysis [284].

Two residues in the catalytic site of PSCK9 are required for binding, in a calcium dependent manner, to EGF regions on the LDLR, and mutations in either residue lead to a more than 90% decrease in binding [278]. Membrane-bound furin or soluble PCSK5 are able to cleave off the pro-domain, resulting in a 53kDa PCSK9 protein [285] with a more than 7-fold greater affinity for LDLR EGF regions [278]. This affinity is increased a further 3-fold when pH drops to 6.0, such as is found in lysosomal compartments [278]. Both the ~60kDa and ~53kDa forms are present in the circulation [285, 286] in concentrations of

around 11 – 600ng/mL [286, 287]. Protein-protein interactions are thought to be mediated by the C-terminal domain [268, 278].

It is known that PCSK9 plasma concentrations fluctuate in a diurnal rhythm similar to that of cholesterol synthesis, peaking at 4:30am and dropping to the lowest levels between 3pm and 9pm [288]. The half-life of PCSK9 protein in plasma is 5 minutes, and it is cleared mainly through LDLRs on the surface of liver cells [289]. A recent study has shown a possible alternative route, which may clear PCSK9 via LDLR-related protein 1 (LRP1), another receptor on liver cells [290]. This receptor appears to bind PCSK9 with lower affinity than the LDLR and increases the half-life of plasma PCSK9 to approximately 15 minutes [289, 291]. The LRP1 receptors bind over 40 different ligands, including triglyceride-rich chylomicrons [291], and competition with PCSK9 for binding to this receptor leads to increased triglyceride levels in plasma [290], which may suggest an explanation for the higher triglyceride levels seen in the plasma of patients with sepsis. Starvation and treatment with growth hormone reduces PCSK9 plasma concentration (80% and 17% respectively), while statin therapy and hepatic cholesterol inhibition increases PCSK9 levels [288].

The active PCSK9 protein circulating in the plasma binds the LDLR and, after internalization, prevents recycling of the receptor back to the cell surface and promotes degradation of the receptor in the lysosome [292], see Figure 1.8. Therefore, in humans, inhibition of PCSK9 results in increased cell surface expression of LDLRs and, consequently, decreased LDL cholesterol levels [293].

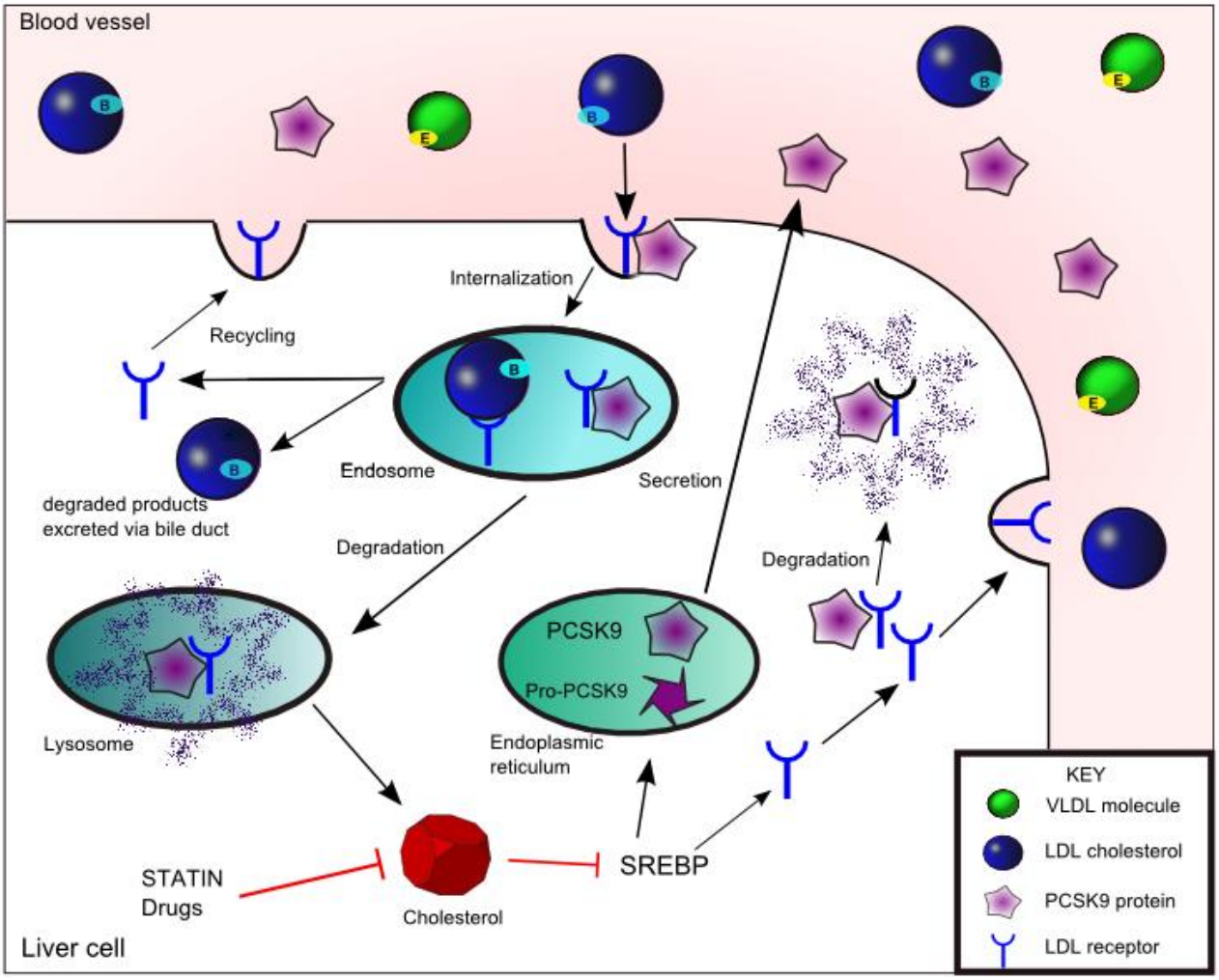

Figure 1.8 Inhibition of LDLR cycling by PCSK9

Association of secreted PCSK9 with the LDL receptor in clathrin-coated pits on the cell surface promotes degradation of the receptor after internalization. The lower pH of the endosomal environment causes increased affinity of PCSK9 for the receptor, promoting trafficking to the lysosome, followed by degradation, thus preventing LDL receptor recycling back to the cell surface. In addition, while trafficking to the cell surface after synthesis, PCSK9 either associates with and directs the LDL receptor to the lysosome, or induces ubiquination of the LDL receptor which also leads to its degradation. Although secreted PCSK9 is known to bind to VLDL receptors, it is not known if PCSK9 is able to modulate VLDL concentrations in a similar manner. LDL cholesterol molecules are associated with apolipoprotein B molecules while VLDL molecules are associated with apolipoprotein E molecules. *Figure created using Inkscape software version 0.48.4*

1.8.2.3 The PCSK9 gene

The *PCSK9* gene localizes to chromosome 1p33-p34.3 (accession number NM_174936.3) and the unprocessed gene contains twelve exons spanning 3617bp, encoding a 692 amino acid protein [268]. The *PCSK9* gene is expressed most commonly in the liver, followed to a lesser extent by the testis and small intestine, with transient expression in the cerebellum and kidney epithelial cells [267].

Schmidt *et al.* (2008) demonstrated in mice that overexpression of *Pcsk9,* or administration of recombinant human PCSK9, reduced mouse LDLR levels in liver tissue to undetectable levels within 30 minutes, and to a lesser extent, in lung, adipose and kidney tissues [294].

1.8.2.4 Genetic variants in the PCSK9 gene

Many mutations in coding regions of the *PCSK9* gene have been well documented [295] and functional effects characterized [280]. Loss of Function (LOF) mutations result in reduced sequestration of the LDL receptor and, as a result, decreased plasma LDL cholesterol concentrations [296, 297]. Presumably LOF mutations would similarly impact other receptors regulated by PCSK9 including the very low-density lipoprotein receptor, APOER2 [298], and CD81 [273]. Three missense LOF variants have been found to be relatively common (MAF>0.5%). The missense variant rs11591147 results in an R46L substitution which is consistently associated with low LDL cholesterol levels and, hence, is a LOF variant [295, 296, 299] (Figure 1.9). This variant results in improved patient outcomes in atherosclerotic disease [300].

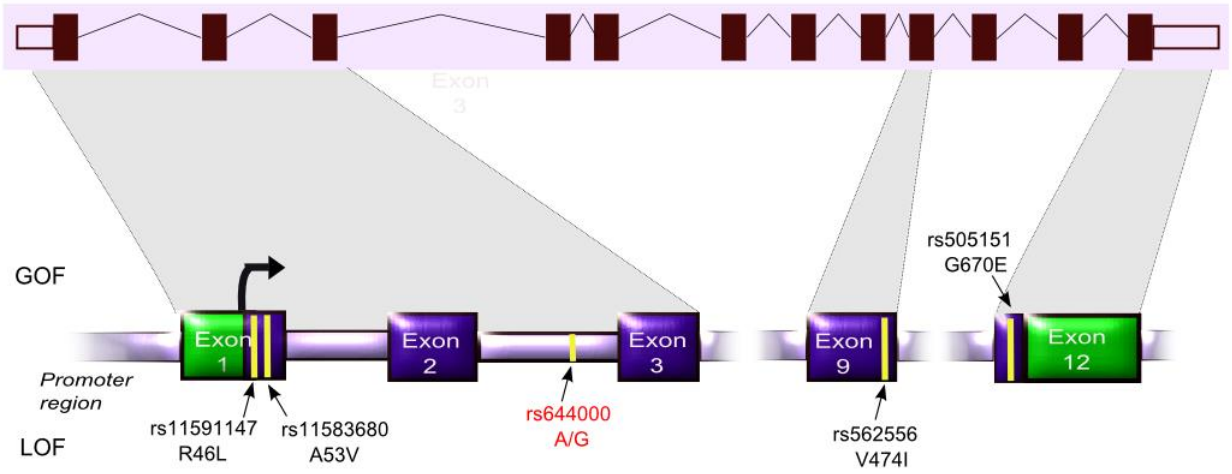

Figure 1.9 Gain-of-Function and Loss-of-Function SNPs in *PCSK9*

The top of the figure depicts the *PCSK9* gene with its 12 exons, also showing the partially untranslated exons 1 and 12. The lower portion of the diagram depicts the positions of the Gain-of-Function (GOF) and Loss-of-Function (LOF) SNPs that were studied in this work, and by other researchers, as well as the tag SNP rs644000 that marks the GOF and LOF SNPs. The shading depicts where the SNPs of interest lie along the gene. The bent arrow indicates the start of translation. *Figure created using Inkscape software version 0.48.4*

Similarly, rs11583680 A53V is common and reported to be a LOF variant [295] (Figure 1.9). The missense variant rs562556 results in a V474I substitution, which results in decreased total cholesterol and LDL cholesterol [301] (Figure 1.9). Conversely, Gain of Function (GOF) variants lead to decreased numbers of LDL receptors at the cell surface of hepatocytes and, as a result, increased plasma LDL cholesterol levels with a concomitant increase in atherosclerosis and cardiovascular disease [282]. Some genetic variants in *PCSK9* may result in LOF or GOF by affecting the affinity with which PCSK9 binds the

LDL receptor [280]. Other genetic variants may affect the degradation of PCSK9 protein, either increasing or decreasing the half-life of PCSK9 [285].

Many GOF mutations in *PCSK9* have been identified in individuals of European, African-American, East Asian, South Asian and Japanese descent [268, 295, 302-304] and have been found to correlate with increased LDL cholesterol and are a risk factor for cardiovascular disease [305], however, most are rare. By the same token, LOF mutations resulting in lower than normal LDL cholesterol levels are common in all populations and are correlated with a lower incidence of cardiovascular disease but again, most are rare [295, 296, 301, 304, 306, 307]. Complete abrogation of *PCSK9* does not appear to be harmful, as evidenced by a healthy graduate carrying *PCSK9* mutations resulting in undetectable PCSK9 levels and extremely low LDL cholesterol levels (14mg/dL) [307]. This woman was heterozygous for two inactivating mutations, one of which she inherited from each of her parents [307]. It has been suggested that there are gender differences in PCSK9 function and regulation, with PCSK9 levels in men, but not women, correlating with LDL cholesterol levels [308]. However, the authors admit the data may be skewed by unknown oral contraceptive use or hormone replacement therapy by the women, as hormones are known to affect LDLR levels [309, 310].

Few studies have looked at non-coding polymorphisms in and around the *PCSK9* gene, however in a recent study Cameron *et al.* (2012) found no effect of four SNPs or three known regulatory elements in the promoter region, on increased or decreased levels of *PCSK9* [290].

1.9 Hypothesis and Aims

The preceding information describes the established role of SNPs in the progression or outcome of disease, including sepsis, however, much remains to be discovered. Specifically, although SNPs in the *PROC* gene have been associated with outcome in sepsis, the causal SNP has not yet been found, and conversely, although many causal SNPs have been identified in the *PCSK9* gene, it is not known whether they have any effect on outcome from sepsis.

This study, therefore, has the following hypothesis: SNPs in the *PROC* and *PCSK9* genes are functional and affect outcome in sepsis.

1.9.1 Specific aims

In order to investigate this hypothesis, the following aims were established:

1. To determine whether inflammatory or coagulation mediators decrease the expression of *PROC*
2. To determine whether any common SNPs in the 5' region of *PROC* bind transcription factors differentially by allele
3. To identify any differentially bound transcription factors and test for functional effects such as decreased protein C concentration
4. To ascertain whether PCSK9 contributes to increased morbidity or mortality from systemic infection and sepsis
5. To determine whether previously identified Loss-of-Function coding SNPs, or others, in the *PCSK9* gene increase survival in patients with sepsis

Chapter 2: Materials and Methods

2.1 Protein C Experiments

2.1.1 Real time-quantitative PCR assays

A series of real time-quantitative PCR (RT-qPCR) assays were performed *in vitro* in Hep-G2 human liver hepatoma cells (American Type Culture Collection (ATCC), Manassas, VA) to determine whether treatment of cells with inflammatory or coagulatory mediators affects expression of *PROC*. Liver cells were seeded at a density of $5x10^5$ cells/mL in Eagles minimum essential media (EMEM, ATCC) and grown to 40% confluency before treatment with LPS (1, 1.5, 2, 5 or 10μg/mL; Sigma-Aldrich, Oakville, Ontario, Canada), IFNG (50 or 100ng/mL; R&D, Burlington, Ontario, Canada), TNF-alpha (30 or 50ng/mL; R&D), dexamethasone (0.001, 0.01, 0.1, 1 or 2μM; Omega, Montreal, Canada), d-dimer (0.5, 1, 2μM; Lee Biosolutions Inc., St Louis, MO), rhAPC (70, 700 and 7000ng/mL; 45, 450, 4500 and 45000ng/mL; Xigris®, Eli Lilly, Indianapolis, IN) and a triple combination (IFNG, 100ng/mL; TNF-alpha, 50ng/mL; d-dimer, 1μM). Cells were harvested in RNAProtect (Qiagen, Mississauga, Ontario, Canada) or TRIzol® (Invitrogen, Carlsbad, CA) after 30 minutes, 1 hour, and then every hour until 8 hours, then at 12 hours and 24 hours. Total RNA was isolated from RNAProtect samples using the Mini RNeasy Mini Kit (Qiagen), as per the manufacturer's protocol, after homogenization of cell lysates using the QIAshredder columns (Qiagen), and from the TRIzol® samples using the phenol/chloroform extraction method [311].

In addition, RT-qPCR assays were performed using RNA isolated from cultured human B-lymphocyte cells (Coriell Cell Repository, (http://ccr.coriell.org/), HeLa cells and a human monocyte cell line (THP-1, ATCC). As B-lymphocytes have limited receptors, specifically no TLR4 receptors, cells were treated with IFNG, dexamethasone or CpG type B (Sigma-Aldrich), a known stimulator of these cells. Moreover, in some experiments the B-lymphocyte cells were "primed" by pre-treatment with IFNG (100ng/mL) for 24 hours prior to treatment with CpG.

Conversion of 1μg RNA/sample to cDNA was achieved by using the Superscript III First-Strand Synthesis for RT-PCR kit (Invitrogen) with oligo$(dT)_{20}$ primers and PCR settings: 65°C (5 mins), placed on ice (1 min), 50°C (50 mins), 85°C (5 mins), placed on ice and added 1 μL RNaseH, then 37°C (20 mins). Products were stored at -20°C.

The cDNA was then used in 384-well format Taqman® Gene Expression assays to quantify *PROC* mRNA concentrations (probe Hs00165584_m1, Applied Biosystems, Carlsbad, CA) with the endogenous control glyceraldehydes-3-phosphate dehydrogenase (*GAPDH*; probe Hs99999905_m1,Applied Biosystems). The probes were chosen specifically to amplify regions spanning exon/exon boundaries to reduce the chance of genomic DNA being erroneously amplified and quantified.

The Taqman® Gene Expression assay is very specific, requiring not only specific complementarity of both the forward and reverse primers but also of the probes bearing fluorescent-reporter dyes. The ABI 7900HT thermal cycler (Applied Biosystems) quantifies the amount of fluorescence of each specific probe at different wavelengths, which correlates with the amount of mRNA for each protein in the log phase of amplification, and is represented by the cycle time (C_T) for each sample. The C_T readings for *PROC* were

normalized to C_T readings of *GAPDH* (*PROC*/*GAPDH*) to remove loading biases. The absolute quantification method, using a standard curve, and the relative quantification method using the $\Delta\Delta C_T$ calculation [312], were both used to compare concentrations of *PROC* mRNA between samples with different treatments. Efficiencies of each primer set were calculated and determined to be within 5% of each other, a requirement when using the $\Delta\Delta C_T$ calculation method [312]. Samples were assayed in triplicate and experiments were performed three times.

2.1.2 B-lymphocyte cells expressing *PROC*

B-lymphocyte cell lines GM10847, GM10846, GM10854, GM11839, GM12144, GM12239 and GM12249 were subcultured (RPMI medium with 10% FBS) into T25 flasks previously coated with Matrigel™ (BD Biosciences, Mississauga, Ontario, Canada) to encourage the normally suspended B-lymphocytes to adhere. Matrigel™ is a protein mixture that resembles the *in vivo* environment for many tissue types and is often used as a substrate for cell culture to elucidate complex cell behavior [313]. After seven days of growth, cells were treated with 100ng/mL hepatocyte growth factor (HGF) and harvested at subsequent days one through seven. Parallel experiments were performed on the same cell lines cultured in RPMI1640 medium plus 10% FBS but without Matrigel™. Conditioned media was collected and cells were harvested in lysis buffer (final concentrations: 1% Triton X-100, 20mM Tris-HCl pH7.5, 150mM NaCl, 1mM EDTA, 1mM EGTA, 2.5mM sodium pyrophosphate, 1mM sodium orthovanadate) with protease inhibitors (Invitrogen) and stored at -80°C until required. Cultured Hep-G2 cells were used as a positive control. Initially, to determine whether the adhered or non-adhered B-lymphocytes treated with HGF had adopted

a hepatocyte-like phenotype, Western blots were performed on cell lysates from cell line GM10847 and probed for alpha-fetoprotein, an ~ 70kDa protein known to be expressed by adult liver cells under some disease conditions, including hepatomas. The alpha-fetoprotein was detected in B-lymphocyte cells cultured on Matrigel™ and treated with 100ng/mL HGF (Figure 2.1), therefore this was the method used to culture B-lymphocyte cells for *PROC* quantification.

Twenty four-well plates were coated with Matrigel™ and placed in an incubator at 37°C and 5% CO_2 for 30 minutes prior to seeding of cells at a density of $2x10^5$ cells/well. The plates were returned to the incubator for four days to allow the cells to adhere and differentiate prior to application of 100ng/mL HGF in fresh media. Cells were harvested, as described previously, at days zero through seven after HGF application and stored at -80°C. Control wells, with no HGF treatment, were harvested at days zero and seven. To determine expression of *PROC* mRNA, *PROC* and *GAPDH* genomic DNA (gDNA) and mRNA (cDNA) were extracted as described previously and amplified in a thermocycler (GeneAmp PCR System 9700, Applied Biosystems, Inc.), set at 94°C for 2 minutes, then 40 cycles of 94°C for 15 seconds, 60°C for 30 seconds, 68°C for 30 seconds, followed by an extra extension period of 68°C for 5 minutes. Samples were held at 4°C until electrophoresis under reducing conditions. Gels were visualized under UV light on a GelDoc imaging system (GENE Flash, Syngene Bio Imaging, Frederick, MD) using GelRed™ nucleic acid stain (Biotium Inc., Hayward, CA).

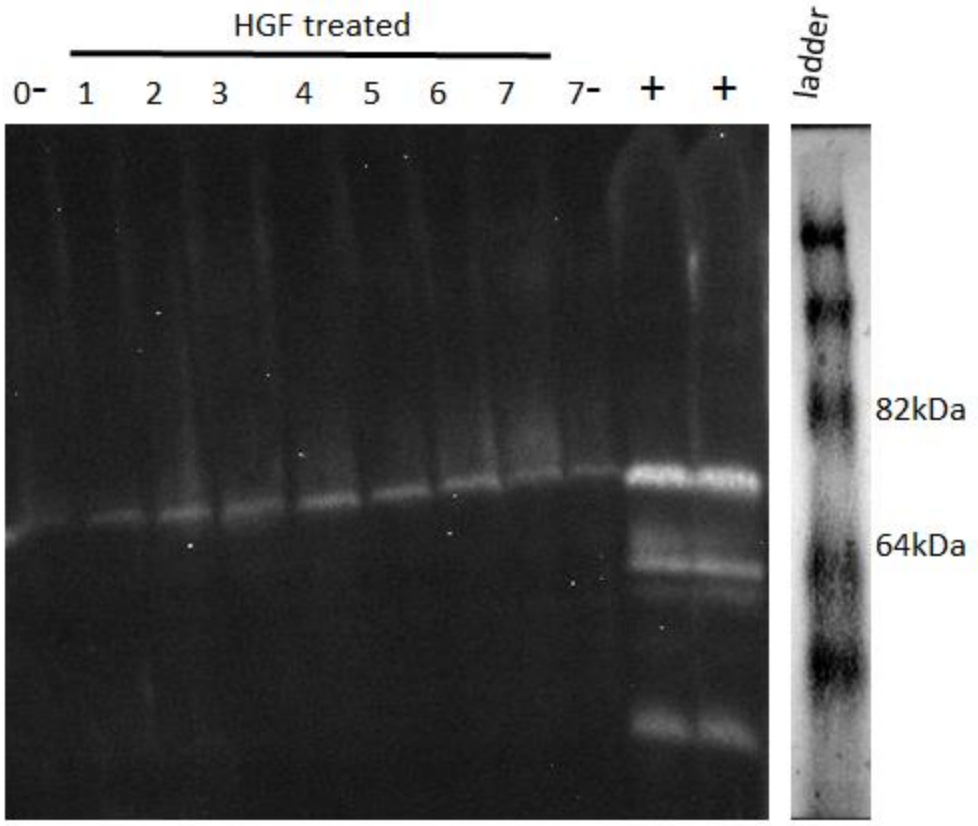

Figure 2.1 B-lymphocytes express a hepatocyte-like phenotype

B-lymphocyte cell line GM10847 was seeded on a Matrigel™ surface to obtain adherent cells then treated for seven days with hepatocyte growth factor (HGF; 100ng/mL). Cell lysate was harvested and 60µg total protein for each sample was separated on an 8% polyacrylamide gel. Untreated adherent B-cell lysates harvested at Day 0 and Day 7 were used as negative controls (0- and 7-). Hep-G2 liver cell lysate was used as a positive control (+). The numbers along the top of the wells indicate the time (days) after HGF treatment the cells were harvested. Although a band of the expected size (~70kDa) was seen when the Western blot was probed for the liver-specific protein, alpha fetoprotein, the concentration in the B-cell line was clearly well below that of the Hep-G2 cells, which was expected as adult hepatoma cells produce an increased level of alpha fetoprotein compared to normal adult liver cells. In addition, viability of the B-cells treated with HGF was considerably less than untreated B-cells.

Samples with potentially positive results were run on a low melting point agarose gel (LM Agarose; Invitrogen) and the bands were excised, purified (QIAquick PCR Purification Kit, Qiagen) and prepared for sequencing. Each sequencing reaction contained a total of 15ng of nucleic acid, 5µM of either the forward (PROC_rs5936gPCR_4593F:5'CGCCCTGTGTCGCAGACGGT3') or reverse (PROC_rs5936gPCR_5157R: 5'TTGCGCTAACAGTGGCCCCG3') primer, 3µL BigDye™ terminators (Nucleic Acid – Protein Service (NAPS) Unit, University of British Columbia, BC, Canada) and water to a total reaction volume of 10µL. Samples for sequencing were run on a GeneAmp PCR System 9700 (Applied Biosystems Inc.) with settings: 96°C for 1 minute followed by 25 cycles of 96°C for 10 seconds, 50°C for 5 seconds and 60°C for 4 minutes. Reactions were then held at 4°C until they were shipped to the NAPS Unit at UBC for sequencing. The sequencing results were analyzed using the PeakPicker software [314] whereby cDNA and gDNA sequences are first aligned then the number of cDNA reads normalized to gDNA reads using the coding SNP rs5936 as a reference point. Ratios 1.5 or greater were considered significant. Each sample was assayed in triplicate for all experiments. All primers used for amplification of *PROC* are listed in Appendix A, Table A.1

2.1.1 Enzyme-linked immunosorbent assay (ELISA)

Endogenous protein C in conditioned media from treated and untreated Hep-G2 cells was measured using the Technozyme® Protein C ELISA kit (Technoclone, Vienna, Austria) according to manufacturer's instructions. Conditioned media (100µL/sample) was added to duplicate wells on a 96-well optical plate, and fluorescence was measured using a

multidetection Rainbow plate reader with XRead Plus software (Tecan U.S. Inc., Durham, NC) at wavelength 450nm and a reference wavelength of 620nm. Protein C concentrations were calculated from the standard curve after subtraction of background readings. Treatments for Hep-G2 cells included all the treatments previously used for the RT-qPCR assays as well as thrombin (100 and 200mIU; Sigma-Aldrich). In addition, several combinations of treatments were used at previously stated concentrations: thrombin/IFNG, thrombin/LPS, thrombin/LPS/IFNG, IFNG/d-dimer, IFNG/LPS and TNF-alpha/d-dimer. Conditioned media was collected at 6, 12, 24 and 48 hours after treatment. Samples were assayed in duplicate and experiments were repeated three times.

Similar ELISA kits and methods were used to measure the concentration of protein C in Hep-G2 conditioned medium 48 hours after siRNA knockdown of USF1.

2.1.2 Viability assay

Viability assays were performed to determine whether any of the treatments used affected cell survival (adapted from Freshney, (1994) [315]). Briefly, Hep-G2 cells were cultured in 24-well plates as previously described and treated with LPS (5μg/mL), IFNG (100ng/mL), rhAPC (45, 450, 4500 and 45000ng/mL) or left untreated as control samples. Cells were harvested at 12 hours and 24 hours. Next, $1x10^6$ cells/mL of each sample was suspended in a 1:1 dilution of 0.4% trypan blue solution (Sigma-Aldrich). After incubation for 2 minutes at room temperature the cells were counted using a haemocytometer. Ratios of stained cells/total cells were compared between treated or untreated samples at the two different time points. In addition, a second method was employed whereby 0.4% trypan blue solution was added to cultured Hep-G2 cells *in-situ* in each well without cell lysis. After

observing the relative number of live:dead cells in each well, some cells were wounded with a pipette tip. Dye up-take by the wounded cells occurred almost immediately, indicating that the assay was capable of differentiating between live cells and dead or wounded cells.

2.1.3 Single nucleotide polymorphism selection in the *PROC* gene

Dense resequencing in a European population by SeattleSNPs (http://pga.mbt.washington.edu/) was used for SNP selection. All SNPs that had a minor allele frequency >10% and were situated between the -1654 polymorphism in the promoter region and the end of intron 2 in *PROC* were selected for study (Table 2.1). Several SNPs in the selected region were found to be in high LD, notably rs2069915, rs2069916 and the promoter SNP -1654 (rs1799808) which together have an r^2>0.83 (Figure 2.2 and Figure 2.3 and Appendix A, Table A.2).

Table 2.1 SNPs in the *PROC* gene selected for study

All SNPs from SeattleSNPs database of European individuals with a minor allele frequency >10% that were situated between the -1654 polymorphism in the *PROC* promoter region and the end of intron 2 were selected for study.

SNP position*	SNP rs ID	Alleles Major/Minor†	Minor allele frequency (%)‡	Gene region	Predicted functional effects§
-1654	rs1799808	C/T	33	Promoter	No known function
-1641	rs1799809	A/G	48	Promoter	No known function
-1479	rs1799810	A/T	48	5'UTR exon 1	Splicing regulation
-141	rs1158867	T/C	47	Intron 1	No known function
453	rs2069910	C/T	39	Intron 2	No known function
670	rs2069912	T/C	26	Intron 2	Enhancer
738	rs2069913	C/G	20	Intron 2	No known function
751	rs2069914	G/A	26	Intron 2	Enhancer
857	rs2069915	G/A	35	Intron 2	No known function
894	rs2069916	C/T	33	Intron 2	Enhancer

* SNP position is with respect to the start of translation in exon 2.

† Major alleles are those most common in European populations.

‡ Minor allele frequencies as per SeattleSNPs European populations.

§ Possible functional effects as predicted by the FastSNP database [316].

UTR, Untranslated Region

Position Numbers		-2653	-1737	-1654	-1641	-1480	-1476	-839	-810	-139	456	673	741	754	860	897	1808	2035	
Clade	rs Numbers	rs2069902	rs2069904	**rs1799808**	**rs1799809**	rs2069936	**rs1799810**	rs2069906	rs2069907	**rs1158867**	**rs2069910**	**rs2069912**	**rs2069913**	**rs2069914**	**rs2069915**	**rs2069916**	rs2069918	rs2069919	Frequency(%)
A	**1**	**G**	**A**	**C**	**G**	**G**	**T**	**G**	**G**	**C**	**C**	**T**	**C**	**G**	**G**	**C**	**G**	**A**	36.96
	2	**G**	**A**	**C**	**G**	**A**	**T**	**G**	**G**	**C**	**C**	**T**	**C**	**G**	**G**	**C**	**G**	**A**	2.17
B	**3**	**C**	**G**	**T**	**A**	**G**	**A**	**G**	**G**	**T**	**C**	**T**	**C**	**G**	**A**	**T**	**G**	**G**	2.17
	4	**C**	**G**	**T**	**A**	**G**	**A**	**G**	**G**	**T**	**T**	**T**	**C**	**G**	**A**	**T**	**G**	**G**	30.43
C	**5**	**C**	**G**	**C**	**A**	**G**	**A**	**G**	**G**	**T**	**C**	**C**	**G**	**A**	**G**	**C**	**A**	**G**	19.57
	6	**C**	**G**	**C**	**G**	**G**	**T**	**A**	**G**	**C**	**T**	**C**	**C**	**A**	**G**	**C**	**G**	**G**	6.52

Figure 2.2 Phased haplotype associations of SNPs in a Caucasian population from SeattleSNPs

The diagram spans a region of 4688bp of the *PROC* gene from upstream of exon 1 to the middle of intron 3. Position numbering is with respect to the start of translation in intron 2. Numbers 1 to 6 represent the different haplotype groups. All 10 SNPs surveyed in this study are represented and marked in bold typeface. The frequency % refers to the frequency that each haplotype was found in the population. In this sample of 23 individuals, rs1799808[C] (also known as -1654[C]) is always associated with the G-C haplotype of rs2069915-rs2069916. Linkage disequilibrium exists between -1654 (rs1799808) and rs2069915 (83%) as well as rs2069916 (94%). Three haplotypes from Clade C were not included as they were not common, together only representing 2 individuals.

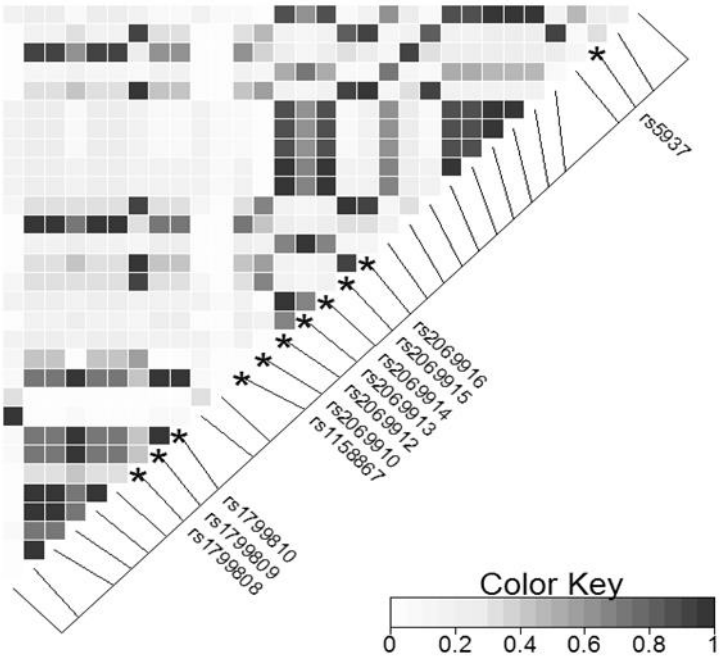

Figure 2.3 Linkage disequilibrium between SNPs in the *PROC* gene

Linkage disequilibrium heatmap showing the degree of association between the ten SNPs in the region of the *PROC* gene surveyed. The darker the squares the greater the LD (and greater the r^2 value) therefore the more likely any two SNPs are inherited together. The SNPs rs2069915 and rs2069916 are in high LD (r^2=0.92). There is also a high degree of LD between these two SNPs and one of the well documented promoter SNPs -1654 (rs1799808), r^2 = 0.83 and 0.92 respectively. *Figure created using R software (version 2.8.1)*

2.1.4 Electrophoretic mobility shift assay (EMSA)

2.1.4.1 Nuclear extracts for EMSA

As protein C is primarily synthesized in the liver, a human hepatoma cell line, Hep-G2 was used to generate nuclear extracts. Cells were cultured, maintained and split as per suppliers' recommendations (ATCC). Nuclear lysates were obtained by seeding cells at a

density of $4x10^5$ cells/mL in 9.6 cm^2 culture plates (6-well plates) and were maintained in EMEM until 90% confluent before harvesting cells and extracting nuclear fractions according to manufacturer's instructions (Nuclear Extraction Kit, Panomics, Fremont, CA). Nuclear proteins were quantified using either a BCA Protein Quantification assay (Pierce, Rockford, IL) or by measuring optical density at 280 nm on a NanoDrop 8000 spectrophotometer (Thermo Fisher Scientific Inc.). Nuclear extracts were obtained from untreated Hep-G2 cells (19 distinct cultures were used) or healthy human liver tissue (Active Motive Inc., Carlsbad, CA) and were used at a concentration of 4 - 10 μg/reaction. As both Hep-G2 and liver tissue lysates returned similar results, the study continued with Hep-G2 lysates.

2.1.4.2 Radiolabeled oligonucleotide sequences for EMSA

Twenty-five base-pair oligonucleotide sequences (oligos) centered on the selected SNPs were designed for the major and minor alleles of each SNP and obtained from Integrated DNA Technologies (IDT, Coralville, IA; Appendix A, Table A.3). The promoter SNP probes contained haplotypes of both SNPs as these two SNPs lie only 13bp apart. The assay was performed following the protocol of the Gel Shift Assay System (Promega, Madison, WI): oligos were 5'end-labeled with $^{[\gamma\text{-}32]}$P-ATP (Perkin Elmer, Waltham, MA). Unlabeled oligos were removed by centrifugation at 1000 x g for 4 minutes in G25 Mini Quick spin DNA columns (Roche, Mississauga, ON). Incorporation of $^{[\gamma 32]}$P-ATP was ascertained by calculating the ratio of labeled oligo to unlabeled oligo after counting in a scintillation counter (BeckMan Coulter LS6500 Multi-Purpose Scintillation counter, Mississauga, ON). Only oligos with >30% incorporation were used, as per the manufacturer's protocol.

2.1.4.3 Electrophoretic mobility shift assay

For each reaction, nuclear lysate (4 - 10µg/reaction) was incubated for 10 minutes at room temperature with 1X binding buffer (20% glycerol, 5mM MgCl2, 2.5mM EDTA, 2.5mM DTT, 250mM NaCl, 50mM Tris-HCl pH 7.5, 0.25mg/mL poly9dI-dC)•(poly(dI-dC) and water to 9µL before the addition of 1µL of labeled oligo (75 000 – 110 000cpm) and a further incubation of 20 minutes at room temperature. Gradient (2-8%) CosmoPAGE native gels (Nacalai USA, Inc,, San Diego, CA) were pre-run for 10 minutes at 250V in 1X native running buffer (20X buffer: 0.8M Tricene, 1.2M Tris pH8.4) to remove any unpolymerized acrylamide. Gels were dried for 45 minutes at 57ºC on a slab gel dryer (Drygel Sr. Model SE1160, Hoefer Scientific Instruments, San Francisco, CA) before being exposed overnight to a Super Resolution storage phosphor screen (Perkin Elmer Life and Analytical Sciences, Shelton, CT) and scanned on a Cyclone® Plus storage phosphor system from Perkin Elmer using OptiQuant Image Analysis software (Perkin Elmer, Waltham, MA).

2.1.4.4 Cold competition and supershift assays

Reactions involving competition with cold (unlabeled) probes were pre-incubated for 20 minutes at room temperature with 50X, 100X or 200X molar excess of unlabeled probe before addition of the labeled probe and continuation of the assay as previously described. Supershift assays were pre-incubated for 20 minutes at room temperature with 2µg of antibody (cMYC and NFκB, Cell Signaling Technology Inc., Boston, MA; USF1, Santa Cruz Biotechnology Inc., Santa Cruz, CA) prior to continuation of the assay.

Consensus sequences for EMSA cold competition assays to identify proteins potentially binding to the SNPs of interest were selected based on a combination of database and literature searches: consensus sequences of transcription factors purported by the

functional analysis database, FastSNP [316] (http://fastsnp.ibms.sinica.edu.tw/pages/input_CandidateGeneSearch.jsp), and the stringent database, ConSite [317] (http://asp.ii.uib.no:8090/cgi-bin/CONSITE/ConSite/), to bind the SNP region were confirmed by comparison against known sequences listed on the MACO database [318] or from literature reports. The final selection of transcription factor consensus sequences included cREL, IRF1, NRF2, TEAD1 and E2F for rs2069915 and cMYC, USF1 and NFKB for rs2069916. Many transcription factors have more than one known consensus sequence, in some cases the sequences are tissue- or pathway-specific, therefore, for completeness, more than one sequence was included for several transcription factors (Appendix A, Table A.4).

2.1.5 Validation of EMSA results by novel bead-based "gel-shift" assay

In collaboration with an industry partner (Panomics Inc., Fremont, CA) a high-throughput quantitative EMSA-type method was developed to screen multiple SNPs for transcription factor binding. This multiplexing method utilizes biotin-conjugated sequences of interest and fluorescent-dyed beads conjugated to specific transcription factor sequences, whole-cell or nuclear lysate and is quantified on the Luminex platform. The work flow is depicted in Figure 2.4.

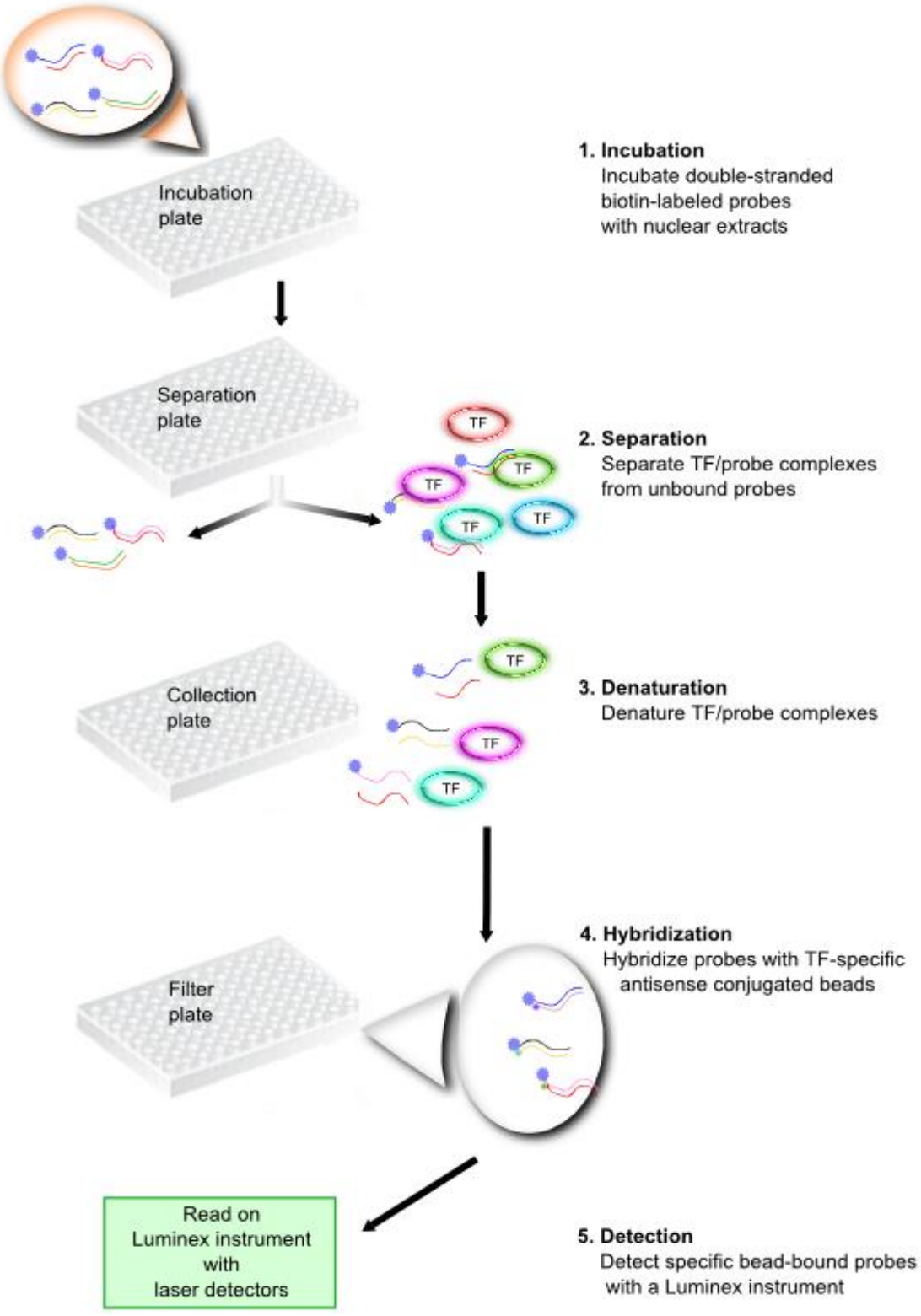

Figure 2.4 Workflow of novel plate-based "gel-shift" assay

Figure created using Inkscape software version 0.48.4

Initially, double-stranded DNA sequences centered on SNPs rs2069912[T/C], rs2069915[G/A] and rs2069916[C/T] were synthesized by IDT and labeled with biotin on the 5' end of the sense stand only (Appendix A, Table A.3). The same sequences were used here as for the EMSA assays but included biotin labeling instead of radionuclide labeling. The transcription factors chosen for this assay were those purported by both the PROMO and ConSite databases to bind the DNA sequence at rs2069916[C], or were known to affect expression in hepatic cells, and were available on the Procarta™ Transcription Factor Assay panel : NFKB, AP1, STAT3, RUNX1/AML, CEBP, GR/PR and HNF1. The sense strands of the consensus sequences for these transcription factors were biotin-labeled at the 5' end and the antisense strands were each conjugated to unique Capture beads by Panomics Inc. Similarly, the antisense strand of rs2069916[C] with a six carbon spacer (rs2069916[C] antisense: 5' XXXXXXCCAGTACACCACGTGCAGCCCCATC 3') was conjugated to a unique Capture bead (Panomics Inc.) capable of being quantified on the Luminex platform and this bead/sequence was added to the pre-mixed Capture bead solution.

The assay was a modified version of the Procarta™ Transcription Factor Assay (Panomics Inc.) whereby 6nM of each sample biotin-labeled double-stranded oligo was incubated with 2µg Hep-G2 nuclear lysate for a total sample volume of 20µL, at 15°C for 30 minutes in a 96-well Incubation plate to enable protein/DNA complexes to form. The assay then continued as per manufacturer's protocol and the plate was read on the Luminex100 instrument and data was analyzed with the accompanying 1.7 Software (Luminex Corporation, Austin, TX). The Luminex instrument was warmed up and calibrated prior to use and gated at 8 000 – 15 000 and set to count 50 events in 25 seconds.

Samples included the three SNPs rs2069912, rs2069915 and rs2069916 with Hep-G2 nuclear lysates which were untreated or treated with TNF-alpha. Samples were assayed in duplicate and negative controls (no Hep-G2 nuclear lysate) were included for each sample type. In addition, positive and negative controls supplied by Panomics were included: untreated HeLa nuclear lysate with the addition of recombinant NFKB protein and untreated HeLa nuclear lysate, respectively. Wells containing only the buffers were included as background controls. All buffers and plates were supplied by Panomics Inc. and formulations are proprietary.

2.1.6 Identification of nuclear factors by SILAC mass spectroscopy

An alternate method to identify nuclear factors binding to the probes of interest is mass spectrometry. As the concentration of nuclear factors binding to the DNA probes is very low, an alternative mass spectrometry method was employed that is able to detect and identify proteins in minuscule concentrations: Stable Isotope Labeling by Amino acids in Cell culture (SILAC) [319]. For this assay, Hep-G2 cells were cultured in T75 flasks in Dulbecco's Minimum Essential Medium without arginine or lysine (DMEM; Caisson Laboratories, Inc., North Logan, UT). Stable heavy isotopes of arginine and lysine ($^{17}C_6$-argenine and D_4-lysine) were added to media in one flask and normal arginine and lysine isotopes (called "light" isotopes for clarity) were added to media in a separate flask. Cells were subcultured through a minimum of seven passages before plating in either "heavy" or "light" media, with harvesting and nuclear extraction as previously described. Nuclear factors binding to SNPs of interest were purified using biotin labeled probes (IDT, Appendix A, Table A.3) and streptavidin-coated magnetic beads (Dynabeads® M-280, 10mg/mL,

Invitrogen) as per manufacturer's instructions. Biotin-labeled probes (1.75µM; IDT) containing the G-allele of rs2069915 or the C-allele of rs2069916 were separately incubated for 20 minutes at room temperature in ~4mg/mL nuclear lysate harvested from cells cultured in media containing "heavy" isotopes while the probe containing the opposite allele of each SNP, the A- and T-alleles respectively, were incubated separately in nuclear extract harvested from cells cultured in "light" medium. The Dynabeads® were washed 3 times in 1X wash/binding buffer (10mM Tris-HCl pH8.8, 1mM EDTA, 0.1mM NaCl) to remove preservatives and resuspended in 1X wash/binding buffer. Twenty microliters of beads were added to each probe/nuclear lysate reaction and incubated for a further 20 minutes at room temperature to immobilize probes to the beads. Each reaction microcentrifuge tube was then appended to a DynaMag™-Spin magnetic particle concentrator (Invitrogen) to concentrate the beads on the sides of the tubes and prevent removal when aspirating nuclear lysate or buffers. Nuclear lysate was then removed and the beads with probes bound were washed once with 1X low-salt binding buffer (20% glycerol, 50mM Tris-HCl, 250mM NaCl, 5mM $MgCl_2$, 25mM EDTA, 2.5mM DTT and 0.25mg/mL poly dI.dC) and resuspended in 20µL of 1X high salt, low pH buffer (20mM Tris-HCL pH6.8, 1M KCl, 1mM EDTA, 1mM DTT). The "heavy" and "light" reactions for each SNP were then combined, the beads immobilized using the magnetic particle concentrator and nuclear factors eluted off the probes by incubation of the reactions at 56°C for 5 minutes. Two reactions were performed for each probe, combined, and the volumes reduced to 20µL by evaporation (Savant SpeedVac SC100, Thermo-Scientific, Nepean, ON, Canada) to concentrate the samples. Samples were stored at -20°C prior to SILAC mass spectrophotometry analysis at the Centre for High-Throughput Biology (CHiBi), University of British Columbia, BC, Canada.

Mass spectroscopy was performed using the OrbiTrap machine (CHiBi, UBC, BC) and Quant analysis was performed by calculating the ratio of "heavy" to "light" isotopes of isolated proteins as per the method of Mittler *et al.*[319]. Ratios greater than 2 or less than 0.5, with a minimum of two identified peptides, were considered positive identifications of proteins bound to the "heavy" or "light" probes, respectively.

2.1.7 siRNA knockdown of USF1

To test whether loss of USF1 binding to rs2069916[C] has a functional effect on protein C expression, a USF1 knock down assay was performed using validated Stealth Select RNAi™ siRNA duplex sequences (Invitrogen) against the human USF1 gene. A medium GC Scrambled Stealth RNAi™ siRNA duplex (Invitrogen) was used as a negative control. Three different siRNA probes were assayed for USF1 knockdown by Western blot analysis using COP1 as the standard. Probe HSS144432 achieved the greatest effect with an 83% knockdown, therefore this probe was used in all subsequent knockdown experiments.

Reverse transfection reactions were performed in triplicate with the siRNA probe and the negative control probe according to manufacturer's recommendations. Whole cell lysates were collected by addition of 300 µL of RNAprotect Cell reagent (Qiagen) to each well after collection of conditioned media, followed by storage at -80°C prior to RNA and DNA extractions.

2.1.8 TaqMan™ SNP genotyping assays

The TaqMan™ SNP genotyping assay (Applied Biosystems Inc.) functions similarly to the TaqMan™ Gene Expression RT-qPCR assay but utilizes two probes instead of one,

each covalently conjugated to a quencher molecule on the 3' end and either a FAM (Excitation 495nm, emission 515nm) or VIC (Excitation 535nm, emission 555nm) [320] fluorophore on the 5' end. The probe sequences span the region flanking the SNP of interest and each is specific for one allele of the SNP. The Taqman™ SNP genotyping assay probes were designed for the *PROC* coding SNP rs1799810 (Validated probes: C-1841975_1_; Applied Biosystems Inc.) which was first tested for quality by RT-qPCR amplification of genomic DNA extracted from genotyped B-lymphocyte cell lines (Coriell Cell Repositories) homozygous or heterozygous for alleles of this SNP: 5ng DNA was used for between four and seven different individuals for each genotype. In addition, an allelic discrimination assay was performed to check the performance of the probes (Figure 2.5). After validation of the probes, total RNA and DNA were extracted (AllPrep RNA/DNA kit; Qiagen) from Hep-G2 cells, as described previously, after 48 hours of USF1 knockdown by siRNA probes, and from Hep-G2 cells treated with control siRNA probes at the same timepoint. The Superscript III First Stand Synthesis system (Invitrogen) was used to convert mRNA to cDNA after Ambion® TURBO DNA-free™ DNase treatment (Life Technologies Corp.). Genomic DNA and cDNA were purified using QIAquick PCR Purification kit (Qiagen) as per manufacturer's recommendations.

For the Taqman™ SNP genotyping assay, 10ng gDNA and, separately, cDNA (total volume 20μL/well) from biological triplicates of each sample were added to separate wells on a 384-well plate, in triplicate, and dried overnight at room temperature under sterile conditions. The following day 10μL/well of a mastermix (2X TaqMan™ Master mix, 40X Taqman™ assay mix containing probes, DNase-free water) was added to each reaction well on the plate as well as to 36 wells containing only Tris-EDTA scattered randomly throughout

the plate as negative controls. The samples were then amplified by RT-qPCR (95°C for 10 minutes followed by 35 cycles of 92°C for 15 seconds then 60°C for 1 minute (Applied Biosystems 7900HT, Applied Biosystems Inc.). Cycle-time readings for cDNA were normalized to the gDNA C_T readings from the same sample prior to averaging of replicates.

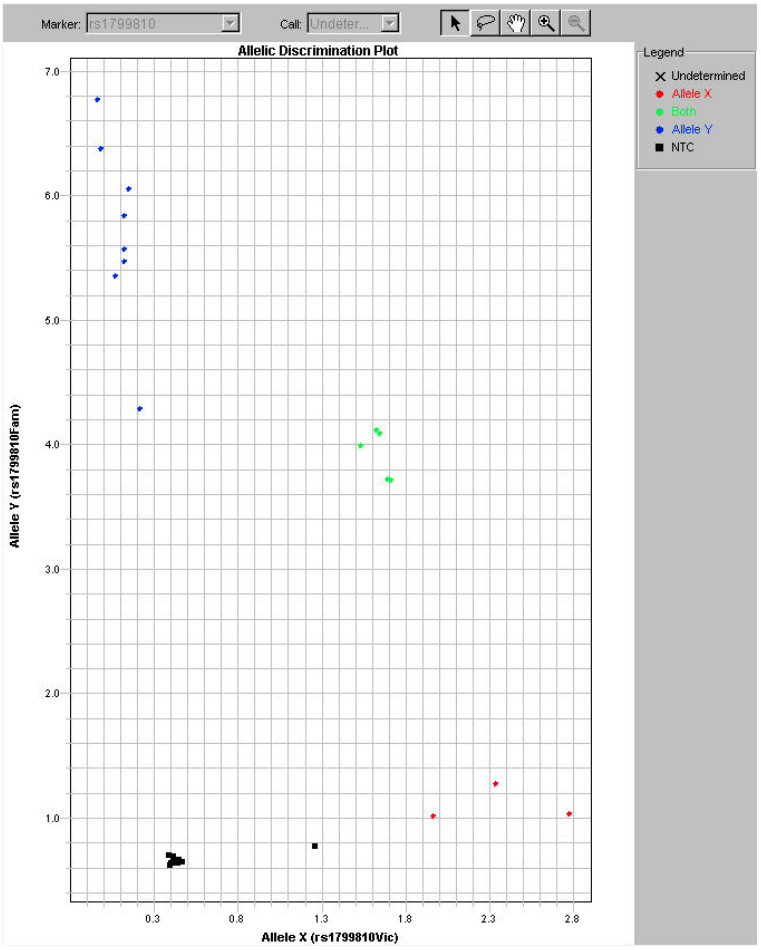

Source: Applied Biosystems PCR system 7900HT

Figure 2.5 Validation of probes by allelic discrimination.

Quality control of the TaqMan™ probes for SNP rs1799810 using DNA from B-lymphocyte cell lines shows clear separation of genotypes: Allele X (red) = rs1799810[AA], Allele Y (blue) = rs1799810[TT], heterozygotes rs1799810[AT] are shown in green. Controls (NTC, containing Tris-EDTA), shown as black squares, are tightly grouped at the bottom left of the graph, indicating no DNA was amplified.

2.1.9 Luciferase reporter assay

2.1.9.1 Construction of vectors

Haplotypes homozygous for the major alleles of SNPs rs2069912, rs2069913 and rs2069914, and major or minor alleles of rs2069915 and rs2069916 (genotypes TCGGC or TCGAT respectively), were amplified by PCR from cDNA derived from individual B-lymphocyte cell lines available at the Coriell Cell Repository (http://ccr.coriell.org/). (Table 2.2).

Table 2.2 Cell lines used for the luciferase reporter assays

	Genotypes of SNPs				
	rs2069912	rs2069913	rs2069914	rs2069915	rs2069916
Cell lines					
GM12005	TT	CC	GG	AA	TT
GM10845	TT	CC	GG	GG	CC

Primers were designed to amplify a 421bp region covering these SNPs. In addition, the forward primer included a Kpn1 restriction site on the 5' end while the reverse primer included a BglII restriction site on the 3' end to facilitate directional cloning (Table 2.3).

Table 2.3 Primers designed for luciferase reporter assay

Primer pair 1 and 2 containing the restrictions site for Kpn1 and BglII at 5' and 3' ends (bold type) was used to amplify the DNA isolated from Coriell cell lines. Primer pair 3 and 4 amplified off the PGL4.23(*luc2*/minP) vector backbone, covering the entire inserted piece of DNA, to check insert orientation. Primer 5 amplified forward off the vector backbone, the reverse primer (primer 6) was situated on the DNA insert near the 5' end to differentiate correctly or incorrectly orientated inserts.

Number	Primers	# bases	Product size	Sequence 5' - 3'
1	PROC_intron2_Kpn1_for421	34	421	GTAC**GGTACC**CCACACCAGGCTGTTGGTTTCATT
2	PROC_intron2_BglII_rev421	34		GCAT**AGATCT**ATAAGTACTCAAGCCCTGGCTGCT
3	pGL4_seq_847F	24	847	AAGAAGGGAATGAGTGCGACACGA
4	pGL4_seq_847R	24		TGGCATCTTCCATGGTGGCTTTAC
5	pGL4_seq_847F	24	494	AAGAAGGGAATGAGTGCGACACGA
6	pGL4_seq_494R	24		GCACAGTTAGGAGGGAGAGATCAA

The amplified regions were cut out of the cellular genomes by a double restriction enzyme digest, purified and cloned into the pGL4.23[*luc2*/minP] vector (Promega), (Figure 2.6).

For the cloning reaction, 1µg each of the vector and the amplified DNA from the three cell lines was double-digested using 2µg each of the Kpn1 and BglII restriction enzymes (New England Biolabs, Pickering, ON, Canada), 1X Buffer 2, BSA (New England Biolabs) and RNase/DNase-free water (New England Biolabs), to a total volume of 50µL. The reactions were incubated in a water bath at 37°C for 1 hour. The vector was then dephosphorylated using Antarctic Phosphatase (New England Biolabs) to prevent self-ligation. The phosphatase was inactivated by incubation at 65°C for 5 minutes. The vector

reaction was run on a 1% agarose gel in 1X TAE buffer (Tris-acetate buffer with EDTA, pH8.0) for 2 hours at 70V.

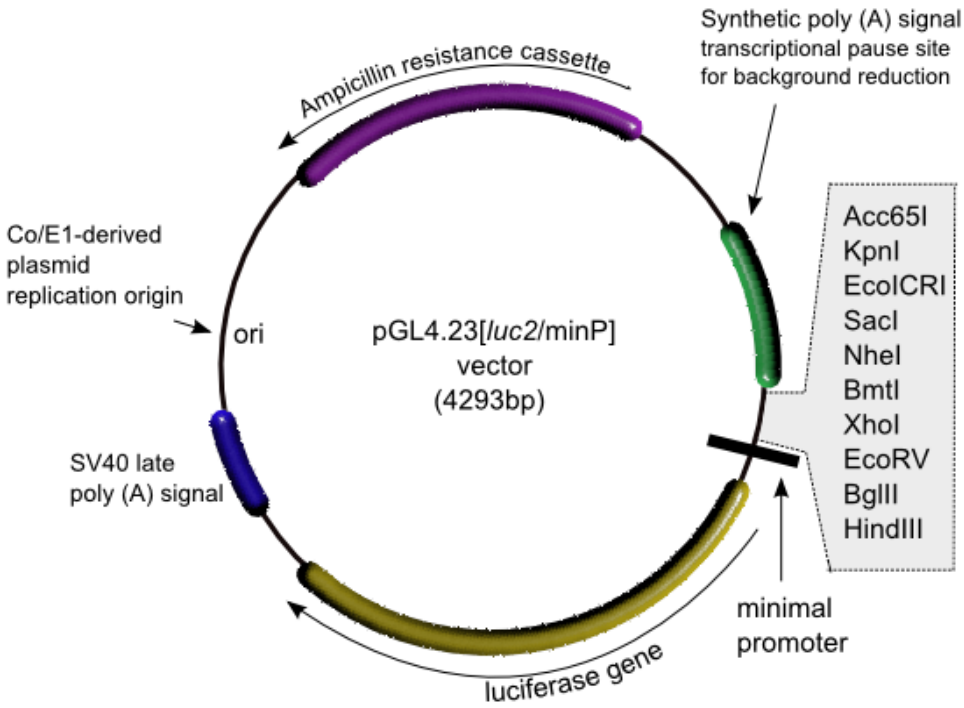

Figure 2.6 Map of the pGL4.23[*luc2*/minP] vector

The pGL4.23[*luc2*/minP] vector was used in the luciferase reporter assays. This high expression vector is designed to reduce aberrant expression. It contains a multiple cloning region (list of restriction sites in box on right) for insertion of a DNA sequence of interest upstream of a minimal promoter and the luciferase gene. *Figure created using Inkscape software version 0.48.4, adapted from www.promega.ca*

The gel was visualized under UV light and the resulting band was cut out and purified using a QIAquick Gel Extraction kit (Qiagen) as per manufacturer's protocol. The DNA fragment to be cloned into the vector was then purified as described previously (QIAquick

PCR Purification Kit, Qiagen). The ligation reactions included insert DNA and vector DNA in a ratio of 3:1, T4 kinase and 1X T4 buffer and water to a total volume of 10µL. The reactions were incubated at room temperature for 10 minutes before transformation into XL-1 Blue competent *Escherichia coli* cells (Agilent Technologies, Palo Alto, CA).

2.1.9.2 Transformation of competent cells

For each reaction, a 40µL aliquot of electro-competent XL-1 Blue *E. coli* (Agilent Technologies) cells were mixed with 2µL of DNA from each ligation reaction in a chilled microcentrifuge tube. The samples were each placed in chilled electroporation cuvettes and electroporated at 1700V, field strength of 17kV/cm, resistance of 200Ω and 25uF capacitance in a BioRad Gene Pulser II Electroporator (Bio-Rad Laboratories (Canada) Ltd, Mississauga, ON, Canada). The cells were immediately resuspended in SOC medium (Invitrogen), transferred to round-bottomed polypropylene tubes and incubated for 1 hour at 37°C, with shaking, at 250 rpm. The cells were then plated with 50µL of culture at various dilutions (1:10, 1:50 and 1:100) on LB (Luria-Bertani) agar (Invitrogen) plates with 100µg/mL ampicillin (Invitrogen) and incubated overnight at 37°C. The following day eight individual colonies for each electroporation reaction were selected and inoculated into 3mL volumes of LB broth (Invitrogen) with ampicillin and allowed to grow overnight at 37°C, with shaking, at 250 rpm.

2.1.9.3 Selection of vectors

One and a half milliliters of the 3mL overnight cultures were purified using the QIAspin Miniprep Kit (Qiagen) as per manufacturer's specifications and run on a 1% agarose gel with 1X SYBR® Safe DNA gel stain (Invitrogen) and a 1kb DNA ladder (Invitrogen) to distinguish those vectors containing a clone from those without. One correct

cloning reaction was selected for each haplotype and the remainder of the 3mL overnight culture for each was used to inoculate 50mL LB broth with 100µg/mL ampicillin. The cultures were allowed to grow overnight at 37°C, with shaking, at 250 rpm. The following day the cultures were purified using a HiSpeed® Plasmid Midi purification kit (Qiagen) as per the manufacturer's specifications and quantified using the BCA Protein Quantification Assay from Pierce (Rockford, IL). Pre-sequencing PCR was performed using BigDye™ terminators as described previously and the samples sent for sequencing (NAPS Unit, UBC,) to ensure the correct haplotypes had been cloned into the vector, in the correct orientation.

2.1.9.4 Dual-Glo luciferase reporter assay

Hep-G2 cells were plated at a density of $5x10^4$ cells/well in 2 cm^2 culture plates and grown to 50% confluency before transfection using Lipofectamine® 2000 (Invitrogen) at a ratio of 5:1 Lipofectamine®:DNA, previously determined to be the optimum ratio. Cells were co-transfected with the *Renilla* luciferase vector (*Renilla reniformis*; Promega), as an internal control, and one of the pGL4.23[luc2/minP] vectors, at a ratio of 1:3 for a total of 20ug DNA/reaction. Reactions were prepared with lipid-free medium and no antibiotics. The DNA and Lipofectamine® reactions were incubated separately for 5 minutes at room temperature before being combined and incubated for a further 20 minutes to allow the complexes to form. Media was then aspirated from each well of the cultured cells and 100µL of the appropriate Lipofectamine®:DNA complex was added drop-wise to each well. An extra 500µL of lipid- and antibiotic-free medium was added to each well and the plates incubated at 37°C and 5% CO_2 for 4 hours. The media was then aspirated and replaced by 1mL/well of medium containing serum but no antibiotics and incubated for a further 24 hours at 37°C and 5% CO_2. After 24 hours the Dual Glo™ Luciferase Assay System (Promega)

assay was performed as per the manufacturer's instructions. The Firefly luciferase (*Photinus pyralis*) luminescence was measured on a FLUOstar OPTIMA microplate reader (Fisher Scientific, Nepean, ON, Canada). After reading the Firefly activity, 70μL of Dual Glo® Stop & Glo® reagent was added to each well and incubated for 10 minutes at room temperature before monitoring of the *Renilla* luciferase activity on the same machine. Background measurements were subtracted and the Firefly luciferase normalized to the *Renilla* luciferase measurements before statistical analysis.

2.1.10 Statistical analysis

For EMSA assays, to enable between-gel comparisons of nuclear factor binding, densitometry measurements (Image J 1.44p software, NiH, USA) were obtained for each allele of a SNP on the same gel using the Image J gel-analysis function which calculates the area under the curve. Ratios of these values were then averaged and graphed. Ratios of densitometry measurements for promoter haplotypes were compared using the ANOVA statistical test (GraphPad Prism 5.02 software, La Jolla, CA). Comparisons of nuclear factor binding between alleles for rs2069915[G/A] and rs2069916[C/T] were performed using 2-tailed, paired Student's t-tests.

Comparisons of luciferase activity were performed using 2-tailed, unpaired t-tests.

For ELISA assays, to reduce variations in readings due to plate differences, background fluorescence was subtracted from sample fluorescence readings prior to calculation of protein C concentrations from standard curves. All measurements were within the range of the standard curves.

A P-value of <0.05 was considered significant throughout.

2.2 PCSK9 Experiments

2.2.1 Animal models

All animal studies were approved by the University of British Columbia animal ethics committee and conformed to NIH and "Guide for the Care and Use of Laboratory Animals' guidelines.

2.2.1.1 Murine experiments

Male C57BL/6 (wildtype genetic background control strain) and *Pcsk9* knock-out (*Pcsk9*$^{-/-}$; B6;129S6- *Pcsk9*$^{tm1Jdh/J}$) mice, body weight 25-30 grams, 10-14 weeks old, were obtained from Jackson Labs (Bar Harbor, ME). Compared to wildtype control mice, *Pcsk9*$^{-/-}$ mice have reduced plasma cholesterol concentrations with nearly undetectable LDL cholesterol concentrations [321]. In addition PCSK9 protein is also undetectable [321]. There are no other reported obvious phenotypic alterations.

Mice had activity level, body temperature, blood pressure, and left ventricular ejection fraction (echocardiography) assessed at baseline. Mice were then injected intra-peritoneally (i.p.) with LPS (20 mg/kg, *E. coli* strain 01 II: B4, Sigma, St. Louis, MO). Their activity level and temperature were measured every hour for six hours. At six hours blood pressure was measured by invasive arterial cannulation, and left ventricular ejection fraction was assessed again. Inflammatory cytokines were measured from blood harvested at this six hour time point.

2.2.1.2 Berberine pretreatment to inhibit hepatic PCSK9 mRNA expression

In separate experiments, pharmacologic inhibition of *Pcsk9* in wildtype male C57BL/6 mice was achieved using berberine (Sigma-Aldrich). At a concentration of 1-10μM berberine inhibits transcription of *Pcsk9* within 24 hours [322, 323]. With a volume of distribution of one and a molecular weight of 371g/mol we targeted plasma levels of 10μM through a bolus followed by maintenance infusion. Mice (body weight approximately 25g) were injected i.p. in the evening 60 hours before exposure to LPS, with 100μg berberine (Sigma-Aldrich) in 100μL sterile saline or saline vehicle. The next morning, a 72 hour osmotic pump (ALZET, Cupertino, CA) with an infusion rate of 1μL/hr was implanted intra-peritoneally. Pumps contained 100μg berberine or vehicle saline. Activity, temperature, blood pressure, and left ventricular ejection fraction were measured following LPS administration, as described below.

To confirm knockdown, livers were harvested at the time of sacrifice and flash frozen in liquid nitrogen. Total cellular RNA was extracted according to manufacturer's instruction (AllPrep DNA/RNA Mini kit, Qiagen) after homogenization using a chilled glass mortar and pestle, in Buffer RLT with Reagent DX added to prevent foaming of samples. Total RNA was DNase treated using Ambion® TURBO DNA-free™ DNase treatment (Life Technologies Corp.) to remove genomic contamination. The PCR products for primers *Pcsk9*_809F (5'CAGTGACCTGTTGGGCCTGGCCCTGAAGTTGC3') and *Pcsk9*_1408R (5'CCGACTGTGATGACCTCTGGAGCAGAAGCTG3') and *Gapdh* loading control primers *Gapdh*_mouse_QRT_F 5'CCAGGTTGTCTCCTGCGACT3' and *Gapdh*_mouse_QRT_R 5'ATACCAGGAAATGAGCTTGACAAAGT3' (94°C for 3 mins, 25 cycles of 94°C for 30 seconds, 64°C for 30 seconds, 72°C for 1 min, followed by 10

minutes at 72°C) were used to verify *Pcsk9* knockdown in the liver of treated mice. Ten microlitres of the product was run on a 2% agarose gel and visualized using GelRed™ nucleic acid stain (Biotium Inc.) under UV light. Densitometry (Image J 1.44p software) was used to estimate percent knockdown (*Pcsk9*/*Gapdh* loading control).

2.2.1.3 Lipopolysaccharide induced systemic inflammation

Healthy mice had activity level, body temperature, blood pressure, and cardiac function (echocardiography) assessed at baseline (time 0). Mice were then injected i.p. with LPS (20mg/kg, *E. coli* strain 01 II: B4, Sigma). This dose was determined from previous experiments where, in the background strain of C57BL/6 mice, LPS 20mg/kg delivered i.p. was the lowest dose which was lethal in all cases within 12 hours [324].

2.2.2 Physiologic assessment of mice

2.2.2.1 Activity index

Every hour post-LPS infusion mice were observed during 2 minutes for posture and activity. A score of 4 (normal) denotes that there were no times with a hunched posture, and the mouse had spontaneous rapid movements interspersed with eating, drinking and grooming. A score of 3 (mild) denotes occasional brief (5-20 seconds) hunched posture which spontaneously reverted to normal with ongoing spontaneous rapid movements interspersed with eating, drinking and grooming. A score of 2 (mild-moderate) denotes a longer (>20 seconds) period with hunched posture which spontaneously reverted to normal with ongoing spontaneous rapid movements interspersed with eating, drinking and grooming. A score of 1 (moderate-severe) denotes nearly continual hunched posture with movement only when subjected to strong external stimuli. Finally, a score of 0 (severe) denotes

continual hunched posture without movement and no response to strong external stimuli. Intervals of 0.5 were used if the mouse exhibited both levels within one observation period.

2.2.2.2 Temperature

Temperature was measured hourly using an infra-red thermometer (IR-101 La Crosse Technology, La Crosse, WI) held 2-3 mm from the abdomen. Once temperatures dropped below 34°C a rectal probe connected to the Vevo 770 ECHO (Visualsonics) machine was employed.

2.2.2.3 Blood pressure

At baseline (time 0) mean arterial blood pressure was measured using a non-invasive tail cuff (CODA 2, Kent Scientific, Torrington, CT). Six hours after LPS injection, mice were anesthetized using inhaled isofluorane (1-3%). Following a small laparotomy, the abdominal aorta was punctured using a 27 gauge needle then a number 2 French micromanometer catheter (Mikro-tip SPR-838, Millar Instruments Inc., Houston, TX) was inserted into the aorta. Mean arterial pressure was measured, and read from analysis software (PVAN 2.9, Millar Instruments Inc.).

2.2.2.4 Echocardiography

Mice were lightly anaesthetized using inhaled isofluorane (1-3%) and placed on a warming blanket. M-mode echocardiograms (ECHO) were targeted from 2D ECHOs obtained using the Vevo 770 ECHO (Visualsonics, Toronto, ON, Canada) operating at a 120Hz frame rate. Left parasternal 2D left ventricular cross-sectional echocardiographic images were obtained. The position and angle of the ECHO transducer is maintained by directing the beam just off the tip of the anterior leaflet of the mitral valve and by maintaining internal anatomic landmarks constant. All measurements were taken from M-

mode traces at end-expiration. Left ventricular internal dimensions were measured at end-diastole (defined as the onset of the QRS complex in lead II of the simultaneously obtained electrocardiogram) and at end-systole (defined as minimum internal ventricular dimension).

2.2.2.5 Multiplex cytokine assay

Plasma from wildtype and *Pcsk9*$^{-/-}$ mice, treated with either saline or 20mg/kg LPS, was diluted 4-50X to ensure that all measurements were within test ranges and 50µL per microplate well was added to duplicate wells of the Fluorokine® MAP mouse base kit microplate (R&D Systems, Minneapolis, MN), and the protocol followed as per the manufacturer's instructions. Microplates were analyzed using the Luminex100 instrument with accompanying 1.7 Software (Luminex Corporation). Cytokines were selected to represent early inflammation (TNF-alpha), an integrated inflammatory marker (IL6), an anti-inflammatory marker (IL10), a representative CC chemokine (JE as a murine homologue of human MCP1, official designation: CCL2) and a CXC chemokine (MIP-2 which is a murine homologue of human IL8).

2.2.2.6 Endotoxin assay

Plasma from the same wildtype and *Pcsk9*$^{-/-}$ mice used in the cytokine assays was diluted 1:10^6, then further diluted 1:2 before combining 50µL of each sample with 50µL of Limulus Amebocyte Lysate (LAL) at 37°C according the manufacturer's instructions (QCL-1000™, endpoint chromogenic LAL assay, Lonza Group, Basel, Switzerland). After 10 minutes, 100µL of substrate solution was added to each reaction and incubated for a further 6 minutes before stopping the reaction. The absorbance of each reaction was read at 410nm and the concentration of endotoxin in each sample was calculated from the standard curve.

Each sample was assayed in duplicate and results are described as endotoxin activity units per mL.

2.2.2.7 Low density lipoprotein receptor null (Ldlr$^{-/-}$) mice response to LPS

In further separate murine experiments low density lipoprotein receptor null (*Ldlr*$^{-/-}$) mice (Strain: B6.129 S7-*Ldlr*$^{tm1Her/J}$, Jackson Labs) were treated with either normal saline or berberine (Sigma-Aldrich) as described previously. Physiologic parameters were observed and/or measured before, and 6 hours after, i.p. administration of LPS (100mg/kg). This higher dose of LPS was required as it has been shown that *Ldlr*$^{-/-}$ mice have a reduced response to LPS compared to wild-type mice and require an ~8-fold higher dose of LPS to induce lethality [325].

These *Ldlr*$^{-/-}$ mice are homozygous for the *Ldlr*^{tm1Her} mutation and have higher than normal serum cholesterol levels when fed a normal diet (200-400 mg/dL compared to the 80-100 mg/dL of normal mice). Most atherosclerotic, diabetic, lipid and cardiovascular abnormalities only become evident after at least 12 weeks on a Western or high fat diet. In our experiments, all mice were fed a normal diet. No other obvious phenotypic differences were reported for mice fed a normal diet.

2.2.3 Human genetic association study

2.2.3.1 Vasopressin and septic shock trial (VASST) derivation cohort

VASST was a multicenter, randomized, double blind, controlled trial evaluating the efficacy of vasopressin versus norepinephrine in 778 patients who had septic shock [326], and vasopressor infusion of at least 5μg/min of norepinephrine, or equivalent [327]. Inclusion criteria and clinical phenotyping are described elsewhere [327]. DNA was

available from 632 patients. The research ethics boards of all participating institutions approved this trial and written informed consent was obtained from all patients or their authorized representatives. The research ethics board at the coordinating center (University of British Columbia) approved the genetic analysis.

2.2.3.2 St Paul's Hospital (SPH) validation cohort

All patients admitted to the ICU at St. Paul's Hospital (SPH) in Vancouver, Canada between July 2000 and January 2004 were screened and of these, 601 patients were classified as having septic shock [326] and had DNA available. Septic shock was defined by the presence of two or more diagnostic criteria for the systemic inflammatory response syndrome, proven or suspected infection, new dysfunction of at least one organ, and hypotension despite adequate fluid resuscitation [326]. Twelve patients were excluded as they had been included in the VASST cohort, leaving the remaining 589 patients for further study. Inclusion criteria and clinical phenotyping are described elsewhere [137]. The Institutional Review Board at St. Paul's Hospital and the University of British Columbia approved the study.

2.2.3.3 Genotyping and SNP selection

DNA was extracted from buffy coat of discarded blood samples using a QIAamp DNA Blood Midi Kit (Qiagen) (VASST cohort) or a QIAamp DNA maxi kit (Qiagen) (SPH cohort). The relatively common (MAF ≥0.5%) *PCSK9* missense LOF variants (rs11591147 R46L, rs11583680 A53V, rs562556 V474I) and a known GOF SNP (rs505151 G670E) were genotyped in the VASST cohort as part of whole genome genotyping using the Illumina Human 1M-Duo genotyping platform (Illumina Inc., San Diego, CA).

To select a tag SNP in *PCSK9* to test for replication in both cohorts, haplotypes were first resolved using PHASE [328] and then applied to dense CEU genotyping of *PCSK9* available from SeattleSNPs (http://pga.mbt.washington.edu/). A crossing over event is evident at approximately the middle of the gene resulting in the requirement for a large number of tag SNPs to resolve all possible haplotypes. It was found that in common haplotypes containing multiple SNPs, one haplotype was in modest linkage disequilibrium with all LOF and GOF variants. The software LDSelect [329] (http://droog.gs.washington.edu/ldSelect.html) was applied to SeattleSNPs dense genotyping to identify haplotype tag SNPs in the *PCSK9* gene. To simplify genotyping, tag SNP choice was limited to bins containing multiple SNPs. Linkage disequilibrium was then measured between tag SNPs within a bin and the three LOF SNPs and one GOF SNP. It was found that the LOF alleles of rs11591147, rs11583680, and rs562556 all preferentially segregated with the minor G-allele of tag SNP, rs644000, while the GOF allele of rs505151 was associated with the opposite A-allele of rs644000 (Figure 2.7). Accordingly, the *PCSK9* SNP best tagging LOF and GOF SNP was rs644000, which was selected for genotyping in both septic shock cohorts using the Illumina Golden Gate™ assay (Illumina Inc., San Diego, CA).

Haplotype	rs11591147 LOF R46L	rs11583680 LOF A53V	rs644000 Best tag SNP	rs562556 LOF V474I	rs505151 GOF G670E	Number of haplotypes in VASST	Percent haplotypes in VASST
1	C	G	A	A	A	735	55.5%
2	C	G	A	A	G	59	4.5%
3	C	A	A	A	A	6	0.5%
4	C	G	A	G	A	57	4.3%
5	C	G	G	A	A	151	11.4%
6	C	G	G	G	A	108	8.2%
7	C	A	G	A	A	136	10.3%
8	C	A	G	G	A	54	4.1%
9	A	G	G	G	A	6	0.5%
					rare haplotypes		0.9%

Figure 2.7 Relationship between Loss-Of-Function (LOF) and Gain-Of-Function (GOF) variants and rs644000 alleles in *PCSK9*

Haplotypes were resolved in VASST using PHASE [328] and haplotypes with MAF ≥0.5% are displayed. Minor alleles are colored for each SNP: LOF yellow, GOF green, rs644000 orange.

2.2.3.4 Primary and secondary outcomes

The primary outcome was 28-day mortality. Secondary outcomes chosen to parallel murine measurements included measurement of cardiovascular organ dysfunction and need for vasopressor administration, which were calculated as days alive and free of organ dysfunction or vasopressor use [157]. These calculations were repeated for other organ dysfunction and other therapeutic support [157] including respiratory, renal, hematologic, hepatic, and neurologic dysfunction as well as need for mechanical ventilation and renal replacement therapy.

2.2.3.5 Cytokine measurements

The systemic inflammatory response was assessed by measuring plasma cytokine levels in 335 patients from VASST cohort at the time of study enrollment. Human multiplex kits (EMD Millipore, Billerica, MA) were used according to the manufacturer's recommendations with modifications as described below. Samples were mixed with antibody-linked magnetic beads on a 96-well plate and incubated overnight at 4°C, with shaking. Plates were washed twice with wash buffer in a Biotek ELx405 washer. Following a one hour incubation at room temperature with biotinylated detection antibody, streptavidin-PE was added for 30 minutes with shaking. Plates were washed as above and PBS added to wells for reading using a Luminex 200 instrument (Illumina Inc.) with a lower bound of 100 beads per cytokine per sample. Each sample was measured in duplicate. To parallel the mouse cytokine measurements, cytokines were selected to represent early inflammation (TNF-alpha), an integrated inflammatory marker (IL6), an anti-inflammatory marker (IL10), and a representative CC chemokine (MCP1) and CXC chemokine (IL8).

2.2.4 Statistical analysis

Repeated measures analysis of variance was used to test for differences in activity level, temperature, and ejection fraction between *Pcsk9* knock-out and background control mice over time. Mann Whitney U tests were used to test for differences in mean arterial pressure because this variable was measured using different instruments at baseline and at 6 hours after LPS administration.

For human experiments, PHASE [328] was used to resolve haplotypes of *PCSK9* containing the LOF and GOF variants and rs644000 in VASST. For human septic shock the

primary analysis used logistic regression to determine the risk of mortality by *PCSK9* genotype, including the covariates of age, gender, Caucasian ancestry, and a surgical versus medical primary diagnosis in the statistical model. Cytokine concentrations were log-normally distributed so differences were tested for in logarithms of concentrations for both murine TNF-alpha, IL6, IL10, JE, and MIP-2 and for replication of directionally similar changes in human homologues TNF-alpha, IL6, IL10, MCP1, and IL8 using a one-way ANOVA.

Univariate analyses was performed using chi-square tests for categorical data and either Kruskal-Wallis tests or one-way ANOVA for continuous data. All tests were two-sided. Differences were considered significant if $P<0.05$. All analyses were performed using R (version 2.8.1, www.R-project.org) and SPSS version 16.0 (SPSS Inc, Chicago, IL) statistical software packages.

Chapter 3: A Common Polymorphism in the 5' Region of the Human *PROC* Gene Binds USF1

3.1 Background

Decreased protein C levels are associated with increased risk of venous thromboembolic events [152], myocardial infarction [330], stroke [331] and adverse outcome from severe sepsis [332]. Rare genetic variants (mutations) in the *PROC* gene result in protein C deficiency states due to decreased protein C production (Type I) or altered protein structure (Type II) [213, 261, 263, 333]. However, common genetic variants (MAF >10%) have also been reported to be associated with relative protein C deficiency [265] and with altered outcome from venous thrombosis [334], pulmonary embolism [207], cardiovascular disease [335], systemic meningococcemia [336] and sepsis [337]. Several investigators have suggested that common SNPs in the 5' region of *PROC* may contribute to the observed phenotypic effects by altering transcriptional regulation [260, 261, 265]. This seems likely since a number of rare genetic variants in the 5' region of *PROC* alter transcriptional regulation [213, 261, 263].

In many genes the promoter region and 5' introns, particularly intron 1 [338-340], contain important regulatory elements, consequently genetic variation in these regions may alter gene transcription [341-343]. The *PROC* gene is complicated by the presence of an untranslated exon 1. Classically, positional numbering of *PROC* is with respect to the start of translation in exon 2 so that exon 1 is generally considered to be part of the promoter region of *PROC* [261, 344], therefore, by extension, *PROC* intron 2 may have regulatory roles analogous to intron 1 of many other genes. Polymorphisms in the 5' region of *PROC*

associated with altered expression of *PROC* include two well documented promoter SNPs 13bp apart and commonly referred to as -1654 (rs1799808[C/T]) and -1641 (rs1799809[A/G]). (Note that this classical numbering of -1654 and -1641 is with respect to the start of translation in exon 2). The C-G and C-A haplotypes of these two SNPs are generally correlated with low circulating levels of protein C and are associated with a higher risk for thrombotic events, while the T-A haplotype is correlated with higher protein C levels and is associated with decreased risk of thrombotic events [265, 334]. Patients with severe sepsis who were homozygous for the C-A haplotypes of -1641 had significantly increased mortality and more organ dysfunction [137]. Exon 1 is untranslated in adults [201, 345] and contains a polymorphism (rs1799810) reported to be associated with altered plasma levels of protein C in healthy subjects [260] and in post-menopausal women [346]. The latter study also found an association with two common SNPs in intron 2 of *PROC*: rs2069910 and rs2069915. Furthermore, regulatory sequences affecting expression of protein C have been found in intron 1, about 500 bases downstream from the core promoter region which extends from upstream of exon 1 into intron 1 [263]. Genotype of the SNP rs2069912 in intron 2 was also found to be associated with adverse outcome in severe sepsis in patients of East Asian ancestry [347]. Thus, a number of high minor allele frequency SNPs in the 5' region of *PROC*, extending from the promoter region to the end of intron 2, are associated with low protein C levels and adverse outcomes in a variety of clinical states.

Whether these reported and other common SNPs within the 5' region of *PROC* causally contribute to transcriptional regulation of *PROC*, or whether they are simply in LD with a causal SNP or haplotype, has not been fully elucidated. Identifying causal SNPs using clinical association studies alone is difficult because there is a high degree of LD between

common SNPs in *PROC*. For example, the C-A haplotype of the -1654/-1641 promoter SNPs is in high LD with the C-allele of rs2069912 but association studies [137, 347] alone cannot determine which of these genetic variants, or others in LD, are causal. Therefore, *in vitro* assays of SNP functional effects are necessary. To identify potentially functional SNPs in the 5' region of *PROC* this study interrogated all SNPs having a minor allele frequency >10% in the region extending from the promoter to the end of intron 2 in *PROC*, reasoning that alteration of transcriptional regulation by differential binding of nuclear factors to different SNP alleles may point to functional SNPs.

3.2 Results

3.2.1 Real time-quantitative PCR assays

To determine whether sepsis processes affect the expression of *PROC in vitro*, a series of RT-qPCR Taqman® Gene Expression Assays (*PROC* probe: Hs00165584_m1 and *GAPDH* probe: Hs99999905_m1; Applied Biosystems Inc.) were performed using treatments designed to mimic these processes. Treatments included LPS, IFNG, TNF-alpha, dexamethasone, d-dimer, rhAPC and a triple combination of IFNG/TNF-alpha/d-dimer. Cells were harvested at 11 different time points, from 30 minutes to 48 hours. The primer sets were validated prior to RT-qPCR assays and were found to amplify fragments of the expected sizes with no primer-dimers (no amplification of the No Template Control (NTC) samples) and no amplification of genomic DNA (no amplification of the negative control No Reverse Transcriptase (-RT) samples) in Hep-G2 samples overexpressing *PROC*.

Expression of *GAPDH* was invariant in all three cells types used (B-lymphocytes, THP-1 and Hep-G2 cells) under all treatments employed (Figure 3.1).

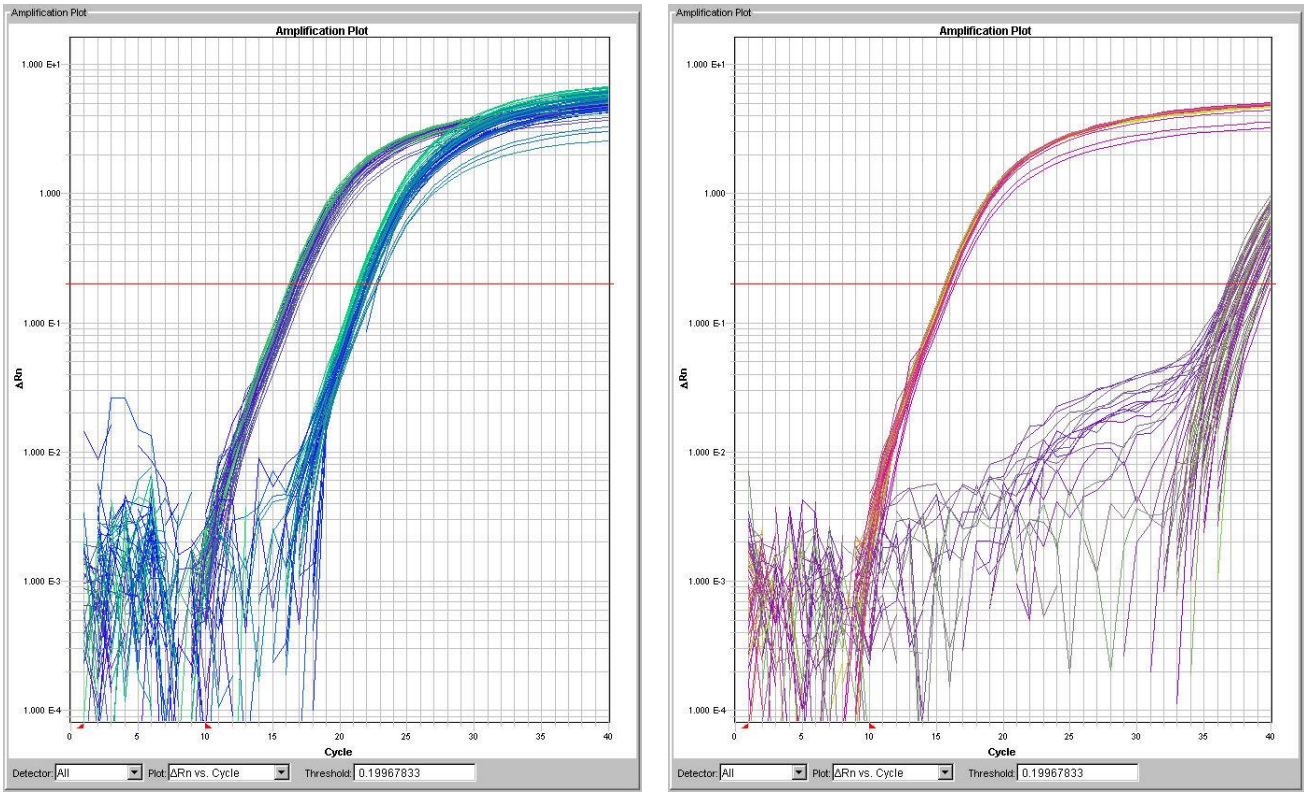

Figure 3.1 Cycle times for *PROC* and *GAPDH* mRNA amplification

Cycle times (C_T) reflect the amount of mRNA present. The panel on the left shows *GAPDH* and *PROC* amplification in Hep-G2 cells, while the panel on the right shows the same amplification in GM10857, a B-lymphocyte cell line. Each line represents a single sample and, in Hep-G2 cells, it can be seen that, for both *GAPDH* (leftmost curves) and *PROC* (rightmost curves), all lines fall in approximately the same place, indicating all mRNA concentrations are similar, regardless of any treatment. The samples for each protein included untreated samples and samples stimulated with a variety of treatments (see text in Methods). The curves for *PROC* in B-lymphocyte cells (panel on right, rightmost curves) only appeared after cycle 35 of 40, which indicates that there is no true amplification of *PROC* in these cells – any amplification curves that appear after cycle 35 are usually regarded as not amplified. Conversely, *GAPDH* amplified in the B-cells in a similar

manner as in the Hep-G2 cells. The horizontal red line in each panel indicates the threshold from which the measurements were taken and was set to ensure measurements were taken during the log phase of amplification.

In Hep-G2 cells, expression of *PROC* mRNA was invariant under all treatment regimens and at all time points tested, albeit at a lower concentration than *GAPDH*, as evinced by the higher cycle times for *PROC* mRNA compared to *GAPDH* mRNA (Figure 3.1). Conversely, although *GAPDH* amplified consistently in THP-1 cells, HeLa cells and in all B-lymphocyte cell lines tested, *PROC* mRNA was always below the level of detection in these cell types Figures 3.1 and 3.2). As results for amplification in THP-1 and HeLa cells were similar to B-lymphocyte cells, only results for the latter are shown.

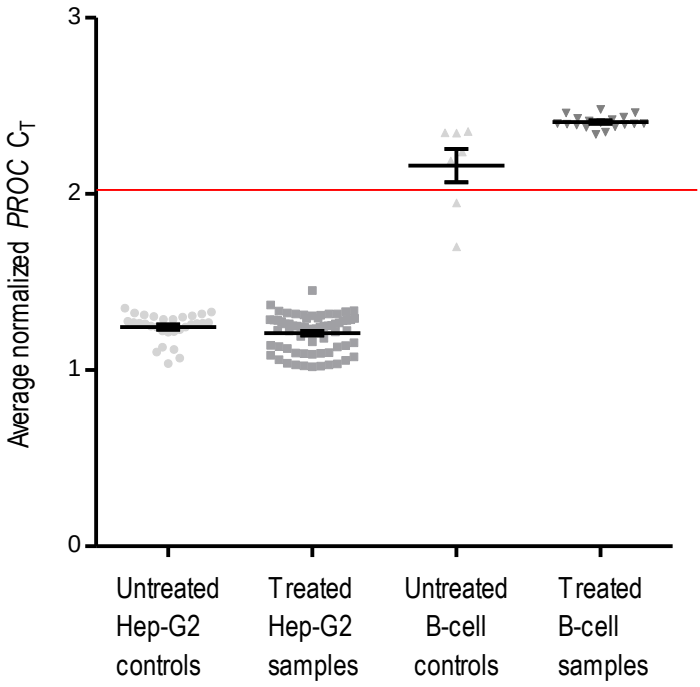

Figure 3.2 Expression of *PROC* mRNA by RT-qPCR assays

PROC and *GAPDH* mRNA were amplified in Hep-G2 and B-lymphocyte cells. Average cycle time (C_T) of *PROC* mRNA was normalized to *GAPDH* mRNA. Samples were quantified in triplicate and average C_Ts ± SD

are shown above. The red line indicates the cut-off C_T value above which quantification is considered undetermined. There was no significant difference in cycle times between treated and untreated samples in Hep-G2 cells (Unpaired t-test, P=0.107, n=66 and 30, respectively), a reflection of invariant *PROC* mRNA concentration between the two groups. As most mRNA concentrations of the B-lymphocyte samples were unquantifiable (untreated = 12, treated = 36), no analysis was possible. Data is shown from four independent, representative assays. The C_T for HeLa cells and THP-1 cells (not shown) were similar to the B-lymphocyte C_T shown here.

3.2.2 Hepatocyte-like gene expression in B-lymphocyte cells

Protein C is expressed primarily in hepatocyte cells but densely genotyped hepatocyte cells are not available, however the study laboratory possessed ~100 densely genotyped B-lymphocyte cell lines (Coriell Cell Repositories). Under normal culture conditions, expression of *PROC* mRNA in B-lymphocyte cells is below the threshold of detection as quantified by RT-qPCR, therefore alternate culture methods were employed in an attempt to force these cells to adopt a more hepatocyte-like expression pattern. Initially, expression of alpha-fetoprotein, a protein expressed specifically in liver cells, was confirmed in both normally-cultured Hep-G2 cells and adherent B-lymphocytes treated with HGF. The expression of alpha-fetoprotein demonstrates the differentiation of B-lymphocytes into a more hepatocyte-like phenotype, although alpha-fetoprotein expression concentrations were low. These low levels may have been due to the decrease in viability seen in all B-lymphocyte cell lines treated with HGF – viability was between 36% and 84%, compared to the usual >97%. Gene expression of *PROC* in these adherent, differentiated B-lymphocyte cells was attempted but, despite using several different primer sets and conditions, results were not conclusive, with several bands being seen for *PROC* where there should have been only two bands as per Hep-G2 cells (Figure 3.3). The internal control used throughout was

GAPDH and this amplified as a single band in all samples, as expected. Eventually one band was obtained in the B-lymphocyte samples and was confirmed by sequencing to be the expected *PROC* product, but this was achieved only after two rounds of PCR amplification of the B-lymphocyte samples. As this accomplishment required such excessive manipulation of the samples this approach was abandoned since it is unlikely to be relevant *in vivo*.

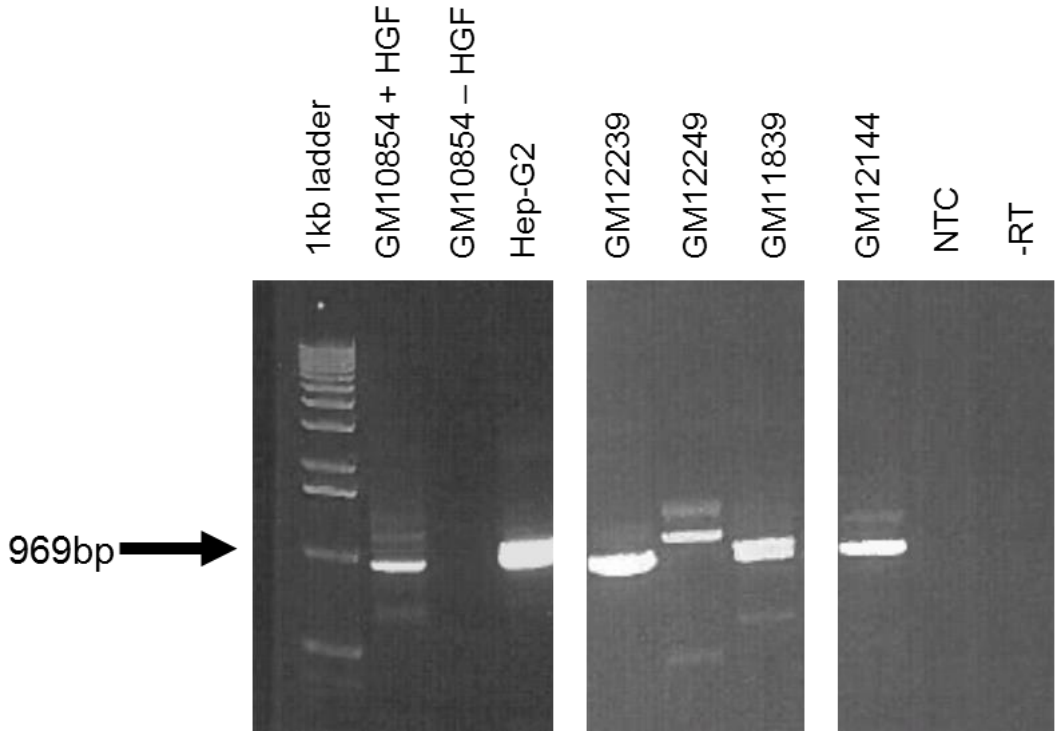

Figure 3.3 B-lymphocyte cells expressing *PROC*

Representative agarose gel images of PCR products after amplification of *PROC* cDNA in several B-lymphocyte cell lines and Hep-G2 cells. Lanes 2 and 3 show the difference in *PROC* expression between cells cultured with and without HGF, respectively. The four other B-lymphocyte cell lines (GM12239, GM12249, GM11839 and GM12144) treated with HGF display a variety of bands corresponding to the expected 969bp product. The positive control was *PROC* amplified in Hep-G2 cells and the two negative controls were NTC (no template control) and –RT (negative reverse transcriptase sample).

3.2.3 ELISA assays of protein C concentration after multiple treatments

In contrast to the consistent *PROC* mRNA expression seen in Hep-G2 cells in the RT-qPCR TaqMan™ Gene Expression assay results, concentration of secreted protein C, as per ELISA quantification, did vary with treatment. However, all treatments resulted in a reduction of protein C concentration compared to untreated controls; none of the six treatments or seven combinations of treatments tested produced an increase in protein C concentration in conditioned media of Hep-G2 cells, compared to untreated controls. Figure 3.4 displays the results of three ELISA assays using conditioned media from Hep-G2 cells harvested at 24 hours. Average absorbance (450nm, reference wavelength 620nm), a relative measure of protein C concentration, of untreated control samples (n=9) was significantly higher than the average absorbance of the treated samples (n=44, unpaired t-test, $P<0.0001$). Conditioned media harvested at 6, 12 and 48 hours showed similar trends between untreated controls and treated samples (data not shown) with absorbance being lower in the 12 hour samples, lowest in the 6 hour samples and highest in the 48 hour samples.

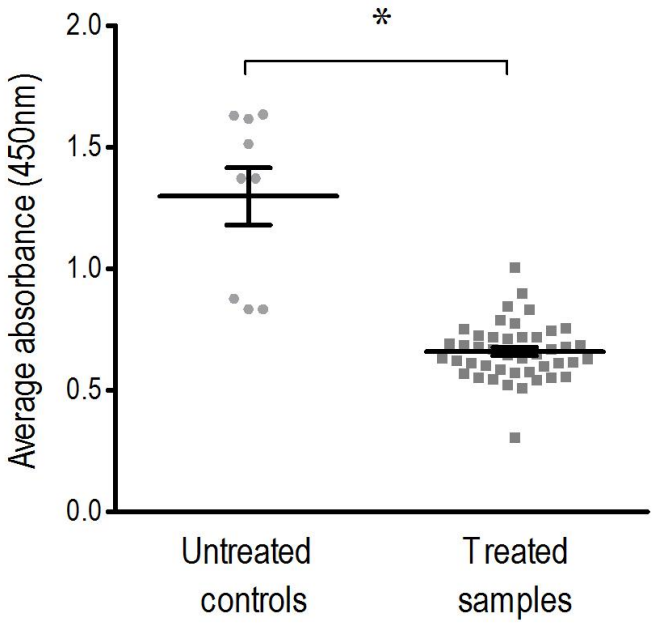

Figure 3.4 Relative protein C differences by ELISA assays

In Hep-G2 cells, average absorbance at 450nm, normalized to absorbance at 620nm, was significantly higher in untreated samples than in samples treated with LPS, IFNG, TNF-alpha, aPC, thrombin, d-dimer or combinations of these, harvested at 24 hours after start of treatment (unpaired t-test, *P<0.0001, n=9 and 44, respectively). Data shown are from three independent assays, mean ± SD, assayed in triplicate.

3.2.4 Viability assays

To further reduce error in interpretation of ELISA results, dye exclusion assays were performed on cells treated with high doses of LPS (5μg/mL), IFNγ (100ng/mL) and rhAPC (45ng/mL, 450ng/mL, 4500ng/mL and 45 000ng/mL). Dead or damaged cells take up trypan blue dye more readily than cells with intact outer membranes and are seen as a distinctive dark blue and are non-refractile when observed under a microscope, whereas live cells exclude the dye so appear light and refractile. Therefore, after counting cells using a

haemocytometer, the percentage of live, undamaged cells was calculated for each treatment type. After 12 and 24 hours of LPS treatment the percentage of viable cells was 91% and 90.2%, respectively, a difference of 0.8%. Similar differences were seen after IFNγ treatment (92.3% and 91.7%, a difference of 0.6%). Slightly higher viability was seen after treatment with aPC: 4500ng/mL, 97.5% and 96.9%, a difference of 0.6%; 45 000ng/mL 99.2% and 98.1%, a difference of 1.1%. The average viability of untreated Hep-G2 cells at the same two timepoints was 99.6% and 99.1%. Trypan blue dye exclusion assay is a crude assessment of cell viability and does not discriminate between necrotic and apoptosing cells, nevertheless in this context it shows that there was <1.5% difference in cell viability in treated or untreated cells over the 12 hours prior to the ELISA measurements. This is important when interpreting results of assays such as the ELISAs where cell concentration differences could contribute to differences seen in protein C concentrations. The <10% difference in viability within and between groups does not account for all the difference between groups (average 50.8%) as measured in ELISA assays (Figure 3.4). The high viability of cells treated with rhAPC may indicate a protective effect of aPC against apoptosis, especially at higher doses.

3.2.5 SNP selection

To limit confounding factors due to population admixture, only SNPs from the European populations listed at the variation discovery resource, SeattleSNPs, were surveyed. Ten SNPs with a minor allele frequency >10% lie between the promoter SNP, -1654, and the end of intron 2 in *PROC* (Table 2.1, Figure 3.5) and these were all selected for functional testing.

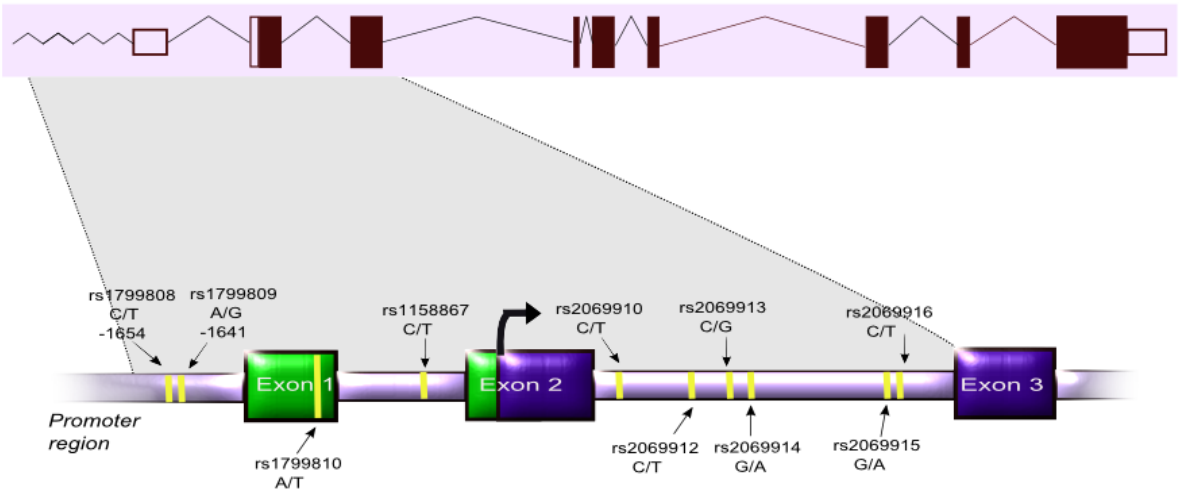

Figure 3.5 Placement of SNPs in the *PROC* gene selected for functional testing

Ten SNPs in the *PROC* gene region from -1654bp upstream of the start of transcription (within exon 2) to the end of intron 2 had a MAF >10% and were selected for functional testing. The diagram depicts the nine exons of *PROC*, including the 5' and 3' UTRs at the beginning and end of exons 1 and 9 respectively. The grey shaded area highlights the gene region under investigation. The bent arrow indicates the start of translation. *Figure created using Inkscape software version 0.48.4*

Several SNPs in the selected region were found to be in high LD, notably rs2069915, rs2069916 and promoter SNP -1654 (rs1799808), which together have an r^2 >0.83 (Figures 2.2 and 2.3).

3.2.6 Transcription factor binding to single nucleotide polymorphisms

Electrophoretic mobility shift assays were performed to determine which, if any, of the 10 selected SNP oligos bound nuclear factors differentially, thus making them likely to

be involved in regulating expression of *PROC*. Figure 3.6 displays the ratios of densitometry measurements for all 10 SNPs, reflecting the average relative binding of nuclear factors to each of the probes tested for at least 3 independent experiments for each SNP.

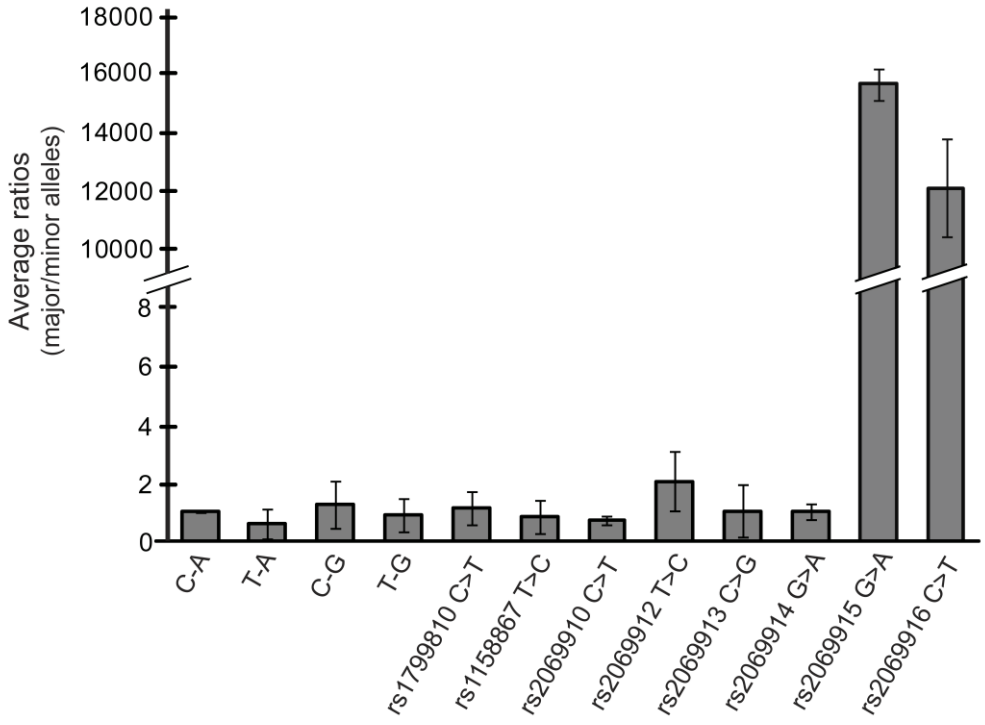

Figure 3.6 Average ratios of densitometry measurements

Measurements from at least 3 separate experiments, normalized to the minor allele of each SNP. The graph shows averaged ratios ± standard deviation of nuclear factor binding to all SNPs with a minor allele frequency >10% in the *PROC* gene region extending from the promoter region to the end of intron 2. Weak binding is seen for all SNPs except for rs2069915[G/A] and rs2069916[C/T]. Nuclear factor binding between the four promoter haplotypes was not significantly different between ratios normalized to the C-A haplotype, the haplotype containing the major alleles in Caucasian populations, (One-way ANOVA, P=0.29). Although some binding to rs2069912 was differential by allele this did not reach significance (Paired t-test, P=0.08, n=5).

Only SNPs rs2069915[G/A] and rs2069916[C/T] displayed differential binding by allele that was statistically significant. Nuclear factor binding to the rs2069915[G] oligo was significantly greater than to the A-allele oligo (Student's paired t-test, $P<1.9x10^{-9}$, n=24) and binding to the rs2069916[C] oligo was significantly greater than to the T-allele oligo (Student's paired t-test, $P<3.7x10^{-6}$, n=19). A representative gel is shown in Figure 3.7 that displays the extent of nuclear factor binding to five SNPs in intron 2.

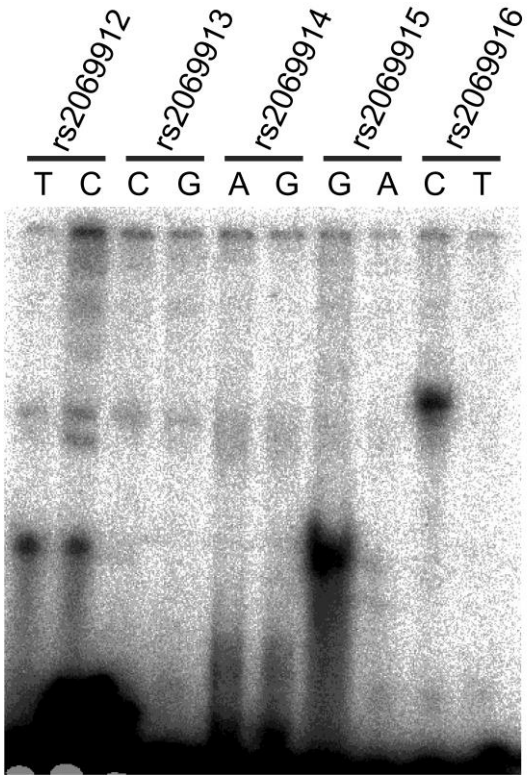

Figure 3.7 A representative gel containing five of the SNPs surveyed in this study

Strong differential binding by allele can be seen for rs2069915[G/A] and rs2069916[C/T]. The SNP rs2069912 shows weak differential binding that was not significantly different between alleles. The SNPs, rs2069913 and rs2069914 do not display differential binding between alleles. Free probe is visible at the bottom of the image.

Nuclear factor binding to the well-studied -1654/-1641 haplotypes (Figure 3.8) was much weaker than that observed for either rs2069915 or rs2069916 and did not differ significantly between haplotypes (Figure 3.6, ANOVA, P=0.29, n=8).

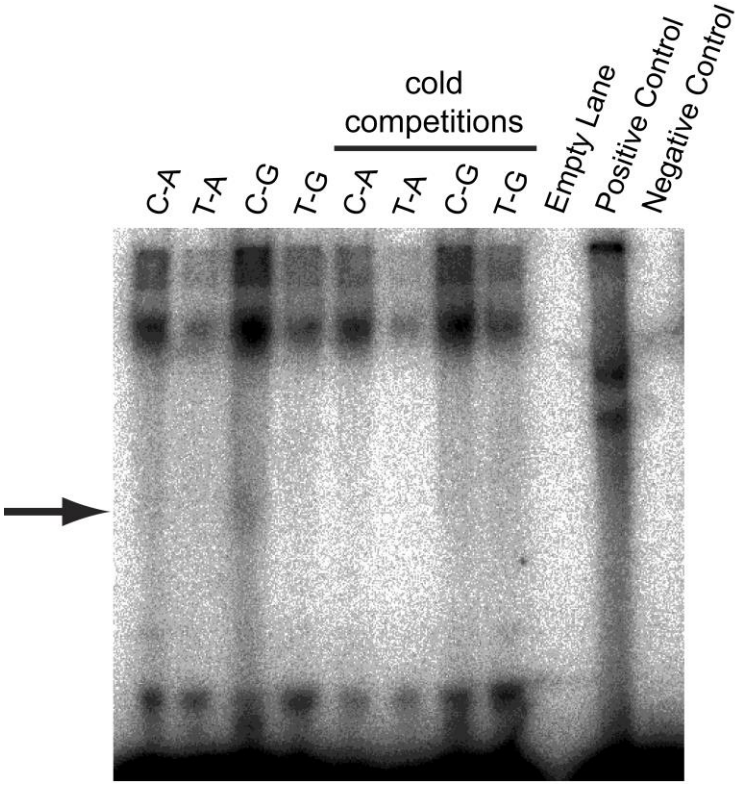

Figure 3.8 Binding of nuclear factors by promoter haplotypes of the *PROC* gene

The promoter haplotypes do not show significantly different binding between haplotypes, although the C-G haplotype appears to bind nuclear factors slightly more avidly than the other three haplotypes (arrow) this did not reach significance (One-way ANOVA, P=0.29, n=8). The apparent nuclear factor binding near the top and the bottom of the gel is likely non-specific binding as cold competition assays were unable to compete these bands away. The positive control contained a labeled probe containing the Sp1 transcription factor consensus sequence incubated in nuclear lysate from HeLa cells overexpressing Sp1. The negative control contained the labeled Sp1 probe and water in place of the nuclear lysate. Free labeled probe is seen at the bottom of the image.

3.2.7 Cold competition assays

To replicate the significant results and to test for specificity of nuclear factor binding to the probes, cold competition assays were performed using an unlabeled specific probe containing the same sequence and, separately, an unlabeled non-specific probe containing a scrambled sequence. For both rs2069915[G] (Figure 3.9) and rs2069916[C] (Figure 3.10) unlabeled specific probes in 50X molar excess competed the visible, labeled band away while non-specific, scrambled probes did not.

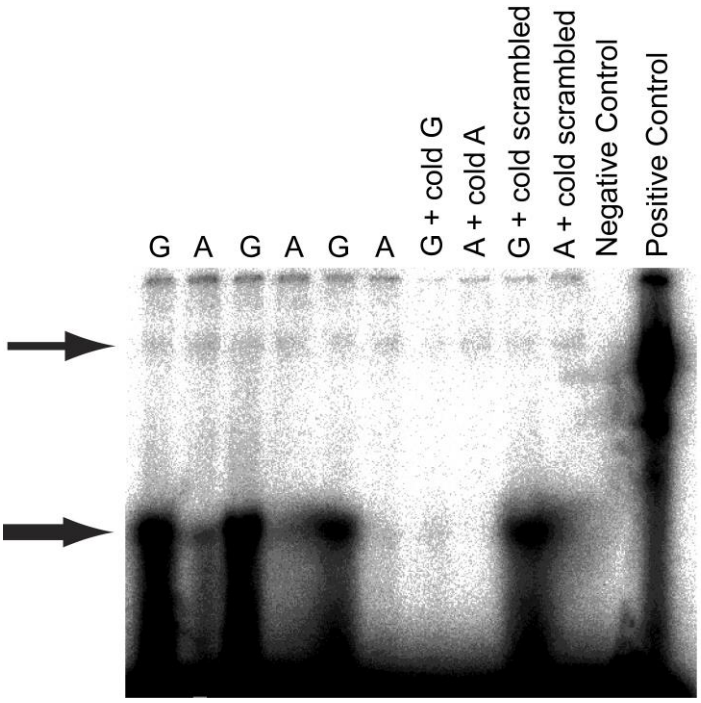

Figure 3.9 Binding of nuclear factors to SNP rs2069915[G/A]

EMSA with nuclear lysates from untreated Hep-G2 cells and ^{32}P labeled probe centered around each allele of the SNP rs2069915[G/A] shows selective nuclear factor binding to the G-allele while the A-allele displays weak or no binding, repeated three times (thick arrow). A 50X molar excess of a specific unlabeled competitor probe is able to reduce binding of the G-allele (G + cold G), while a non-specific unlabeled probe is not (G + cold scrambled). Non-specific binding (thin arrow) is evident in all lanes except the negative control lane. The

positive control contained a labeled probe containing the Sp1 transcription factor consensus sequence incubated in nuclear lysate from HeLa cells overexpressing Sp1. The negative control contained the labeled Sp1 probe and water in place of the nuclear lysate. Free probe is visible at the bottom of the image.

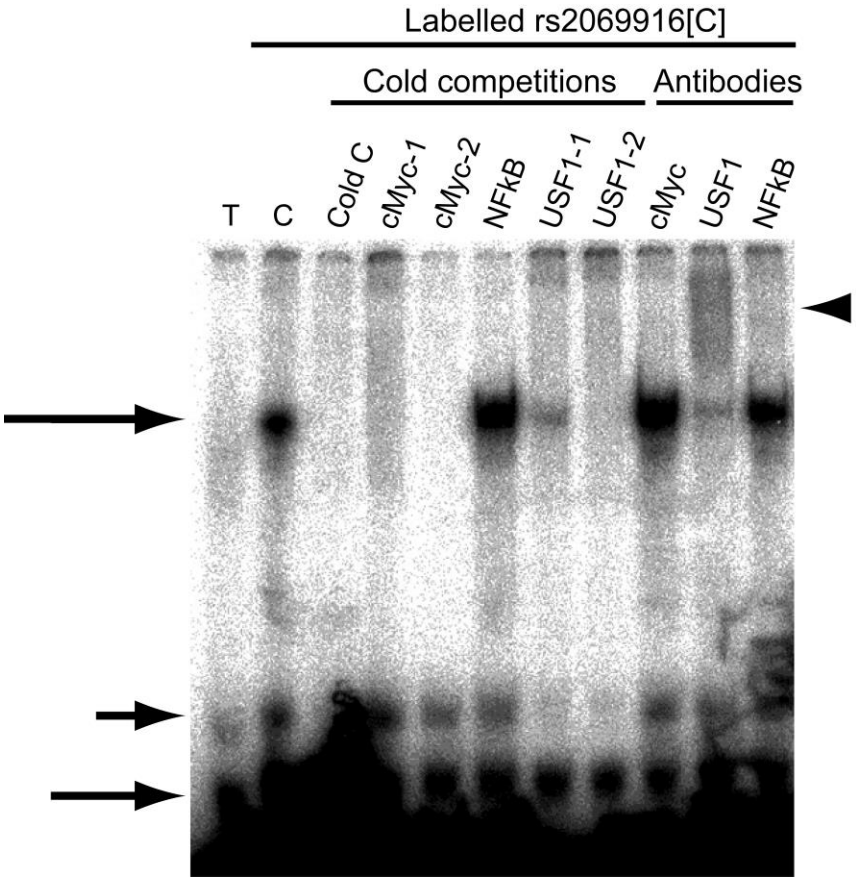

Figure 3.10 Binding of nuclear factors to SNP rs2069916[C/T]

The first two lanes show no protein binding by the T-allele but strong binding by the C-allele of rs2069916, and specificity of binding is indicated by the ability of a 50X molar excess of unlabeled probe containing the same sequence (cold C) to compete the band away (long arrow). Cold competition assays for rs2069916[C], using unlabeled probes containing consensus sequences of nuclear factors purported to bind this region, show that both cMYC and USF1 are likely candidates: a 50X molar excess of both consensus sequences completely competes the band away, while the probe containing the NFKB consensus sequence is unable to do so.

Supershift assays show that USF1, but not cMYC, is likely the nuclear factor that binds this probe, the arrowhead shows the supershifted band for USF1 while the bands for cMYC and NFKB are unchanged. This supershift result was obtained in six independent assays. The two lower arrows point to likely non-specific binding (long arrow) as this does not compete away and a possible accessory protein (short arrow) as, although this band competes away with 50X molar excess of unlabeled USF1 probe it unchanged by addition of USF1 antibody. Free probe is seen at the bottom of the image directly below the non-specific bands.

3.2.8 Identification of nuclear factors

To identify the nuclear factors that bind differentially to the DNA regions across the SNPs rs2069915 and rs2069916, database searches were performed using the ConSite and FastSNP databases. Using a stringency threshold of 70% and a minimum specificity of 10 bits, ConSite revealed that cREL, IRF1, NRF2, TEAD1 and E2F may bind at rs2069915, while USF1, cMYC and NFKB were possible binding candidates for rs2069916. The FastSNP database did not predict any nuclear factor binding partners for rs2069915 but did corroborate the results for rs2069916 by predicting USF1 (score 100.0) and N-Myc (the mouse equivalent of human cMYC, score 93.3) to bind across this SNP.

3.2.9 EMSA supershift assays

Subsequent cold competition EMSAs using 50X molar excess of unlabeled probes containing consensus sequences for these nuclear factors did not clearly identify potential binding partners for rs2069915. However, cold competition assays with oligos containing consensus sequences for NFKB, cMYC or USF1 showed the latter two competed away the visible rs2069916[C] band (Figure 3.10) suggesting these transcription factors as possible

binding candidates for this SNP. To test the validity of these results for rs2069916, EMSA supershift assays were performed using antibodies against USF1, cMYC, or NFKB. The binding of the protein complex to rs2069916[C] was supershifted by addition of a human polyclonal antibody against USF1 but not by addition of antibodies against either cMYC or NFKB (Figure 3.10).

3.2.10 Novel assay to identify SNPs binding transcription factors

Corroboration of the gel shift assay results was obtained by performing a novel bead-based assay in collaboration with Panomics Inc. In line with the gel shift assays, results of this bead-based assay clearly showed binding of a nuclear protein to the sequence surrounding the SNP rs2069916[C] (Figure 3.11A) but not to rs2069916[T]. From this assay it was not possible to identify the nuclear factor binding to rs2069916[C], except to say that the binding protein was not one of the transcription factors included in the panel.

Neither of the other two SNPs tested in the bead-based assay (rs2069912 and rs2069915) displayed binding of the transcription factors tested here (AP1, CEBP, GR/PR, HNF1, NFKB, RUNX1 (previously AML1), STAT3) above background levels for either allele (Figure 3.11B). All positive and negative controls behaved as expected (Figure 3.11B).

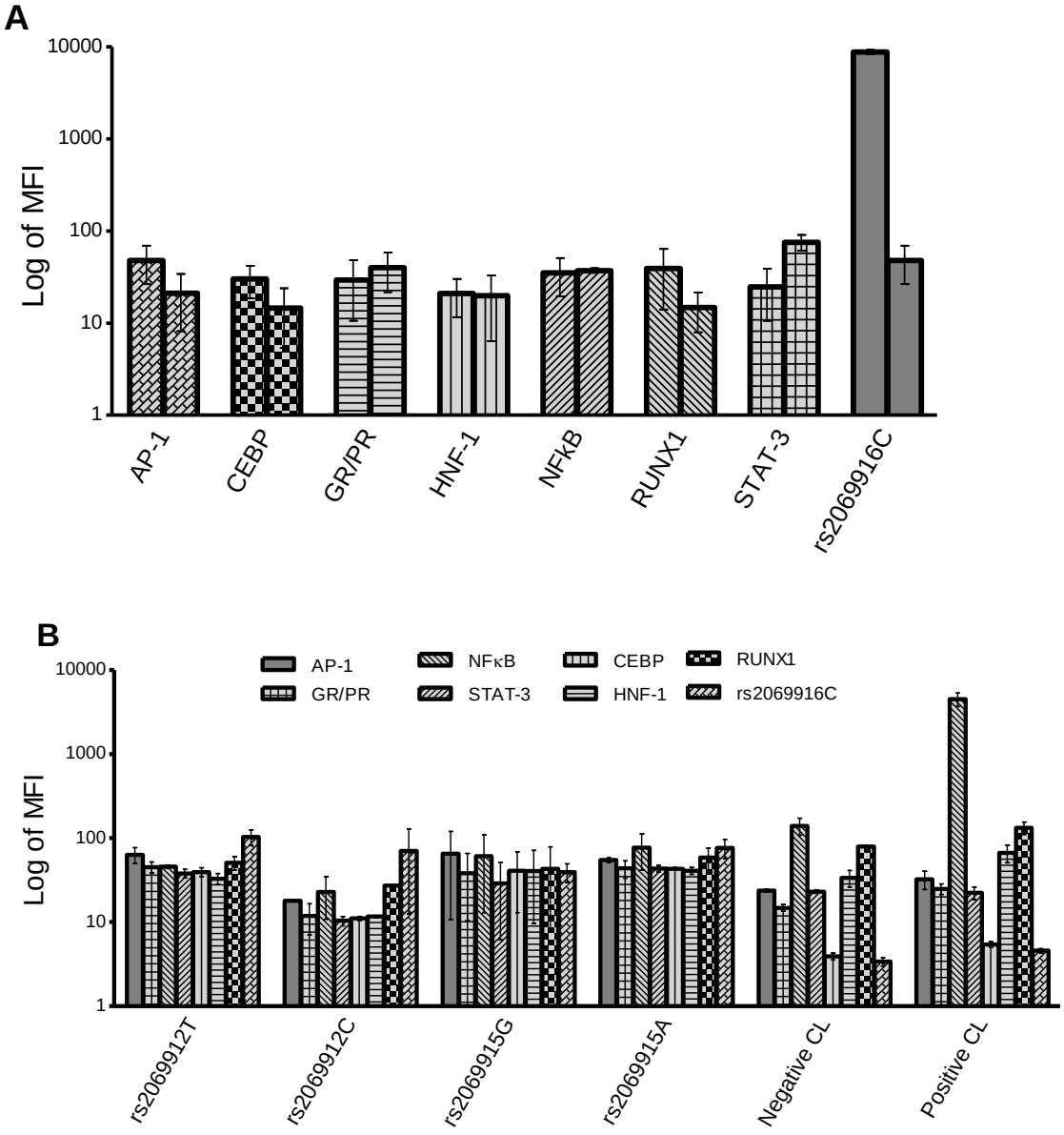

Figure 3.11 Results of novel bead-based "gel-shift" assay

Data were log transformed to ensure all data can be visualized. **A.** Untreated Hep-G2 nuclear lysate was incubated with probes containing the sequences for rs2069916[C] and [T] in separate reactions. Only the sequence for rs2069916[C] was found to bind a nuclear factor, however, the binding protein was not one of the transcription factors included in this assay. X-axis = Capture beads with conjugated transcription factor sequences as shown or the sequence surrounding rs2069916[C]. Each pair of columns reflects binding to first the major then the minor allele of rs2069916[C/T]. **B.** Untreated Hep-G2 nuclear lysate was incubated with

probes containing the sequences for rs2069912[T/C] or rs2069915[G/A]. Neither of the alleles of these two SNPs bound any of the transcription factors shown here, MFI was always in line with background levels (not shown, invariant from negative controls) and negative controls. As these sequences were not conjugated to Capture beads it is not possible to tell if these probes bound any other transcription factors. The positive control contained lysate from cells overexpressing NFKB. MFI, mean fluorescent intensity.

3.2.11 Identifying nuclear factors using SILAC mass spectroscopy analysis

Quant analysis of protein fragments containing either "heavy" or "light" isotopes of lysine and arginine amino acids and identification using MASCOT software (Matrix Science Inc., Boston, MA) indicates that the complex bound to the probe sequence centered on rs2069915[G] contains, almost exclusively, histone cluster 1 family members (Table 3.1).

Table 3.1 SILAC mass spectroscopy results for rs2069915[A/G]

# Peptides	Heavy/Light Ratio	Description	Protein function	UniProtKB Accession Number
8	4.438	histone H1b	Histones H1 are necessary for the condensation of nucleosome chains into higher order structures. Binds to linker DNA between nucleosomes forming the macromolecular structure known as the chromatin fiber.	P10412
8	3.650	histone cluster 1, H1c	Histone H1 protein binds to linker DNA between nucleosomes forming the macromolecular structure known as the chromatin fiber. Histones H1 are necessary for the condensation of nucleosome chains into higher-order structured fibers. Acts also as a regulator of individual gene transcription through chromatin remodeling, nucleosome spacing and DNA methylation	P16403
4	4.489	H1 histone family, member 0	Histones H1 are necessary for the condensation of nucleosome chains into higher-order structures. The H1F0 histones are found in cells that are in terminal stages of differentiation or that have low rates of cell division.	P07305

# Peptides	Heavy/Light Ratio	Description	Protein function	UniProtKB Accession Number
3	3.044	histone cluster 1, H1b	Acts also as a regulator of individual gene transcription through chromatin remodeling, nucleosome spacing and DNA methylation	P10412 and P16401
2	15.983	nucleolar protein 1, 120kDa	May act as ribosomal RNA methyltransferase.	P46087
18	0.439	ATP-dependent DNA helicase II, 70 kDa subunit	Key enzyme involved in DNA replication and DNA repair in nucleus and mitochondrion.	P51530
14	0.457	ATP-dependent DNA helicase II	Key enzyme involved in DNA replication and DNA repair in nucleus and mitochondrion.	P51530
10	0.010	unnamed protein product		
10	0.010	unnamed protein product		
6	0.231	unnamed protein product		
5	0.215	unnamed protein product		
4	0.015	unnamed protein product		
3	0.118	chaperone protein HSP90 beta	Molecular chaperone that promotes the maturation, structural maintenance and proper regulation of specific target proteins involved for instance in cell cycle control and signal transduction. Undergoes a functional cycle that is linked to its ATPase activity. This cycle probably induces conformational changes in the client proteins, thereby causing their activation..	P08238
3	0.386	unnamed protein product		
2	0.010	unnamed protein product		
2	0.011	unnamed protein product		
2	0.011	unnamed protein product		
2	0.292	unnamed protein product		
2	0.408	Chain A, Crystal Structure Of Human 17-Beta-Hydroxysteroid Dehydrogenase Type 4 In Complex With Nad	Lipid metabolism	P51659

Dark mauve colour = binding of nuclear factors to rs2069915[G]

Light mauve colour = binding of nuclear factors to rs2069915[A]

While the probe sequence centered on s2069916[C] also binds a histone cluster 1 protein family member, this complex also contains nucleic acid-associating proteins such as NHP2, HNRPM as well as actinin, a structural stabilizing protein, and others (see Table 3.2). In addition, proteins normally associated with ribosomal assembly or stabilization (ribosomal proteins SA and S8, NHP2, NCL) were also seen to bind to this probe, however, the most abundant protein binding to the rs2069916[C] probe was unidentifiable. Interestingly, the ribosomal associating proteins and NCL, DEAH and HNRPM are known to associate in the same complex on untranslated mRNA [348-350].

The probes containing sequences centered on the minor alleles of each SNP, rs2069915[A] and rs2069916[T], were found to bind proteins known to be involved with transcription, such as ATP-dependent DNA helicase and poly (ADP-ribose) polymerase family, member 1. In fact, these two proteins were identified as the most common proteins binding to rs2069915[A] and rs2069916[T], respectively (Tables 3.1 and 3.2). The probe containing the sequence centered on rs2069916[T] was also found to bind other proteins involved with active transcriptions, such as a protein with the ability to cause DNA bending (High-mobility group box 2) and a protein involved in unwinding double-stranded DNA (High-mobility group box 3). In addition, this sequence also bound several proteins involved in enzymatic reactions related to transcription such as ATP binding (HSP90AB1), DNA ligase II, polynucleotide kinase and DNA polymerase-beta interaction (DNA repair protein XRCC1) (Table 3.2). Both Tables 3.1 and 3.2 contain selected results: proteins with ratios falling between 0.5 and 2.0 or with <2 identifying peptides, as well as contaminating proteins such as keratin and albumin were removed for clarity. For a complete lists of all SILAC mass spectroscopy results see Appendix A, Tables A.5 and A.6.

Table 3.2 SILAC mass spectroscopy results for rs2069916[C/T]

# Peptides	Heavy/Light ratio	Description	Protein function	UniProtKB Accession Number
6	2.130	unnamed protein product		
5	2.726	HSP90AB1 protein	ATP binding, stress response, protein and unfolded protein binding	Q6PK50
3	2.197	unnamed protein product		
2	2.236	NHP2 non-histone chromosome protein 2-like 1	Binds to the 5'-stem-loop of U4 snRNA and may play a role in the late stage of spliceosome assembly. The protein undergoes a conformational change upon RNA-binding.	P55769
2	2.260	ribosomal protein SA, isoform CRA_c	Required for the assembly and/or stability of the 40S ribosomal subunit. Required for the processing of the 20S rRNA-precursor to mature 18S rRNA in a late step of the maturation of 40S ribosomal subunits.	P08865
2	2.312	Chain A, The Crystal Structure Of The Exon Junction Complex*	Component of a splicing-dependent multiprotein exon junction complex deposited at splice junction on mRNAs. Phosphorylation redistributes it from the nuclear speckles to the nucleoplasm.	Q9UKV3
2	2.326	NCL protein *	Found in the nucleolus. Binds both RNA and DNA.	Q9BQ02
2	2.391	actinin alpha4 isoform*	Localized in nucleus. Has been found bound to unprocessed mRNA. F-actin cross-linking protein which is thought to anchor actin to a variety of intracellular structures and HNR proteins.	O43707
2	2.477	ribosomal protein S8 *	In complex, bound to untranslated mRNA, composed, in part, of HNRPM, actinin alpha4 and NCL.	P62241
2	2.503	DEAH (Asp-Glu-Ala-His) box polypeptide 9, isoform CRA_a*	Unwinds double-stranded DNA and RNA in a 3' to 5' direction. Alteration of secondary structure may subsequently influence interactions with proteins or other nucleic acids. Identified in a complex bound to untranslated mRNA.	Q08211
2	2.757	HNRPM protein*	Heterogeneous nuclear ribonucleoprotein M; Pre-mRNA binding protein in vivo. Involved in splicing.	Q6P2D7
2	3.324	hypothetical protein		
2	4.314	histone 1, H2bj, isoform CRA_b	Core component of nucleosome. Nucleosomes wrap and compact DNA into chromatin, limiting DNA accessibility to the cellular machineries which require DNA as a template.	P06899

# Peptides	Heavy/Light Ratio	Description	Protein function	UniProtKB Accession Number
32	0.426	poly (ADP-ribose) polymerase family, member 1	Involved in DNA repair processes. Positively regulates transcription of certain genes.	P09874
32	0.427	poly(ADP-ribose) polymerase	as above	P09874
11	0.010	unnamed protein product		
9	0.359	glyceraldehyde-3-phosphate dehydrogenase	Participates in nuclear events including transcription, RNA transport, DNA replication and apoptosis. Upon interferon-gamma treatment assembles into the GAIT complex which binds to stem loop-containing GAIT elements in the 3'-UTR of diverse inflammatory mRNAs and suppresses their translation.	P04406
7	0.010	unnamed protein product		
7	0.433	unnamed protein product		
6	0.423	unnamed protein product		
5	0.363	DNA repair protein XRCC1	Corrects defective DNA strand-break repair. Interacts with polynucleotide kinase, DNA polymerase-beta and DNA ligase III.	P18887
5	0.397	high-mobility group box 2	DNA binding proteins that associates with chromatin and has the ability to bend DNA	P26583
5	0.434	MAP4 protein	Non-neuronal microtubule-associated protein. Promotes microtubule assembly. Phosphorylated upon DNA damage, causing detachment from microtubules, and their disassembly.	P27816
4	0.040	filaggrin family member 2	Possibly involved in calcium ion binding	Q5D862
3	0.026	unnamed protein product		
3	0.373	inosine monophosphate dehydrogenase 2	Catalyzes the conversion of inosine 5'-phosphate (IMP) to xanthosine 5'-phosphate (XMP), the first committed and rate-limiting step in the de novo synthesis of guanine nucleotides, and therefore plays an important role in the regulation of cell growth. Could also have a single-stranded nucleic acid-binding activity and could play a role in RNA and/or DNA metabolism.	P12268
3	0.389	high-mobility group box 3	Binds preferentially single-stranded DNA and unwinds double stranded DNA	O15347

# Peptides	Heavy/Light Ratio	Description	Protein function	UniProtKB Accession Number
3	0.446	Chain B, Human ApurinicAPYRIMIDINIC ENDONUCLEASE-1 (Ape1)	Multifunctional protein that plays a central role in the cellular response to oxidative stress. The two major activities are DNA repair and redox regulation of transcriptional factors.Plays a role in regulating MYC mRNA turnover by preferentially cleaving in between UA and CA dinucleotides of the MYC coding region determinant. Binds DNA and RNA.	P27695
3	0.461	protein disulfide isomerase A5 precursor	Catalyzes the rearrangement of -S-S- bonds in proteins.	Q14554
2	0.011	unnamed protein product		
2	0.406	unnamed protein product		
2	0.408	Chain A, Crystal Structure Of Human Recq-Like Dna Helicase	DNA helicase that may play a role in the repair of DNA that is damaged by ultraviolet light or other mutagens.	P46063
2	0.432	endothelial differentiation-related factor 1 isoform beta	Transcriptional coactivator stimulating transcriptional activities. Enhances the DNA-binding activity of ATF1, ATF2, CREB1 and NR5A1. May function in endothelial cells differentiation, hormone-induced cardiomyocytes hypertrophy and lipid metabolism.	
2	0.462	hypothetical protein		
2	0.464	CGI-55	May play a role in the regulation of mRNA stability. Binds to the 3'-most 134 nt of the SERPINE1/PAI1 mRNA, a region which confers cyclic nucleotide regulation of message decay.	Q8NC51
2	0.474	unnamed protein product		

Dark mauve colour = binding of nuclear factors to rs2069916[C]

Light mauve colour = binding of nuclear factors to rs2069916[T]

*These proteins have been seen forming part of the same complex binding to unprocessed mRNA

3.2.12 siRNA knockdown of USF1

Knockdown of USF1, the nuclear factor shown by EMSA cold competition and supershift assays to bind rs2069916[C], by siRNA techniques resulted in an increase of secreted protein C compared to controls as measured by protein C ELISA assays. Protein C was measured in conditioned media harvested 48 hours after transfection with either the USF1 siRNA probe or a control siRNAprobe. The difference in protein C concentration in the conditioned media of cells transfected with the siRNA probe and those transfected with the control siRNA probe was statistically significant at 48 hours (Mann Whitney U test, P=0.004, n=6; Figure 3.12).

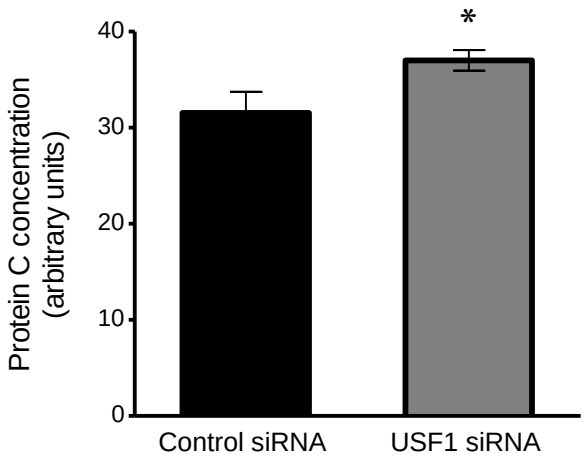

Figure 3.12 Increase in protein C expression after inhibition of USF1

After transfection into Hep-G2 cells, the siRNA probe was able to knockdown expression of USF1, resulting in a statistically significant increase in expression of protein C compared to cells transfected with a control siRNA probe that did not affect USF1 expression, as measured by ELISA assay (Mann Whitney U test, P=0.004, n=6). Data are mean ± SD.

3.2.13 TaqMan™ SNP genotyping assays

To determine whether siRNA knockdown of USF1 affects expression of *PROC* mRNA in Hep-G2 cells we utilized TaqMan™ SNP genotyping assays to quantify mRNA transcripts containing each allele of the *PROC* coding SNP, rs1799810[A/T]. By comparing the number of transcripts of each allele before and after USF1 knockdown it is possible to determine if inhibiting USF1 affects *PROC* expression. The cDNA of each sample was normalized to the gDNA amplified in the same sample to remove any loading bias. Comparison of the normalized samples showed no difference in expression between the control siRNA samples when amplified using probes containing either the T-allele or A-allele of rs1799810 (2-tailed Student's t-test, P=0.366). Moreover, there was no difference in expression between the USF1 siRNA samples amplified using either of these probes (2-tailed Student's t-test, P=0.874). Furthermore, no expression differences were seen between the control siRNA samples and the USF1 knockdown (siRNA) samples for either allele (2-tailed Student's t-test, P=0.721 and 0.167 for rs1799810[A] and rs1799810[T], respectively).

3.2.14 Luciferase assays

To determine whether haplotypes of rs2069915 and rs2069916 could modify transcription, Hep-G2 cells were transiently transfected with constructs containing the TCG alleles of rs2069912, rs2069913 and rs2069914 and either the A-T or G-C haplotypes of rs2069915 and rs2069916: TCGAT and TCGGC, respectively. Luciferase activity was significantly greater with the construct containing the A-T haplotype compared to the construct containing the C-G haplotype (Mann Whitney U test, P=0.022, n=12, Figure 3.14).

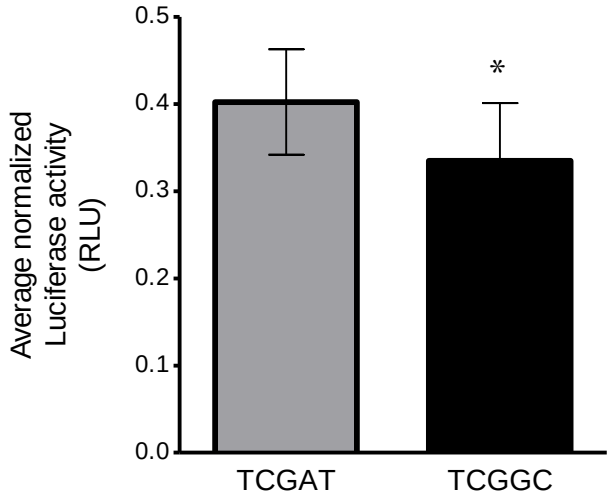

Figure 3.13 Luciferase reporter activity in two haplotypes of *PROC*

Luciferase reporter activity was compared between two different constructs spanning a 421bp region of *PROC* intron 2. The constructs were homozygous for the major alleles of SNPs rs2069912, rs2069913 and rs2069914 (TCG) and either the major or minor alleles of rs2069915 and rs2069916: TCGGC and TCGAT, respectively. Luciferase reporter assays show the vector containing the G-C haplotype of rs2069915[G/A] and rs2069916[C/T] (TCGGC) has a significantly limited ability to drive expression of the firefly luciferase gene compared to the vector containing the A-T haplotype of these two SNPs (TCGAT). The assay was performed in Hep-G2 cells (Mann Whitney U test, P=0.022, n=12, data are mean ± SD). RLU, Relative Light Units.

3.3 Discussion

Severe sepsis and septic shock are conditions known to have extremely high mortality rates despite many available drugs and interventions being employed. Protein C plays an important role in modulating outcome in patients in the ICU with these conditions as protein C is known to be active in several pathways shown to be important in the course of sepsis. Although protein C is most well known as an anti-coagulant molecule it also acts as an anti-

inflammatory modulator, a pro-fibrinolytic molecule, an anti-apoptotic molecule and plays a role in the innate immune system.

To determine whether sepsis affects expression of *PROC*, this study first attempted to find a treatment for *in vitro* assays that would a) increase and b) decrease expression of *PROC* mRNA. Treatments were chosen that are known to invoke the inflammatory and immune responses of patients with sepsis, as well as molecules known to play a role in the coagulation cascade, the most well-known of all the functions of protein C. None of the treatments employed perturbed expression of *PROC* mRNA in Hep-G2 cells. Clearly, a feedback system does not appear to be triggered by aPC to replenish endogenous protein C as it is consumed by conversion to aPC during a sepsis event. It was impossible to induce B-lymphocyte cells to express *PROC* in measureable concentrations without excessive manipulation, therefore the approach to use the densely genotyped B-lymphocyte cell lines was abandoned.

Interestingly, all treatments employed reduced secreted protein C concentration in conditioned media of Hep-G2 cells. It was not possible to increase protein C concentration in conditioned media, despite trying several different treatment concentrations, treatment combinations and harvesting time points. As the ELISA assay used here measures endogenous protein C as well as aPC, the lower concentrations observed do not necessarily reflect an increase in conversion of endogenous protein C to aPC in the treated cells, but rather an overall reduction. From the results of these assays it is not possible to determine whether endogenous protein C or aPC contributes most to the measurements obtained here. It is tempting to speculate that the results reflect a reduction in endogenous protein C due to

conversion to aPC and that much of the aPC was bound to various receptors and was therefore unavailable for quantification.

The viability assays confirmed that the ELISA assay results likely reflect true differences in protein C concentrations due to treatment type, and not to a disparity in cell number between samples caused by the treatments. The maximum viability difference between samples was less than 10%, while the protein C differences between treated and untreated samples as measured by ELISA was an average of 50.8%.

Screening for potential functional effects of common polymorphisms (MAF >10%) was undertaken in the 5' region of *PROC*. A number of mutations in the untranslated exon 1 and beginning of the first intron have been shown to have a functional effect in modulating *PROC* expression but these mutations are rare in Caucasian populations and therefore do not appear to account for associations between common SNPs and disease outcomes [260, 261, 263]. Many common genetic variations in the promoter and 5' region of the *PROC* gene have previously been associated with outcome in a variety of disease states [265, 334, 351] but, to date, have not been determined to be the causal or functional mutations. Recently, as part of the large ARIC (Atherosclerosis Risk in Communities) study, Tang *et al.* (2010) found an association between one of the SNPs tested here, rs1158867, and plasma levels of protein C [351]. In this study, rs1158867 was tested by gel shift assay for differential nuclear factor binding by allele but no difference was found and any binding was very weak, barely above background levels, reducing the probability that this SNP was the causal SNP accounting for this observation. Smith *et al.* (2007) tested for association between SNPs in coagulation pathway genes and venous thrombosis in peri- and post-menopausal women and found four SNPs in *PROC* to be significantly associated: rs1799810, rs2069910, rs2069915

and rs5937 [346]. The first three of these SNPs are found in the 5' region of *PROC* and were included in this study. Of these three SNPs, only rs2069915 showed strong, differential binding by allele. Interestingly, rs1799810 and rs1158867 are in complete LD (r^2=1) and although the FastSNP database does not propose any function for rs1158867, it suggests rs1799810 may be involved in regulating splicing events. However, rs1799810 is in 23% LD with rs2069915 and 41% LD with rs2069916, while rs1158867 is in 15% and 26% LD, respectively (Appendix A, Table A.2). Further studies need to be undertaken to determine the extent to which SNPs with other functions, such as altering splicing sites, affect protein C deficient states. Russell *et al.* (2008) found an association between rs2069912 and increased mortality in East Asian patients with severe sepsis [347] and in this study this SNP did display differential binding by allele. However, binding was minimal and further tests are needed to determine if this SNP plays a functional or supporting role – as rs2069912 lies just 224bp upstream from rs2069916 it is possible that nuclear factors binding these SNPs may form part of the same complex, although there is little LD between rs2069912 and rs2069915 (19%) or rs2069916 (17%). In addition, only Caucasian patients were used in this study which may not reflect racial differences of SNP effects.

Many reports in the current literature have examined -1654 and -1641 promoter region SNPs (rs1799808[C/T] and rs1799809[A/G]) and their haplotypes. The T-A haplotype is associated with the highest levels of protein C *in vitro* and *in vivo* while the C-G and C-A haplotypes are associated with the lowest levels of protein C *in vitro* [352] as well as in plasma, with a worse outcome in patients in a variety of disease states [265, 334, 336]. To date the identity of potential nuclear factor(s) binding these promoter haplotypes have not been elucidated. Very little nuclear factor binding to oligonucleotides centered on these

promoter SNPs was found in this study, reducing the probability that these SNPs or their haplotypes functionally alter transcription, and increasing the possibility that SNPs in LD with haplotypes of these promoter region SNPs may be functionally more important. Indeed, this was found in this study, with the T-A haplotype of the promoter SNPs being in 100% LD with the A-T haplotype of rs2069915-rs2069916 (Figure 2.2) and the latter haplotype was associated with increased transcription in luciferase reporter assays compared to the G-C haplotype of these SNPs (Figure 3.14).

Dramatic differential binding of nuclear factor(s) between the alleles of SNP rs2069915[G/A] was found, with the G-allele evincing very strong binding, while binding to the A-allele was very weak. Similarly, the C-allele of SNP rs2069916[C/T] showed significantly stronger binding than the T-allele. None of the other SNPs interrogated displayed significant differential binding by allele and therefore, of the SNPs interrogated, rs2069915[G/A] and rs2069916[C/T] appear most likely to be functional and were selected for further testing. These two SNPs are in very high linkage disequilibrium (r^2=0.91) and lie only 37 bases apart therefore it is possible that either proteins binding to both regions form part of the same complex, or that protein binding to one region is influenced by the other.

Identification of the nuclear factors binding these regions was attempted first by adding an excess of unlabeled probe containing the consensus sequences of nuclear factors purported to bind these particular regions. Potential binding partners were selected after database and literature searches. For SNP rs2069916, cMYC, USF1 or NFKB were imputed to bind this region and indeed, cold competition assays showed cMYC and USF1 were able to compete for nuclear factor binding, but NFKB was not. Cold competition EMSA assays demonstrated the high affinity and specificity of nuclear factor binding to rs2069915[G] and

rs2069916[C] and supershift assays showed that the factor binding to the latter was likely the transcription factor, USF1. The shift in the visible gel band to a higher position in the gel indicates affinity of the antibody for the protein, resulting in a larger complex with slower migration through the gel and a visibly "supershifted" band in the gel. This affinity identifies USF1 as the nuclear factor binding the DNA in this region – if USF1 was merely part of a complex it is likely the visible band would only have been reduced in cold competition and supershift assays, and not completely abrogated as seen here. Binding of an antibody to a protein/DNA complex will increase the size of the complex, causing further retardation as the complex moves through the gel resulting in a supershifted band at a higher position. Alternatively, nuclear factor binding to DNA may be disrupted if the epitope recognized by the antibody is the same as the DNA binding region: steric hindrance will result in less protein binding the DNA and, consequently, a less visible band.

Luciferase reporter assays with vectors containing the haplotypes of the major alleles of these two SNPs showed significantly decreased transcription compared to the vector containing the minor allele haplotype, A-T. The well-studied transcription factor USF1 has been reported to be an activator of transcription in some systems and a repressor in others [353-355]. In addition, a report of USF1 binding to motifs downstream of a transcription start site shows USF1 functioning as a repressor [356].

The unlabeled probe containing the consensus sequence for cMYC was able to successfully compete for the binding site across rs2969916[C] but the results of the supershift assay using an antibody against cMYC was negative. The DNA-binding consensus sequences for USF1 and cMYC are very similar (5'CACGTG3') [357], in fact these two transcription factors are well known to have antagonistic transcriptional activities

of the same gene [353, 354, 358]. A search of PubMed (http://www.ncbi.nlm.nih.gov/pubmed/) and STRING 9.0 (http://string-db.org) [359] a protein/protein interaction database, did not reveal any known instances of USF1 and cMYC either binding to each other or in the same complex, therefore the positive cold competition assay and negative supershift of cMYC is most likely due to cMYC and USF1 having similar DNA-binding consensus sequences. Furthermore, for several different genes, investigators have reported that cMYC and USF1 compete for the same site, with binding by cMYC leading to increased transcription of the gene and binding by USF1 suppressing transcription [353, 356, 358], therefore it cannot be ruled out that cMYC may compete for binding at this site. Ubiquitously expressed USF1 forms homodimers, heterodimers with USF2 or multimers before binding DNA consensus sequences to modulate gene expression. Activity of USF1 is modulated by phosphorylation: phosphorylation at three sites in leucine zipper domains increases DNA binding while phosphorylation of two sites in basic domains disrupts DNA binding [360], therefore a measure of the total phosphorylation state of USF1 is not indicative of USF1 activity.

Antibodies against cMYC and NFKB were unable to shift the visible bands indicating that they are not the nuclear factors binding the DNA in this region. It is not clear from this assay if these proteins form part of the protein complex that binds this region. In order to be able to identify the whole complex of proteins binding to the SNPs an alternate mass spectroscopy method was used – the SILAC mass spectroscopy method in which ratios of "heavy" and "light" isotopes are used to identify all the proteins in a complex attached to a DNA region. As rs2069915 and rs2069916 are only 37 bases apart it is reasonable to suppose that some of the proteins in the complexes are common to both SNPs and this is

indeed what was seen. The histone 1 protein appears in complexes binding to both rs2069915[G] and rs2069916[C]. Histone cluster 1 family members are almost exclusively the only proteins identified by the SILAC analysis to bind rs2069915[G], whereas the complex binding rs2069916[C] includes structural proteins and histone-binding adaptor proteins as well. Binding of histone cluster 1 members and associated proteins would cause the DNA in this region to become, or remain, tightly wound which reduces accessibility of transcriptional machinery and thus transcription of this region would be low. The structural proteins such as actinin that form part of the complex binding to rs2069916[C] lend credence to the suppression of transcription as it is known that structural proteins such as actin help stabilize the closed conformation of DNA when it is not being transcribed. Interestingly, several of the proteins binding to the major allele of rs2069916 (NCL, ribosomal protein S8, ribosomal protein SA, DEAH and HNRPM) are known to bind together in a complex on unprocessed mRNA and may be involved in splicing events or translation suppression. This suggests a mechanism justifying the differences seen in protein C concentrations in ELISA assays, despite no differences being evident in *PROC* mRNA concentrations as quantified by RT-qPCR assays. In support of this theory, a recent study by Chen *et al.* (2012) found NCL interacts with *TP53* mRNA and suppresses translation after DNA damage [361]. In contrast, the minor alleles of both SNPs do not bind any histone proteins or structural proteins, instead the minimal binding seen in EMSA assays for these alleles was identified by SILAC mass spectroscopy as both helicases and polymerase family members which would suggest that active gene expression occurs when the minor alleles are present.

In collaboration with an industry partner, results of a novel bead-based assay corroborated the binding of nuclear protein(s) to rs2069916[C] as well as the lack of nuclear

factor binding to rs2069916[T], as seen in the EMSA assays. This assay was unable to duplicate the binding to rs2069915[G] seen in EMSA assays, likely because the nuclear protein binding rs2069915[G] was not one of the transcription factors included in the assay. The prohibitive cost, at the time, of hybridizing all the *PROC* DNA sequences to unique Capture beads prevented this for all SNPs of interest, therefore it was only possible to fully test one SNP – rs2069916[C/T]. The assay indicated that rs2069916[C] binds nuclear protein and that this protein was not one of the transcription factors included in the panel. In 2013 the cost of conjugating sequences to beads has been vastly reduced and it might be worthwhile developing this assay as a high throughput method of screening SNPs for nuclear protein binding. Any SNPs displaying binding could then be included in standard EMSA assays using ^{32}P, a more hazardous, labor-intensive, but very sensitive and trusted method.

Possible biological differences were exhibited between the rs2069915-rs2069916 haplotypes using luciferase reporter assays. These assays demonstrated that the A-T haplotype binds transcription factors minimally and is able to drive transcription of an artificial luciferase gene significantly more than the C-G haplotype which binds USF1, suggesting that USF1 may repress transcription, which is consistent with reports in the literature showing USF1 suppressing transcription when binding regions downstream of the start site of genes [356].

A second method, quantifying allele-specific expression of *PROC*, using TaqMan™ SNP genotyping assays, supported the earlier RT-qPCR results by evincing no difference in expression between alleles of the *PROC* SNP rs1799810[T/A] after siRNA knockdown of USF1. The haplotype diagram (Figure 2.2) shows that the alleles for rs1799810[T] and

rs2069916[C] are 100% correlated, hence allelic expression of rs1799810[T] is a reasonable approximation of the allelic expression of rs2069916[C].

Whether endogenous protein C levels are associated with genotypes of rs2069915 and rs2069916 has not been previously reported. However, results from previous studies may be extrapolated: it has been shown by several groups that the common promoter SNPs, -1654 and -1641, are associated with low protein C levels and a worse outcome in sepsis, thrombosis and other inflammatory conditions [265, 337, 362]. The two SNPs in this study which show significant protein binding, rs2069915 and rs2069916, are in very high LD with one of the promoter SNPs, -1654 (r^2 = 0.83 and 0.94, respectively), therefore the genotypes of the two intronic SNPs should mirror closely the genotype of this promoter SNP and, concomitantly, the measured protein C levels in previous studies. From phased haplotype data of Caucasian populations at SeattleSNPs, the C-allele of -1654 is almost always associated with the G-allele of rs2069915 and the C-allele of rs2069916 (Figures 2.2 and 2.3; Appendix A, Table A.2). As both the C-G and C-A haplotypes of -1654/-1641 have been shown by several groups to be associated with low circulating levels of protein C and a worse outcome in patients, it is reasonable to suppose that the nuclear factors seen here to bind to rs2069915[G] and rs2069916[C] may repress transcription, resulting in lower levels of protein C at baseline. As patients with severe sepsis and other inflammatory conditions are known to have low plasma levels of protein C, and that low concentrations of protein C are correlated with increased mortality or worse outcomes [137, 362], this discovery suggests that individuals with the G-C haplotype of rs2069915 and rs2069916 are likely to have more transcriptional inhibition, correspondingly low endogenous levels of protein C and,

consequently, a worse outcome during sepsis, thrombosis or other inflammatory conditions than individuals with the A-T haplotype at these positions.

Chapter 4: Reduced PCSK9 Function Protects Against Adverse Outcomes in Murine Systemic Inflammation and Human Septic Shock

4.1 Background

Significant interaction occurs between lipid metabolism and inflammation pathways leading to altered incidence and/or outcome of sepsis when lipid metabolism is altered. Statin treatment reduces the incidence of pneumonia [363] and reduces mortality associated with in-hospital pneumonia [364]. Similarly, HDL may be protective in sepsis [365]. However, the evidence is not conclusive [366]. For example, continuation of pre-hospitalization statin therapy did not improve outcomes in patients hospitalized with sepsis [367] and actively increasing plasma HDL using cholesterylester transfer protein (CETP) inhibitors such as torcetrapib appeared to result in increased sepsis deaths [368]. There have been no pivotal randomized controlled trials to date of statins in sepsis. Thus, there appears to be a clinically important interaction between lipid metabolism and inflammatory pathways, although apparently contradictory observations indicate that our understanding is very incomplete.

The mechanisms involved in the interaction between lipid metabolism and the septic inflammatory response are similarly unclear although bacterial cell wall products, such as endotoxins LPS and LTA, contain lipid moieties. Triglyceride-rich lipoproteins contribute by binding to LPS and LTA fragments of Gram-positive and Gram-negative pathogens, respectively, which are then internalized via the LDL receptor and cleared by the liver, thereby potentially reducing activation of macrophages [34, 35, 369, 370]. A number of macrophage-expressed receptors that modulate the inflammatory response, including PPAR

and LXR, are activated by cholesterol [371]. High density lipoprotein augments human monocyte responses to LPS by suppressing the inhibitory activity of high concentrations of LPS binding protein, where APOA2 appears to be the active component [372]. Statins have multiple effects which may cause immune modulation including reduction of C-reactive protein levels [373], reduction in NFKB activation [374], and improving endothelial eNOS responses thus reducing leukocyte adhesion within the microcirculation [375] and leukocyte recruitment to the infected site [376]. Statins also inhibit protein isoprenylation, including farnesylation, which abrogates pro-apoptotic effects of sepsis on splenic lymphocytes [377].

The primary effect of statins is to decrease serum LDL. Thus, the mechanism of statin effect may also be related to LDL or ligation of its receptor leading to downstream signaling. Low density lipoprotein receptor knock-out ($Ldlr^{-/-}$) mice are protected against lethal endotoxemia and severe Gram-negative infections [325]. However, potentially contradictory observations have been made. For example, LDL receptor-deficient mice have been reported to be more susceptible to sepsis induced by cecal ligation and puncture (CLP) than corresponding genetic background mice [378]. In $Ldlr^{-/-}$ mice a number of inflammatory mediators were altered. Prior to CLP, $Ldlr^{-/-}$ mice had an elevation in serum amyloid A protein, lipopolysaccharide binding protein (LBP), and soluble CD14 (sCD14). Following CLP, IL1-beta increased more in $Ldlr^{-/-}$ mice than controls. In experimental models of murine sepsis, statin treatment [379] and treatment with an apolipoprotein A-I mimetic protein [380] appears to be beneficial.

In summary, lipid metabolism pathways interact with the inflammatory response, potentially with important clinical consequences. However, the exact mechanisms and whether this effect impacts patient outcome are uncertain. Whether, in addition to statins,

other molecules influencing these lipid metabolism pathways would alter the inflammatory response and outcome in human sepsis is unknown. Recently *PCSK9* has been identified as a key regulator of LDL receptors [381] and other receptors such as very low-density lipoprotein receptor (VLDLR), ApoER2 [298], and CD81 [273]. To date, there are no publications regarding PCSK9 and models of human sepsis.

In view of the interaction of lipid metabolism and inflammatory pathways, the hypothesis that PCSK9 alters the systemic inflammatory response in mice and in human septic shock was tested. Indeed, it was found that *Pcsk9* knock-out mice had a diminished inflammatory response to LPS and were protected against adverse aspects of the physiologic phenotype of a severe inflammatory response, compared to background control mice. To determine whether this observation could have clinically significant consequences, genetic polymorphisms of *PCSK9* in human sepsis were examined. Genetic variants in *PCSK9* have been highly characterized so it was possible to parse and sort several common variants into known LOF variants and compare these to a known GOF variant. Variants in *PCSK9* were genotyped in two cohorts of patients with septic shock. In accord with the murine LPS observations, it was found that humans with septic shock who carry LOF variants of *PCSK9* had a reduced inflammatory cytokine response and decreased mortality whereas individuals with GOF variants had the opposite effect.

In conclusion: reduction of activity of PCSK9 reduces the inflammatory response and improves physiologic outcome in mice and in human patients who have severe sepsis and septic shock.

4.2 Results

4.2.1 Murine physiological measurements

The *Pcsk9* knock-out mice had a blunted general and cardiovascular response to LPS. By six hours after LPS injection all 10 C57BL/6 wildtype control mice exhibited continuously hunched posture and did not move despite strong physical stimuli (Activity index of 0/4) **(**Figure 4.1A) and demonstrated a progressive loss of body temperature over the six hours following LPS administration, such that 6 of the 10 mice had a final body temperature <32°C (mean 30.5 ± 2.8°C) (Figure 4.1B). In contrast, the *Pcsk9*$^{-/-}$ mice had a mean activity index of 1.6 ± 0.9 ($P<0.0001$ vs. control) corresponding to a maximum of 20-30 seconds of hunched posture which spontaneously reverted to normal with ongoing spontaneous rapid movements interspersed with eating and drinking (Figure 4.1A) and none of the 10 *Pcsk9*$^{-/-}$ mice had their temperature drop below 32°C (mean 35.2 ± 1.8°C, $P<0.0001$ vs. control) (Figure 4.1B). Lipopolysaccharide induced an acute decrease in mean arterial pressure and left ventricular ejection fraction (Figure 4.1C and D) within six hours in C57BL/6 wildtype control mice [324, 382]. Both of these cardiovascular effects were significantly ameliorated in *Pcsk9*$^{-/-}$ mice (Figure 4.1C and D).

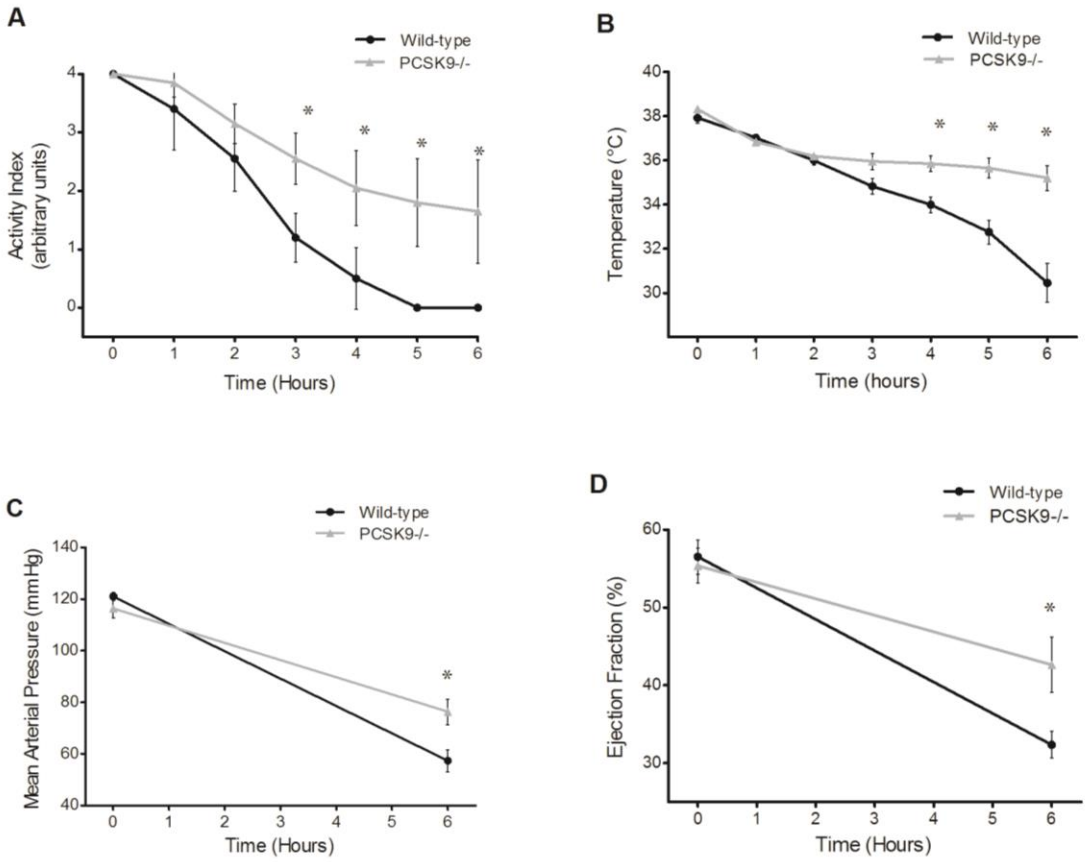

Figure 4.1 Phenotypic responses to LPS in wild-type and *Pcsk9*$^{-/-}$ mice

A. *Activity phenotype*. All 10 wild-type control mice (C57BL/6) had an activity index of 0 (no movement) six hours post LPS administration compared to none of 10 *PCSK9* knock-out (*Pcsk9*$^{-/-}$**)** mice. Comparison of group means demonstrates a statistically significant effect (* $p<0.05$) in hours 3 - 6. Typically an activity index less than 0.5 represents a terminal state. **B**. *Body temperature.* Wild-type control mice (C57BL/6) demonstrated a progressive loss of body temperature over the six hours post LPS administration such that 6 of the 10 mice had a body temperature <32°C, while none of 10 *Pcsk9*$^{-/-}$ mice had their temperature drop below 32°C. Comparison of group means demonstrates a statistically significant effect ($p<0.05$) in hours 4 - 6. Typically a sustained temperature less than 32°C represents a terminal state. **C**. *Blood pressure*. Mean arterial pressure is preserved in *Pcsk9*$^{-/-}$ mice compared to wild-type control mice 6 hours post LPS administration (Mann Whitney U test, P=0.014). **D**. *Left ventricular ejection fraction*. Cardiac function is preserved in *Pcsk9*$^{-/-}$ mice compared to wild-type control mice as evidenced by significantly higher left ventricular ejection fraction 6 hours post LPS administration (Repeated measures ANOVA, P=0.024,). All data are mean ± SD.

4.2.2 Murine replication

Independent replication of these results was examined using pharmacologic inhibition of *Pcsk9* with berberine, which resulted in a 65±20% reduction in hepatic *Pcsk9* mRNA expression (P<0.05). It was found that, similar to *Pcsk9* knock-out, pharmacologic inhibition of *Pcsk9* also blunted the effect of LPS on activity (Repeated measures ANOVA, P<0.001) and body temperature (Repeated measures ANOVA, P<0.001) (Figure 4.2 A and B).

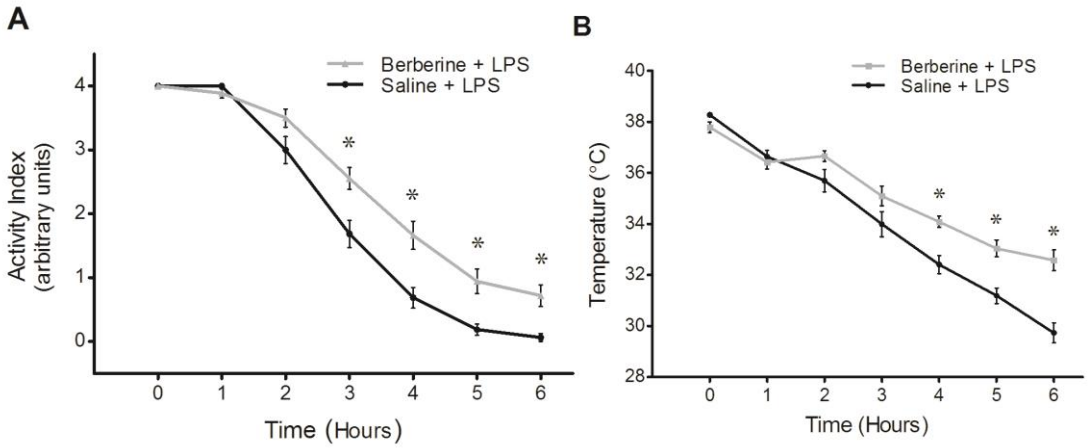

Figure 4.2 Phenotypic responses of wild-type mice treated with saline or berberine

A. *Activity phenotype.* 7/8 saline treated C57BL/6 wild-type control mice had an activity index of 0 (no movement) by six hours post LPS administration compared to 2/9 of the berberine treated mice. Comparison of group means demonstrated a statistically significant effect (* P<0.05) in hours 3-6. **B**. *Body temperature*. Saline treated mice demonstrated a progressive loss of body temperature over the six hours following LPS administration such that all 8 mice had a body temperature <32°C, while only 2/9 of the berberine treated mice had their temperature drop to <32°C. Comparison of group means demonstrated a statistically significant effect (*P<0.05) in hours 4, 5 and 6. Data are mean ± SD.

4.2.3 Murine *PCSK9* knock-out had a blunted inflammatory cytokine response

Pcsk9$^{-/-}$ mice also had an attenuated inflammatory cytokine response measured in plasma at 6 hours after LPS infusion (Table 4.1).

Table 4.1 Cytokine measurement of mouse and human plasma

Cytokine measurements in *Pcsk9*$^{-/-}$ and wild-type control mouse plasma 6 hours following 20 mg/kg LPS injection i.p., and in human plasma from VASST septic shock patients at time of study entry.

Mouse	TNF-alpha	IL6	IL10	JE	MIP-2
Pcsk9$^{-/-}$ (n=8)	26.4 (22.3-31.2)	2420 (2040-2880)	39 (32-48)	1000 (800-1250)	850 (680-1080)
Controls (n=9)	47.6 (41.1-55.1)	6750 (5290-8620)	101 (85-121)	2190 (1940-2480)	2280 (1710-3040)
P-values	0.018	0.004	0.003	0.006	0.019
Human	**TNF-alpha**	**IL6**	**IL10**	**MCP1**	**IL8**
LOF (n=178)	13.4 (12.3-14.5)	182 (153-216)	42 (37-48)	717 (644-799)	70 (61-79)
GOF (n=35)	18.5 (15.0-22.8)	338 (221-519)	101 (66-155)	1140 (884-1470)	129 (89-188)
P-values	0.061	0.076	0.009	0.043	0.035

Data are median (25^{th} – 75^{th} quartiles) of log transformed data, converted back to pg/mL throughout.
LOF indicates patients having at least one Loss of Function allele and GOF indicates patients having at least one Gain of Function allele.

Specifically, compared to wildtype control mice at 6 hours after LPS administration, *Pcsk9*$^{-/-}$ mice had lower plasma concentrations of TNF-alpha (P=0.018), IL6 (P=0.004), IL10 (P=0.003), JE (P=0.006) and MIP-2 (P=0.019). There were no differences in cytokine concentrations between *Pcsk9*$^{-/-}$ mice and wildtype control mice, measured in saline-treated mice (Table 4.2).

Table 4.2 Cytokine concentrations in saline-treated mice

	TNF-alpha pg/mL	IL6 pg/mL	IL10 pg/mL	JE pg/mL	MIP-2 pg/mL
Wild-type mice	0.33 (0.33-0.47)	2.0 (1.2-2.9)	0.31 (0.31-0.31)	15.2 (11.4-18.4)	3.3 (2.7-5.1)
Pcsk9$^{-/-}$ mice	0.00 (0.00-0.67)	2.0 (1.7-25.3)	0.49 (0.24-1.62)	7.6 (7.4-62.4)	2.1 (1.3-6.9)
P-value	0.969	0.433	0.46	0.509	0.87

Data are median (25^{th} – 75^{th} quartiles)
n=3 for each group

4.2.4 Murine endotoxin clearance rates

As a simple first step to elucidate the mechanism responsible for the increased survival seen in LPS-treated *Pcsk9*$^{-/-}$ mice, plasma clearance of endotoxin in *Pcsk9*$^{-/-}$ mice was measured and compared to wild-type controls. It was found that *Pcsk9*$^{-/-}$ mice cleared endotoxin approximately twice as quickly as wild-type controls (Mann Whitney U test, P=0.023; Figure 4.3A).

As a second step, endotoxin clearance in berberine treated mice was compared to saline treated mice and, although the trend was similar, with berberine treated mice evincing a slightly more rapid endotoxin clearance than saline treated mice, the difference was not significant (Mann Whitney U test. P=0.160) (Figure 4.3B).

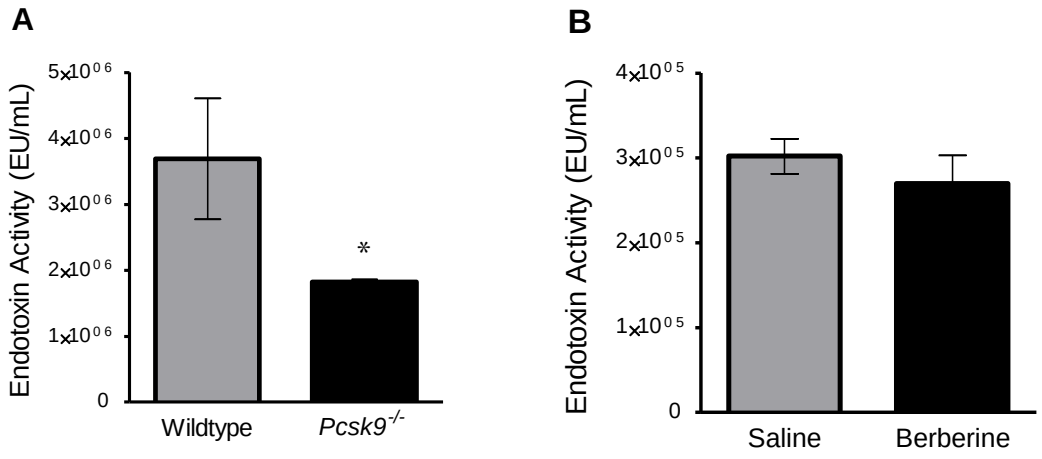

Figure 4.3 Endotoxin clearance 6 hours post LPS infusion

A. Endotoxin activity was measured in plasma from the cytokine experiments of *Pcsk9*$^{-/-}$ (n=11) and wild-type control mice (n=8) using a limulus amebocyte lysate assay. At 6 hours following intra-peritoneal injection of 20mg/kg LPS the *Pcsk9*$^{-/-}$ mice had significantly reduced endotoxin activity compared to wild-type mice exposed to the same dose of LPS (Mann Whitney U test. P=0.023). **B**. Similarly, although berberine-treated C57BL/6 mice (n=8) had reduced endotoxin activity compared to saline-treated controls (n=8), this difference was not significant (Mann Whitney U test. P=0.160). Data mean ± SD.

4.2.5 Preserved cardiac function in *Ldlr*$^{-/-}$ mice treated with berberine

To try and determine whether the protective effect seen in *Pcsk9*$^{-/-}$ mice is due to binding of PCSK9 to the LDL receptor, *Ldlr*$^{-/-}$ mice were treated with either berberine or saline prior to LPS challenge. Body temperature, activity index and cardiac physiology were measured as described for the previous experiments. There was no difference between the two groups at baseline in body temperature, activity index, ejection fraction or mean arterial pressure (Table 4.3).

Table 4.3 Responses to LPS in *Ldlr*$^{-/-}$ mice treated with either saline or berberine

	Activity baseline	Activity 6hrs LPS	Temp baseline	Temp 6hrs LPS	EF baseline	EF 6hrs LPS	MAP baseline	MAP 6hrs LPS
Saline-treated mice	0 (0-0)	4 (3.8-4.3)	37.1 (36.2-37.9)	28.3 (26.0-30.6)	54.2 (36.6-71.8)	21.3 (16.3-26.3)	124 (118-129)	53 (32-74)
Berberine-treated mice	0 (0-0)	4 (3.8-4.3)	37.0 (36.2-37.9)	28.5 (26.1-30.8)	50.4 (38.2-62.6)	26.0 (23.0-29.0)	109 (93-125)	53 (52-54)
P-value	NA	0.356	0.806	0.898	0.844	0.045	0.565	0.477

Data are median (95% CI)
All groups n=4

Moreover, 6 hours after LPS challenge there was no body temperature or activity index differences between groups (Table 4.3). However, there was a significant difference in ejection fraction with the berberine treated mice having a slightly conserved ejection fraction compared to the saline group 6 hours after LPS challenge (Repeated measures ANOVA, P=0.045, Table 4.3 and Figure 4.4). There was no difference in mean arterial blood pressure at 6 hours after LPS challenge (Mann Whitney U test, P=0.477, Table 4.3).

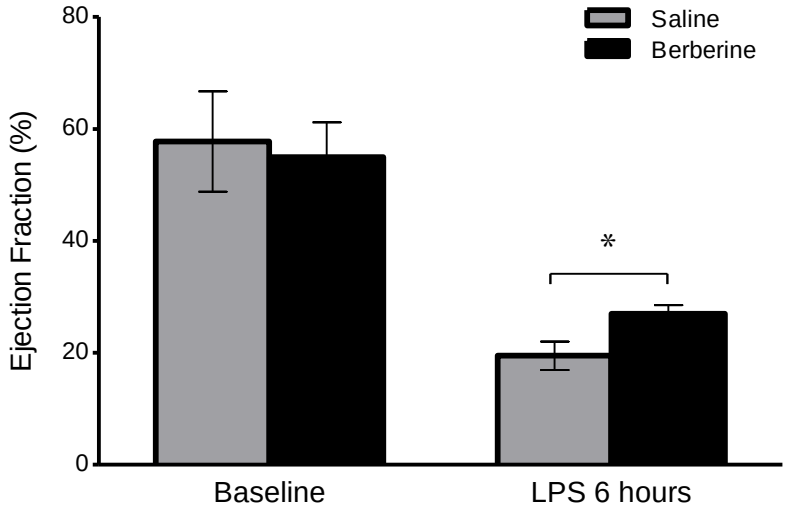

Figure 4.4 Preserved ejection fraction in *Ldlr* null mice after berberine infusion

At baseline there was no significant difference between *Ldlr*$^{-/-}$ mice treated with either saline or berberine (Mann Whitney U test, P=0.844, n=4/group) but six hours after LPS infusion the berberine-treated mice had a significantly preserved ejection fraction (Repeated measures ANOVA, P=0.045, n=4/group).

4.2.6 Human *PCSK9* LOF had a blunted general and cardiovascular response

The human *PCSK9* gene has been highly characterized and several relatively common missense variants (MAF ≥0.5%) and many rare missense and nonsense variants have been identified that are associated with decreased LDL levels, as an indicator of LOF of *PCSK9* (Figure 2.7). The relationship between LDL levels and genotype of *PCSK9* has also been identified using an unbiased genome-wide association study (GWAS) approach. One fairly common missense variant and many rare missense variants have been found to be associated with increased LDL levels and, based on this, are considered GOF (Figure 2.7). Accordingly, the relatively common *PCSK9* LOF variants (MAF ≥0.5%, rs11591147 R46L, rs11583680 A53V, rs562556 V474I) were genotyped along with the relatively common

PCSK9 GOF variant (rs505151 G670E) in the VASST cohort. All SNPs tested were in Hardy-Weinberg equilibrium (Appendix B, Table B.1).

It was found that patients in the VASST cohort having at least one *PCSK9* LOF allele had decreased mortality over 28 days (29.1% 28-day mortality, Figure 4.5A) compared to patients without a LOF allele (39.6% 28-day mortality, P=0.0037 by log-rank test).

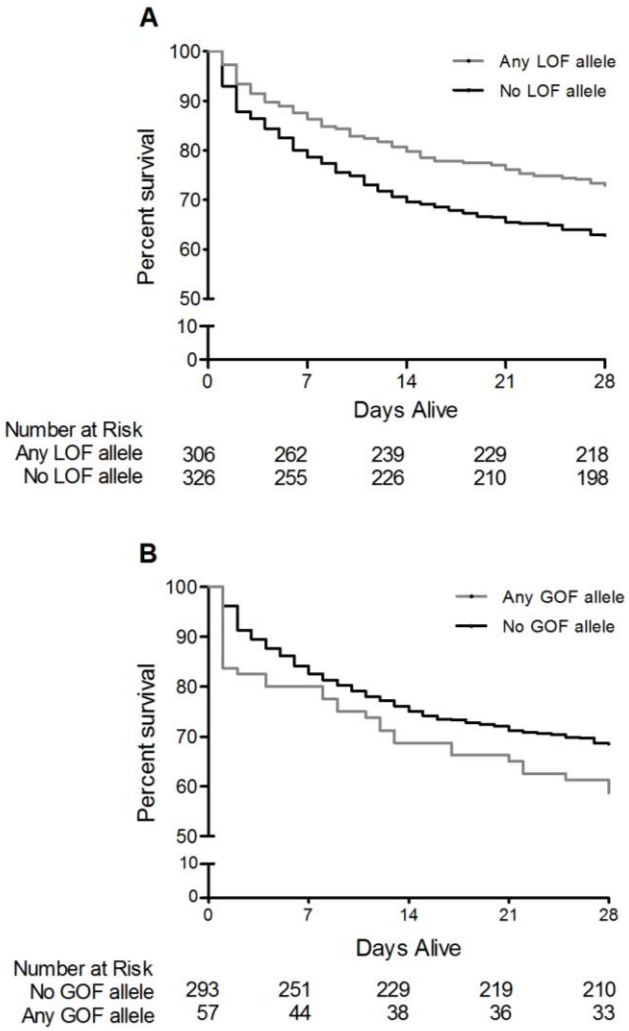

Figure 4.5 Kaplan Meier 28-day survival curves in VASST

A. *Loss-Of-Function (LOF).* Patients in VASST having at least one *PCSK9* LOF allele had decreased mortality over 28 days (any LOF allele = grey line, n total = 306 with 89 deaths, 29.1% 28-day mortality) compared to patients without a LOF allele (black line, n total = 326 with 129 deaths, 39.6% 28-day mortality) (P=0.0037 by log-rank test). **B**. *Gain-Of-Function (GOF).* Patients in VASST having at least one *PCSK9* GOF allele (grey line, n total = 57 with 25 deaths, 43.9% mortality at 28 days) had increased mortality over 28 days compared to patients having at least one *PCSK9* Loss-Of-Function allele but no GOF alleles (black line, n total = 293 with 83 deaths, 28.3% mortality at 28 days, P=0.011 by log-rank test).

Using logistic regression to identify and adjust for potentially important covariates, it was found that having at least one *PCSK9* LOF allele remained significantly associated with decreased mortality (Odds Ratio 0.64, 95% confidence interval 0.46-0.89, P<0.009) (Table 4.4).

Table 4.4 Logistic regression testing for Loss-Of-Function and Gain-Of-Function effects on 28-day mortality in VASST

	Loss-Of-Function		**Gain-Of-Function**	
	Odds Ratio (95% Confidence interval)	*P*	Odds Ratio (95% Confidence interval)	*P*
Age -per year	1.017 (1.007-1.029)	0.001	1.007 (0.997-1.027)	0.11
Gender - Female	0.99 (0.71-1.40)	0.97	0.81 (0.50-1.29)	0.37
Ethnicity - Caucasian	0.80 (0.51-1.26)	0.33	0.91 (0.46-1.77)	0.77
Surgical diagnosis	0.75 (0.50-1.14)	0.18	0.64 (0.51-1.52)	0.63
Effect of genetic variant	0.64 (0.46-0.89)	0.009	1.92 (1.06-3.48)	0.031

LOF patients had at least one LOF allele
GOF patients had at least one GOF allele

The number of GOF-containing haplotypes was less than the number of LOF variants. Despite this, it was found that patients in VASST having a GOF variant had a directionally opposite effect to LOF variants, having increased mortality over 28 days (43.9% 28-day mortality, Figure 4.5B) compared to patients with a LOF variant (28.3% 28-day mortality, Figure 4.5B) (P=0.011 by log-rank test). Logistic regression, adjusting for potentially important covariates, similarly found that the *PCSK9* GOF allele was significantly

associated with increased mortality (Odds Ratio 1.92, 95% confidence interval 1.06-3.48, P<0.031) (Table 4.4).

4.2.7 Human *PCSK9* LOF had a blunted inflammatory cytokine response

Similar to the *PCSK9* knock-out mouse cytokine measurements, patients with at least one LOF allele had a trend towards or a significantly blunted inflammatory cytokine response compared to those with at least one GOF allele for TNF-alpha (P=0.061), IL6 (P=0.076), IL10 (P=0.009), MCP1 (P=0.043), and IL8 (P=0.035) (Table 4.1).

4.2.8 A single SNP is suitable to test for replication of LOF/GOF

This study found that the LOF alleles of rs11591147, rs11583680, and rs562556 all preferentially segregated with the minor G allele of the tag SNP, rs644000 (Figure 2.7). Out of 1324 total observed haplotypes a LOF allele was observed 442 times within 309 haplotypes. Moreover, 83.5% of these LOF alleles were contained within haplotypes that also contained the rs644000 minor G-allele. Only 15.5% of the LOF alleles were contained within rs644000 major A-allele haplotypes. Thus, the minor allele of rs644000 is a marker of the most common *PCSK9* LOF genetic variants. Conversely, the relatively common GOF variant preferentially segregated with the major A-allele of rs644000: 95.2% of these GOF alleles were contained within haplotypes that also contained the rs644000 major A-allele (Figure 2.7). Only 4.8% of the GOF alleles were contained within the rs644000 minor G-allele haplotypes. Thus, overall, the minor G-allele of rs644000 is preferentially associated with LOF alleles and the major A-allele of rs644000 is preferentially associated with GOF alleles of known relatively common genetic variants of *PCSK9*.

Therefore, rs644000 was used as a tagging SNP for replication analysis. It was found that the minor G-allele (LOF marker) of *PCSK9* rs644000[A/G] was highly associated with decreased mortality over 28 days in both the VASST cohort (P=0.005 by log-rank test; Figure 4.6A) and in the SPH cohort (P=0.034, Figure 4.6B).

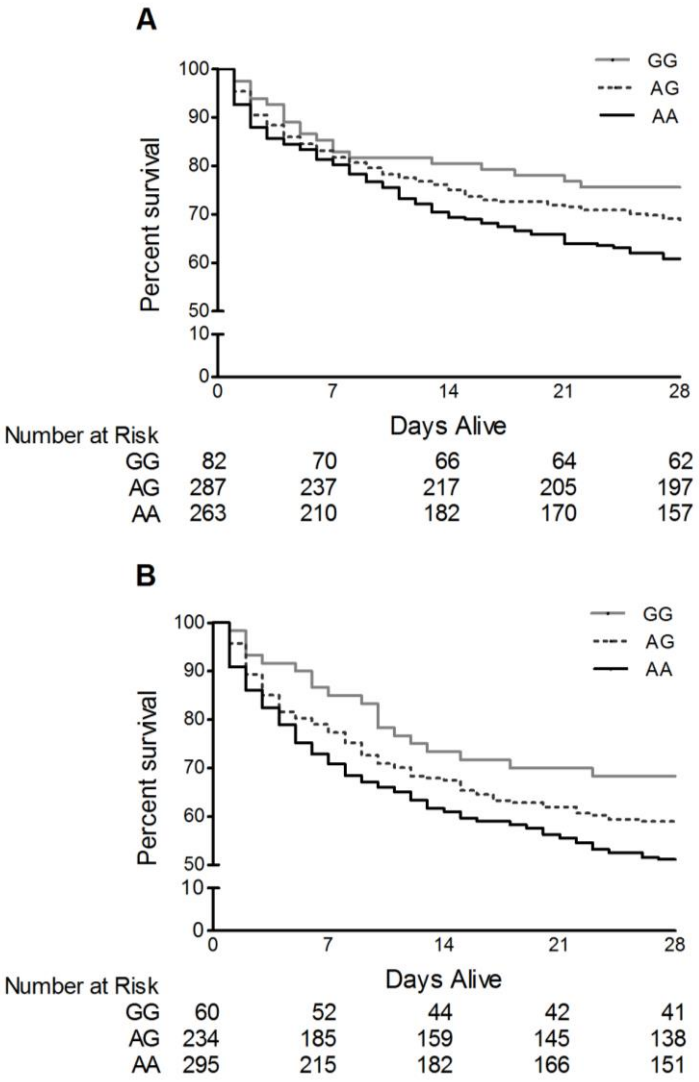

Figure 4.6 Kaplan Meier 28-day survival curves by *PCSK9* rs644000 genotype

A. *Survival curve for VASST cohort*. In the VASST derivation cohort patients with the GG genotype of SNP rs644000[A/G] had increased survival compared to patients with either the AG or AA genotypes (P=0.005 by log rank test). **B**. *Survival curve for SPH cohort.* Similarly, in the SPH replication cohort patients with the GG genotype of rs644000 displayed increased survival compared to the other two genotypes (P=0.034 by log rank test).

No consistent significant differences in baseline characteristics in these two cohorts were identified that could potentially confound this result (Appendix B, Table B.2B). Logistic regression adjusting for key covariates supported this conclusion (VASST Odds Ratio 0.68, 95% confidence interval 0.53 - 0.89, P=0.0044; SPH Odds Ratio 0.54, 95% confidence interval 0.12 - 0.88, P=0.0045) (Table 4.5).

Table 4.5 Logistic regression of rs644000 genotype with 28-day mortality in VASST and SPH cohorts

	VASST Cohort Odds Ratio (95% Confidence interval)	*P*	**SPH Cohort** Odds Ratio (95% Confidence interval)	*P*
Age	0.98 (0.97-0.99)	0.001	1.007 (1.004-1.010)	<0.001
Gender_Female	0.98 (0.70-1.38)	0.895	1.14 (0.88-1.48)	0.313
Ethnicity_Caucasian	1.19 (0.75-1.87)	0.465	0.87 (0.66-1.16)	0.349
Surgical Diagnosis	0.81 (0.57-1.13)	0.211	1.09 (0.83-1.42)	0.547
PCSK9 rs644000 G-allele	0.68 (0.53-0.89)	0.0044	0.54 (0.12-0.88)	0.0045

In accord with the murine observations, it was also found that the G-allele (LOF marker) of rs644000 was associated with decreased cardiovascular dysfunction (VASST P<0.001, SPH P<0.009) and decreased need for vasopressor administration (VASST P<0.001, SPH P<0.019). There were significant differences and directionally similar trends across both cohorts for respiratory, renal, hematologic, hepatic, and neurologic organ systems (Table 4.6) as well as a decreased need for mechanical ventilation and renal replacement therapy (Table 4.6).

Table 4.6 Organ dysfunction in VASST and SPH cohorts by rs644000 genotype

PCSK9 rs644000 genotype	VASST Cohort GG (n=82)	GA (n=287)	AA (n=263)	P	SPH Cohort GG (n=60)	GA (n=234)	AA (n=295)	P
Days Alive and Free (DAF) of organ dysfunction								
Cardiovascular	22(1-25)	21(1-24)	15(0-23)	0.001	18(5-25)	15(1-24)	8(0-23)	0.009
Respiratory	9(1-15)	3(0-16)	3(0-15)	0.047	18(1-25)	10(0-24)	4(0-22)	0.009
Renal	26(13-28)	23(6-28)	18(1-28)	0.001	22(3-28)	17(2-28)	11(1-27)	0.062
Hematologic	28(12-28)	26(11-28)	22(3-28)	<0.001	27(6-28)	24(6-28)	20(3-28)	0.068
Hepatic	28(9-28)	27(8-28)	21(4-28)	0.001	28(6-28)	24(4-28)	17(2-28)	0.041
Neurologic	19(2-26)	16(0-25)	15(0-23)	0.029	26(8-28)	24(5-28)	20(3-27)	0.084
Days Alive and Free (DAF) of artificial organ support								
Vasopressors	22(1-25)	21(1-24)	17(0-24)	<0.001	24(9-27)	21(2-26)	17(1-26)	0.019
Ventilator	13(0-22)	10(0-21)	7(0-20)	0.121	17(0-23)	8(0-22)	2(0-21)	0.019
Renal replacement therapy	28(13-28)	27(9-28)	21(3-28)	<0.001	28(4-28)	23(3-28)	12(1-28)	0.008

4.3 Discussion

This study found that *Pcsk9* knock-out mice, versus genetic background controls, are protected against the adverse effects of LPS administration; an important pre-clinical model of the systemic inflammatory response relevant to sepsis and septic shock. It was found that *Pcsk9* knock-out beneficially ameliorated the adverse effect of LPS on activity and body temperature, as well as on adverse LPS-induced cardiovascular phenotypes of hypotension and decreased left ventricular ejection fraction. Additionally, *Pcsk9* knock-out decreased the plasma inflammatory cytokine response in response to LPS. In essence, knocking out *Pcsk9* was very protective of the important and common adverse effects of LPS.

As a first step to elucidate mechanism of PCSK9 action, plasma clearance of endotoxin in *Pcsk9*$^{-/-}$ mice was measured and compared to wildtype controls. It was found that *Pcsk9*$^{-/-}$ mice cleared endotoxin approximately twice as quickly as wildtype controls (Figure 4.3A), potentially suggesting a mechanism of beneficial effect.

These results were only partially replicated when pharmacologic inhibition of *Pcsk9* by berberine was applied to *Ldlr*$^{-/-}$ mice prior to LPS challenge: 6 hours after LPS challenge there was no difference in body temperature, activity index or mean arterial pressure, both groups were equally sick. However, the berberine group did have a slightly preserved ejection fraction compared to the saline group. The preserved ejection fractions seen in the *Ldlr*$^{-/-}$ mice may be due to direct action of berberine on the heart rather than to any effects of berberine-reduced PCSK9 function as berberine is known to have pleotropic effects, including cardiovascular effects [323]. A key physiologic response in mice after endotoxin challenge is the development of fever, hunched posture and unwillingness to move which was observed in all control mouse groups as well as the *Ldlr*$^{-/-}$/berberine group which is

suggestive of a slower rate of endotoxin clearance. Credence is given to this observation with the faster endotoxin clearance measured in both the *Pcsk9*$^{-/-}$ mice and the C57/BL6 mice treated with berberine compared to controls: both the former groups should have an increased number of LDL receptors compared to either the wildtype controls or the *Ldlr*$^{-/-}$ mice. Taken together, these results suggest that LPS endotoxin clearance may occur primarily via the LDL receptor, although other receptor(s) may also be utilized, as a previous study showed a survival benefit in *Ldlr* null mice after LPS endotoxin challenge [325], although another group had opposite results after endotoxin challenge via CLP [378]. In this study, cardiac function was preserved in all mouse models, including the *Ldlr*$^{-/-}$ model, which suggests that this effect may be coordinated via a receptor other than the LDLR.

To determine whether the impact of PCSK9 was relevant in human sepsis, a tag SNP approach was used, followed by using the knowledge that *PCSK9* LOF and GOF genetic variants have been characterized. The genotype of the *PCSK9* tag SNP, rs644000, was found to be highly associated with 28-day mortality in the VASST septic shock cohort and this result replicated in the SPH septic shock cohort. Loss-Of-Function missense variants were then shown to be associated with decreased 28-day mortality while GOF missense variants were associated with increased 28-day mortality. All three relatively common LOF variants (MAF $\geq$0.5%) were predominately found within haplotypes tagged by the minor allele of rs644000 and the relatively common GOF variant was almost exclusively found within haplotypes tagged by the major allele of rs644000, likely accounting for the strong association of the minor G-allele of rs644000 with decreased 28-day mortality. Further, it was found that plasma concentrations of inflammatory cytokines and chemokines were elevated in patients having GOF variants compared to those with LOF variants. These

human septic shock results align with the mouse model of systemic inflammation indicating that decreased PCSK9 activity results in a decreased inflammatory cytokine response and increased survival. These results support the conclusion that reduction of activity of PCSK9 reduces the inflammatory response and improves physiologic outcome in mice following LPS administration and also increases survival in human patients who have severe sepsis and septic shock.

Chapter 5: Conclusion

Genetic association studies have identified many SNPs in many genes that are associated with outcome in complex diseases [383], including sepsis, but to date few have been identified as the causal or functional SNP [384, 385]. The aim of this study was to identify causal SNPs that affect outcome in sepsis. Two candidate genes were focused upon: one known to impact sepsis but with no proven causal SNPs (*PROC*) and a second gene with proven causal SNPs but without known impact on sepsis (*PCSK9*).

There are a variety of ways a SNP can be causal, as discussed earlier in detail (see Introduction), however, for the *PROC* SNPs, it was decided to test for potentially causal SNPs by examining differences in transcription factor binding between alleles. The rationale being that low levels of protein C are known to be associated with a poor outcome in sepsis [193], and differential expression of *PROC* due to SNP-caused differences in transcription factor binding may lead to differences in protein C concentration. In addition, reliable and reproducible methods exist to test this function: EMSA assays to detect transcription factor binding, "supershift" EMSA and mass spectroscopy assays to identify DNA binding partners, allele-specific expression assays to test mRNA expression differences between alleles, luciferase assays to determine haplotypic differences in functional expression of protein and siRNA knockdown to show alteration of protein expression. Results of *in vitro* experiments indicated that *PROC* mRNA expression appears consistent, even in the face of excessive coagulation and a robust inflammatory response, whereas secreted protein C levels varied significantly in these settings, pointing to a post-transcriptional mechanism. That there was no difference in allele-specific expression either with or without USF1 gene knockdown

lends credence to this supposition. Transcription factor binding was positive for the major alleles of two common SNPs tested, rs2069915 and rs2069916, and likely binding partners were identified as both DNA transcription inhibitors (USF1 and histone 1) and untranslated mRNA modifyers (ribosomal protein 8, HNRPM, actinin alpha 4, NCL and DEAH, known to bind as a cluster on untranslated mRNA). Genetic variation of these two SNPs was shown to affect luciferase reporter activity and concentration of protein C after siRNA knockdown of USF1. Together these results suggest major alleles of two common variants in the *PROC* gene decrease secreted protein C concentrations via a post-transcriptional mechanism, possibly by inhibition of untranslated mRNA processing, potentially leading to a worse outcome in sepsis.

A different approach was required to test the functionality of SNPs in the *PCSK9* gene as, although many SNPs in the *PCSK9* gene have been shown to be functional, resulting in differences in plasma LDL cholesterol levels and impacting incidence of cardiovascular disease and atherosclerosis [282, 296], it is not known whether these SNPs also impact outcome in patients with sepsis. The first step was to determine whether PCSK9 even plays a role in sepsis outcome, and to this end, a *Pcsk9* knock-out mouse model of systemic infection was employed wherein intermediate phenotypes such as activity indices, body temperature, cardiovascular parameters and plasma cytokine levels were measured and compared to wildtype controls. These experiments were repeated in a wildtype murine model using pharmacological inhibition of *Pcsk9*, as well as in an *Ldlr* knock-out model. Once it was established that PCSK9 appeared to play a role in murine systemic infection, known functional SNPs and a tag SNP were tested for outcome and similar intermediate phenotypes in a large human cohort of densely genotyped patients with septic shock. In

addition, the tag SNP was tested for replication in a second large septic shock cohort. Results of these assays point to a hitherto unknown role for PCSK9 in outcome of systemic inflammation in mice and in human septic shock. Abrogation of PCSK9 in both mice and human patients with septic shock appears to confer a survival benefit, possibly by supporting cardiac function and reducing pro-inflammatory mediators.

Work performed in this thesis has identified two novel functional intronic SNPs in the *PROC* gene and suggested a novel mechanism of protein C regulation which highlights the possible direct involvement of intronic variants in post-transcriptional regulation, a role more commonly attributed to miRNA molecules.

In addition, a novel role has been purported for PCSK9 as a player in the course and outcome of sepsis which suggests that PCSK9-inhibitors may be a logical target to pursue as a treatment for sepsis patients in the ICU, individuals undergoing cardiac surgery or those with other systemic inflammatory conditions. Moreover, this work demonstrates that previously identified functional non-synonymous SNPs in PCSK9 are likely also functional in causing differences in outcome from septic shock.

5.1 Protein C

In clinical trials, most drugs tested to date have shown no or mixed efficacy in the treatment of patients with sepsis. For example, in many cases a survival benefit has been shown in the sickest patients treated with rhAPC (PROWESS trial [96]), low-dose corticosteroids [386], eritoran tetrasodium (competitively inhibits binding of LPS molecules to TLR4) [387] and afelimomab (monoclonal anti-TNF antibody) [63] whereas no benefit was seen in patients with less severe illness, as stratified by APACHE II scores. In fact,

follow up trials using rhAPC in patients with less severe illness (ADDRESS [388]) and in children with severe sepsis (RESOLVE trial [389]) showed no survival benefits. However, while the ENHANCE trial evaluating safety of rhAPC found an increased bleeding risk in patients treated with rhAPC, it also found a likelihood that earlier treatment with rhAPC would be more beneficial [390]. The latest randomized, double-blind, placebo-controlled multicenter trial assessing the effects of rhAPC in patients with septic shock (PROWESS-SHOCK [97]) showed no survival benefit at 28 or 90 days compared to placebo. The patients in this trial were administered rhAPC or placebo within 24 hours of receiving a vasopressor, which itself was administered within a median time of 2.5 hours after antibiotic treatment was initiated. However, there is no data detailing the initiation of illness in the patients and it is possible that the negative results of this, and other, trials reflects a fault in study design – the window of opportunity for beneficial outcome with drug treatment may have been missed. In addition, although co-morbidities of the patients were controlled for in the analyses, there was no way to control for the different genomic backgrounds of individuals and this may have influenced not only the progression and severity of disease but also the response to the treatments. Despite the mixed results of the randomized controlled trials to date, aPC remains a logical drug target to pursue in the treatment of sepsis as it acts at the intersection of several pathways engaged in the response to infection and inflammation – coagulation, inflammation, fibrinolysis, innate immunity and apoptotic pathways. Being able to target treatments more accurately by stratifying patients according to genotype of candidate genes may go some way towards determining the most timely and efficacious treatments and reducing poor outcomes. This approach is not trivial and involves the selection of appropriate candidate genes, the identification and testing of potential functional

variants that may affect outcome and, eventually, stratification and treatment of study groups by genotype.

Infusion of endogenous protein C into patients with severe sepsis or septic shock and protein C levels <50% of normal [100] appeared to alleviate some of the coagulopathy usually seen in these patients, however the mortality rate was still high at 35%, which is within the range expected for patients with this severity of illness. In addition, the study was small (20 patients), therefore larger follow up studies should be planned.

Identifying functional SNPs in non-coding regions of genes is a challenging task but doing so in the context of complex diseases is a formidable undertaking. Once a candidate gene has been selected for study, a first step in elucidating a functional SNP is to determine the relationship between all the SNPs in the region. Dense genotyping information is now available from several sources such as the HapMap Project, SeattleSNPs, the 1000 Genomes Project, ENCODE and others and it is possible to identify regions in high LD that contain almost all known SNPs. The LD between SNPs in and around the *PROC* genes is extensive; therefore only very common SNPs were selected for this study, those with a minor allele frequency of >10%, found in populations of European ancestry, as more than 80% of patients in the study ICU fall into this group. By selecting such common SNPs it is possible rare SNPs may have been missed that have a high potential to affect protein C expression and/or function. However, it has been postulated that, in complex diseases, it is likely that many SNPs, with small effects, in many genes, contribute to outcome [391, 392]. In addition, by considering the percentage of a common disease that would be eliminated upon removal of the risk factor, the population attributable fraction (PAF), it seems more likely that common variants with modest effects contribute more to the PAF in common diseases than do high-

risk, rare variants: in short, the common disease/common variant theory [393]. For example, in Alzheimer's disease one common apolipoprotein E4 allele has a PAF of around 20% [394] whereas more than 150 rare high-risk alleles in three genes have a combined PAF of <5% [395].

Association studies, in particular GWASs, have the ability to interrogate the whole genome in an unbiased fashion and compare SNPs found in patients with those of healthy controls to elucidate differences between the two groups. The GWAS has the capacity to be very powerful, with the potential to uncover modest-risk variants contributing to common diseases, in genes previously not connected with the disease. However, some true positive associations may be missed if they do not reach the very low statistical significance (P-value of 10^{-7} or 10^{-8}) required to overcome bias due to multiple testing; this will become increasingly problematic in future with greater density of genotyping forcing the cut-off P-value even lower as well as possibly increasing the false-discovery rate. Other potential problems include small sample sizes, population admixture, insufficient matching between test and control groups and classification of inclusion criteria and outcome measures or phenotypes. These are study design issues and may, in part, contribute to the fact that, to date, findings in most GWA studies have not been replicated. Candidate gene studies are usually less expensive to perform than GWA studies and have greater power to detect SNP effects, not least because a greater depth of SNP genotyping can be performed. However, because only the candidate gene is being considered, co-effects of variations in other genes are not taken into account.

Once the SNPs of interest have been selected, the next undertaking is to determine whether there is a difference in gene expression between individuals homozygous for the

minor allele, compared to individuals homozygous for the major allele. One method to achieve this is to use allele-specific assays. Allele-specific expression differences have been shown by several groups to be heritable ([396, 397], moreover it has been shown that SNPs with modest expression differences (1.5 – 2-fold) can have functional effects. An estimate of allele-specific expression in the murine genome is 6% [398], while in human B-lymphocyte cells it is around 20% [396, 397]. Several confounding factors could mask any real differences: expression may be spatially and temporally specific or the background genomic make-up may affect expression of the gene of interest. In addition, differences in response to external or local environmental influences may alter expression of the gene of interest between individuals [391].

In addition to affecting splicing sites and mRNA stability, a common function of non-coding SNPs is to bind transcription factors, which may be activators, enhancers or suppressors. The gel shift assay using radioactively labeled probes is a sensitive and specific method to identify the relative DNA binding efficiencies of two alleles of a SNP. Cold competitions and "supershift" assays, using an excess of unlabeled probes or antibodies, respectively, are able to show specificity of transcription factor binding and to identify the bound protein. However there are limitations: assays are strictly *in vitro* and there is no way to show that any specific transcription factor binding actually occurs *in vivo*. In addition, probes are necessarily short therefore they do not contain flanking sequences and cannot attain native conformation, often a requirement for correct binding of proteins. Further, for "supershift" assays to be successful the potential binding partner needs to be known, or at least a short list identified, otherwise it becomes prohibitively expensive in reagents and man-hours to test all known transcription factors for protein binding identity. Publically

available, curated databases predicting binding partners and/or potential functions for given sequences are becoming more common (STRING, PolyPhen, PROMO, ConSite, Transfac, FastSNP, IntAct) and these do at least provide a starting point for generating a short list of potential candidates, however consensus sequences for binding of transcription factors to DNA sequences are often context- and tissue-specific. Moreover, the choice of antibody is critical for the "supershift" assays – the best antibody will bind an epitope on the protein of interest with high affinity and without interfering with the DNA binding site, which will then render a clear "supershifted" band.

Further functional information can be gained from performing experiments in transgenic mice or *in vitro* gene knockdown experiments using siRNA probes. In this study the latter was chosen to better correlate with previous experiments. Recognized limitations exist for this methodology: knockdown of the gene of interest is transient and the effective knockdown period is driven primarily by the rate of cell growth and the half-life of the protein as the siRNA probes appear to be relatively resistant to degradation [399]. Rapid cell growth (doubling every 24 hours) quickly dilutes the concentration of siRNA probes below a threshold necessary to maintain gene inhibition therefore the optimum analysis time must be determined. Maximum knockdown of such cells has been found to be ~72 hours after siRNA transfection [400], whereas longer doubling times means effective knockdown is not seen until 96 hours after transfection and may be maintained for several days [399]. Doubling time for Hep-G2 cells tends to vary depending on confluency of the cells, averaging approximately 26 hours. In this study maximum knockdown of USF1 in Hep-G2 cells occurred between 48 and 72 hours. Transfection conditions for Hep-G2 cells were optimized

and commercially validated siRNA probes were used, consequently the resulting data is likely robust.

The recently published ChiP-seq data from the ENCODE Consortium [401] corroborates the findings of this study by showing binding of USF1 to intron 2 of *PROC* at the position of the SNP rs2069916 (Figure 5.1). In addition, ENCODE data also shows USF1 binding in intron 1 and in the promoter region (Figure 5.1).

Source: http://genome.ucsc.edu, ENCODE HAIB transcription factor track

Figure 5.1 ENCODE ChiP-seq data of transcription factor binding in Hep-G2 cells

Transcription factor binding from ENCODE data sets is shown. The vertical red line indicates position of rs2069916, rs2069915 lies 37bp to the left of the line. The horizontal blue line underlines USF1 binding, for clarity, where it can be seen that USF1 does indeed bind the region spanning rs2069915/6 in Hep-G2 cells.

It is possible that the binding of USF1 seen in EMSA assays reflects the ability of chromatin to bend and bring up- or downstream enhancers and repressors into contact with regulatory regions of genes (Figure 5.2B), as has been shown for USF1 binding in the promoter region of the fragile X mental retardation 1 gene [402]; alternatively, USF1 may bind each region independently, possibly under different environmental conditions (Figure 5.2A) as described by Sanchez *et al*. who showed that USF1 activity increased under high glucose conditions, whereas under fasting conditions USF1 is deacetylated and does not translocate to the nucleus [403].

Results of EMSA assays (including cold competitions and supershift assays), luciferase assays and the siRNA knockdown of USF1 assays strengthen the conclusion that USF1 binds the sequence surrounding rs2069916[C]. The binding of USF1 as indicated by EMSA assays was very strong, whereas the ENCODE data shows weak binding of USF1 (as indicated by the paleness of the grey marker) and, taking the ELISA results into account, this may suggest that the majority of the binding of USF1 occurs on unprocessed mRNA, which still retains introns. The nuclear lysate used in the EMSA assays contained both DNA and unprocessed mRNA, whereas ENCODE data was generated using DNA. Taken together with the mass spectrometry and ENCODE data, this suggests that rs2069916[C] binds USF1 and recruits several co-factors to suppress *PROC* mRNA processing (Figure 5.2C).

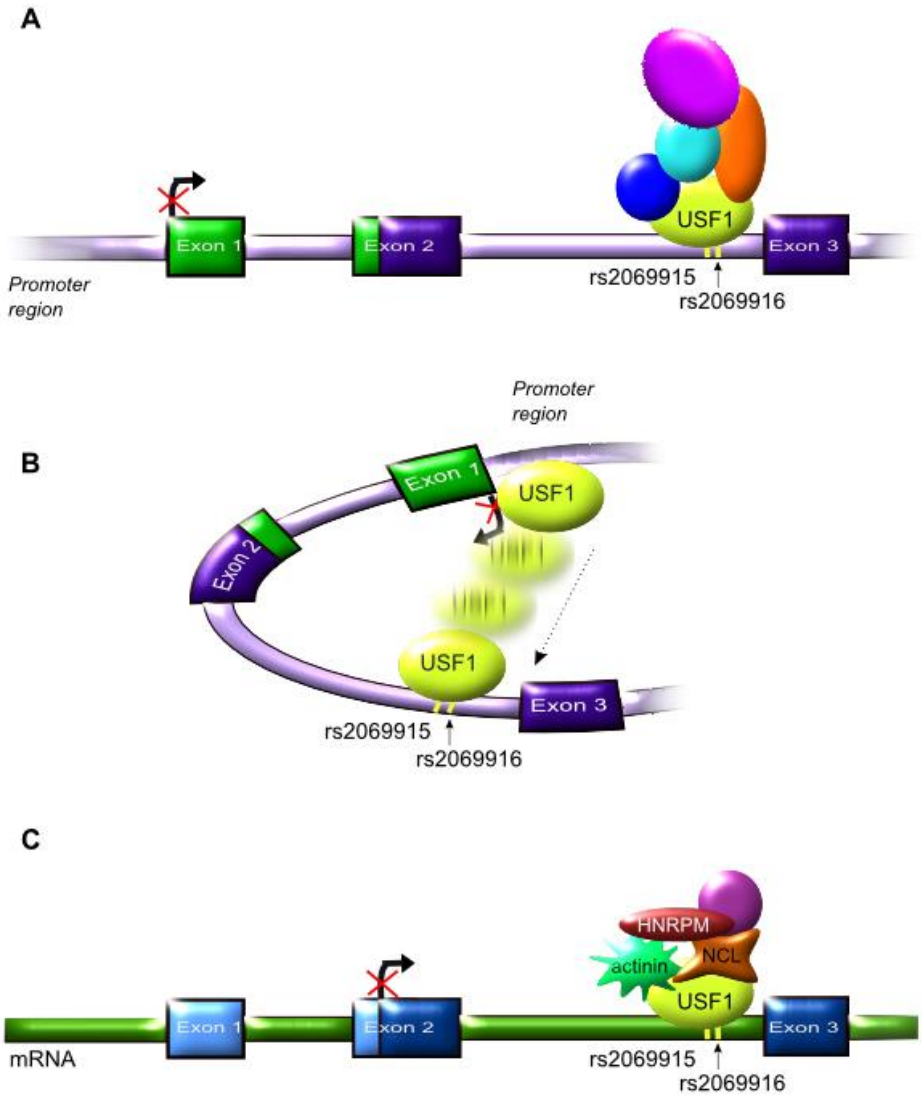

Figure 5.2 Proposed actions of USF1 binding *PROC* DNA or mRNA

A. USF1 and co-factors directly bind DNA and suppress transcription. **B.** USF1 binds a consensus sequence in the promoter region, with or without cofactors, that initiates a conformational change in chromatin. USF1 is then positioned close to rs2069916 for which USF1 has high affinity, causing DNA to become tightly wound and inaccessible to transcriptional machinery. **C.** USF1 and co-factors bind unprocessed mRNA causing suppression of translation, resulting in lower concentrations of functional protein C. Alternatively, binding could interfere with splicing events due to steric hindrance and cause non-functional protein products to be produced, which are likely quickly degraded. *Figure created using Inkscape software version 0.48.4*

Although the SILAC mass spectroscopy was unable to explicitly identify USF1 as a protein binding to rs2069916[C], the most prolific and third most prolific proteins remained unidentified (Table 3.2). This may be due to ambiguity in the amino acid sequences or subjectiveness of the analysis – if one amino acid differs from the expected sequence of a protein it will not be called as such but may in fact still be that protein. Interestingly, although ENCODE data did not include histone 1 family members, there are several tracks that show open chromatin regions relating to active transcription (Faire, DNase 1 hypersensitivity and histones related to active transcription: H3K4Me3 and H3K36Me3). None of the binding of these proteins cover the positions of rs2069915 and rs2069916 (Figure 5.3), indicating that this region is likely normally closed to transcription, which is supported by the ENCODE track showing transcriptionally inactive regions, such as sites bound by the transcriptional repressor CCCTC-binding factor (CTCF), across the two SNPs (Figure 5.3). However, the histone H3K27Me3 is a marker of inactive transcription and ENCODE data does not show this protein binding the region across the SNPs of interest. It must be kept in mind that *PROC* appears to be constitutively expressed at a particular rate (indicated by RT-qPCR assays) and would therefore be constantly switching between transcriptionally active and inactive states.

Source: http://genome.ucsc.edu, ENCODE tracks

Figure 5.3 ENCODE tracks displaying open and closed DNA regions

The tracks for FAIRE, DNase hypersensitivity sites and histones H3K4M3 and H3K36M3 indicate regions where transcription is likely active. None of these sites are evident across *PROC* SNPs rs2069915 and rs2069916 (vertical red line). The tracks for histone H3K27M3 and nuclear factor CTCF indicate regions of closed chromatin where transcription is unlikely to occur. The histone site does not cross the region of the SNPs of interest in this study, however the CTCF site does but not with great affinity, likely why it was not identified in the SILAC mass spectroscopy assays.

Histone 1, seen to bind to the major allele of rs2069915 (37bp upstream of rs2069916), is known to both stabilize and protect DNA from nucleases, topoisomerases, helicases, recombinases and others, as well as to assist in the compaction of DNA into 30nm fibers in the presence of nucleosomes [404]. In addition, histone 1 is able to bend and compact DNA without nucleosome involvement, in this instance the binding of histone 1 to DNA is transient and rapid, allowing immediate inhibition of transcription without the lengthy delay of nucleosome formation [404]. As *PROC* appears to be constitutively transcribed, the transient and rapid binding of histone 1 to the intronic SNP rs2069915 may

cause natural regulation of *PROC* expression. Individuals with the minor A-allele at this position displayed far less histone 1 binding and should therefore have naturally higher *PROC* expression with a concomitant increase in protein C levels and survival, as documented in the literature [193]. However, no difference was observed in *PROC* expression in this study, either overall or by allele, although a difference in secreted protein C was observed, which suggests regulation of *PROC* occurs post-transcriptionally. In substantiation of this, it has recently been shown that histone 1 exhibits protein-protein binding, specifically binding to ribosomal proteins, unconnected with its well-known function of chromatin binding [405-407], therefore it is possible that histone 1 binding to rs2069915[G] forms part of the same complex of ribosomal proteins suggested here to bind to rs2069916[C] [407]. This is possible since the two SNPs lie so close together that a complex binding across one SNP likely overlaps the other.

The major alleles of SNPs rs2069915[G/A] and rs2069916[C/T] in the *PROC* gene displayed differential binding of nuclear factors that may suppress translation. As low plasma levels of protein C are correlated with increased mortality in sepsis, carriers of these mutations will likely display a worse outcome during severe sepsis, when circulating plasma concentrations are already low. Treating these patients, who may benefit from rhAPC administration, earlier in the course of sepsis may prevent deterioration from sepsis to severe sepsis, septic shock and, ultimately, death. Knowing the genotype of an individual may allow clinicians to treat patients carrying the G-C haplotype of rs2069915 and rs2069916 with rhAPC at an earlier time point, before much of the cellular damage caused by severe sepsis has occurred. This should go some way towards alleviating the enormous burden on

the health care system currently caused by the extended care and treatment of patients with severe sepsis and septic shock, as well as to improve the quality of life of survivors.

5.2 PCSK9

Although, since its discovery in 2003, PCSK9 has been extremely well studied in the realms of dyslipidemias, diabetes, cardiovascular disease and interactions with cholesterol-lowering statin drugs, little is known about its role in infection, and sepsis in particular.

Many coding SNPs in the *PCSK9* gene have been shown to be functional and associated with disease phenotypes, most of them very rare and termed either Gain-of-Function or Loss-of-Function if they result in higher- or lower-than-normal LDL cholesterol plasma concentrations, respectively. These LOF variants are currently proving to be favorable with the increasing obesity and high cholesterol levels seen today in North American populations, due to the high-fat Western diet consumed in North America and elsewhere. Historically, LOF variants must have undergone strong positive selection to have remained in the population, at a time when a high fat diet was not the norm. At that time, death before puberty from parasitic infections was common. For parasites such as *Trypanosoma brucei*, *T. cruzi*, *Schistosoma mansoni* and *S. japonicum*, cholesterol is the major sterol, but these parasites are unable to synthesize it themselves and rely on the host to deliver this resource [408-411]. The parasites use cholesterol for survival functions such as proliferation, infectivity and evading the hosts' immune system. In this setting, LOF mutations in *PCSK9*, resulting in low LDL cholesterol levels, would have been advantageous and would likely have been positively selected for in populations living in areas where parasitic infections were common.

There are, however, as many highly conserved GOF as LOF mutations in *PCSK9*, which likely have also been retained in the genome by positive selection. There is evidence that some viruses such as HCV and some rhinoviruses use the LDLR to gain access to host cells [412, 413], therefore it is likely that *PCSK9* GOF variants, with their reduced levels of LDLR, would have conferred a survival benefit to these individuals. Pathogens are known to bind directly to LDLR [414, 415], soluble LDLR [416] as well as circulating LDL cholesterol molecules, which are then cleared via the LDLR [417-419]. For North Americans, in today's climate of high-fat diets and increasing obesity, coupled with good health care and declining incidence of death due to such viruses, the GOF variants are likely not as advantageous as they once were.

There appear to be few individuals homozygous for GOF or LOF alleles in *PCSK9*, however, one of the two LOF homozygotes that are known, appears to be healthy and without any serious disease problems despite having undetectable plasma PCSK9 levels [307].

It has been shown that *Ldlr*$^{-/-}$ mice have a survival benefit after LPS infusion and Gram-negative infections, but not after CLP [325, 378]; this is plausible as CLP releases an assortment of infective agents, some of which are likely Gram-positive, and it has been shown that cholesterol substantially increases growth of some Gram-positive agents such as *Staphylococcus aureus* [113]. Therefore increasing the direct pathogen-clearing potential of LDLR and other PCSK9- regulated receptors, such as the VLDL receptor, by reducing PCSK9 activity, may benefit all patients, with or without low LDL cholesterol pathogen sequestration capabilities. In support of the beneficial effects of PCSK9 inhibition, a recent study by Bieghs *et al*. (2012) demonstrated an increased inflammatory response by *Ldlr*$^{-/-}$

mice due to increased sensitivity of bone-marrow-derived macrophages to oxidized LDL [420], therefore increasing the LDLR cell surface concentration by inhibition of PCSK9 may increase clearance of oxidized LDL particles via the LDL receptors on liver cells, thus reducing the oxidized LDL-mediated secretion of pro-inflammatory molecules from activated macrophages. Although obese individuals have increased circulating pro-inflammatory markers [421], and obese patients in the ICU are known to have more co-morbidities and an increased risk of infection [422], obese ICU patients have a lower risk of mortality [423, 424], however, the reason for this apparent paradox is not clear. The possibility exists that this protective effect may be modulated by the higher lipoprotein and LDLR levels usually present in obese individuals, which may increase the rate of endotoxin clearance, however this remains to be elucidated.

Clearly, reducing PCSK9 levels confers advantages such as decreased mortality in sepsis as shown here and reduction of atherosclerosis and cardiovascular disease as shown by many other groups, with no obvious side effects. What then was the evolutionary advantage of maintaining the *PCSK9* gene in the genome? All biologic systems have checks and balances and PCSK9 modulates cholesterol levels via LDLR regulation. In addition to its role of endotoxin clearance, cholesterol is an essential component of vertebrate cell membranes, including neurons, and serves as a precursor for the biosynthesis of vitamin D, steroid hormones and bile acids. Synthesis of PCSK9 mirrors that of LDLR, ensuring that cholesterol levels remain within a specified range sufficient for normal cellular processes. In addition, in the brain PCSK9 is important during development where it is involved in directing axons, which may be the function that has allowed this gene to be maintained in the genome over time, even though adults with low or no PCSK9 seem to have no obvious ill-

effects. Indeed, transiently reducing PCSK9 during an acute event such as sepsis may not prove to be harmful, particularly if normal PCSK9 levels (and normal cellular processes of cholesterol) are resumed once the patient has recovered.

Although there remains much work to be done in order to determine all targets for PCSK9 interactions, it is currently thought that PCSK9 modulates the APOER2, VLDL [298] and LRP1 [290] receptors, all members of the LDLR-family of receptors. It is not known whether PCSK9 mediates cell surface concentrations of these receptors as it does for the LDLR, or whether treatment of sepsis patients with a pharmacological inhibitor of PCSK9 will adversely affect patient outcome due to the potentially diverse functions of this protein.

A recent study has shown that withholding nutrition for the first week in sepsis patients decreased incidence of new infections, duration of organ support and ICU stay [425], which correlates well with the early use of PCSK9 inhibitors to treat sepsis, as starvation is known to decrease PCSK9 concentration [288, 426]. Conversely, statin therapy is known to increase PCSK9 concentration [288], therefore future studies to test the efficacy of PCSK9 inhibitors in treatment of sepsis must include tight stratification of patients according to prior disease status, prior chronic treatment regimens as well as *PCSK9* genotype.

To elucidate functional SNPs in non-coding regions of the *PCSK9* gene, a small number of tag SNPs were used that gave good coverage of the gene. One tag SNP was found that clearly marked the known GOF and LOF variants that were genotyped in the VASST cohort. Carriers of the minor allele of tag SNP rs644000[A/G], that segregated with most of the LOF alleles, had increased survival compared to carriers of the major allele of this SNP.

Murine systemic inflammation and human septic shock results replicate and are concordant. Therefore, it is concluded that decreased PCSK9 activity results in amelioration

of adverse consequences of systemic inflammation including adverse cardiovascular effects (hypotension, decreased left ventricular ejection fraction in mice; cardiovascular organ dysfunction and need for vasoactive agents in humans), adverse global phenotypes (activity and body temperature in mice; multiple organ dysfunction in humans), amelioration of the inflammatory cytokine response (similar pattern in mice and humans), and reduction in mortality (the surrogate mortality endpoint of temperature <32°C in mice, 28-day mortality in humans). There are a number of PCSK9 inhibitors currently in development for treatment of lipid disorders, but none are focused on sepsis. It is also concluded that reduction in PCSK9 activity using pharmacologic or siRNA blockade or inhibition could improve outcomes of human sepsis and many other inflammatory conditions.

5.3 Limitations and Strengths of the Studies

A limitation of the *PROC* study is that the study does not have access to a genotyped cohort of patients with sepsis or septic shock in whom endogenous protein C levels were measured; an interesting study to undertake in the future would be to compare endogenous protein C and aPC levels, *PROC* genotype and outcome in patients with sepsis, severe sepsis and septic shock. A strength of this study is that all known common SNPs within the *PROC* region were included, in a population stratified by ethnicity. In addition, all functional experiments were performed on the same genetic background of Hep-G2 cells; however, no functional information on the cumulative effects of all genomic variations in these cells is available.

Experimental design is important to mitigate the effects of as many of the confounding factors as possible. A limitation of this study is that it has proved challenging to

discover a genotyped cell line that can express protein C in measureable concentrations in which to perform functional genetic studies. Work to induce the densely genotyped B-lymphocyte cell lines from the Coriell Institute (www.coriell.org) to express higher concentrations of *PROC* mRNA, which they naturally produce only minimally, proved disappointing: excessive manipulation was required and a variety of transcripts were produced, possibly due, in part, to the variety of genomic backgrounds between the individual cell lines. Therefore the well-know hepatoma cell line, Hep-G2, was used. The resulting *in vitro* assays were robust as the genetic background of all samples was identical and only differed by the carefully orchestrated treatments and genetic manipulations.

The attempts, using RT-qPCR assays, to illustrate *PROC* mRNA expression differences in Hep-G2 cells met with little success as expression remained invariant over several timepoints and many treatment alternatives. In fact, expression was so consistent *PROC* could likely be developed as a "housekeeping" gene in expression assays performed with Hep-G2 cells.

Luciferase reporter assays are a well-known and trusted assay to demonstrate genetic functionality but also have recognized limitations. The same cell line, (Hep-G2), was used for all reporter assays which removed any bias from differing genetic backgrounds between the samples and strengthened the results. However, the 421bp fragment of DNA that was cloned into the vector was short and may have lacked native chromatin conformation, thus natural function. The fragment contained five SNP sites and the DNA was excised from B-lymphocyte cell lines with specific genotypes. The alternative, to be more certain that native conformation and function would be attained, was to have cloned the entire *PROC* gene, with flanking sequences, into the vector and then performed site-directed mutagenesis to change

the SNPs of interest. After consideration this idea was rejected as the entire vector would be ~19 000bp, transfection of which is both challenging and predisposed to a lower success rate.

A potential confounding factor with the murine experiments described in this work is that mice and primates are known to have different cholesterol metabolism responses to LPS. Mice show an increase in cholesterol synthesis and total serum concentrations, whereas human and non-human primates exhibit either a decrease or no change in LDL and serum cholesterol concentrations [427]. However, humans would likely display a similar difference between cases and controls as was seen in the murine experiments, as blockade of PCSK9 activity results in an increase in LDLR and LDL-like receptors, and the difference in pathogen-bound LDL cholesterol would be relative.

A limitation of the experimental design was that an LPS-mediated murine model of endotoxemia was chosen for initial experiments in preference to a CLP model. The LPS-mediated model has been extensively used as a model of systemic infection, and removes confounding of infection by multiple pathogens, as would be the case with the CLP model of severe sepsis. The CLP model would more closely mimic conditions seen in human patients with severe sepsis, but the responses of different pathways invoked may mask or overwhelm any specific effects seen in the simpler LPS model. The murine experiments need to be repeated in a CLP model of severe sepsis before a definitive evaluation can be made as to the likely efficacy of PCSK9 blockade as a potential therapeutic treatment for sepsis patients. General availability of a specific *PCSK9* inhibitor is limited and berberine is imperfect: In addition to down-regulating *PCSK9* [323], berberine reduces LDL cholesterol [428] and upregulates LDL and insulin receptors [429]. Additionally, the data presented does not directly address the mechanism of the beneficial effect of reduced PCSK9 function. It seems

plausible that it is related to the LDL receptor and clearance of plasma lipid moieties, but other receptors and mechanisms may play a role. The *Pcsk9*$^{-/-}$ mice were found to clear endotoxin approximately twice as quickly as wild-type controls, potentially suggesting a mechanism of beneficial effect. These promising results raise the possibility that PCSK9 inhibition may be beneficial in prevention of adverse outcomes from human sepsis. However, *Pcsk9* knock-out, *Pcsk9* inhibition using berberine (prolonged pre-treatment is required to inhibit *Pcsk9* mRNA expression [322]) and human genotype all preceded the inflammatory stimulus in these studies. Therefore, an important limitation of these data is that they do not address the potential benefit of acute *PCSK9* inhibition in established sepsis and septic shock.

An explanation for the disparity of results obtained between the *Pcsk9*$^{-/-}$ and *Ldlr*$^{-/-}$ experiments may be that the lipid profiles of *Ldlr*$^{-/-}$ mice mimic human lipid profiles more closely than do wildtype C57BL/6J mice: cholesterol in the *Ldlr*$^{-/-}$ mice is mostly associated with LDL particles as in humans, whereas in wildtype C57BL/6J mice it is mostly associated with HDL particles [420]. The *Pcsk9*$^{-/-}$ mice, and berberine-treated wildtype mice, had preserved activity indices and body temperature profiles after LPS treatment compared to controls, whereas there was no difference between the saline and berberine-treated groups of *Ldlr*$^{-/-}$ mice. This might suggest that the benefit of *Pcsk9* knock-out was acting through the LDL pathway as opposed to the HDL pathway. However, both the *Pcsk9*$^{-/-}$ and *Ldlr*$^{-/-}$ mice exhibited preserved ejection fractions 6 hours after LPS infusion. The most likely explanation for these inconsistencies is that berberine has so many physiological effects it is not possible to elucidate from these experiments which pathways are involved, therefore experiments should be repeated with a more targeted PCSK9 inhibitor.

A limitation of the human data in the PCSK9 study is that data on the lipid profiles of these patients was not available. An important follow-up study would be to discern how differences in lipid profiles correlate with *PCSK9* genotype in patients with sepsis, severe sepsis and septic shock.

5.4 The Final Word

The goal of this study was to identify functional SNPs in the *PROC* and *PCSK9* genes that impact outcome from sepsis. The work here has elucidated intronic SNPs in *PROC* that are likely to have a modifying effect on unprocessed *PROC* mRNA and are correlated with lower protein C concentrations. This is a novel finding with clinical implications.

Recombinant human APC (Drotecogin-alfa activated, Xigris®, Eli Lilly) was withdrawn in 2011 as a treatment for sepsis due to lack of efficacy being shown in follow-up trials and the propensity for increasing bleeding events, but was, in any event, only approved for treatment in patients with an APACHE II score of >25. The results shown here indicate rhAPC should not be relegated to the 'back of the shelf' and tagged as yet another failed treatment for sepsis. Future studies into the efficacy of rhAPC as a treatment for sepsis should, however, include stratification of subjects by genotype as well as disease severity.

Also novel are the findings that PCSK9 modulates outcome in patients with septic shock, and that an intronic SNP in the *PCSK9* gene seems to mark the known coding LOF and GOF variations, and the correlation of LOF variations with increased survival. Results shown here suggest several possible mechanisms whereby PCSK9 knock-out may exert beneficial effect in sepsis, from increased pathogen clearance and preserved cardiac function to a reduction in production of pro-inflammatory mediators. This has significant potential for

future studies aimed at developing new treatments for patients with sepsis. Future association studies for PCSK9 in sepsis should be performed in more densely genotyped populations where data on serum lipid levels, PCSK9 concentrations, co-morbidities, chronic drug use (including statins and diabetic treatments) and BMI are collected.

The finding that SNPs in such diverse genes as *PROC* and *PCSK9* can affect outcome in patients with sepsis augments the common disease/common variation hypothesis, as all the intronic SNPs tested here were common and affected outcome in a complex disease. Additionally, these findings highlight the interplay between physiological systems in the fight against systemic infection and inflammation. These data add to the accumulating wealth of knowledge suggesting that the treatment of complex diseases should become more personal and include an individual's genomic information.

References

1. Harder MN, Ribel-Madsen R, Justesen JM et al. Type 2 diabetes risk alleles near BCAR1 and in ANK1 associate with decreased beta-cell function whereas risk alleles near ANKRD55 and GRB14 associate with decreased Insulin sensitivity in the Danish Inter99 cohort. J Clin Endocrinol Metab 2013.

2. Sawhney V, Brouilette S, Abrams D et al. Current genomics in cardiovascular medicine. Curr Genomics 2012;13:446-462.

3. Thomsen M, Nordestgaard BG, Kobzik L and Dahl M. Genetic variation in the scavenger receptor MARCO and its association with chronic obstructive pulmonary disease and lung infection in 10,604 individuals. Respiration 2013;85:144-153.

4. Rogers AJ, Chu JH, Darvishi K et al. Copy number variation prevalence in known asthma genes and their impact on asthma susceptibility. Clin Exp Allergy 2013;43:455-462.

5. Feldmann R, Fischer C, Kodelja V et al. Genome-wide analysis of LXRalpha activation reveals new transcriptional networks in human atherosclerotic foam cells. Nucleic Acids Res 2013.

6. Thompson CM, Holden TD, Rona G et al. Toll-like receptor 1 polymorphisms and associated outcomes in sepsis after traumatic injury: a candidate gene association study. Ann Surg 2013.

7. Bone RC. Toward an epidemiology and natural history of SIRS (systemic inflammatory response syndrome). JAMA - J Am Med Assoc 1992;268:3452-3455.

8. Bailey JM. Parvovirus B19 presenting with severe sepsis in a previously healthy 25-year-old female. J Am Board Fam Med 2006;19:317-319.

9. Newberry AM, Williams DN, Stauffer WM et al. Strongyloides hyperinfection presenting as acute respiratory failure and gram-negative sepsis. Chest 2005;128:3681-3684.

10. Dellinger RP, Levy MM, Carlet JM et al. Surviving Sepsis Campaign: international guidelines for management of severe sepsis and septic shock: 2008. Crit Care Med 2008;36:296-327.

11. Heron M. Deaths: leading causes for 2004. Natl Vital Stat Rep 2007;56:1-95.

12. Angus D, Linde-Zwirble W, Lidicker J et al. Epidemiology of severe sepsis in the United States: analysis of incidence, outcome, and associated costs of care. Crit Care Med 2001;29:1303-1310.

13. Wheeler DS, Zingarelli B, Wheeler WJ and Wong HR. Novel pharmacologic approaches to the management of sepsis: targeting the host inflammatory response. Recent Pat Inflamm Allergy Drug Discov 2009;3:96-112.

14. Liaw PC, Esmon CT, Kahnamoui K et al. Patients with severe sepsis vary markedly in their ability to generate activated protein C. Blood 2004;104:3958-3964.

15. Karlsson S, Ruokonen E, Varpula T et al. Long-term outcome and quality-adjusted life years after severe sepsis. Crit Care Med 2009;37:1268-1274.

16. Quartin AA, Schein RM, Kett DH and Peduzzi PN. Magnitude and duration of the effect of sepsis on survival. Department of Veterans Affairs Systemic Sepsis Cooperative Studies Group. JAMA - J Am Med Assoc 1997;277:1058-1063.

17. Reinhart K, Bauer M, Riedemann NC and Hartog CS. New Approaches to Sepsis: Molecular Diagnostics and Biomarkers. Clin Microbiol Rev 2012;25:609-634.

18. Edbrooke DL, Hibbert CL, Kingsley JM et al. The patient-related costs of care for sepsis patients in a United Kingdom adult general intensive care unit. Crit Care Med 1999;27:1760-1767.

19. Sørensen TIA, Nielsen GG, Andersen PK and Teasdale TW. Genetic and environmental influences on premature death in adult adoptees. N Engl J Med 1988;318:727-732.

20. King MC, Lee GM, Spinner NB et al. Genetic epidemiology. Annu Rev Public Health 1984;5:1-52.

21. Obel N, Christensen K, Petersen I et al. Genetic and environmental influences on risk of death due to infections assessed in Danish twins, 1943-2001. Am J Epidemiol 2010;171:1007-1013.

22. Monneret G, Venet F, Pachot A and Lepape A. Monitoring immune dysfunctions in the septic patient: a new skin for the old ceremony. Mol Med 2008;14:64-78.

23. Schefold JC, Hasper D, Volk HD and Reinke P. Sepsis: time has come to focus on the later stages. Med Hypotheses 2008;71:203-208.

24. Cohen J. The immunopathogenesis of sepsis. Nature 2002;420:885-891.

25. Annane D, Bellissant E and Cavaillon JM. Septic shock. Lancet 2005;365:63-78.

26. Vincent JL and Abraham E. The last 100 years of sepsis. Am J Respir Crit Care Med 2006;173:256-263.

27. Limaye AP, Kirby KA, Rubenfeld GD et al. Cytomegalovirus reactivation in critically ill immunocompetent patients. JAMA - J Am Med Assoc 2008;300:413-422.

28. Otto GP, Sossdorf M, Claus RA et al. The late phase of sepsis is characterized by an increased microbiological burden and death rate. Crit Care 2011;15:R183-R190.

29. Volk HD, Reinke P, Krausch D et al. Monocyte deactivation--rationale for a new therapeutic strategy in sepsis. Int Care Med 1996;Supp 4:S474-S481.

30. Wolk K, Kunz S, Crompton NEA et al. Multiple mechanisms of reduced major histocompatibility complex Class II expression in endotoxin tolerance. J Biol Chem 2003;278:18030-18036.

31. Lekkou A, Karakantza M, Mouzaki A et al. Cytokine production and monocyte HLA-DR expression as predictors of outcome for patients with community-acquired severe infections. Clin Diagn Lab Immunol 2004;11:161-167.

32. Monneret G, Lepape A, Voirin N et al. Persisting low monocyte human leukocyte antigen-DR expression predicts mortality in septic shock. Intensive Care Med 2006;32:1175-1183.

33. Berbee JF, Havekes LM and Rensen PC. Apolipoproteins modulate the inflammatory response to lipopolysaccharide. J Endotoxin Res 2005;11:97-103.

34. Harris HW, Grunfeld C, Feingold KR et al. Chylomicrons alter the fate of endotoxin, decreasing tumor necrosis factor release and preventing death. J Clin Invest 1993;91:1028-1034.

35. Harris HW, Rockey DC and Chau P. Chylomicrons alter the hepatic distribution and cellular response to endotoxin in rats. Hepatology 1998;27:1341-1348.

36. Vermont CL, den Brinker M, Kakeci N et al. Serum lipids and disease severity in children with severe meningococcal sepsis. Crit Care Med 2005;33:1610-1615.

37. Flegel WA, Baumstark MW, Weinstock C et al. Prevention of endotoxin-induced monokine release by human low- and high-density lipoproteins and by apolipoprotein A-I. Infect Immun 1993;61:5140-5146.

38. Levine DM, Parker TS, Donnelly TM et al. In vivo protection against endotoxin by plasma high density lipoprotein. Proc Natl Acad Sci USA 1993;90:12040-12044.

39. Casas AT, Hubsch AP, Rogers BC and Doran JE. Reconstituted high-density lipoprotein reduces LPS-stimulated TNF alpha. J Surg Res 1995;59:544-552.

40. Hubsch AP, Casas AT and Doran JE. Protective effects of reconstituted high-density lipoprotein in rabbit gram-negative bacteremia models. J Lab Clin Med 1995;126:548-558.

41. Pajkrt D, Doran JE, Koster F et al. Antiinflammatory effects of reconstituted high-density lipoprotein during human endotoxemia. J Exp Med 1996;184:1601-1608.

42. Behnes M, Brueckmann M, Liebe V et al. Levels of oxidized low-density lipoproteins are increased in patients with severe sepsis. J Crit Care 2008;23:537-541.

43. Safa O, Hensley K, Smirnov MD et al. Lipid oxidation enhances the function of activated protein C. J Biol Chem 2001;276:1829-1836.

44. Rensen PC, Oosten M, Bilt E et al. Human recombinant apolipoprotein E redirects lipopolysaccharide from Kupffer cells to liver parenchymal cells in rats in vivo. J Clin Invest 1997;99:2438-2445.

45. Laskowitz DT, Lee DM, Schmechel D and Staats HF. Altered immune responses in apolipoprotein E-deficient mice. J Lipid Res 2000;41:613-620.

46. Lynch JR, Tang W, Wang H et al. APOE genotype and an ApoE-mimetic peptide modify the systemic and central nervous system inflammatory response. J Biol Chem 2003;278:48529-48533.

47. Grainger DJ, Reckless J and McKilligin E. Apolipoprotein E modulates clearance of apoptotic bodies in vitro and in vivo, resulting in a systemic proinflammatory state in apolipoprotein E-deficient mice. J Immunol 2004;173:6366-6375.

48. Ali K, Middleton M, Pure E and Rader DJ. Apolipoprotein E suppresses the type I inflammatory response in vivo. Circ Res 2005;97:922-927.

49. van den Elzen P, Garg S, Leon L et al. Apolipoprotein-mediated pathways of lipid antigen presentation. Nature 2005;437:906-910.

50. Sinnis P, Willnow TE, Briones MR et al. Remnant lipoproteins inhibit malaria sporozoite invasion of hepatocytes. J Exp Med 1996;184:945-954.

51. Roselaar SE and Daugherty A. Apolipoprotein E-deficient mice have impaired innate immune responses to Listeria monocytogenes in vivo. J Lipid Res 1998;39:1740-1743.

52. de Bont N, Netea MG, Demacker PN et al. Apolipoprotein E-deficient mice have an impaired immune response to *Klebsiella pneumoniae*. Eur J Clin Invest 2000;30:818-822.

53. Recalde D, Ostos MA, Badell E et al. Human apolipoprotein A-IV reduces secretion of proinflammatory cytokines and atherosclerotic effects of a chronic infection mimicked by lipopolysaccharide. Arterioscler Thromb Vasc Biol 2004;24:756-761.

54. Rivers E, Nguyen B, Havstad S et al. Early goal-directed therapy in the treatment of severe sepsis and septic shock. N Engl J Med 2001;345:1368-1377.

55. Hayes M, Timmins A, Yau E et al. Elevation of systemic oxygen delivery in the treatment of critically ill patients. N Engl J Med 1994;330:1717-1722.

56. Gattinoni L, Brazzi L, Pelosi P et al. A trial of goal-oriented hemodynamic therapy in critically ill patients. N Engl J Med 1995;333:1025-1032.

57. Kriegler M, Perez C, DeFay K et al. A novel form of TNF/cachectin is a cell surface cytotoxic transmembrane protein: Ramifications for the complex physiology of TNF. Cell 1988;53:45-53.

58. Qiu P, Cui X, Barochia A et al. The evolving experience with therapeutic TNF inhibition in sepsis: considering the potential influence of risk of death. Expert Opin Investig Drugs 2011;20:1555-1564.

59. Mira JP, Cariou A, Grall F et al. Association of TNF2, a TNF-alpha promoter polymorphism, with septic shock susceptibility and mortality: a multicenter study. JAMA - J Am Med Assoc 1999;282:561-568.

60. Tang GJ, Huang SL, Yien HW et al. Tumor necrosis factor gene polymorphism and septic shock in surgical infection. Crit Care Med 2000;28:2733-2736.

61. Stuber F, Petersen M, Bokelmann F and Schade U. A genomic polymorphism within the tumor necrosis factor locus influences plasma tumor necrosis factor-alpha concentrations and outcome of patients with severe sepsis. Crit Care Med 1996;24:381-384.

62. Majetschak M, Flohe S, Obertacke U et al. Relation of a TNF gene polymorphism to severe sepsis in trauma patients. Ann Surg 1999;230:207-214.

63. Panacek EA, Marshall JC, Albertson TE et al. Efficacy and safety of the monoclonal anti-tumor necrosis factor antibody F(ab')2 fragment afelimomab in patients with severe sepsis and elevated interleukin-6 levels. Crit Care Med 2004;32:2173-2182.

64. Sutton BT,. Anti-tnf antibody therapy in rheumatoid arthritis and the risk of serious infections and malignancies: Systematic review and meta-analysis of rare harmful effects in randomized controlled trials. JAMA - J Am Med Assoc 2006;295:2275-2285.

65. Saint Marcoux B and De Bandt M. Vasculitides induced by TNFα antagonists: a study in 39 patients in France. Joint Bone Spine 2006;73:710-713.

66. Mangat P, Whittle S, Cleland L and Limaye V. Digital vasculitis: a late complication of anti-tumour necrosis factor alpha therapy. Clin Rheumatol 2008;27:1593-1595.

67. Siebenlist U, Franzoso G and Brown K. Structure, regulation and function of NF-kappaB. Annu Rev Cell Biol 1994;10:405-455.

68. Liou H and Baltimore D. Regulation of the NF-kB/rel transcription factor and IkB inhibitor system. Curr Opin Cell Biol 1993;5:477-487.

69. Abraham E, Nick JA, Azam T et al. Peripheral blood neutrophil activation patterns are associated with pulmonary inflammatory responses to lipopolysaccharide in humans. J Immunol 2006;176:7753-7760.

70. Hwang D. Modulation of the expression of cyclooxygenase-2 by fatty acids mediated through Toll-like receptor 4-derived signaling pathways. FASEB J 2001;15:2556-2564.

71. Kang Y, Wingerd BA, Arakawa T and Smith WL. Cyclooxygenase-2 gene transcription in a macrophage model of inflammation. J Immunol 2006;177:8111-8122.

72. Wang C, Guttridge DC, Mayo MW and Baldwin AS. NF-κB induces expression of the Bcl-2 homologue A1/Bfl-1 to preferentially suppress chemotherapy-induced apoptosis. Mol Cell Biol 1999;19:5923-5929.

73. Baldwin Jr. AS. The NF-κB and IκB proteins: New discoveries and insights. Rev Immunol 1996;14:649-683.

74. Kumar A, Takada Y, Boriek AM and Aggarwal BB. Nuclear factor-kB: its role in health and disease. J Mol Med 2004;82:434-448.

75. Lee CH, Jeon Y, Kim S and Song Y. NF-κB as a potential molecular target for cancer therapy. Biofactors 2007;29:19-35.

76. Schön M, Wienrich BG, Kneitz S et al. KINK-1, a novel small-molecule inhibitor of IKKβ, and the susceptibility of melanoma cells to antitumoral treatment. J Natl Cancer I 2008;100:862-875.

77. Miller SC, Huang R, Sakamuru S et al. Identification of known drugs that act as inhibitors of NF-κB signaling and their mechanism of action. Biochem Pharmacol 2010;79:1272-1280.

78. Courtois G and Gilmore TD. Mutations in the NF-kappaB signaling pathway: implications for human disease. Oncogene 2006;25:6831-6843.

79. Brown MA and Jones WK. NF-kappaB action in sepsis: the innate immune system and the heart. Front Biosci 2004;9:1201-1217.

80. Gilmore TD and Herscovitch M. Inhibitors of NF-kappaB signaling: 785 and counting. Oncogene 2006;25:6887-6899.

81. Marra F. Nuclear factor-κB inhibition and non-alcoholic steatohepatitis: inflammation as a target for therapy. Gut 2008;57:570-572.

82. Levi, Marcel van der P and Tom. Inflammation and coagulation. Crit Care Med 2010;38:S26-S34.

83. de Jonge E, Dekkers PEP, Creasey AA et al. Tissue factor pathway inhibitor dose-dependently inhibits coagulation activation without influencing the fibrinolytic and cytokine response during human endotoxemia. Blood 2000;95:1124-1129.

84. Abraham E, Reinhart K, Svoboda P et al. Assessment of the safety of recombinant tissue factor pathway inhibitor in patients with severe sepsis: a multicenter, randomized, placebo-controlled, single-blind, dose escalation study. Crit Care Med 2001;29:2081-2089.

85. Abraham E, Reinhart K, Opal S et al. Efficacy and safety of tifacogin (recombinant tissue factor pathway inhibitor) in severe sepsis: a randomized controlled trial. JAMA - J Am Med Assoc 2003;290:238-247.

86. Creasey AA, Chang AC, Feigen L et al. Tissue factor pathway inhibitor reduces mortality from *Escherichia coli* septic shock. J Clin Invest 1993;91:2850-2860.

87. Levi M and ten Cate H. Disseminated intravascular coagulation. N Engl J Med 1999;341:586-592.

88. Ammollo CT, Semeraro F, Xu J et al. Extracellular histones increase plasma thrombin generation by impairing thrombomodulin-dependent protein C activation. J Thromb Haemost 2011;9:1795-1803.

89. Levi M. The coagulant response in sepsis and inflammation. Hamostaseologie 2010;30:10-16.

90. Levi M, Schouten M and van der Poll T. Sepsis, coagulation, and antithrombin: old lessons and new insights. Semin Thromb Hemos 2008;34:742-746.

91. Warren BL, Eid A, Singer P et al. Caring for the critically ill patient. High-dose antithrombin III in severe sepsis: a randomized controlled trial. JAMA - J Am Med Assoc 2001;286:1869-1878.

92. Avidan MS, Levy JH, van Aken H et al. Recombinant human antithrombin III restores heparin responsiveness and decreases activation of coagulation in heparin-resistant patients during cardiopulmonary bypass. J Thorac Cardiovasc Surg 2005;130:107-113.

93. van Sluis GL, Bruggemann LW, Esmon CT et al. Endogenous activated protein C is essential for immune-mediated cancer cell elimination from the circulation. Cancer Lett 2011;306:106-110.

94. Soh UJK and Trejo J. Activated protein C promotes protease-activated receptor-1 cytoprotective signaling through β-arrestin and dishevelled-2 scaffolds. Proc Natl Acad Sci 2011;108:E1372-E1380.

95. Madhusudhan T, Wang H, Straub BK et al. Cytoprotective signaling by activated protein C requires protease-activated receptor-3 in podocytes. Blood 2012;119:874-883.

96. Bernard GR, Vincent JL, Laterre PF et al. Efficacy and safety of recombinant human activated protein C for severe sepsis. N Engl J Med 2001;344:699-709.

97. Ranieri VM, Thompson BT, Barie PS et al. Drotrecogin alfa (activated) in adults with septic shock. N Engl J Med 2012;366:2055-2064.

98. Weiler H and Kerschen E. Modulation of sepsis outcome with variants of activated protein C. J Thromb Haemost 2009;7 Suppl 1:127-131.

99. Schuepbach RA, Velez K and Riewald M. Activated protein C up-regulates procoagulant tissue factor activity on endothelial cells by shedding the TFPI Kunitz 1 domain. Blood 2011;117:6338-6346.

100. Baratto F, Michielan F, Meroni M et al. Protein C concentrate to restore physiological values in adult septic patients. Intens Care Med 2008;34:1707-1712.

101. Wu A, Hinds CJ and Thiemermann C. High-density lipoproteins in sepsis and septic shock: metabolism, actions, and therapeutic applications. Shock 2004;21:210-221.

102. Gordon BR, Parker TS, Levine DM et al. Relationship of hypolipidemia to cytokine concentrations and outcomes in critically ill surgical patients. Crit Care Med 2001;29:1563-1568.

103. Emancipator K, Csako G and Elin RJ. In vitro inactivation of bacterial endotoxin by human lipoproteins and apolipoproteins. Infect Immun 1992;60:596-601.

104. Eggesbø JB, Hjermann I, Høstmark AT and Kierulf P. LPS induced release of IL-1β, IL-6, IL-8 and TNF-α in EDTA or heparin anticoagulated whole blood from persons with high or low levels of serum HDL. Cytokine 1996;8:152-160.

105. Cockerill GW, Rye K, Gamble JR et al. High-density lipoproteins inhibit cytokine-induced expression of endothelial cell adhesion molecules. Arterioscler Thromb Vasc Biol 1995;15:1987-1994.

106. Cockerill GW, Mcdonald MC, Mota-Filipe H et al. High density lipoproteins reduce organ injury and organ dysfunction in a rat model of hemorrhagic shock. FASEB J 2001;15:1941-1952.

107. Uittenbogaard A, Shaul PW, Yuhanna IS et al. High density lipoprotein prevents oxidized low density lipoprotein-induced inhibition of endothelial nitric-oxide synthase localization and activation in caveolae. J Biol Chem 2000;275:11278-11283.

108. Gong M, Wilson M, Kelly T et al. HDL-associated estradiol stimulates endothelial NO synthase and vasodilation in an SR-BI-dependent manner. J Clin Invest 2003;111:1579-1587.

109. Mackness M, Durrington P and Mackness B. How high-density lipoprotein protects against the effects of lipid peroxidation. Curr Opin Lipidol 2000;11:383-388.

110. Boisfer E, Stengel D, Pastier D et al. Antioxidant properties of HDL in transgenic mice overexpressing human apolipoprotein A-II. J Lipid Res 2002;43:732-741.

111. Cué JI, DiPiro JT, Brunner LJ,et al. Reconstituted high density lipoprotein inhibits physiologic and tumor necrosis factor α responses to lipopolysaccharide in rabbits. Arch Surg-CHICAGO 1994;129:193-197.

112. Netea MG, Curfs JHAJ, Demacker PNM et al. Infusion of lipoproteins into volunteers enhances the growth of *Candida albicans*. Clin Infect Dis 1999;28:1148-1151.

113. Shine WE, Silvany R and McCulley JP. Relation of cholesterol-stimulated *Staphylococcus aureus* growth to chronic blepharitis. Invest Ophth Vis Sci 1993;34:2291-2296.

114. Gautier T and Lagrost L. Plasma PLTP (phospholipid-transfer protein): an emerging role in 'reverse lipopolysaccharide transport' and innate immunity. Biochem Soc Trans 2011;39:984-988.

115. Liappis AP, Kan VL, Rochester CG and Simon GL. The effect of statins on mortality in patients with bacteremia. Clin Infect Dis 2001;33:1352-1357.

116. Almog Y. Statins, inflammation, and sepsis: hypothesis. Chest 2003;124:740-743.

117. Hackam DG, Mamdani M, Li P and Redelmeier DA. Statins and sepsis in patients with cardiovascular disease: a population-based cohort analysis. Lancet 2006;367:413-418.

118. Almog Y, Novack V, Eisinger M et al. The effect of statin therapy on infection-related mortality in patients with atherosclerotic diseases. Crit Care Med 2007;35:372-378.

119. Ando H, Takamura T, Ota T et al. Cerivastatin improves survival of mice with lipopolysaccharide-induced sepsis. J Pharmacol Exp Ther 2000;294:1043-1046.

120. Mulhaupt F, Matter CM, Kwak BR et al. Statins (HMG-CoA reductase inhibitors) reduce CD40 expression in human vascular cells. Cardiovasc Res 2003;59:755-766.

121. Greenwood J and Mason JC. Statins and the vascular endothelial inflammatory response. Trends Immunol 2007;28:88-98.

122. Ayala A, Wesche-Soldato DE, Perl M et al. Blockade of apoptosis as a rational therapeutic strategy for the treatment of sepsis. Novartis Found Symp 2007;280:37-49.

123. Annane D, Sebille V, Charpentier C et al. Effect of treatment with low doses of hydrocortisone and fludrocortisone on mortality in patients with septic shock. JAMA - J Am Med Assoc 2002;288:862-871.

124. Sprung CL, Goodman S and Weiss YG. Steroid therapy of septic shock. Crit Care Clin 2009;25:825-34, x.

125. COIITSS Study Investigators, Annane D, Cariou A et al. Corticosteroid treatment and intensive insulin therapy for septic shock in adults: a randomized controlled trial. JAMA - J Am Med Assoc 2010;303:341-348.

126. Berger MM and Chiolero RL. Antioxidant supplementation in sepsis and systemic inflammatory response syndrome. Crit Care Med 2007;35:S584-90.

127. Harbrecht BG. Therapeutic use of nitric oxide scavengers in shock and sepsis. Curr Pharm Des 2006;12:3543-3549.

128. Minneci P, Deans K, Natanson C and Eichacker PQ. Increasing the efficacy of anti-inflammatory agents used in the treatment of sepsis. Eur J Clin Microbiol 2003;22:1-9.

129. Ayala FJ, Escalante A, O'Huigin C and Klein J. Molecular genetics of speciation and human origins. Proc Natl Acad Sci USA 1994;91:6787-6794.

130. Miller RD and Kwok P. The birth and death of human single-nucleotide polymorphisms: new experimental evidence and implications for human history and medicine. Hum Mol Genet 2001;10:2195-2198.

131. Chakravarti A. Population genetics - making sense out of sequence. Nat Genet 1999.

132. Collins FS, Brooks LD and Chakravarti A. A DNA polymorphism discovery resource for research on human genetic variation. Genome Res 1998;8:1229-1231.

133. Wang Z and Moult J. SNPs, protein structure, and disease. Hum Mutat 2001;17:263-270.

134. Wang DG, Fan J, Siao C et al. Large-scale identification, mapping, and genotyping of single-nucleotide polymorphisms in the human genome. Science 1998;280:1077-1082.

135. Corder EH, Saunders AM, Strittmatter WJ et al. Gene dose of apolipoprotein E type 4 allele and the risk of Alzheimer's disease in late onset families. Science 1993;261:921-923.

136. Saunders AM, Strittmatter WJ, Schmechel D et al. Association of apolipoprotein E allele epsilon 4 with late-onset familial and sporadic Alzheimer's disease. Neurology 1993;43:1467-1472.

137. Walley KR and Russell JA. Protein C -1641 AA is associated with decreased survival and more organ dysfunction in severe sepsis. Crit Care Med 2007;35:12-17.

138. Chen G, Bentley A, Adeyemo A et al. Genome-wide association study identifies novel loci association with fasting insulin and insulin resistance in African Americans. Hum Mol Genet 2012;21:4530-4536.

139. Martinelli-Boneschi F, Esposito F, Brambilla P et al. A genome-wide association study in progressive multiple sclerosis. Mult Scler J 2012;18:1384-1394.

140. Vimaleswaran KS, Tachmazidou I, Zhao JH et al. Candidate genes for obesity-susceptibility show enriched association within a large genome-wide association study for BMI. Hum Mol Genet 2012;21:4537-4542.

141. Wilk JB, Shrine NRG, Loehr LR et al. Genome-wide association studies identify CHRNA5/3 and HTR4 in the development of airflow obstruction. Am J Resp Crit Care 2012;186:622-632.

142. Church DM, Goodstadt L, Hillier LW et al. Lineage-specific biology revealed by a finished genome assembly of the mouse. PLoS Biol 2009;7:e1000112.

143. Meader S, Ponting CP and Lunter G. Massive turnover of functional sequence in human and other mammalian genomes. Genome Res 2010;20:1335-1343.

144. Pfeifer D, Kist R, Dewar K et al. Campomelic dysplasia translocation breakpoints are scattered over 1 mb proximal to sox9: evidence for an extended control region. Am J Hum Genet 1999;65:111-124.

145. Kleinjan DA, Seawright A, Schedl A et al. Aniridia-associated translocations, DNase hypersensitivity, sequence comparison and transgenic analysis redefine the functional domain of PAX6. Hum Mol Genet 2001;10:2049-2059.

146. Lettice LA, Horikoshi T, Heaney SJH et al. Disruption of a long-range cis-acting regulator for Shh causes preaxial polydactyly. Proc Natl Acad Sci 2002;99:7548-7553.

147. Blackwood EM and Kadonaga JT. Going the distance: A current view of enhancer action. Science 1998;281:60-63.

148. Howard ML and Davidson EH. cis-Regulatory control circuits in development. Dev Biol 2004;271:109-118.

149. Slatkin M. Linkage disequilibrium mdash] understanding the evolutionary past and mapping the medical future. Nat Rev Genet 2008;9:477-485.

150. Brookes AJ. The essence of SNPs. Gene 1999;234:177-186.

151. Drake JA, Bird C, Nemesh J et al. Conserved noncoding sequences are selectively constrained and not mutation cold spots. Nat Genet 2006;38:223-227.

152. Allaart CF, Poort SR, Rosendaal FR et al. Increased risk of venous thrombosis in carriers of hereditary protein C deficiency defect. Lancet 1993;341:134-138.

153. Poort SR, Rosendaal FR, Reitsma PH and Bertina RM. A common genetic variation in the 3' untranslated region of the prothrombin gene is associated with elevated prothrombin levels and an increase in venous thrombosis. Blood 1996;88:3698-3703.

154. Hubacek JA, Stuber F, Frohlich D et al. Gene variants of the bactericidal/ permeability increasing protein and lipopolysaccharide binding protein in sepsis patients: gender-specific predisposition to sepsis. Crit Care Med 2001;29:557-561.

155. Sapru A, Wiemels JL, Witte JS et al. Acute lung injury and the coagulation pathway: Potential role of gene polymorphisms in the protein C and fibrinolytic pathways. Intensive Care Med 2006;32:1293-1303.

156. Sapru A, Hansen H, Ajayi T et al. 4G/5G polymorphism of plasminogen activator inhibitor-1 gene is associated with mortality in intensive care unit patients with severe pneumonia. Anesthesiology 2009;110:1086-1091.

157. Manocha S, Russell JA, Sutherland AM et al. Fibrinogen-beta gene haplotype is associated with mortality in sepsis. J Infect 2007;54:572-577.

158. Sachidanandam R, Weissman D, Schmidt SC et al. A map of human genome sequence variation containing 1.42 million single nucleotide polymorphisms. Nature 2001;409:928-933.

159. Sneath P. Relations between chemical structure and biological activity in peptides. J Theor Biol 1966;12:157-195.

160. Segal MR, Cummings MP and Hubbard AE. Relating amino acid sequence to phenotype: analysis of peptide-binding data. Biometrics 2001;57:632-642.

161. Gulukota K, Sidney J, Sette A and DeLisi C. Two complementary methods for predicting peptides binding major histocompatibility complex molecules. J Mol Biol 1997;267:1258-1267.

162. Xia X and Xie Z. Protein structure, neighbor effect, and a new index of amino acid dissimilarities. Mol Biol Evol 2002;19:58-67.

163. Ruivo R, Anne C, Sagné C and Gasnier B. Molecular and cellular basis of lysosomal transmembrane protein dysfunction. BBA-Mol Cell Res 2009;1793:636-649.

164. Cao A, Galanello R and Rosatelli MC. Genotype-phenotype correlations in β-thalassemias. Blood Rev 1994;8:1-12.

165. Aartsma-Rus A, Van Deutekom JC, Fokkema IF et al. Entries in the Leiden Duchenne muscular dystrophy mutation database: an overview of mutation types and paradoxical cases that confirm the reading-frame rule. Muscle Nerve 2006;34:135-144.

166. Welsh MJ and Smith AE. Molecular mechanisms of CFTR chloride channel dysfunction in cystic fibrosis. Cell 1993;73:1251-1254.

167. Nudelman I, Glikin D, Smolkin B et al. Repairing faulty genes by aminoglycosides: Development of new derivatives of geneticin (G418) with enhanced suppression of diseases-causing nonsense mutations. Bioorg Med Chem 2010;18:3735-3746.

168. Dobson CM. Protein folding and misfolding. Nature 2003;426:884-890.

169. Vendruscolo M, Zurdo J, MacPhee CE and Dobson CM. Protein folding and misfolding: a paradigm of self–assembly and regulation in complex biological systems. Philos T Roy Soc A 2003;361:1205-1222.

170. Fitzpatrick AW, Knowles TP, Waudby CA et al. Inversion of the balance between hydrophobic and hydrogen bonding interactions in protein folding and aggregation. PLoS Comput Biol 2011;7:e1002169.

171. O'Brien EP, Christodoulou J, Vendruscolo M and Dobson CM. Trigger factor slows co-translational folding through kinetic trapping while sterically protecting the nascent chain from aberrant cytosolic interactions. J Am Chem Soc 2012;134:10920-10932.

172. Kahali B, Basak S and Ghosh TC. Reinvestigating the codon and amino acid usage of S. cerevisiae genome: a new insight from protein secondary structure analysis. Biochem Biophys Res Commun 2007;354:693-699.

173. Pagani F, Raponi M and Baralle FE. Synonymous mutations in CFTR exon 12 affect splicing and are not neutral in evolution. Proc Natl Acad Sci USA 2005;102:6368-6372.

174. Mandal M and Breaker RR. Gene regulation by riboswitches. Nat Rev Mol Cell Biol 2004;5:451-463.

175. Collier AJ, Gallego J, Klinck R et al. A conserved RNA structure within the HCV IRES eIF3-binding site. Nat Struct Mol Biol 2002;9:375-380.

176. Neilson JR and Sandberg R. Heterogeneity in mammalian RNA 3′ end formation. Exp Cell Res 2010;316:1357-1364.

177. von Roretz C and Gallouzi I. Decoding ARE-mediated decay: is microRNA part of the equation? J Cell Biol 2008;181:189-194.

178. Chen K, Song F, Calin GA et al. Polymorphisms in microRNA targets: a gold mine for molecular epidemiology. Carcinogenesis 2008;29:1306-1311.

179. Ha M, Pang M, Agarwal V and Chen ZJ. Interspecies regulation of microRNAs and their targets. BBA-Gene Reg Mech 2008;1779:735-742.

180. Mattick JS and Gagen MJ. The evolution of controlled multitasked gene networks: The role of introns and other noncoding RNAs in the development of complex organisms. Mol Biol Evol 2001;18:1611-1630.

181. Kleinjan DA and van Heyningen V. Long-range control of gene expression: Emerging mechanisms and disruption in disease. Am J Hum Genet 2005;76:8-32.

182. Shastry B. SNPs: Impact on Gene Function and Phenotype. In:. Single Nucleotide Polymorphisms. Editor: Komar AA. Humana Press; 2009. p 3-22.

183. Locke JM, Da Silva Xavier G, Rutter GA and Harries LW. An alternative polyadenylation signal in TCF7L2 generates isoforms that inhibit T cell factor/lymphoid-enhancer factor (TCF/LEF)-dependent target genes. Diabetologia 2011;54:3078-3082.

184. Sun G, Yan J, Noltner K et al. SNPs in human miRNA genes affect biogenesis and function. RNA 2009;15:1640-1651.

185. Jiang Q, Wang Y, Hao Y et al. miR2Disease: a manually curated database for microRNA deregulation in human disease. Nucleic Acids Res 2009;37:D98-D104.

186. Law JA and Jacobsen SE. Establishing, maintaining and modifying DNA methylation patterns in plants and animals. Nat Rev Genet 2010;11:204-220.

187. Ehrlich M, Gama-Sosa MA, Huang L et al. Amount and distribution of 5-methylcytosine in human DNA from different types of tissues or cells. Nucleic Acids Res 1982;10:2709-2721.

188. Shoemaker R, Deng J, Wang W and Zhang K. Allele-specific methylation is prevalent and is contributed by CpG-SNPs in the human genome. Genome Res 2010;20:883-889.

189. Cargill M, Altshuler D, Ireland J et al. Characterization of single-nucleotide polymorphisms in coding regions of human genes. Nat Genet 1999;22:231-238.

190. Strittmatter WJ, Saunders AM, Schmechel D et al. Apolipoprotein E: high-avidity binding to beta-amyloid and increased frequency of type 4 allele in late-onset familial Alzheimer disease. Proc Natl Acad Sci 1993;90:1977-1981.

191. Bertina RM, Koeleman BP, Koster T et al. Mutation in blood coagulation factor V associated with resistance to activated protein C. Nature 1994;369:64-67.

192. Esmon CT. Protein C anticoagulant pathway and its role in controlling microvascular thrombosis and inflammation. Crit Care Med 2001;29:S48-S51.

193. Yan S, Helterbrand J, Hartman D et al. Low levels of protein C are associated with poor outcome in severe sepsis. Chest 2001;120:915-922.

194. Mammen EF, Thomas WR and Seegers WH.Activation of purified prothrombin to autoprothrombin-I or autoprothrombin-II (platelet cofactor-II or autoprothrombin II-A). Thromb Diath Haemorrh 1960;5:218-249.

195. Stenflo J. A new vitamin K-dependent protein. Purification from bovine plasma and preliminary characterization. J Biol Chem 1976;251:355-363.

196. Stenflo J. Structure and function of protein-C. Semin Thromb Hemost 1984;10:109-121.

197. Fisher CL, Greengard JS and Griffin JH. Models of the serine-protease domain of the human antithrombotic plasma factor-activated protein-C and its zymogen. Protein Sci 1994;3:588-599.

198. Gandrille S, Alhenc-Gelas M, Gaussem P et al. Five novel mutations located in exons III and IX of the protein C gene in patients presenting with defective protein C anticoagulant activity. Blood 1993;82:159-168.

199. Beckmann RJ, Schmidt RJ, Santerre RF et al. The structure and evolution of a 461 amino acid human protein C precursor and its messenger RNA, based upon the DNA sequence of cloned human liver cDNAs. Nucleic Acids Res 1985;13:5233-5247.

200. Esmon NL, DeBault LE and Esmon CT. Proteolytic formation and properties of gamma-carboxyglutamic acid-domainless protein C. J Biol Chem 1983;258:5548-5553.

201. Foster D and Davie EW. Characterization of a cDNA coding for human protein C. Proc Natl Acad Sci USA 1984;81:4766-4770.

202. Sun YH, Shen L and Dahlback B. Gla domain-mutated human protein C exhibiting enhanced anticoagulant activity and increased phospholipid binding. Blood 2003;101:2277-2284.

203. Danese S, Vetrano S, Zhang L et al. The protein C pathway in tissue inflammation and injury: pathogenic role and therapeutic implications. Blood 2010;115:1121-1130.

204. Esmon CT. Thrombomodulin as a model of molecular mechanisms that modulate protease specificity and function at the vessel surface. FASEB J 1995;9:946-955.

205. Esmon CT. The protein C anticoagulant pathway. Arterioscler Thromb 1992;12:135-145.

206. Seligsohn U, Berger A, Abend M et al. Homozygous protein C deficiency manifested by massive venous thrombosis in the newborn. N Engl J Med 1984;310:559-562.

207. Broekmans AW, Veltkamp JJ and Bertina RM. Congenital protein C deficiency and venous thromboembolism. A study of three Dutch families. N Engl J Med 1983;309:340-344.

208. Miletich J, Sherman L and Broze G. Absence of thrombosis in subjects with heterozygous protein-C deficiency. N Engl J Med 1987;317:991-996.

209. Mesters R, Helterbrand J, Utterback B et al. Prognostic value of protein C concentrations in neutropenic patients at high risk of severe septic complications. Crit Care Med 2000;28:2209-2216.

210. de Kleijn E, de Groot R, Hack C et al. Activation of protein C following infusion of protein C concentrate in children with severe meningococcal. sepsis and purpura fulminans: A randomized, double-blinded, placebo-controlled, dose-finding study. Crit Care Med 2003;31:1839-1847.

211. Griffin JH, Evatt B, Zimmerman TS et al. Deficiency of protein C in congenital thrombotic disease. J Clin Invest 1981;68:1370-1373.

212. Conard J, Horellou MH, Teger-Nilsson AC et al. The fibrinolytic system in patients with congenital protein C deficiency. Thromb Res 1984;36:363-367.

213. Spek CA, Greengard JS, Griffin JH et al. Two mutations in the promoter region of the human protein C gene both cause type I protein C deficiency by disruption of two HNF-3 binding sites. J Biol Chem 1995;270:24216-24221.

214. Marlar RA and Mastovich S. Hereditary protein C deficiency: a review of the genetics, clinical presentation, diagnosis and treatment. Blood Coagul Fibrin 1990;1:319-330.

215. Broekmans AW, Bertina RM, Loeliger EA et al. Protein C and the development of skin necrosis during anticoagulant therapy. Thromb Haemost 1983;49:251.

216. Casella JF, Lewis JH, Bontempo FA et al. Successful treatment of homozygous protein C deficiency by hepatic transplantation. Lancet 1988;1:435-438.

217. Hartman KR, Manco-Johnson M, Rawlings JS et al. Homozygous protein C deficiency: early treatment with warfarin. Am J Pediatr Hematol Oncol 1989;11:395-401.

218. Scully MF, Toh CH, Hoogendoorn H et al. Activation of protein C and its distribution between its inhibitors, protein C inhibitor, alpha 1-antitrypsin and alpha 2-macroglobulin, in patients with disseminated intravascular coagulation. Thromb Haemost 1993;69:448-453.

219. Kurosawa S, Stearns-Kurosawa D, Carson C et al. Plasma levels of endothelial cell protein C receptor are elevated in patients with sepsis and systemic lupus erythematosus: Lack of correlation with thrombomodulin suggests involvement of different pathological processes. Blood 1998;91:725-727.

220. Hook KM and Abrams CS. The loss of homeostasis in hemostasis: New approaches in treating and understanding acute disseminated intravascular coagulation in critically ill patients. Clin Trans Sci 2012;5:85-92.

221. Wheeler A and Bernard G. Treating patients with severe sepsis. N Engl J Med 1999;340:207-214.

222. vanderPoll T, Jansen P, VanZee K et al. Pretreatment with a 55-kDa tumor necrosis factor receptor immunoglobulin fusion protein attenuates activation of coagulation, but not of fibrinolysis, during lethal bacteremia in baboons. J Infect Dis 1997;176:296-299.

223. Mestries J, Kruithof E, Gascon M et al. In-vivo modulation of coagulation and fibrinolysis by recombinant glycosylated human interleukin-6 in baboons. Eur Cytokine Netw 1994;5:275-281.

224. Levi M, Dorffler-Melly J, Reitsma P et al. Aggravation of endotoxin-induced disseminated intravascular coagulation and cytokine activation in heterozygous protein-C-deficient mice. Blood 2003;101:4823-4827.

225. Houng A, Maggini L, Clement C and Reed G. Identification and structure of activated-platelet protein-1, a protein with RNA-binding domain motifs that is expressed by activated platelets. Eur J Biochem 1997;243:209-218.

226. Grey ST, Tsuchida A, Hau H et al. Selective inhibitory effects of the anticoagulant activated protein C on the responses of human mononuclear phagocytes to LPS, IFN-gamma, or phorbol ester. J Immunol 1994;153:3664-3672.

227. Murakami K, Okajima K, Uchiba M et al. Activated protein C prevents LPS-induced pulmonary vascular injury by inhibiting cytokine production. Am J Physiol-Lung C 1997;272:L197-L202.

228. Yuksel M, Okajima K, Uchiba M et al. Activated protein C inhibits lipopolysaccharide-induced tumor necrosis factor-alpha production by inhibiting activation of both nuclear factor-kappa B and activator protein-1 in human monocytes. Thromb Haemost 2002;88:267-273.

229. Esmon CT, Xu J and Lupu F. Innate immunity and coagulation. J Thromb Haemost 2011;9 Suppl 1:182-188.

230. Degen JL, Bugge TH and Goguen JD. Fibrin and fibrinolysis in infection and host defense. J Thromb Haemost 2007;5:24-31.

231. Bergmann S and Hammerschmidt S. Fibrinolysis and host response in bacterial infections. Thromb Haemost 2007;98:512-520.

232. Kwiecinski J, Josefsson E, Mitchell J et al. Activation of plasminogen by staphylokinase reduces the severity of *Staphylococcus aureus* systemic infection. J Infect Dis 2010;202:1041-1049.

233. Herwald H, Morgelin M, Olsen A et al. Activation of the contact-phase system on bacterial surfaces - a clue to serious complications in infectious diseases. Nat Med 1998;4:298-302.

234. Pixley RA, Cadena DL, Page JD et al. The contact system contributes to hypotension but not disseminated intravascular coagulation in lethal bacteremia. In vivo use of a monoclonal anti-factor XII antibody to block contact activation in baboons. J Clin Invest 1993;91:61-68.

235. Colman R and Schmaier A. The contact activation system - Biochemistry and interactions of these surface-mediated defense reactions. Crit Rev Oncol Hemat 1986;5:57-85.

236. Kaplan A and Silverberg M. The coagulation-kinin pathway of human-plasma. Blood 1987;70:1-15.

237. Hall J. Bradykinin receptors - Pharmacological properties and biological roles. Pharmacol Ther 1992;56:131-190.

238. Arnout J and Vermylen J. Current status and implications of autoimmune antiphospholipid antibodies in relation to thrombotic disease. J Thromb Haemost 2003;1:931-942.

239. Pennings MTT, Derksen RHWM, Urbanus RT et al. Platelets express three different splice variants of ApoER2 that are all involved in signaling. J Thromb Haemost 2007;5:1538-1544.

240. White TC, Berny MA, Tucker EI et al. Protein C supports platelet binding and activation under flow: role of glycoprotein Ib and apolipoprotein E receptor 2. J Thromb Haemost 2008;6:995-1002.

241. Stephenson DA, Toltl LJ, Beaudin S and Liaw PC. Modulation of monocyte function by activated protein c, a natural anticoagulant. J Immunol 2006;177:2115-2122.

242. Sturn DH, Kaneider NC, Feistritzer C et al. Expression and function of the endothelial protein C receptor in human neutrophils. Blood 2003;102:1499-1505.

243. Joyce DE, Gelbert L, Ciaccia A et al. Gene expression profile of antithrombotic protein c defines new mechanisms modulating inflammation and apoptosis. J Biol Chem 2001;276:11199-11203.

244. Joyce DE and Grinnell BW. Recombinant human activated protein C attenuates the inflammatory response in endothelium and monocytes by modulating nuclear factor-kappaB. Crit Care Med 2002;30:S288-93.

245. White B, Schmidt M, Murphy C et al. Activated protein C inhibits lipopolysaccharide-induced nuclear translocation of nuclear factor kappaB (NF-kappaB) and tumour necrosis factor alpha (TNF-alpha) production in the THP-1 monocytic cell line. Br J Haematol 2000;110:130-134.

246. Toltl LJ, Beaudin S, Liaw PC and Canadian Critical Care Translational Biology Group. Activated protein C up-regulates IL-10 and inhibits tissue factor in blood monocytes. J Immunol 2008;181:2165-2173.

247. Yamazaki S, Inamori S, Nakatani T and Suga M. Activated protein C attenuates cardiopulmonary bypass-induced acute lung injury through the regulation of neutrophil activation. J Thorac Cardiovasc Surg 2011;141:1246-1252.

248. Della Valle P, Pavani G and D'Angelo A. The protein C pathway and sepsis. Thromb Res 2012;129:296-300.

249. Esmon CT. Extracellular histones zap platelets. Blood 2011;118:3456-3457.

250. Xu J, Zhang X, Pelayo R et al. Extracellular histones are major mediators of death in sepsis. Nat Med 2009;15:1318-U117.

251. Wang H, Yang H, Czura C et al. HMGB1 as a late mediator of lethal systemic inflammation. Am J Respir Crit Care Med 2001;164:1768-1773.

252. Fiuza C, Bustin M, Talwar S et al. Inflammation-promoting activity of HMGB1 on human microvascular endothelial cells. Blood 2003;101:2652-2660.

253. van Zoelen MA, Yang H, Florquin S et al. Role of toll-like receptors 2 and 4, and the receptor for advanced glycation end products in high-mobility group box 1-induced inflammation in vivo. Shock 2009;31:280-284.

254. Bae J and Rezaie AR. Activated protein C inhibits high mobility group box 1 signaling in endothelial cells. Blood 2011.

255. Papathanassoglou EDE, Moynihan JA and Ackerman MH. Does programmed cell death (apoptosis) play a role in the development of multiple organ dysfunction in critically ill patients? A review and a theoretical framework. Crit Care Med 2000;28.

256. McVerry BJ and Garcia JGN. Endothelial cell barrier regulation by sphingosine 1-phosphate. J Cell Biochem 2004;92:1075-1085.

257. Riewald M, Petrovan RJ, Donner A et al. Activation of endothelial cell protease activated receptor 1 by the protein C pathway. Science 2002;296:1880-1882.

258. Mosnier L and Griffin J. Inhibition of staurosporine-induced apoptosis of endothelial cells by activated protein C requires protease-activated receptor-1 and endothelial cell protein C receptor. Biochem J 2003;373:65-70.

259. Yamamoto K and Loskutoff D. Extrahepatic expression and regulation of protein C in the mouse. Am J Pathol 1998;153:547-555.

260. Spek CA, Koster T, Rosendaal FR et al. Genotypic variation in the promoter region of the protein C gene is associated with plasma protein C levels and thrombotic risk. Arterioscler Thromb Vasc Biol 1995;15:214-218.

261. Miao CH, Ho WT, Greenberg DL and Davie EW. Transcriptional regulation of the gene coding for human protein C. J Biol Chem 1996;271:9587-9594.

262. Alhenc-Gelas M, Gandrille S, Aubry ML and Aiach M. Thirty-three novel mutations in the protein C gene. French INSERM network on molecular abnormalities responsible for protein C and protein S. Thromb Haemost 2000;83:86-92.

263. Shamsher MK, Chuzhanova NA, Friedman B et al. Identification of an intronic regulatory element in the human protein C (*PROC*) gene. Hum Genet 2000;107:458-465.

264. Zhang K, Kurachi S and Kurachi K. Genetic mechanisms of age regulation of protein C and blood coagulation. J Biol Chem 2002;277:4532-4540.

265. Aiach M, Nicaud V, Alhenc-Gelas M et al. Complex association of protein C gene promoter polymorphism with circulating protein C levels and thrombotic risk. Arterioscler Thromb Vasc Biol 1999;19:1573-1576.

266. Chen QX, Wu SJ, Wang HH et al. Protein C -1641A/-1654C haplotype is associated with organ dysfunction and the fatal outcome of severe sepsis in Chinese Han population. Hum Genet 2008;123:281-287.

267. Seidah NG, Benjannet S, Wickham L et al. The secretory proprotein convertase neural apoptosis-regulated convertase 1 (NARC-1): liver regeneration and neuronal differentiation. Proc Natl Acad Sci USA 2003;100:928-933.

268. Abifadel M, Varret M, Rabes JP et al. Mutations in PCSK9 cause autosomal dominant hypercholesterolemia. Nat Genet 2003;34:154-156.

269. Seidah NG. PCSK9 as a therapeutic target of dyslipidemia. Expert Opin Ther Targets 2009;13:19-28.

270. Davignon J, Dubuc G and Seidah N. The influence of PCSK9 polymorphisms on serum low-density lipoprotein cholesterol and risk of atherosclerosis. Curr Ather Rep 2010;12:308-315.

271. Ranheim T, Mattingsdal M, Lindvall JM et al. Genome-wide expression analysis of cells expressing gain of function mutant D374Y-PCSK9. J Cell Physiol 2008;217:459-467.

272. Bingham B, Shen R, Kotnis S et al. Proapoptotic effects of NARC 1 (= PCSK9), the gene encoding a novel serine proteinase. Cytometry A 2006;69:1123-1131.

273. Labonte P, Begley S, Guevin C et al. PCSK9 impedes hepatitis C virus infection in vitro and modulates liver CD81 expression. Hepatology 2009;50:17-24.

274. Feingold KR, Moser AH, Shigenaga JK et al. Inflammation stimulates the expression of PCSK9. Biochem Biophys Res Commun 2008;374:341-344.

275. Miyazawa H, Honda T, Miyauchi S et al. Increased serum PCSK9 concentrations are associated with periodontal infection but do not correlate with LDL cholesterol concentration. Clin Chim Acta 2012;413:154-159.

276. Abifadel M, Rabes JP, Devillers M et al. Mutations and polymorphisms in the proprotein convertase subtilisin kexin 9 (*PCSK9*) gene in cholesterol metabolism and disease. Hum Mutat 2009;30:520-529.

277. Naureckiene S, Ma L, Sreekumar K et al. Functional characterization of Narc 1, a novel proteinase related to proteinase K. Arch Biochem Biophys 2003;420:55-67.

278. Kwon HJ, Lagace TA, McNutt MC et al. Molecular basis for LDL receptor recognition by PCSK9. Proc Natl Acad Sci USA 2008;105:1820-1825.

279. Benjannet S, Rhainds D, Essalmani R et al. NARC-1/PCSK9 and its natural mutants: zymogen cleavage and effects on the low density lipoprotein (LDL) receptor and LDL cholesterol. J Biol Chem 2004;279:48865-48875.

280. Cunningham D, Danley DE, Geoghegan KF et al. Structural and biophysical studies of PCSK9 and its mutants linked to familial hypercholesterolemia. Nat Struct Mol Biol 2007;14:413-419.

281. McNutt MC, Kwon HJ, Chen C et al. Antagonism of secreted PCSK9 increases low density lipoprotein receptor expression in HepG2 cells. J Biol Chem 2009;284:10561-10570.

282. Horton JD, Cohen JC and Hobbs HH. Molecular biology of PCSK9: its role in LDL metabolism. Trends Biochem Sci 2007;32:71-77.

283. Basak A, Palmer-Smith H and Mishra P. Proprotein convertase subtilisin kexin9 (PCSK9): a novel target for cholesterol regulation. Protein Pept Lett 2012;19:575-585.

284. Dewpura T, Raymond A, Hamelin J et al. PCSK9 is phosphorylated by a Golgi casein kinase-like kinase ex vivo and circulates as a phosphoprotein in humans. FEBS J 2008;275:3480-3493.

285. Benjannet S, Rhainds D, Hamelin J et al. The proprotein convertase (PC) PCSK9 is inactivated by furin and/or PC5/6A: functional consequences of natural mutations and post-translational modifications. J Biol Chem 2006;281:30561-30572.

286. Lagace TA, Curtis DE, Garuti R et al. Secreted PCSK9 decreases the number of LDL receptors in hepatocytes and in livers of parabiotic mice. J Clin Invest 2006;116:2995-3005.

287. Alborn WE, Cao G, Careskey HE et al. Serum proprotein convertase subtilisin kexin type 9 is correlated directly with serum LDL cholesterol. Clin Chem 2007;53:1814-1819.

288. Persson L, Cao G, Ståhle L et al. Circulating Proprotein Convertase Subtilisin Kexin type 9 has a diurnal rhythm synchronous with cholesterol synthesis and is reduced by fasting in humans. Arterioscler Thromb Vasc Biol 2010;30:2666-2672.

289. Grefhorst A, McNutt MC, Lagace TA and Horton JD. Plasma PCSK9 preferentially reduces liver LDL receptors in mice. J Lipid Res 2008;49:1303-1311.

290. Cameron J, Bogsrud MP, Tveten K et al. Serum levels of proprotein convertase subtilisin/kexin type 9 in subjects with familial hypercholesterolemia indicate that proprotein convertase subtilisin/kexin type 9 is cleared from plasma by low-density lipoprotein receptor–independent pathways. Translation Res 2012;160:125-130.

291. Boucher P and Herz J. Signaling through LRP1: Protection from atherosclerosis and beyond. Biochem Pharmacol 2011;81:1-5.

292. Zhang DW, Lagace TA, Garuti R et al. Binding of proprotein convertase subtilisin/kexin type 9 to epidermal growth factor-like repeat A of low density lipoprotein receptor decreases receptor recycling and increases degradation. J Biol Chem 2007;282:18602-18612.

293. Stein EA, Gipe D, Bergeron J et al. Effect of a monoclonal antibody to PCSK9, REGN727/SAR236553, to reduce low-density lipoprotein cholesterol in patients with heterozygous familial hypercholesterolaemia on stable statin dose with or without ezetimibe therapy: a phase 2 randomised controlled trial. Lancet 2012;380:29-36.

294. Schmidt RJ, Beyer TP, Bensch WR et al. Secreted proprotein convertase subtilisin/kexin type 9 reduces both hepatic and extrahepatic low-density lipoprotein receptors in vivo. Biochem Biophys Res Commun 2008;370:634-640.

295. Kotowski IK, Pertsemlidis A, Luke A et al. A spectrum of PCSK9 alleles contributes to plasma levels of low-density lipoprotein cholesterol. Am J Hum Genet 2006;78:410-422.

296. Cohen JC, Boerwinkle E, Mosley TH, Jr. and Hobbs HH. Sequence variations in PCSK9, low LDL, and protection against coronary heart disease. N Engl J Med 2006;354:1264-1272.

297. Musunuru K, Lettre G, Young T et al. Candidate gene association resource (CARe): design, methods, and proof of concept. Circ Cardiovasc Genet 2010;3:267-275.

298. Poirier S, Mayer G, Benjannet S et al. The proprotein convertase PCSK9 induces the degradation of low density lipoprotein receptor (LDLR) and its closest family members VLDLR and ApoER2. J Biol Chem 2008;283:2363-2372.

299. Scartezini M, Hubbart C, Whittall RA et al. The PCSK9 gene R46L variant is associated with lower plasma lipid levels and cardiovascular risk in healthy U.K. men. Clin Sci (Lond) 2007;113:435-441.

300. Kathiresan S and Myocardial Infarction Genetics Consortium. A PCSK9 missense variant associated with a reduced risk of early-onset myocardial infarction. N Engl J Med 2008;358:2299-2300.

301. Shioji K, Mannami T, Kokubo Y et al. Genetic variants in PCSK9 affect the cholesterol level in Japanese. J Hum Genet 2004;49:109-114.

302. Timms K, Wagner S, Samuels M et al. A mutation in PCSK9 causing autosomal-dominant hypercholesterolemia in a Utah pedigree. Hum Genet 2004;114:349-353.

303. Sun X, Eden ER, Tosi I et al. Evidence for effect of mutant PCSK9 on apolipoprotein B secretion as the cause of unusually severe dominant hypercholesterolaemia. Hum Mol Genet 2005;14:1161-1169.

304. Teslovich TM, Musunuru K, Smith AV et al. Biological, clinical and population relevance of 95 loci for blood lipids. Nature 2010;466:707-713.

305. Kathiresan S, Melander O, Anevski D et al. Polymorphisms associated with cholesterol and risk of cardiovascular events. N Engl J Med 2008;358:1240-1249.

306. Cohen J, Pertsemlidis A, Kotowski IK et al. Low LDL cholesterol in individuals of African descent resulting from frequent nonsense mutations in PCSK9. Nat Genet 2005;37:161-165.

307. Zhao Z, Tuakli-Wosornu Y, Lagace TA et al. Molecular characterization of Loss-of-Function mutations in PCSK9 and identification of a compound heterozygote. Am J Hum Genet 2006;79:514-523.

308. Mayne J, Raymond A, Chaplin A et al. Plasma PCSK9 levels correlate with cholesterol in men but not in women. Biochem Biophys Res Commun 2007;361:451-456.

309. Croston GE, Milan LB, Marschke KB et al. Androgen receptor-mediated antagonism of estrogen-dependent low density lipoprotein receptor transcription in cultured hepatocytes. Endocrinology 1997;138:3779-3786.

310. Smith PM, Cowan A and White BA. The low-density lipoprotein receptor is regulated by estrogen and forms a functional complex with the estrogen-regulated protein Ezrin in pituitary GH3 somatolactotropes. Endocrinology 2004;145:3075-3083.

311. Chomczynski P and Sacchi N. Single-step method of RNA isolation by acid guanidinium thiocyanate-phenol-chloroform extraction. Anal Biochem 1987;162:156-159.

312. Bookout AL and Mangelsdorf DJ. Quantitative real-time PCR protocol for analysis of nuclear receptor signaling pathways. Nucl Recept Signal 2003;1:e012.

313. Hughes CS, Postovit LM and Lajoie GA. Matrigel: a complex protein mixture required for optimal growth of cell culture. Proteomics 2010;10:1886-1890.

314. Ge B, Gurd S, Gaudin T et al. Survey of allelic expression using EST mining. Genome Res 2005;15:1584-1591.

315. Freshney RI. Cytotoxicity. In: Culture of Animal Cells. John Wiley & Sons, Inc; 2010. p 365-381.

316. Yuan H, Chiou J, Tseng W et al. FASTSNP: an always up-to-date and extendable service for SNP function analysis and prioritization. Nucl Acids Res 2006;34:W635-W641.

317. Sandelin A, Wasserman WW and Lenhard B. ConSite: web-based prediction of regulatory elements using cross-species comparison. Nucleic Acids Res 2004;32:W249-W252.

318. Su G, Mao B and Wang J. MACO: a gapped-alignment scoring tool for comparing transcription factor binding sites. In Silico Biol 2006;6:307-310.

319. Mittler G, Butter F and Mann M. A SILAC-based DNA protein interaction screen that identifies candidate binding proteins to functional DNA elements. Genome Res 2009;19:284-293.

320. Marras SE. Selection of fluorophore and quencher pairs for fluorescent nucleic acid hybridization probes. In: Fluorescent Energy Transfer Nucleic Acid Probes. Editor: Didenko V, Humana Press; 2006. p 3-16.

321. Rashid S, Curtis DE, Garuti R et al. Decreased plasma cholesterol and hypersensitivity to statins in mice lacking Pcsk9. Proc Natl Acad Sci USA 2005;102:5374-5379.

322. Cameron J, Ranheim T, Kulseth MA et al. Berberine decreases PCSK9 expression in HepG2 cells. Atherosclerosis 2008;201:266-273.

323. Li H, Dong B, Park SW et al. Hepatocyte nuclear factor 1alpha plays a critical role in PCSK9 gene transcription and regulation by the natural hypocholesterolemic compound berberine. J Biol Chem 2009;284:28885-28895.

324. Boyd JH, Mathur S, Wang Y et al. Toll-like receptor stimulation in cardiomyoctes decreases contractility and initiates an NF-kappaB dependent inflammatory response. Cardiovasc Res 2006;72:384-393.

325. Netea MG, Demacker PN, Kullberg BJ et al. Low-density lipoprotein receptor-deficient mice are protected against lethal endotoxemia and severe gram-negative infections. J Clin Invest 1996;97:1366-1372.

326. Bone RC, Balk RA, Cerra FB, et al. American College of Chest Physicians/Society of Critical Care Medicine Consensus Conference: definitions for sepsis and organ failure and guidelines for the use of innovative therapies in sepsis. Crit Care Med 1992;20:864-874.

327. Russell JA, Walley KR, Singer J et al. Vasopressin versus norepinephrine infusion in patients with septic shock. N Engl J Med 2008;358:877-887.

328. Stephens M and Donnelly P. A comparison of bayesian methods for haplotype reconstruction from population genotype data. Am J Hum Genet 2003;73:1162-1169.

329. Carlson CS, Eberle MA, Rieder MJ et al. Selecting a maximally informative set of single-nucleotide polymorphisms for association analyses using linkage disequilibrium. Am J Hum Genet 2004;74:106-120.

330. Folsom AR, Ohira T, Yamagishi K and Cushman M. Low protein C and incidence of ischemic stroke and coronary heart disease: the Atherosclerosis Risk in Communities (ARIC) Study. J Thromb Haemost 2009;7:1774-1778.

331. Chiu YN, Wang TG and Chang CW. Early-onset stroke in a patient with nasopharyngeal cancer associated with protein C deficiency. J Formos Med Assoc 2009;108:592-594.

332. Macias WL and Nelson DR. Severe protein C deficiency predicts early death in severe sepsis. Crit Care Med 2004;32:S223-8.

333. Spek CA, Lannoy VJ, Lemaigre FP et al. Type I protein C deficiency caused by disruption of a hepatocyte nuclear factor (HNF)-6/HNF-1 binding site in the human protein C gene promoter. J Biol Chem 1998;273:10168-10173.

334. Pomp ER, Doggen CJ, Vos HL et al. Polymorphisms in the protein C gene as risk factor for venous thrombosis. Thromb Haemost 2009;101:62-67.

335. Conlan MG, Folsom AR, Finch A et al. Correlation of plasma protein C levels with cardiovascular risk factors in middle-aged adults: the Atherosclerosis Risk in Communities (ARIC) Study. Thromb Haemost 1993;70:762-767.

336. Binder A, Endler G, Rieger S et al. Protein C promoter polymorphisms associate with sepsis in children with systemic meningococcemia. Hum Genet 2007;122:183-190.

337. Borgel D, Bornstain C, Reitsma PH et al. A comparative study of the protein c pathway in septic and nonseptic patients with organ failure. Am J Respir Crit Care Med 2007;176:878-885.

338. Hegen A, Koidl S, Weindel K et al. Expression of angiopoietin-2 in endothelial cells is controlled by positive and negative regulatory promoter elements. Arterioscler Throm Vasc Biol 2004;24:1803-1809.

339. Donaldson IJ, Chapman M, Kinston S et al. Genome-wide identification of cis-regulatory sequences controlling blood and endothelial development. Hum Mol Genet 2005;14:595-601.

340. Koinuma D, Tsutsumi S, Kamimura N et al. Chromatin immunoprecipitation on microarray analysis of Smad2/3 binding sites reveals roles of ETS1 and TFAP2A in transforming growth factor beta signaling. Mol Cell Biol 2009;29:172-186.

341. Spek CA, Bertina RM and Reitsma PH. Identification of evolutionarily invariant sequences in the protein C gene promoter. J Mol Evol 1998;47:663-669.

342. Ott CJ, Blackledge NP, Kerschner JL et al. Intronic enhancers coordinate epithelial-specific looping of the active CFTR locus. Proc Natl Acad Sci USA 2009;106:19934-19939.

343. Fan LQ, Hardy DO, Catterall JF et al. Identification and characterization of an androgen-responsive Kap promoter enhancer located in the intron II region of human angiotensinogen gene. J Steroid Biochem Mol Biol 2010;119:135-140.

344. Tsay W, Lee YM, Lee SC et al. Characterization of human protein C gene promoter: insights from natural human mutants. DNA Cell Biol 1996;15:907-919.

345. Plutzky J, Hoskins JA, Long GL and Crabtree GR. Evolution and organization of the human protein C gene. Proc Natl Acad Sci USA 1986;83:546-550.

346. Smith NL, Hindorff LA, Heckbert SR et al. Association of genetic variations with nonfatal venous thrombosis in postmenopausal women. JAMA - J Am Med Assoc 2007;297:489-498.

347. Russell JA, Wellman H and Walley KR. Protein C rs2069912 C allele is associated with increased mortality from severe sepsis in North Americans of East Asian ancestry. Hum Genet 2008;123:661-663.

348. Tenenbaum SA, Carson CC, Lager PJ and Keene JD. Identifying mRNA subsets in messenger ribonucleoprotein complexes by using cDNA arrays. Proc Natl Acad Sci USA 2000;97:14085-14090.

349. Zhou Z, Licklider LJ, Gygi SP and Reed R. Comprehensive proteomic analysis of the human spliceosome. Nature 2002;419:182-185.

350. Jonson L, Vikesaa J, Krogh A et al. Molecular composition of IMP1 ribonucleoprotein granules. Mol Cell Proteomics 2007;6:798-811.

351. Tang W, Basu S, Kong X et al. Genome-wide association study identifies novel loci for plasma levels of protein C: the ARIC study. Blood 2010;116:5032-5036.

352. Scopes D, Berg LP, Krawczak M et al. Polymorphic variation in the human protein C (PROC) gene promoter can influence transcriptional efficiency in vitro. Blood Coagul Fibrinolysis 1995;6:317-321.

353. Luo X and Sawadogo M. Antiproliferative properties of the USF family of helix-loop-helix transcription factors. Proc Natl Acad Sci 1996;93:1308-1313.

354. McMurray HR and McCance DJ. Human papillomavirus type 16 E6 activates TERT gene transcription through induction of c-Myc and release of USF-mediated repression. J Virol 2003;77:9852-9861.

355. Selva DM, Hogeveen KN and Hammond GL. Repression of the human sex hormone-binding globulin gene in sertoli cells by upstream stimulatory transcription factors. J Biol Chem 2005;280:4462-4468.

356. Horikawa I, Cable PL, Mazur SJ et al. Downstream E-box-mediated regulation of the human telomerase reverse transcriptase (hTERT) gene transcription: evidence for an endogenous mechanism of transcriptional repression. Mol Biol Cell 2002;13:2585-2597.

357. Sirito M, Lin Q, Maity T and Sawadogo M. Ubiquitous expression of the 43- and 44-kDa forms of transcription factor USF in mammalian cells. Nucleic Acids Res 1994;22:427-433.

358. Hadjiagapiou C, Borthakur A, Dahdal RY et al. Role of USF1 and USF2 as potential repressor proteins for human intestinal monocarboxylate transporter 1 promoter. Am J Physiol-Gastr L 2005;288:G1118-G1126.

359. Jensen LJ, Kuhn M, Stark M et al. STRING 8—a global view on proteins and their functional interactions in 630 organisms. Nucl Acids Res 2009;37:D412-D416.

360. Xiao Q, Kenessey A and Ojamaa K. Role of USF1 phosphorylation on cardiac α-myosin heavy chain promoter activity. Am J Physiol-Heart C 2002;283:H213-H219.

361. Chen J, Guo K and Kastan MB. Interactions of nucleolin and ribosomal protein L26 (RPL26) in translational control of human p53 mRNA. J Biol Chem 2012;287:16467-16476.

362. Grinnell BW and Joyce D. Recombinant human activated protein C: a system modulator of vascular function for treatment of severe sepsis. Crit Care Med 2001;29:S53-S60.

363. Novack V, MacFadyen J, Malhotra A et al. The effect of rosuvastatin on incident pneumonia: results from the JUPITER trial. Can Med Assoc J 2012;184:E367-E372.

364. Rothberg MB, Bigelow C, Pekow PS and Lindenauer PK. Association between statins given in hospital and mortality in pneumonia patients. J Gen Intern Med 2012;27:280-286.

365. Grion CM, Cardoso LT, Perazolo TF et al. Lipoproteins and CETP levels as risk factors for severe sepsis in hospitalized patients. Eur J Clin Invest 2010;40:330-338.

366. Chalmers JD, Short PM, Mandal P et al. Statins in community acquired pneumonia: Evidence from experimental and clinical studies. Respir Med 2010;104:1081-1091.

367. Kruger PS, Harward ML, Jones MA et al. Continuation of statin therapy in patients with presumed infection: a randomized controlled trial. Am J Respir Crit Care Med 2011;183:774-781.

368. Barter PJ, Caulfield M, Eriksson M et al. Effects of torcetrapib in patients at high risk for coronary events. N Engl J Med 2007;357:2109-2122.

369. Read TE, Harris HW, Grunfeld C et al. The protective effect of serum lipoproteins against bacterial lipopolysaccharide. Eur Heart J 1993;14 Suppl K:125-129.

370. Read TE, Grunfeld C, Kumwenda ZL et al. Triglyceride-rich lipoproteins prevent septic death in rats. J Exp Med 1995;182:267-272.

371. de Lima-Salgado TM, Cruz LM and Souza HP. Lipid-activated nuclear receptors and sepsis. Endocr Metab Immune Disord Drug Targets 2010;10:258-265.

372. Thompson PA, Berbee JF, Rensen PC and Kitchens RL. Apolipoprotein A-II augments monocyte responses to LPS by suppressing the inhibitory activity of LPS-binding protein. Innate Immun 2008;14:365-374.

373. Abe M, Maruyama N, Okada K et al. Effects of lipid-lowering therapy with rosuvastatin on kidney function and oxidative stress in patients with diabetic nephropathy. J Atheroscler Thromb 2011;18:1018-1028.

374. Fraunberger P, Grone E, Grone HJ and Walli AK. Simvastatin reduces endotoxin-induced nuclear factor kappaB activation and mortality in guinea pigs despite lowering circulating low-density lipoprotein cholesterol. Shock 2009;32:159-163.

375. McGown CC, Brown NJ, Hellewell PG et al. Beneficial microvascular and anti-inflammatory effects of pravastatin during sepsis involve nitric oxide synthase III. Br J Anaesth 2010;104:183-190.

376. Winkler F, Angele B, Pfister HW and Koedel U. Simvastatin attenuates leukocyte recruitment in experimental bacterial meningitis. Int Immunopharmacol 2009;9:371-374.

377. Yang W, Yamada M, Tamura Y et al. Farnesyltransferase inhibitor FTI-277 reduces mortality of septic mice along with improved bacterial clearance. J Pharmacol Exp Ther 2011;339:832-841.

378. Lanza-Jacoby S, Miller S, Jacob S et al. Hyperlipoproteinemic low-density lipoprotein receptor-deficient mice are more susceptible to sepsis than corresponding wild-type mice. J Endotoxin Res 2003;9:341-347.

379. Rosch JW, Boyd AR, Hinojosa E et al. Statins protect against fulminant pneumococcal infection and cytolysin toxicity in a mouse model of sickle cell disease. J Clin Invest 2010;120:627-635.

380. Zhang Z, Datta G, Zhang Y et al. Apolipoprotein A-I mimetic peptide treatment inhibits inflammatory responses and improves survival in septic rats. Am J Physiol Heart Circ Physiol 2009;297:H866-73.

381. Steinberg D and Witztum JL. Inhibition of PCSK9: A powerful weapon for achieving ideal LDL cholesterol levels. Proc Natl Acad Sci 2009;106:9546-9547.

382. Boyd JH, Kan B, Roberts H et al. S100A8 and S100A9 mediate endotoxin-induced cardiomyocyte dysfunction via the receptor for advanced glycation end products. Circ Res 2008;102:1239-1246.

383. Zaitlen N, Pasaniuc B, Gur T et al. Leveraging genetic variability across populations for the identification of causal variants. Am J Hum Genet 2010;86:23-33.

384. Gao L, Grant A, Halder I et al. Novel polymorphisms in the myosin light chain kinase gene confer risk for acute lung injury. Am J Respir Cell Mol Biol 2006;34:487-495.

385. Song Z, Yin J, Yao C et al. Variants in the Toll-interacting protein gene are associated with susceptibility to sepsis in the Chinese Han population. Crit Care 2011;15:R12.

386. Minneci PC, Deans KJ, Eichacker PQ and Natanson C. The effects of steroids during sepsis depend on dose and severity of illness: an updated meta-analysis. Clin Microbiol Infec 2009;15:308-318.

387. Tidswell M, Tillis W, Larosa SP et al. Phase 2 trial of eritoran tetrasodium (E5564), a toll-like receptor 4 antagonist, in patients with severe sepsis. Crit Care Med 2010;38:72-83.

388. Abraham E, Laterre PF, Garg R et al. Drotrecogin alfa (activated) for adults with severe sepsis and a low risk of death. N Engl J Med 2005;353:1332-1341.

389. Nadel S, Goldstein B, Williams MD et al. Drotrecogin alfa (activated) in children with severe sepsis: a multicentre phase III randomised controlled trial. Lancet 2007;369:836-843.

390. Vincent JL, Bernard GR, Beale R et al. Drotrecogin alfa (activated) treatment in severe sepsis from the global open-label trial ENHANCE: further evidence for survival and safety and implications for early treatment. Crit Care Med 2005;33:2266-2277.

391. Glazier AM, Nadeau JH and Aitman TJ. Finding genes that underlie complex traits. Science 2002;298:2345-2349.

392. Knight J. Regulatory polymorphisms underlying complex disease traits. J Mol Med 2005;83:97-109.

393. Carlson CS, Eberle MA, Kruglyak L and Nickerson DA. Mapping complex disease loci in whole-genome association studies. Nature 2004;429:446-452.

394. Slooter AC, Cruts M, Kalmijn S,et al. Risk estimates of dementia by apolipoprotein E genotypes from a population-based incidence study: The Rotterdam study. Arch Neurol 1998;55:964-968.

395. Rocchi A, Pellegrini S, Siciliano G and Murri L. Causative and susceptibility genes for Alzheimer's disease: a review. Brain Res Bull 2003;61:1-24.

396. Yan H, Yuan W, Velculescu VE et al. Allelic variation in human gene expression. Science 2002;297:1143-1143.

397. Pastinen T, Sladek R, Gurd S et al. A survey of genetic and epigenetic variation affecting human gene expression. Physiol Genomics 2004;16:184-193.

398. Cowles CR, Hirschhorn JN, Altshuler D and Lander ES. Detection of regulatory variation in mouse genes. Nat Genet 2002;32:432-437.

399. Dykxhoorn DM, Novina CD and Sharp PA. Killing the messenger: short RNAs that silence gene expression. Nat Rev Mol Cell Biol 2003;4:457-467.

400. Elbashir SM, Harborth J, Weber K and Tuschl T. Analysis of gene function in somatic mammalian cells using small interfering RNAs. Methods 2002;26:199-213.

401. ENCODE Project Consortium., Myers RM, Stamatoyannopoulos J et al. A user's guide to the encyclopedia of DNA elements (ENCODE). PLoS Biol 2011;9:e1001046.

402. Kumari D, Gabrielian A, Wheeler D and Usdin K. The roles of Sp1, Sp3, USF1/USF2 and NRF-1 in the regulation and three-dimensional structure of the Fragile X mental retardation gene promoter. Biochem J 2005;286:297-303.

403. Sanchez AP, Zhao J, You Y et al. Role of the USF1 transcription factor in diabetic kidney disease. Am J Physiol Renal Physiol 2011;301:F271-F279.

404. Xiao B, Freedman BS, Miller KE et al. Histone H1 compacts DNA under force and during chromatin assembly. Mol Biol Cell 2012;23:4864-4871.

405. Ni JQ, Liu LP, Hess D et al. Drosophila ribosomal proteins are associated with linker histone H1 and suppress gene transcription. Genes Dev 2006;20:1959-1973.

406. Kraus WL. Transcriptional control by PARP-1: chromatin modulation, enhancer-binding, coregulation, and insulation. Curr Opin Cell Biol 2008;20:294-302.

407. McBryant SJ, Lu X and Hansen JC. Multifunctionality of the linker histones: an emerging role for protein-protein interactions. Cell Res 2010;20:519-528.

408. Coppens I, Baudhuin P, Opperdoes FR and Courtoy PJ. Receptors for the host low density lipoproteins on the hemoflagellate *Trypanosoma brucei*: purification and involvement in the growth of the parasite. Proc Natl Acad Sci USA 1988;85:6753-6757.

409. Rumjanek FD, Campos EG and Afonso LC. Evidence for the occurrence of LDL receptors in extracts of schistosomula of *Schistosoma mansoni*. Mol Biochem Parasitol 1988;28:145-152.

410. Bennett MW and Caulfield JP. Specific binding of human low-density lipoprotein to the surface of *Schistosoma mansoni* and ingestion by the parasite. Am J Pathol 1991;138:1173-1182.

411. Rogers MV. Do parasites express receptors for host lipoproteins? Parasitol Today 1991;7:117-120.

412. Hofer F, Gruenberger M, Kowalski H et al. Members of the low density lipoprotein receptor family mediate cell entry of a minor-group common cold virus. Proc Natl Acad Sci USA 1994;91:1839-1842.

413. Monazahian M, Bohme I, Bonk S et al. Low density lipoprotein receptor as a candidate receptor for hepatitis C virus. J Med Virol 1999;57:223-229.

414. Vlasak M, Roivainen M, Reithmayer M et al. The minor receptor group of human rhinovirus (HRV) includes HRV23 and HRV25, but the presence of a lysine in the VP1 HI loop is not sufficient for receptor binding. J Virol 2005;79:7389-7395.

415. Fuchs R and Blaas D. Uncoating of human rhinoviruses. Rev Med Virol 2010;20:281-297.

416. Fischer DG, Tal N, Novick D et al. An antiviral soluble form of the LDL receptor induced by interferon. Science 1993;262:250-253.

417. Agnello V, Abel G, Elfahal M et al. Hepatitis C virus and other flaviviridae viruses enter cells via low density lipoprotein receptor. Proc Natl Acad Sci USA 1999;96:12766-12771.

418. Wunschmann S, Medh JD, Klinzmann D et al. Characterization of hepatitis C virus (HCV) and HCV E2 interactions with CD81 and the low-density lipoprotein receptor. J Virol 2000;74:10055-10062.

419. Zeisel MB, Fofana I, Fafi-Kremer S and Baumert TF. Hepatitis C virus entry into hepatocytes: Molecular mechanisms and targets for antiviral therapies. J Hepatol 2011;54:566-576.

420. Bieghs V, Van Gorp PJ, Wouters K et al. LDL receptor knock-out mice are a physiological model particularly vulnerable to study the onset of inflammation in non-alcoholic fatty liver disease. PLoS One 2012;7:e30668.

421. Geffken DF, Cushman M, Burke GL et al. Association between physical activity and markers of inflammation in a healthy elderly population. Am J Epidemiol 2001;153:242-250.

422. Dossett LA, Dageforde LA, Swenson BR et al. Obesity and site-specific nosocomial infection risk in the intensive care unit. Surg Infect 2009;10:137-142.

423. Akinnusi ME, Pineda LA and El Solh AA. Effect of obesity on intensive care morbidity and mortality: A meta-analysis. Crit Care Med 2008;36:151-158.

424. Oliveros H and Villamor E. Obesity and mortality in critically ill adults: a systematic review and meta-analysis. Obesity 2008;16:515-521.

425. Casaer MP, Coenegrachts J, De Rijdt T et al. Early versus late parenteral nutrition in ICU patients: cost analysis of the EPaNIC trial. Crit Care 2012;16:R96.

426. Costet P, Cariou B, Lambert G et al. Hepatic PCSK9 expression is regulated by nutritional status via insulin and sterol regulatory element-binding protein 1c. J Biol Chem 2006;281:6211-6218.

427. Hardardottir I, Grunfeld C and Feingold KR. Effects of endotoxin on lipid metabolism. Biochem Soc Trans 1995;23:1013-1018.

428. Kong W, Wei J, Abidi P et al. Berberine is a novel cholesterol-lowering drug working through a unique mechanism distinct from statins. Nat Med 2004;10:1344-1351.

429. Wang Y, Wang Y, Zhang H et al. Synthesis and biological evaluation of berberine analogues as novel up-regulators for both low-density-lipoprotein receptor and insulin receptor. Bioorg Med Chem Lett 2009;19:6004-6008.

Appendices

Appendix A Supplementary data for Chapter 3

A.1 Primer sequences for amplifying *PROC* and *GAPDH*

Primer	Direction	Sequence (5' – 3')	Length (bp)
PROC_RTPCR_60F	Forward	CCAGTGCCTCCAGAATGTG	19
PROC_RTPCR_68F	Forward	GGAGAGTATGACCTGCGGCG	20
PROC_RTPCR_301F	Forward	GGATGACACACTGGCCTTCT	20
PROC_RTPCR_664F	Forward	GAAACGAGACACAGAAGACC	20
PROC_RTPCR_227R	Reverse	GCAGACCATAGTGCCCATCT	20
PROC_RTPCR_705R	Reverse	CGCGGATCTACTTGGTCTTC	20
PROC_RTPCR_779R	Reverse	GCTTCTTCTTTGAGTCCAGC	20
PROC_RTPCR_1028R	Reverse	AGATGGGCACTATGGTCTGC	20
PROC_RTPCR_1459R	Reverse	CTAAGGTGCCCAGCTCTTCT	20
PROC_DNA_1815F	Forward	GTGCTGATCTTGGGCAAACT	20
PROC_DNA_2002F	Forward	GGAGGAGGCCATGATTCTT	19
PROC_DNA_2574R	Reverse	CCCGATCTCTGTGTGACCTT	20
PROC_DNA_-1473R	Reverse	GGGTCGTGGAGATACTGCAA	20
GAPDH-1_Forward_QRT	Forward	CATGGCCTCCAAGGAGTAAG	20
GAPDH-1_Reverse_QRT	Reverse	AGGGGTCTACATGGCAACTG	20

A.2 Linkage disequilibrium for SNPs in *PROC*

Linkage disequilibrium from Seattle SNPs (http://pga.mbt.washington.edu/). Chromosome 2: 127892487 - 127903288, minor allelle frequency >10%, combined sample with combined variations from 4 populations: PGA- EUROPEAN-PANEL, HapMap-CEU(unrelated only), CEU_GENO_PANEL, AFD_EUR_PANEL. Highlighted boxes show LD between the common promoter SNP, -1641 and rs2069915 and rs2069916.

SNP 1	SNP 2	LD (r^2)
rs1799808	rs1799810	0.281
rs1799808	rs2069910	0.696
rs1799808	rs2069912	0.220
rs1799808	rs2069913	0.118
rs1799808	rs2069914	0.171
rs1799808	rs2069915	0.829
rs1799808	rs2069916	0.940
rs1799809	rs1799810	0.947
rs1799809	rs2069910	0.005
rs1799809	rs2069912	0.206
rs1799809	rs2069913	0.223
rs1799809	rs2069914	0.174
rs1799809	rs2069915	0.074
rs1799809	rs2069916	0.194
rs1799810	rs2069910	0.007
rs1799810	rs2069912	0.167
rs1799810	rs2069913	0.248
rs1799810	rs2069914	0.167
rs1799810	rs2069915	0.256
rs1799810	rs2069916	0.407
rs1158867	rs1799810	1
rs1158867	rs2069910	0.040
rs1158867	rs2069912	0.154
rs1158867	rs2069913	0.216
rs1158867	rs2069914	0.154
rs1158867	rs2069915	0.263
rs1158867	rs2069916	0.447
rs2069910	rs2069912	0.001
rs2069910	rs2069913	0.156
rs2069910	rs2069914	0.001
rs2069910	rs2069915	0.652
rs2069910	rs2069916	0.574
rs2069912	rs2069913	0.689
rs2069912	rs2069914	1

SNP 1	SNP 2	LD (r^2)
rs2069912	rs2069915	0.188
rs2069912	rs2069916	0.171
rs2069913	rs2069914	0.689
rs2069913	rs2069915	0.130
rs2069913	rs2069916	0.118
rs2069914	rs2069915	0.188
rs2069914	rs2069916	0.171
rs2069915	rs2069916	0.907

A.3 Probe sequences for SNPs tested in EMSA assays

Probe	Strand	Sequence (5' – 3')	Length (bp)
-1654/-1641[C-A]	sense	GCTGGACGGCATCCTTGGTAGGCAGA	26
	antisense	TCTGCCTACCAAGGATGCCGTCCAGC	
-1654/-1641[T-A]	sense	GCTGGATGGCATCCTTGGTAGGCAGA	26
	antisense	TCTGCCTACCAAGGATGCCATCCAGC	
-1654/-1641[C-G]	sense	GCTGGACGGCATCCTTGGTGGGCAGA	26
	antisense	TCTGCCCACCAAGGATGCCGTCCAGC	
-1654/-1641[T-G]	sense	GCTGGATGGCATCCTTGGTGGGCAGA	26
	antisense	TCTGCCCACCAAGGATGCCATCCAGC	
rs1158867[C]	sense	CAAGGACCCTCAATCCCAGCTTCCGCCC	28
	antisense	GGGCGGAAGCTGGGATTGAGGGTCCTTG	
rs1158867[T]	sense	CAAGGACCCTCAATTCCAGCTTCCGCCC	28
	antisense	GGGCGGAAGCTGGAATTGAGGGTCCTTG	
rs1799810[T]	sense	GCGGCAGGACGGCGTACTTGCAGTATCTC	29
	antisense	GAGATACTGCAAGTACGCCGTCCTGCCGC	
rs1799810[A]	sense	GCGGCAGGACGGCGAACTTGCAGTATCTC	29
	antisense	GAGATACTGCAAGTTCGCCGTCCTGCCGC	
rs2069910[C]	sense	GCACACTGGCCTCACGGCTGCCCTGCCCC	29
	antisense	GGGGCAGGGCAGCCGTGAGGCCAGTGTGC	
rs2069910[T]	sense	GCACACTGGCCTCATGGCTGCCCTGCCCC	29
	antisense	GGGGCAGGGCAGCCATGAGGCCAGTGTGC	
rs2069912[T]	sense	TAGGATGCCTTTTCCCCCATCCCTT	25
	antisense	AAGGGATGGGGGAAAAGGCATCCTA	
rs2069912[C]	sense	TAGGATGCCTTTCCCCCCATCCCTT	25
	antisense	AAGGGATGGGGGGAAAGGCATCCTA	
rs2069913[C]	sense	CTGCACCCAAGACAGACACTTCACA	25
	antisense	TGTGAAGTGTCTGTCTTGGGTGCAG	
rs2069913[G]	sense	CTGCACCCAAGAGAGACACTTCACA	25
	antisense	TGTGAAGTGTCTCTCTTGGGTGCAG	
rs2069914[A]	sense	GACAGACACTTCACAAAGCCCAGGAGACACC	29
	antisense	GGTGTCTCCTGGGCTTTGTGAAGTGTCTGTC	
rs2069914[G]	sense	GACAGACACTTCACAGAGCCCAGGAGACACC	29
	antisense	GGTGTCTCCTGGGCTCTGTGAAGTGTCTGTC	
rs2069915[G]	sense	GTTGGGGGAGGAGAGGAAGACTGGG	25
	antisense	CCCAGTCTTCCTCTCCTCCCCCAAC	
rs2069915[A]	sense	GTTGGGGGAGGAAAGGAAGACTGGG	25
	antisense	CCCAGTCTTCCTTTCCTCCCCCAAC	
rs2069916[C]	sense	GATGGGGCTGCACGTGGTGTACTGG	25
	antisense	CCAGTACACCACGTGCAGCCCCATC	
rs2069916[T]	sense	GATGGGGCTGCATGTGGTGTACTGG	25
	antisense	CCAGTACACCACATGCAGCCCCATC	

A.4 Probe sequences for transcription factors and cold competitions for EMSA assays

Nuclear Factor	Strand	Sequence (5' - 3')	Length (bases)
rs2069915[G]_scrambled	sense	GATGGGGCTGCATGTGGTGTACTGG	25
	antisense	CCAGTACACCACATGCAGCCCCATC	25
rs2069916[C]_scrambled	sense	CTGCACCCAAGACAGACACTTCACA	25
	antisense	TGTGAAGTGTCTGTCTTGGGTGCAG	25
NFKB	sense	AGTTGAGGGGACTTTCCAGGC	22
	antisense	GCCTGGGAAAGTCCCCTCAACT	22
USF18	sense	CGGGAACACCTGCGGACA	18
	antisense	TGTCCGCAGGTGTTCCCG	18
USF20	sense	ACAGCCCACCTCGTGACTGG	20
	antisense	CCAGTCACGAGGTGGGCTGT	20
USF45	sense	AGTGCCTGAGAGCTCATGAACAAGCATGTGACCTTGGATCCAGCT	45
	antisense	AGCTGGATCCAAGGTCACATGCTTGTTCATGAGCTCTCAGGCACT	45
cMYC1	sense	GACCACGTGCACGTGGTC	18
	antisense	GACCACGTGCACGTGGTC	18
cMYC2	sense	CGTTTTCGATGACCACGTGGTCGGTATACGAT	32
	antisense	ATCGTATACCGACCACGTGGTCATCGAAAACG	32
cREL	sense	GTC CTG GAG TTT CCT ACC GGG	21
	antisense	CCC GGT AGG AAA CTC CAG GAC	21
E2F	sense	ATTTAAGTTTCGCGCCCTTTCTCAA	25
	antisense	TTGAGAAAGGGCGCGAAACTTAAAT	25
IRF1	sense	AAGTGAAAGTGAAAGTGAAAAGTGAAACT	29
	antisense	AGTTTCACTTTTCACTTTCACTTTCACTT	29
NRF2	sense	TCTGTTTTCGCTGAGTCATGGTTCCCGTTG	30
	antisense	CAACGGGAACCATGACTCAGCGAAAACAGA	30
NRF2_long	sense	GCACAGCAATGCTGAGTCATGATGAGTCATGCTG	34
	antisense	CAGCATGACTCATCATGACTCAGCATTGCTGTGC	34
TEAD1-1	sense	AGTGTTGCATTCCTCTCTGG	20
	antisense	CCAGAGAGGAATGCAACACT	20

A.5 Complete results for SILAC mass spectrometry for rs2069915[A/G]

Accession	# Peptides	Heavy/Light	Heavy/Light Variability [%]	Description
gi190167	26	0.856	5.0	poly(ADP-ribose) polymerase [Homo sapiens]
gi194382466	26	0.852	6.1	unnamed protein product [Homo sapiens]
gi47132620	26	**0.010**	0.0	keratin 2 [Homo sapiens]
gi11935049	22	**0.010**	0.0	keratin 1 [Homo sapiens]
gi195972866	19	**0.010**	0.0	keratin 10 [Homo sapiens]
gi435476	18	**0.010**	0.0	cytokeratin 9 [Homo sapiens]
gi4503841	18	**0.439**	10.7	ATP-dependent DNA helicase II, 70 kDa subunit [Homo sapiens]
gi10863945	14	**0.457**	5.2	ATP-dependent DNA helicase II [Homo sapiens]
gi12803709	10	**0.010**	0.0	Keratin 14 [Homo sapiens]
gi119617041	10	**0.010**	0.0	keratin 5 (epidermolysis bullosa simplex, Dowling-Meara/Kobner/Weber-Cockayne types), isoform CRA_d [Homo sapiens]
gi194388850	10	**0.010**	0.0	unnamed protein product [Homo sapiens]
gi194387918	10	**0.010**	0.0	unnamed protein product [Homo sapiens]
gi1195531	9	**0.011**	9.0	type I keratin 16 [Homo sapiens]
gi119617032	8	**0.010**	0.0	keratin 6B, isoform CRA_a [Homo sapiens]
gi356168	8	**4.438**	59.4	histone H1b
gi4885375	8	**3.650**	32.3	histone cluster 1, H1c [Homo sapiens]
gi221045918	6	**0.231**	25.0	unnamed protein product [Homo sapiens]
gi148921602	6	0.573	5.4	EML4 protein [Homo sapiens]
gi31645	5	0.535	7.3	glyceraldehyde-3-phosphate dehydrogenase [Homo sapiens]
gi19550955	5	1.321	9.1	ligase III, DNA, ATP-dependent [Homo sapiens]
gi193785596	5	**0.215**	27.7	unnamed protein product [Homo sapiens]
gi55958544	4	0.695	1.2	heterogeneous nuclear ribonucleoprotein K [Homo sapiens]
gi4885371	4	**4.489**	43.3	H1 histone family, member 0 [Homo sapiens]
gi51476762	4	0.517	5.6	hypothetical protein [Homo sapiens]
gi1310882	4	0.682	3.8	Chain A, Cyclophilin B Complexed With [d-(Cholinylester)ser8]- Cyclosporin
gi21754583	4	0.015	51.2	unnamed protein product [Homo sapiens]
gi54696428	3	0.582	12.0	high-mobility group box 2 [Homo sapiens]
gi119612724	3	1.038	6.5	actin, alpha, cardiac muscle, isoform CRA_c [Homo sapiens]
gi21619981	3	1.179	2.5	LMNA protein [Homo sapiens]
gi194382662	3	0.386	0.1	unnamed protein product [Homo sapiens]
gi119626284	3	0.747	3.9	heterogeneous nuclear ribonucleoprotein D (AU-rich element RNA binding protein 1, 37kDa), isoform CRA_f [Homo sapiens]
gi119627830	3	0.625	9.6	splicing factor proline/glutamine-rich (polypyrimidine tract binding protein associated), isoform CRA_e [Homo sapiens]

Accession	# Peptides	Heavy/Light	Heavy/Light Variability [%]	Description
gi119590557	3	0.145	8.1	heat shock 60kDa protein 1 (chaperonin), isoform CRA_c [Homo sapiens]
gi9082289	3	0.118	4.9	chaperone protein HSP90 beta [Homo sapiens]
gi4885381	3	3.044	22.0	histone cluster 1, H1b [Homo sapiens]
gi16751921	3	0.013	22.8	dermcidin preproprotein [Homo sapiens]
gi75517570	2	0.835	18.4	HNRPA1 protein [Homo sapiens]
gi113414871	2	**0.010**	0.0	Keratin 77 [Homo sapiens]
gi119580687	2	1.162	0.6	apolipoprotein B mRNA editing enzyme, catalytic polypeptide-like 3C, isoform CRA_a [Homo sapiens]
gi194388468	2	0.531		unnamed protein product [Homo sapiens]
gi6470150	2	0.261	11.7	BiP protein [Homo sapiens]
gi21750830	2	0.010	0.0	unnamed protein product [Homo sapiens]
gi194387512	2	0.292	0.5	unnamed protein product [Homo sapiens]
gi10637825	2	0.585	13.1	ribosome binding protein 1 homolog 180kDa (dog) [Homo sapiens]
gi119609186	2	15.983	4024.7	nucleolar protein 1, 120kDa [Homo sapiens]
gi38014092	2	0.010	0.0	KRT4 protein [Homo sapiens]
gi194390544	2	0.555		unnamed protein product [Homo sapiens]
gi71143137	2	0.637		high-mobility group box 3 [Homo sapiens]
gi194384486	2	0.739	0.9	unnamed protein product [Homo sapiens]
gi9954649	2	1.213	1.8	XRCC1 DNA repair protein [Homo sapiens]
gi11513832	2	0.873	2.8	Chain A, Core Of The Alu Domain Of The Mammalian Srp
gi66361418	2	0.408	18.0	Chain A, Crystal Structure Of Human 17-Beta-Hydroxysteroid Dehydrogenase Type 4 In Complex With Nad
gi134105047	2	0.692	12.9	Chain A, Crystal Structure Of Human P100 Tudor Domain
gi5542151	2	0.135	20.0	Chain A, Macrophage Migration Inhibitory Factor (Mif) With Hydroxphenylpyruvate
gi119626079	2	0.032	430.1	albumin, isoform CRA_p [Homo sapiens]
gi194373749	2	0.011	9.0	unnamed protein product [Homo sapiens]
gi207028494	2	1.715	6715.2	lactate dehydrogenase A isoform 2 [Homo sapiens]
gi33875177	1	0.758		YBX1 protein [Homo sapiens]
gi6730357	1	0.425		Chain A, Role Of Amino Acid Residues At Turns In The Conformational Stability And Folding Of Human Lysozyme
gi159163560	1	0.039	614.7	Chain A, The Solution Structure Of The Second Thioredoxin-Like Domain Of Human Protein Disulfide-Isomerase
gi268612104	1	0.828		Chain A, Nmr Structure Of Dimerization Domain Of Human Ribosomal Protein P2
gi306549	1	1.182		homology to rat ribosomal protein L23 [Homo sapiens]
gi10645195	1	100.000		histone cluster 1, H2ae [Homo sapiens]
gi109940083	1	7.290		RecName: Full=Histone H2B type 1-C/E/F/G/I; AltName: Full=H2B.a/g/h/k/l; AltName: Full=H2B.1 A; Short=H2B/a; AltName: Full=H2B/g; AltName: Full=H2B/h; AltName: Full=H2B/k; AltName: Full=H2B/l
gi52545921	1	0.619		hypothetical protein [Homo sapiens]
gi194390750	1	0.359		unnamed protein product [Homo sapiens]

Accession	# Peptides	Heavy/Light	Heavy/Light Variability [%]	Description
gi158255378	1	0.086		unnamed protein product [Homo sapiens]
gi73998790	1	0.687		PREDICTED: similar to BUB3 budding uninhibited by benzimidazoles 3 isoform a isoform 3 [Canis familiaris]
gi4758876	1	0.373		poly(A) binding protein, nuclear 1 [Homo sapiens]
gi119609127	1	0.119		triosephosphate isomerase 1, isoform CRA_a [Homo sapiens]
gi52545510	1	4.302		hypothetical protein [Homo sapiens]
gi194377326	1	0.810		unnamed protein product [Homo sapiens]
gi4826860	1	2.517		NHP2 non-histone chromosome protein 2-like 1 [Homo sapiens]
gi5174449	1	2.090		H1 histone family, member X [Homo sapiens]
gi4432750	1	0.802		ribosomal protein L11 [Homo sapiens]
gi197099116	1			signal recognition particle 14kDa (homologous Alu RNA binding protein) [Pongo abelii]
gi3915733	1	0.771		RecName: Full=Dehydrogenase/reductase SDR family member 2; AltName: Full=HEP27 protein; AltName: Full=Protein D
gi50542195	1	2.556		histone H4 [Gallus gallus]
gi223278387	1	0.010		calmodulin-like 5 [Homo sapiens]
gi307066	1	0.386		inosine-5'-monophosphate dehydrogenase (EC 1.1.1.205) [Homo sapiens]
gi28931	1	0.286		beta-subunit (AA 1-312) [Homo sapiens]
gi119630058	1	0.659		high-mobility group nucleosome binding domain 1, isoform CRA_d [Homo sapiens]
gi119609679	1	0.674		hCG1789827 [Homo sapiens]
gi119593357	1			hCG1643801 [Homo sapiens]
gi56203186	1			RNA binding protein, autoantigenic (hnRNP-associated with lethal yellow homolog (mouse)) [Homo sapiens]
gi73983054	1	0.010		PREDICTED: similar to Cofilin-1 (Cofilin, non-muscle isoform) (18 kDa phosphoprotein) (p18) isoform 2 [Canis familiaris]
gi3088342	1	0.703		ribosomal protein S23 [Homo sapiens]
gi119592203	1	0.161		malate dehydrogenase 2, NAD (mitochondrial), isoform CRA_b [Homo sapiens]
gi32187319	1	1.259		SHUJUN-1 [Homo sapiens]
gi194373457	1	1.652		unnamed protein product [Homo sapiens]
gi54792071	1	0.224		SMT3 suppressor of mif two 3 homolog 2 isoform b precursor [Homo sapiens]
gi159163287	1	2.040		Chain A, Solution Structure Of Rrm Domain In Hnrpc Protein
gi181400	1			cytokeratin 8 [Homo sapiens]
gi62122917	1	0.101		filaggrin family member 2 [Homo sapiens]
gi55669565	1	0.521		Chain A, Solution Structure Of Alpha Subunit Of Human Eif2
gi119582136	1	0.599		Treacher Collins-Franceschetti syndrome 1, isoform CRA_a [Homo sapiens]
gi78101498	1	0.601		Chain A, Crystal Structure Of Kh1 Domain Of Human Poly(C)-Binding Protein-2 With C-Rich Strand Of Human Telomeric Dna
gi340058	1	0.931		ubiquitin precursor [Homo sapiens]
gi118142840	1	0.535		ABCF1 protein [Homo sapiens]
gi73535681	1	0.202		Chain B, Human Vinculin Head Domain (Vh1, 1-258) In Complex With Human Alpha-Actinin's Vinculin-Binding Site (Residues 731- 760)

Accession	# Peptides	Heavy/Light	Heavy/Light Variability [%]	Description
gi4506715	1	0.407		ribosomal protein S28 [Homo sapiens]
gi52695617	1	0.354		Chain A, Crystal Structure Of The C-Terminal Domain Of Uap56
gi73968359	1	1.751		PREDICTED: similar to Myosin light polypeptide 6 (Myosin light chain alkali 3) (Myosin light chain 3) (MLC-3) (LC17) isoform 3 [Canis familiaris]
gi61104919	1			heat shock protein 90Bf [Homo sapiens]
gi41472460	1	0.249		unknown [Homo sapiens]
gi226438295	1	1.338		Chain A, Human Mitochondrial Transcription Factor A Box B
gi5803165	1	0.386		Sec61 beta subunit [Homo sapiens]
gi119569330	1	0.722		hCG1640785, isoform CRA_b [Homo sapiens]
gi187761435	1	0.458		calcyclin binding protein [Homo sapiens]
gi194377686	1	0.567		unnamed protein product [Homo sapiens]
gi40737308	1	0.010		C4B1 [Homo sapiens]
gi80475848	1			KRT73 protein [Homo sapiens]
gi57997041	1	2.051		hypothetical protein [Homo sapiens]
gi55959888	1	0.069		peroxiredoxin 1 [Homo sapiens]
gi6730226	1	0.010		Chain B, Crystal Structure Of The D3b Subcomplex Of The Human Core Snrnp Domain At 2.0a Resolution
gi119602641	1	0.343		eukaryotic translation elongation factor 1 delta (guanine nucleotide exchange protein), isoform CRA_f [Homo sapiens]
gi119585586	1	1.298		ribosomal protein L29, isoform CRA_a [Homo sapiens]
gi63991119	1	0.919		unknown [Homo sapiens]
gi18490813	1	0.295		PYCR1 protein [Homo sapiens]
gi119597481	1	0.123		fatty acid binding protein 1, liver, isoform CRA_a [Homo sapiens]
gi50262342	1	0.555		activated RNA polymerase II transcription cofactor 4 [Homo sapiens]
gi55640591	1	0.753		PREDICTED: hypothetical protein [Pan troglodytes]

Bold red, keratin contaminants
Bold pink, probe sequence for rs2069915[A], cultured in medium with “light” Arg and Lys isotopes
Bold blue, probe sequence for rs2069915[G], cultured in medium with “heavy” Arg and Lys isotopes
Black non-bold, ratio falls within 0.5 and 2 and is usually not considered significant
Variability (%), variability between biological samples; for preference should be <50

A.6 Complete results for SILAC mass spectrometry for rs2069916[C/T]

Accession	# Peptides	Heavy/Light	Heavy/Light Variability [%]	Description
gi190167	32	0.427	11.8	poly(ADP-ribose) polymerase [Homo sapiens]
gi156523968	32	0.426	11.8	poly (ADP-ribose) polymerase family, member 1 [Homo sapiens]
gi4503841	23	1.224	8.3	ATP-dependent DNA helicase II, 70 kDa subunit [Homo sapiens]
gi47132620	23	0.010	0.0	keratin 2 [Homo sapiens]
gi181402	23	0.010	0.0	epidermal cytokeratin 2 [Homo sapiens]
gi10863945	22	1.251	10.6	ATP-dependent DNA helicase II [Homo sapiens]
gi11935049	21	0.010	0.0	keratin 1 [Homo sapiens]
gi195972866	16	0.010	0.0	keratin 10 [Homo sapiens]
gi435476	14	0.010	0.0	cytokeratin 9 [Homo sapiens]
gi10637825	14	0.858	12.0	ribosome binding protein 1 homolog 180kDa (dog) [Homo sapiens]
gi12803709	12	0.010	0.0	Keratin 14 [Homo sapiens]
gi27436946	11	1.321	13.8	lamin A/C isoform 1 precursor [Homo sapiens]
gi126032350	11	0.870	13.1	protein kinase, DNA-activated, catalytic polypeptide isoform 2 [Homo sapiens]
gi1195531	11	0.010	0.0	type I keratin 16 [Homo sapiens]
gi194387918	11	0.010	0.0	unnamed protein product [Homo sapiens]
gi119617032	10	0.010	0.0	keratin 6B, isoform CRA_a [Homo sapiens]
gi31645	9	0.359	11.9	glyceraldehyde-3-phosphate dehydrogenase [Homo sapiens]
gi356168	8	0.976	11.4	histone H1b
gi4885375	8	0.948	7.8	histone cluster 1, H1c [Homo sapiens]
gi148921602	8	0.562	19.0	EML4 protein [Homo sapiens]
gi119617041	8	0.011	19.2	keratin 5 (epidermolysis bullosa simplex, Dowling-Meara/Kobner/Weber-Cockayne types), isoform CRA_d [Homo sapiens]
gi55958544	7	0.916	5.8	heterogeneous nuclear ribonucleoprotein K [Homo sapiens]
gi21754583	7	0.010	0.0	unnamed protein product [Homo sapiens]
gi189065399	7	0.433	4.6	unnamed protein product [Homo sapiens]
gi194375299	6	2.130	1.5	unnamed protein product [Homo sapiens]
gi194378192	6	0.423	7.9	unnamed protein product [Homo sapiens]
gi221040048	6	0.540	16.8	unnamed protein product [Homo sapiens]
gi54696428	5	0.397	14.4	high-mobility group box 2 [Homo sapiens]
gi221042312	5	1.786	6.9	unnamed protein product [Homo sapiens]
gi189053345	5	1.789	5.4	unnamed protein product [Homo sapiens]
gi119576011	5	1.364	2.7	hCG1992406, isoform CRA_b [Homo sapiens]
gi39644662	5	2.726	18.8	HSP90AB1 protein [Homo sapiens]

Accession	# Peptides	Heavy/Light	Heavy/Light Variability [%]	Description
gi139820	5	0.363	1.6	RecName: Full=DNA repair protein XRCC1; AltName: Full=X-ray repair cross-complementing protein 1
gi109096516	5	1.346	6.4	PREDICTED: alpha tubulin isoform 2 [Macaca mulatta]
gi5729877	5	1.760	8.2	heat shock 70kDa protein 8 isoform 1 [Homo sapiens]
gi14250528	5	0.434	3.4	MAP4 protein [Homo sapiens]
gi4885371	4	0.759	9.7	H1 histone family, member 0 [Homo sapiens]
gi119626284	4	0.523	0.9	heterogeneous nuclear ribonucleoprotein D (AU-rich element RNA binding protein 1, 37kDa), isoform CRA_f [Homo sapiens]
gi194388468	4	0.735	1.7	unnamed protein product [Homo sapiens]
gi6470150	4	1.325	8.7	BiP protein [Homo sapiens]
gi62122917	4	0.040	169.6	filaggrin family member 2 [Homo sapiens]
gi153791158	4	0.031	393.1	keratin 75 [Homo sapiens]
gi38014544	4	1.256	1.6	Tubb5 protein [Rattus norvegicus]
gi148352331	4	0.633	12.9	cell division cycle 10 isoform 1 [Homo sapiens]
gi4506597	4	1.875	26.4	ribosomal protein L12 [Homo sapiens]
gi197927454	4	1.145	10.1	DEK oncogene isoform 2 [Homo sapiens]
gi75517570	3	0.722	2.0	HNRPA1 protein [Homo sapiens]
gi230867	3	**0.368**	11.1	Chain R, Twinning In Crystals Of Human Skeletal Muscle D- Glyceraldehyde-3-Phosphate Dehydrogenase
gi1310882	3	0.752	19.9	Chain A, Cyclophilin B Complexed With [d-(Cholinylester)ser8]- Cyclosporin
gi55956921	3	0.636	19.3	heterogeneous nuclear ribonucleoprotein A/B isoform b [Homo sapiens]
gi189299	3	0.636	12.0	DNA-binding protein [Homo sapiens]
gi5803121	3	0.461	28.9	protein disulfide isomerase A5 precursor [Homo sapiens]
gi4504431	3	0.900	5.3	high mobility group AT-hook 2 isoform a [Homo sapiens]
gi6980804	3	0.446	12.6	Chain B, Human ApurinicAPYRIMIDINIC ENDONUCLEASE-1 (Ape1) Bound To Abasic Dna
gi48429165	3	0.895	7.3	RecName: Full=THO complex subunit 4; Short=Tho4; AltName: Full=Ally of AML-1 and LEF-1; AltName: Full=Transcriptional coactivator Aly/REF; AltName: Full=bZIP-enhancing factor BEF
gi71143137	3	0.389	9.0	high-mobility group box 3 [Homo sapiens]
gi255311804	3	1.281	24.8	Chain A, Crystal Structure Of The R482w Mutant Of Lamin AC
gi4557976	3	1.432	1.3	Chain A, Human Muscle Fructose 1,6-Bisphosphate Aldolase Complexed With Fructose 1,6-Bisphosphate
gi194388596	3	1.716	14.1	unnamed protein product [Homo sapiens]
gi119600604	3	0.835	5.6	ligase III, DNA, ATP-dependent, isoform CRA_b [Homo sapiens]
gi63991119	3	0.565	11.6	unknown [Homo sapiens]
gi119703744	3	0.010	0.0	desmoglein 1 preproprotein [Homo sapiens]

Accession	# Peptides	Heavy/Light	Heavy/Light Variability [%]	Description
gi194373749	3	0.026	58.0	unnamed protein product [Homo sapiens]
gi194386068	3	2.197	14.7	unnamed protein product [Homo sapiens]
gi194378642	3	0.845	3.5	unnamed protein product [Homo sapiens]
gi66933016	3	0.373	10.3	inosine monophosphate dehydrogenase 2 [Homo sapiens]
gi14198278	3	2.469	34.6	KRT8 protein [Homo sapiens]
gi1732421	3	0.704	3.0	C2f [Homo sapiens]
gi119626074	3	0.152	4253.4	albumin, isoform CRA_k [Homo sapiens]
gi119580379	3	0.562	16.2	developmentally regulated GTP binding protein 1, isoform CRA_b [Homo sapiens]
gi203282367	3	1.891	8.3	Chain A, Crystal Structure Of Human Enolase 1
gi62087444	3	0.645	2.5	hydroxysteroid (17-beta) dehydrogenase 4 variant [Homo sapiens]
gi197101499	3	1.706	5.2	interleukin enhancer binding factor 2, 45kDa [Pongo abelii]
gi194387672	3	1.397	4.8	unnamed protein product [Homo sapiens]
gi119617051	3	0.096	90.0	keratin 3, isoform CRA_a [Homo sapiens]
gi113414871	2	0.012	25.7	Keratin 77 [Homo sapiens]
gi114649280	2	0.436	2.7	PREDICTED: hypothetical protein isoform 9 [Pan troglodytes]
gi221041662	2	0.918	1.5	unnamed protein product [Homo sapiens]
gi119615473	2	1.144	5.5	ribosomal protein L11, isoform CRA_a [Homo sapiens]
gi119609127	2	1.470	15.8	triosephosphate isomerase 1, isoform CRA_a [Homo sapiens]
gi194378348	2	1.200	10.0	unnamed protein product [Homo sapiens]
gi82802708	2	0.753	0.2	eFI-2-gamma [Homo sapiens]
gi50949460	2	0.462	9.3	hypothetical protein [Homo sapiens]
gi6730357	2	0.733	24.6	Chain A, Role Of Amino Acid Residues At Turns In The Conformational Stability And Folding Of Human Lysozyme
gi194388148	2	0.911	13.1	unnamed protein product [Homo sapiens]
gi13097759	2	1.183	16.6	Unknown (protein for IMAGE:3544292) [Homo sapiens]
gi31455187	2	2.326	19.9	NCL protein [Homo sapiens]
gi119627830	2	0.755	0.8	splicing factor proline/glutamine-rich (polypyrimidine tract binding protein associated), isoform CRA_e [Homo sapiens]
gi11513832	2	0.756	20.4	Chain A, Core Of The Alu Domain Of The Mammalian Srp
gi151568124	2	0.408	17.3	Chain A, Crystal Structure Of Human Recq-Like Dna Helicase
gi194376170	2	1.783		unnamed protein product [Homo sapiens]
gi55669565	2	0.823	2.1	Chain A, Solution Structure Of Alpha Subunit Of Human Eif2
gi119582136	2	0.965	18.2	Treacher Collins-Franceschetti syndrome 1, isoform CRA_a [Homo sapiens]
gi2896146	2	0.852		transcriptional coactivator ALY [Homo sapiens]

Accession	# Peptides	Heavy/Light	Heavy/Light Variability [%]	Description
gi119623487	2	4.314	46.3	histone 1, H2bj, isoform CRA_b [Homo sapiens]
gi21750830	2	0.011	16.2	unnamed protein product [Homo sapiens]
gi4826860	2	2.236	13.7	NHP2 non-histone chromosome protein 2-like 1 [Homo sapiens]
gi119611543	2	2.503	27.8	DEAH (Asp-Glu-Ala-His) box polypeptide 9, isoform CRA_a [Homo sapiens]
gi219520997	2	0.577	3.1	SEPT8 protein [Homo sapiens]
gi33874022	2	2.757	0.2	HNRPM protein [Homo sapiens]
gi194389932	2	0.406	12.4	unnamed protein product [Homo sapiens]
gi90655152	2	2.391	29.4	actinin alpha4 isoform [Homo sapiens]
gi38014092	2	0.010		KRT4 protein [Homo sapiens]
gi89574029	2	1.321	14.9	mitochondrial ATP synthase, H+ transporting F1 complex beta subunit [Homo sapiens]
gi158255378	2	1.638	5.0	unnamed protein product [Homo sapiens]
gi164698496	2	0.507	16.5	septin 9 isoform e [Homo sapiens]
gi40795897	2	0.061	357.5	hornerin precursor [Homo sapiens]
gi194388336	2	0.474	21.9	unnamed protein product [Homo sapiens]
gi4506743	2	2.477	36.7	ribosomal protein S8 [Homo sapiens]
gi119584991	2	2.260	71.1	ribosomal protein SA, isoform CRA_c [Homo sapiens]
gi6841314	2	0.543		HSPC332 [Homo sapiens]
gi194389318	2	0.609	8.0	unnamed protein product [Homo sapiens]
gi125628632	2	0.014	53.4	keratin 80 isoform b [Homo sapiens]
gi52632385	2	0.685	9.4	heterogeneous nuclear ribonucleoprotein L isoform b [Homo sapiens]
gi55613379	2	0.491	9.7	CLE [Homo sapiens]
gi14029171	2	0.464	3.4	CGI-55 [Homo sapiens]
gi24497601	2	0.432		endothelial differentiation-related factor 1 isoform beta [Homo sapiens]
gi5174449	2	1.046	7.9	H1 histone family, member X [Homo sapiens]
gi148612803	2	0.010		keratin 6 irs4 [Homo sapiens]
gi194382840	2	0.824	2.3	unnamed protein product [Homo sapiens]
gi114794876	2	2.312	1.6	Chain A, The Crystal Structure Of The Exon Junction Complex At 3.2 A Resolution
gi194387038	2	1.553	11.2	unnamed protein product [Homo sapiens]
gi10834770	2	0.555	0.6	PNAS-107 [Homo sapiens]
gi6729803	2	1.502	7.5	Chain A, Heat-Shock 70kd Protein 42kd Atpase N-Terminal Domain
gi11513833	2	0.632	13.7	Chain B, Core Of The Alu Domain Of The Mammalian Srp
gi30581135	2	1.029		structural maintenance of chromosomes 1A [Homo sapiens]
gi18490813	2	0.614	65.7	PYCR1 protein [Homo sapiens]
gi50542195	2	2.905	2.6	histone H4 [Gallus gallus]
gi57997041	2	3.324	8.1	hypothetical protein [Homo sapiens]

Accession	# Peptides	Heavy/Light	Heavy/Light Variability [%]	Description
gi119569329	2	1.103	60.6	hCG1640785, isoform CRA_a [Homo sapiens]
gi553328	1	1.014	7.4	histone H1 [Homo sapiens]
gi29387268	1	1.886		ILF3 protein [Homo sapiens]
gi1017823	1	1.342		RNA polymerase II subunit [Homo sapiens]
gi31958	1	0.579		glutaminyl-tRNA synthetase [Homo sapiens]
gi119600188	1	1.242		ribosomal protein L24, isoform CRA_c [Homo sapiens]
gi18033272	1	0.448		histidyl-tRNA synthetase [Homo sapiens]
gi145580402	1	2.326		Chain A, Crystal Structure Of Human Nucleophosmin-Core
gi17426163	1	0.335		macrophin 1 isoform [Homo sapiens]
gi183448176	1	0.972		Chain A, Crystal Structure Of Human Peroxisomal Delta3,5, Delta2,4-Dienoyl Coa Isomerase
gi159163719	1	2.092		Chain A, Solution Structure Of Polypyrimidine Tract Binding Protein Rbd2 Complexed With Cucucu Rna
gi12583614	1	0.495		FUS/CHOP chimaeric fusion protein [Homo sapiens]
gi33873325	1	0.824		KHDRBS1 protein [Homo sapiens]
gi6807709	1	0.488		hypothetical protein [Homo sapiens]
gi226438295	1	0.977		Chain A, Human Mitochondrial Transcription Factor A Box B
gi45476309	1	0.425		damage-specific DNA binding protein 2 splicing variant D4 [Homo sapiens]
gi237649049	1	2.416		small nuclear ribonucleoprotein D2 isoform 2 [Homo sapiens]
gi306549	1	1.203		homology to rat ribosomal protein L23 [Homo sapiens]
gi168984316	1	1.937		heterochromatin protein 1, binding protein 3 [Homo sapiens]
gi119580687	1	1.322		apolipoprotein B mRNA editing enzyme, catalytic polypeptide-like 3C, isoform CRA_a [Homo sapiens]
gi119615454	1	0.553		transcription elongation factor A (SII), 3, isoform CRA_a [Homo sapiens]
gi119592222	1	1.747		ribosomal protein S4, X-linked, isoform CRA_b [Homo sapiens]
gi119621546	1			hCG1643126, isoform CRA_b [Homo sapiens]
gi62202489	1	0.717		CIP29 protein [Homo sapiens]
gi33187705	1	1.125		unknown [Homo sapiens]
gi2624694	1			Chain A, Human Mitochondrial Single-Stranded Dna Binding Protein
gi40254924	1	1.160	3.1	leucine rich repeat containing 59 [Homo sapiens]
gi162280796	1	0.010		caspase 14 precursor [Homo sapiens]
gi241913102	1	0.077		Chain A, Crystal Structure Of Human Filamin B Actin Binding Domain At 1.9 Angstroms Resolution
gi119620549	1	1.718		spectrin, beta, non-erythrocytic 1, isoform CRA_f [Homo sapiens]
gi119611769	1	0.637		ladinin 1, isoform CRA_a [Homo sapiens]

Accession	# Peptides	Heavy/Light	Heavy/Light Variability [%]	Description
gi193787171	1	1.355		unnamed protein product [Homo sapiens]
gi114793397	1	1.849		Chain A, Nmr Structure Of The N-Terminal Domain A Of The Glycoprotein Chaperone Erp57
gi57209130	1	0.672		paraspeckle component 1 [Homo sapiens]
gi895845	1	1.933		p64 CLCP [Homo sapiens]
gi159163287	1	3.525		Chain A, Solution Structure Of Rrm Domain In Hnrpc Protein
gi159162530	1	1.234		Chain A, Solution Structure Of Reduced Recombinant Human Cytochrome C
gi119572748	1	2.687		ribosomal protein L18, isoform CRA_e [Homo sapiens]
gi73998790	1	0.620		PREDICTED: similar to BUB3 budding uninhibited by benzimidazoles 3 isoform a isoform 3 [Canis familiaris]
gi59016837	1	0.608		hypothetical protein [Homo sapiens]
gi57997098	1	2.630		hypothetical protein [Homo sapiens]
gi221044626	1	0.596		unnamed protein product [Homo sapiens]
gi60552474	1	2.412		SSRP1 protein [Homo sapiens]
gi15341985	1	1.009		SERPINA3 protein [Homo sapiens]
gi52695617	1	2.093		Chain A, Crystal Structure Of The C-Terminal Domain Of Uap56
gi15147219	1	0.321		purine-rich element binding protein B [Homo sapiens]
gi82802829	1			rcNSEP1 [Homo sapiens]
gi62421162	1	3.048		actin-like protein [Homo sapiens]
gi194391216	1	0.252		unnamed protein product [Homo sapiens]
gi119609186	1	1.971		nucleolar protein 1, 120kDa [Homo sapiens]
gi56204904	1	1.531		synaptotagmin binding, cytoplasmic RNA interacting protein [Homo sapiens]
gi243123	1	1.213		cytochrome c oxidase subunit VIIa='liver-type' isoform {EC 1.9.3.1} [human, skeletal muscle, Peptide Partial, 30 aa]
gi159163871	1	2.177		Chain A, Solution Structure Of The N-Terminal Domain Of Human Ribosomal Protein L9
gi13477169	1			Vitronectin [Homo sapiens]
gi194377686	1	0.556		unnamed protein product [Homo sapiens]
gi119611898	1	0.653		zinc finger CCCH-type containing 11A, isoform CRA_a [Homo sapiens]
gi119585586	1	1.451		ribosomal protein L29, isoform CRA_a [Homo sapiens]
gi5542151	1	1.705		Chain A, Macrophage Migration Inhibitory Factor (Mif) With Hydroxphenylpyruvate
gi119591666	1	0.597		septin 2, isoform CRA_c [Homo sapiens]
gi114653233	1	1.042		PREDICTED: similar to Proteasome (prosome, macropain) subunit, alpha type, 3 isoform 1 [Pan troglodytes]
gi10835240	1	0.581		high mobility group nucleosomal binding domain 4 [Homo sapiens]
gi119612777	1	0.464		family with sequence similarity 98, member B, isoform CRA_c [Homo sapiens]
gi34528529	1	1.212		unnamed protein product [Homo sapiens]

Accession	# Peptides	Heavy/Light	Heavy/Light Variability [%]	Description
gi221039618	1	1.556		unnamed protein product [Homo sapiens]
gi3088342	1	0.909		ribosomal protein S23 [Homo sapiens]
gi10835230	1	2.164		metallothionein 1G [Homo sapiens]
gi189030	1	2.640		nonmuscle myosin heavy chain-A [Homo sapiens]
gi111309288	1	0.469		CKAP5 protein [Homo sapiens]
gi40737308	1	0.010		C4B1 [Homo sapiens]
gi157879202	1	0.674		Chain B, Crystal Structures Of Native And Inhibited Forms Of Human Cathepsin D: Implications For Lysosomal Targeting And Drug Design
gi194388578	1	1.370		unnamed protein product [Homo sapiens]
gi119616090	1	1.240		golgi apparatus protein 1, isoform CRA_c [Homo sapiens]
gi21614544	1	0.025		S100 calcium-binding protein A8 [Homo sapiens]
gi6330302	1	0.603		KIAA1185 protein [Homo sapiens]
gi1673514	1	1.774		B-cell receptor associated protein [Homo sapiens]
gi257471008	1	1.594		glypican 3 isoform 3 precursor [Homo sapiens]
gi16307468	1	1.077		LRPPRC protein [Homo sapiens]
gi3088349	1	2.478		ribosomal protein L13 [Homo sapiens]
gi13385036	1	2.571		ribosomal protein L15 [Mus musculus]
gi119621354	1	1.489		protein disulfide isomerase family A, member 6, isoform CRA_a [Homo sapiens]
gi159162698	1	0.640		Chain A, C-Terminal Domain Of Midkine
gi157834124	1	1.264		Chain A, Nmr Study Of Vigilin, Repeat 6, 40 Structures
gi194374163	1	2.078		unnamed protein product [Homo sapiens]
gi55957202	1	0.357		chromosome 20 open reading frame 72 [Homo sapiens]
gi268612104	1	2.275		Chain A, Nmr Structure Of Dimerization Domain Of Human Ribosomal Protein P2
gi119596625	1	1.990		integrin beta 4 binding protein, isoform CRA_a [Homo sapiens]
gi20150229	1	0.037		Chain A, Crystal Structure Of The Mrp14 Complexed With Chaps
gi119619436	1	6.076		hCG1983058 [Homo sapiens]
gi33877895	1	1.021		MARCKS protein [Homo sapiens]
gi182642	1	0.783		rapamycin-binding protein [Homo sapiens]
gi4502847	1			cold inducible RNA binding protein [Homo sapiens]
gi16751921	1	0.010		dermcidin preproprotein [Homo sapiens]
gi194384322	1	1.259		unnamed protein product [Homo sapiens]
gi253722876	1	0.654		Chain A, Lem-Like Domain Of Human Inner Nuclear Membrane Protein Lap2
gi28948850	1	0.903		Chain A, Human Topoisomerase I Ara-C Complex
gi5454090	1	1.420		signal sequence receptor, delta precursor [Homo sapiens]

Accession	# Peptides	Heavy/Light	Heavy/Light Variability [%]	Description
gi52545510	1	2.730		hypothetical protein [Homo sapiens]
gi338497	1	1.734		SS-B/La protein [Homo sapiens]
gi119571986	1	0.774		granulin, isoform CRA_b [Homo sapiens]
gi193787257	1	0.010		unnamed protein product [Homo sapiens]
gi41350399	1	1.967		migration-inducing gene 9 protein [Homo sapiens]
gi42542978	1	4.195		Chain B, X-Ray Crystal Structure Of Human Galectin-1
gi42542977	1			Chain A, X-Ray Crystal Structure Of Human Galectin-1
gi57208257	1	1.388		ribophorin II [Homo sapiens]
gi194383306	1	0.518		unnamed protein product [Homo sapiens]
gi5803165	1	1.059		Sec61 beta subunit [Homo sapiens]
gi183448388	1	2.562		Chain A, Crystal Structure Of Human Eukaryotic Translation Initiation Factor Eif5a
gi33112669	1	0.601		RecName: Full=Ribosomal RNA processing protein 1 homolog B; AltName: Full=RRP1-like protein B
gi19352984	1	1.894		CAPZB protein [Homo sapiens]
gi7770137	1	2.255		PRO1608 [Homo sapiens]
gi4506715	1	1.641		ribosomal protein S28 [Homo sapiens]
gi55960696	1	2.061		aldehyde dehydrogenase 1 family, member A1 [Homo sapiens]
gi56203186	1			RNA binding protein, autoantigenic (hnRNP-associated with lethal yellow homolog (mouse)) [Homo sapiens]
gi6729889	1	0.433		Chain A, Human 3-Methyladenine Dna Glycosylase Complexed To Dna
gi41472460	1	1.231		unknown [Homo sapiens]
gi36796	1	1.658		t-complex polypeptide 1 [Homo sapiens]
gi221044494	1	0.208		unnamed protein product [Homo sapiens]
gi193785141	1	1.933		unnamed protein product [Homo sapiens]
gi194379584	1	0.462		unnamed protein product [Homo sapiens]
gi159164372	1	0.913		Chain A, Solution Structure Of Rsgi Ruh-069, A Gtf2i Domain In Human Cdna
gi45384773	1	2.905		ribosomal protein L8 [Chinchilla lanigera]
gi93359803	1	1.241		RUVBL1-FK [Homo sapiens]
gi119572383	1	1.932		Tu translation elongation factor, mitochondrial, isoform CRA_b [Homo sapiens]
gi119584403	1	4.266		hCG1995701, isoform CRA_b [Homo sapiens]
gi159164137	1	1.989		Chain A, The Solution Structure Of The Third Thioredoxin Domain Of Human Thioredoxin Domain-Containing Protein 5
gi119602640	1	1.078		eukaryotic translation elongation factor 1 delta (guanine nucleotide exchange protein), isoform CRA_e [Homo sapiens]
gi10863895	1	3.267		thymosin, beta 10 [Homo sapiens]
gi119624177	1	0.509		high mobility group AT-hook 1, isoform CRA_g [Homo sapiens]
gi194377426	1	1.603		unnamed protein product [Homo sapiens]
gi62630233	1			unknown [Homo sapiens]

Accession	# Peptides	Heavy/Light	Heavy/Light Variability [%]	Description
gi8574449	1	1.784		rheumatoid arthritis-related antigen RA-A47 [Homo sapiens]
gi194391388	1	0.012		unnamed protein product [Homo sapiens]
gi66392203	1	2.204		NME1-NME2 protein [Homo sapiens]
gi4507793	1	1.813		ubiquitin-conjugating enzyme E2N [Homo sapiens]
gi61104919	1			heat shock protein 90Bf [Homo sapiens]
gi260436922	1	0.083		suprabasin isoform 1 precursor [Homo sapiens]
gi56203545	1	2.080		nucleolar protein 5A (56kDa with KKE/D repeat) [Homo sapiens]
gi51476156	1			hypothetical protein [Homo sapiens]
gi36535	1	1.303		unnamed protein product [Homo sapiens]
gi223480	1			dismutase,Cu/Zn superoxide
gi4261582	1	2.019		prothymosin alpha [Homo sapiens]
gi34526989	1	0.020		unnamed protein product [Homo sapiens]
gi24308271	1	1.362		DC2 protein [Homo sapiens]
gi16878197	1	2.772		VIL1 protein [Homo sapiens]
gi62897523	1	0.479		cytidine 5'-monophosphate N-acetylneuraminic acid synthetase variant [Homo sapiens]
gi54792071	1	1.673		SMT3 suppressor of mif two 3 homolog 2 isoform b precursor [Homo sapiens]
gi78101271	1	0.456		Chain C, Human Complement Component C3c
gi194382012	1	20.176		unnamed protein product [Homo sapiens]
gi1335208	1	0.500		LLDBP [Homo sapiens]
gi4929565	1	2.673		CGI-48 protein [Homo sapiens]
gi116283653	1	0.393		FAM98A protein [Homo sapiens]
gi119622066	1	0.011		hCG1820678 [Homo sapiens]
gi1663708	1	2.211		KIAA0007 [Homo sapiens]
gi14278207	1	1.305		Chain B, Ran-Rcc1-So4 Complex
gi61651996	1	1.634		ribosomal protein L18a-like protein [Homo sapiens]
gi6730225	1	1.473		Chain A, Crystal Structure Of The D3b Subcomplex Of The Human Core Snrnp Domain At 2.0a Resolution
gi260099885	1	0.456		Chain A, Crystal Structure Of The Duf55 Domain Of Human Thymocyte Nuclear Protein 1
gi180687	1	1.018		2',3'-cyclic-nucleotide 3'-phosphodiesterase (EC 3.1.4.37) [Homo sapiens]
gi239746153	1			PREDICTED: similar to cytoskeletal beta actin [Homo sapiens]
gi197927207	1	0.583		crystallin, zeta isoform c [Homo sapiens]
gi52545962	1	1.310		hypothetical protein [Homo sapiens]
gi119574244	1	0.294		septin 10, isoform CRA_b [Homo sapiens]
gi15342081	1			Mitochondrial ribosomal protein L38 [Homo sapiens]
gi119587722	1			centrosomal protein 164kDa, isoform CRA_a [Homo sapiens]
gi57160644	1	1.132		ribosomal protein L35 [Homo sapiens]

Accession	# Peptides	Heavy/Light	Heavy/Light Variability [%]	Description
gi194380082	1	0.856		unnamed protein product [Homo sapiens]
gi4758302	1	1.756		enhancer of rudimentary homolog [Homo sapiens]
gi5803137	1	1.408		RNA binding motif protein 3 [Homo sapiens]

Bold red, keratin contaminants
Bold pink, probe sequence for rs2069916[T], cultured in medium with “light” Arg and Lys isotopes
Bold blue, probe sequence for rs2069915[C], cultured in medium with “heavy” Arg and Lys isotopes
Black non-bold, ratio falls within 0.5 and 2 and is usually not considered significant
Variability (%), variability between biological samples; for preference should be <50

Appendix B Supplementary data for Chapter 4

B.1 Allele frequency and Hardy Weinberg equilibrium in VASST cohort

PCSK9 SNPs	Major (minor) allele	Minor Allele Frequency	HWE P-value
rs11591147	C(A)	0.006	0.841
rs11583680	G(A)	0.134	0.677
rs562556	A(G)	0.170	0.592
rs644000	A(G)	0.338	0.840
rs505151	A(G)	0.053	0.882

B.2 Baseline characteristics of patients in the VASST and SPH cohorts by *PCSK9* genotype

	VASST Cohort				SPH Cohort			
***PCSK9* rs644000 genotype**	**GG**	**GA**	**AA**		**GG**	**GA**	**AA**	
	(n=82)	(n=287)	(n=263)	P	(n=60)	(n=234)	(n=295)	P
Age –yr	64(51-73)	63(50-73)	63(50-73)	0.76	63(51-72)	62(49-72)	62(46-73)	0.89
Gender -% male	62.2	56.5	59.6	0.57	73.3	62.4	61.4	0.21
Caucasian -n (%)	78(95.0)	251(87.5)	201(85.1)	0.06	48(80.0)	194(82.9)	211(71.5)	0.13
APACHE II	25(20-31)	26(21-32)	27(22-32)	0.19	24(18-29)	26(21-31)	27(20-33)	0.16
Surgical -%	20.7	22.6	19.4	0.64	25	29.1	31.5	0.67
Pre-existing conditions -n (%)								
Chronic heart failure	8(9.8)	17(5.9)	25(9.5)	0.24	4(6.7)	20(8.5)	13(4.4)	0.15
Chronic pulmonary disease	11(13.4)	46(16.0)	50(19.0)	0.43	10(16.7)	41(17.5)	49(16.6)	0.96
Chronic liver disease	10(12.2)	35(12.2)	27(10.3)	0.75	6(10.0)	18(7.7)	34(11.5)	0.34
Chronic renal failure	8(9.8)	26(9.1)	34(12.9)	0.33	5(8.3)	12(5.1)	22(7.5)	0.48
Chronic corticosteroid use	13(15.9)	54(18.8)	65(24.7)	0.11	5(8.3)	13(5.6)	20(6.8)	0.70
Cardiovascular variables -Day 1								
Heart rate –bpm	120(107-133)	127(112-141)	130(112-141)	0.05	106(95-120)	110(95-130)	115(96-135)	0.06
Mean arterial pressure -mmHg	56(50-62)	56(50-62)	55(50-60)	0.30	54(50-58)	55(50-59)	55(49-59)	0.45
Central venous pressure -mmHg*	14(11-18)	14(11-18)	14(11-18)	0.88	11(6-13)	11(7-15)	12(8-15)	0.22
Norepinephrine -µg/min	15(9-26)	14(8-25)	16(10-27)	0.12	10(6-23)	15(7-25)	15(8-29)	0.59
Dobutamine -µg/kg/min†	3(2-5)	3(2-5)	5(4-7)	0.86	5(3-10)	7(5-10)	8(5-12)	0.40
Laboratory variables- Day 1								
White blood cell count -10^3/mm^3	14.5(8.7-21.2)	14.1(7.7-21.0)	13.2(7.2-20.8)	0.74	14.6(10.2-21.6)	15.6(10.4-21.3)	14.1(9.3-19.0)	0.22
Platelet count -10^3/mm^3	151(89-234)	162(92-245)	156(66-263)	0.75	206(85-300)	162(95-243)	161(90-240)	0.19
PaO_2/F_IO_2 -torr‡	198(151-254)	185(128-249)	186(128-255)	0.71	160(91-216)	142(93-220)	145(89-214)	0.91
Blood creatinine -µmol/L	146(88-250)	150(90-239)	153(94-267)	0.44	142(80-271)	145(83-283)	150(90-272)	0.69
Blood lactate -mmol/L	1.7(0.8-3.4)	1.8(1.0-3.8)	1.9(1.0-3.9)	0.29	2.0(1.4-5.9)	2.3(1.4-4.4)	2.3(1.4-5.1)	0.89

* Cases missing in VASST: GG/9, AG/34 and AA/30

† Data only includes those patients that received dobutamine

‡ Cases missing in VASST: GG/2, AG/9 and AA/7